The role of plant extracts on islet function in vivo and in vitro

Alromaiyan, Altaf

Awarding institution:
King's College London

Title: The role of plant extracts on islet function in vivo and in vitro

Author: Altaf Alromaiyan

The role of plant extracts on islet function *in vivo* and *in vitro*

A thesis submitted by

Altaf Al-Romaiyan

For the degree of Doctor of Philosophy

from University of London

Diabetes Research Group

Division of Diabetes and Nutritional Sciences

School of Medicine

King's College London

University of London

Table of Contents

Abstract

Plant-derived extracts have been used as folk remedies for Type 2 diabetes mellitus (T2DM) for many centuries, and offer the potential of cheap and readily available alternatives to conventional pharmaceuticals in developing countries. Extracts of *Gymnema sylvestre* (GS) and *Costus pictus* (CP) are reported to have antidiabetic activity *in vivo*. The exact molecular mode of action(s) of GS and CP is unclear but the antihyperglycemic effect seen in animal studies was associated with dramatic increases in insulin secretion so in my thesis I have examined the effect of alcoholic aqueous GS extract, named OSA®, on blood glucose and plasma insulin levels *in vivo* from animals and humans with T2DM and I have measured the effect of GS aqueous alcoholic and CP methanolic extracts on insulin secretion *in vitro* from the MIN6 β-cell line and isolated mouse and human islets. The *in vivo* data showed that OSA® increased insulin levels and reduced blood glucose in patients with T2DM and ameliorated glucose intolerance in animal model of diabetes. The *in vitro* data demonstrated that OSA® and CP have a direct stimulatory effect on insulin secretion which was not associated with compromised membrane integrity or decreased β-cell viability. OSA®-, but not CP-, induced insulin secretion was coupled with elevations in insulin gene expression suggesting that GS may reserve β-cell insulin store following chronic stimulation of insulin.

Single cell calcium microfluorimetry measurements showed that OSA® and CP elevated intracellular Ca^{2+} concentrations ($[Ca^{2+}]_i$) in Fura-2-loaded β-cell, an effect which was completely abolished by the removal of extracellular Ca^{2+} or blockade of voltage-gated Ca^{2+} channels (VGCC). These *in vitro* observations suggest that one

mode of action of OSA® and CP is through stimulating insulin secretion which may be mediated, in part, by the ability of OSA® and CP to increase $[Ca^{2+}]_i$ levels through VGCC. In addition, OSA®-induced insulin secretion was partially associated with protein kinase activation and was independent of classical PKC, CaMKII or cAMP activation.

OSA® was also found to protect β-cells from cytokine-induced apoptosis. Our measurement of caspase-3 and -7 production showed partial reduction in OSA®-treated MIN6 cells and mouse islets following cytokines exposure. These data were further supported by our microarray analysis of mouse islets when challenged with cytokines in the presence of OSA®. Enrichment analysis indicated that OSA® reduced caspase-3 gene expression most likely through activation of PI3K/AKT pathway and subsequent downstream effectors including MnSOD.

Acknowledgments

I would like to begin by thanking both of my supervisors Prof. Peter Jones and Prof. Shanta Persaud for their guidance and help. It was really a great privilege to work under their supervision. I have learnt a lot from their academic expertise.

Many thanks to Dr. Bo liu for her help and support throughout the work of my thesis. My thanks also directed to the entire Diabetes Research Group members especially Dr. Aileen King and Dr. James Bowe for helping me with some of the animal work.

I would like to gratefully acknowledge C. R. Maity, S. K. Chatterjee, N. Koley, T. Biswas and A. K. Chatterji for conducting the clinical human studies discussed in this thesis. I also want to thank our collaborators A. K. Chatterji and M.A. Jayasri for supplying and preparing the *Gymnema sylvestre* and *Costus pictus* powder, respectively.

Many thanks for Dr. Matthew Arno and Dr. Estibaliz Aldecoa-otalora Astarloa from the genomic center, King's College London for their great help with the microarray experiment.

I sincerely thank Kuwait University and Government of Kuwait for offering me a scholarship and for their financial support.

Last but not least, I would like to express my special gratitude to my family and friends who overwhelmed me with their constant love, support and encouragement.

List of abbreviations

$[Ca^{2+}]_i$	Intracellular Ca^{2+} concentration
5-HT	Serotonin
aa	Amino acids
AA	Arachidonic acid
Ab	Antibody
ABC	ATP-binding cassette
AC	Adenylate cyclase
Ach	Acetylcholine
ADP	Adenosine diphosphate
Ag	Antigen
AKT	Murine thymoma viral oncogene homolog
Ala	Alanine
AM	Acetoxymethyl
Apaf-1	Apoptosin protease activating factor-1
Arg	Arginine
ATP	Adenosine triphosphate
Bard1	BRCA1 associated RING domain 1

Bax	BCL2-associated X protein
Bcl2	B-cell leukemia/lymphoma 2
beta2/NeuroD	Neurogenic differentiation
BH	Bcl-2 homology domains
Bid	BH3 interacting domain death agonist
bp	Base pair
BSA	Bovine serum albumin
Ca^{2+}	Calcium ion
CAD	Caspase-activated DNase
CaMK	Ca^{2+}-calmodulin-dependent kinase
cAMP	Cyclic adenylate monophosphate
CARD	Caspase recruitment domain
Casp	Caspase
CCK	Cholecystokinin
$CD4^{+}$	Cluster of differentiation 4
$CD8^{+}$	Cluster of differentiation 8
CDKAL1	CDK5 regulatory subunit associated protein 1 like 1 gene
CDKN2A	Cyclin-dependent kinase inhibitor 2A gene;

CDKN2B	Cyclin-dependent kinase inhibitor 2B gene;
CgA	Chromogranin A peptide
CHOP	C/EBP homologous protein
cIAP	Cellular inhibitor of apoptosis
CMRL	Connaught Medical Research Laboratories
CNS	Central nervous system
CoA	Coenzyme A
CP	*Costus pictus*
Cpm	Counts per minute
Creb1	cAMP responsive element binding protein 1
DAG	Diacylglycerol
dATP	Deoxy adenosine triphosphate
DD	Death domain
DED	Death effector domain
DISC	Death-inducing signaling complex
DM	Diabetes mellitus
DMEM	Dulbecco's modified Eagle's medium
DMSO	Dimethyl sulfoxide

Dnajc3	DnaJ (Hsp40) homolog, subfamily C, member 3
DPP-4	Dipeptidyl peptidase-4
ds	Double stranded
E2f1	E2F transcription factor 1
EDTA	Ethylenediaminetetraacetic acid
EGTA	Ethylene glycol tetraacetic acid
Epac	Exchange proteins activated by cAMP
ER	Endoplasmic reticulum
Ern1/ire1	Endoplasmic reticulum (ER) to nucleus signaling 1
FACS	Fluorescence Activated Cell Sorting
FADD	Fas-associated death domain
FasL	Fas ligand
FCS	Foetal Calf Serum
FFAs	Free fatty acids
Foxo	Forkhead box
FSK	Forskolin
FTO	Fat mass and obesity associated gene;
GA	Gymnemic acids

GABA	Gamma-aminobutyric acid
GAD	Glutamatic acid decarboxylase
GADD	DNA damage-inducible gene
GIP	Gastric inhibitory polypeptide
GK	Glucokinase
GLP-1	Glucagon-like peptide-1
GLUT1	Glucose transporter type 1
GLUT2	Glucose transporter type 2
GLUT3	Glucose transporter type 3
GLUT4	Glucose transporter type 4
Gly	Glycine
GPCR	G-protein coupled receptor
GRP	Gastrin releasing peptide
GS	*Gymnema sylvestre*
GTT	Glucose tolerance test
HCl	Hydrochloric acid
HHEX	Haematopoietically expressed homoebox gene
HLA	Human leukocyte Ag

HNF	Hepatic nuclear factor
Hspa5/Gpr78	Heat shock protein 5
I	Iodine
I^+	Iodous ion
IAPP	Islet amyloid polypeptide
IAPs	Inhibitors of apoptosis proteins
IBMX	3-Isobutyl-1-methylxanthine
ICAD	Inhibitor of caspase-activated DNase
IDE	Insulin-degrading enzyme gene
IDF	International Diabetes Federation
IGF2BP2	Insulin-like growth factor 2 mRNA binding protein 2 gene
IL-1β	Interleukin-1β
Ile	Isoleucine
INF-γ	Interferon-γ
iNOS	Inducible nitric oxide synthase
IP3	Phosphotidyl inositol tri-phosphate
IRF-1	INF-γ regulatory factors-1
IVT	*In vitro* transcription

IκB	Inhibitor of NF-κB
IκK	IκB kinase
JAK	Janus kinase
JNK	c-Jun NH2-terminal kinase
K^+	Potassium ion
KCNJ11	Inwardly rectifying ATP-sensitive potassium channel subfamily J member 11 gene
KDa	Kilo Dalton
K_{IR}	Inward-rectifying K^+ channel
Km	Michaelis constant
Lys	Lysine
MafA/L-Maf	v-maf musculoaponeurotic fibrosarcoma oncogene homolog A
MAPKs	Mitogen activated protein kinases
MB	Maximum binding
Mcl1	Myeloid cell leukemia sequence 1
MHC	Major histocompatibility complex
MIN	Mouse insulinoma
MLCK	Myosin-light chain kinase

mmLV-RT	Moloney Murine Leukemia Virus Reverse Transcriptase
MODY	Maturity onset diabetes of the young
Na^+	Sodium ion
NADH	Nicotinamide adenine dinucleotide hydrogen
NCS	Neonatal calf serum
NE	Norepinephrine
NF-κB	Nuclear factor kappa B
NO	Nitric oxide
NOXA	Phorbol-12-myristate-13-acetate-induced protein 1
NPY	Neuropeptide Y
NSB	Non-specific binding
OM	ob/ob mouse
PACAP	Pituitary adenylate cyclase-activating polypeptide
PBS	Phosphate buffered saline
PC 1/3	Prohormone convertase 1/3
PC 2	Prohormone convertase 2
PCR	Polymerase chain reaction
Pdx-1	Pancreatic/duodenal homeobox 1

PEG	Polyethelenglycol
PI3K	Phosphatidylinositol-3 kinase
PIP2	Phosphatidylinositol bis phosphate
PIs	Pseudoislets
PKA	Protein kinase A
PKB	Protein kinase B
PKC	Protein kinase C
PKCα	Protein kinase C alpha
PKCβ	Protein kinase C beta
PKCγ	Protein kinase C gamma
PKCδ	Protein kinase C delta
PKCε	Protein kinase C epsilon
PKCζ	Protein kinase C zeta
PKCη	Protein kinase C eta
PKCθ	Protein kinase C theta
PKCι/λ	Protein kinase C Iota/ lambda
PKCμ	Protein kinase C mu
PLA_2	Phospholipase A_2

PLC	Phospholipase C
PLD	Phospholipase D
PPARG	Peroxisome proliferator-activated receptor γ gene
PtdIns-3,4,5-P3	Phosphatidylinositol 3,4,5 triphosphate
PtdIns-3,4-P2	Phosphatidylinositol 3,4 bisphosphate
PtdIns-3-P	Phosphatidylinositol 3-phosphate
PYY	Peptide YY
Rela	v-rel reticuloendotheliosis viral oncogene homolog A
RIA	Radioimmunoassay
ROS	Reactive oxygen radicals
RPMI	Roswell Park Memorial Institute medium
RXR	Retinoid X receptor
Ser	Serine
SGLT2	Type 2 sodium-glucose co-transporter
SLC30A8	Family 30 (zinc transporter) member 8 gene;
SNAP-25	Synaptosome-associated protein of 25,000 daltons
SNARE	Soluble N-Ethylmaleimide-Sensitive Factor Attachment Protein Receptor
ss	Single stranded

STAT	Signal transducer and activator of transcription
STZ	Streptozotocin
SUR	Sulphonylurea receptor
SUs	Sulphonylureas
T1DM	Type 1 diabetes mellitus
T2DM	Type 2 diabetes mellitus
TBM	Tetramethylbenzidine
TCF7L2	Transcription factor 7-like 2 (T cell specific) gene
TG	Triglyceride
Thr	Threonine
Tnfaip	Tumor necrosis factor, alpha-induced protein
TNFR	TNF receptor
TNF-α	Tumor necrosis factor-α
Traf	TNF receptor associated factor
TRAIL	TNF-related apoptosis-inducing ligand
Trp73	Transformation related protein 73
Val	Valine
VAMP	Vesicle-associated membrane protein

VGCC	Voltage gated Ca^{2+} channels
VIP	Vasoactive intestinal polypeptide
WFS1	Wolfram syndrome 1 gene
WHO	World Health Organization
Xaf1	XIAP associated factor 1
Xiap	X-linked inhibitor of apoptosis

Chapter 1

Introduction

1.1 History

It is believed that diabetes mellitus (DM) was known as a disease in as early as Egyptian times (1500 BC). However, it was not until the 1st & 2nd centuries when the Greeks used the term "Diabetes" to describe the disorder. Diabetes was derived from the Greek ward "diabainein" which means "passing through". The name referred to the excessive passing of urine. Although the symptoms of diabetes have been further studied in the middle age by Arabs, the "sweetness of urine" was only noticed and investigated in the mid of 17th century by Thomas Willis. The early classification of diabetes into diabetes mellitus and diabetes insipidus has been introduced in the 18th century (Schadewaldt, 1989). In 1869, the islets were discovered by Paul Langerhans but the association between these islets and DM was first noticed in 1889 when Von Mering and Minkowski induced DM by pancreatimizing dogs. After approximately 35 years, a break-through in science was made by Banting and Best in collaboration with Macleod and Collip when they were able to treat diabetic dogs by administering pancreatic extract which when purified led to the discovery of insulin (Pratt, 1989). With the advances in technology, many discoveries regarding insulin structure, gene sequence, and diabetes have been made. Introducing insulin as a potential treatment of DM in the late 1920 saved patients lives. Shortly afterward, the therapy of diabetes was further advanced with the introduction of sulphonylurea class of drugs to treat DM especially type 2 DM. To date, many other treatments have been introduced for a complete cure and management of diabetes.

1.2 Structure of the pancreas

The adult pancreas consists of two parts: exocrine tissue which comprises the majority (98-99%) of the pancreas and involves in carbohydrate digestion and enzyme secretion and islets of Langerhans which make up only 1-2% of the total volume of the pancreas and form part of the endocrine system. Islets of Langerhans are composed of at least 5 different types of cells. The size of an islet ranges from 100-500μM and each islet has 1000-3000 cells. In rodent islets, β-cells, which comprise at least 60-80% of islet volume, are located in the center of the islet and secrete mainly insulin. Glucagon and somatostatin-secreting cells are called α and δ-cells, respectively. Both types of cells are localized in the mantle of the islet and comprise 10-20% of total cell number. The last two cell types are γ and ε-cells. They comprise collectively 1-2% of cell volume. γ-Cells secrete pancreatic polypeptide but the exact function of this peptide is unknown (Goodman, 2003, Pipeleers *et al.*, 1992). Recently, ε-cells have been identified and they secrete ghrelin. Ghrelin may be involved in the regulation of insulin release and action. However, the physiological role of ghrelin on glucose homeostasis needs to be fully elucidated (Tritos and Kokkotou, 2006). In human islets, however; the composition and architecture of the islets are different than that of the rodent ones. β-Cells are less abundant (48-59%) while α-cells can reach 33-46%. The number of other cells is similar to that seen in rodent islets. The distribution of these cells follows random patterns with the majority of β-cells are in contact with non-β-cells (In't Veld and Marichal, 2010). The pancreatic islets are highly vascularized receiving approximately 10-20% of cardiac output through pancreatic afferent arterioles. This to ensure a rapid sensing of blood glucose and thus allows for appropriate

secretory responses and tight regulation of glucose homeostasis (Ballian and Brunicardi, 2007). Cells within islets communicate with each other either through gap junctions as seen in β-β cells communication or by releasing hormones locally (autocrine and paracrine regulation).

1.3 Insulin gene and structure

The insulin gene sequence is highly conserved among higher vertebrates (Table 1.1) (Harris *et al.*, 1956, Nicol and Smith, 1960). In these species, except rodents, insulin is encoded by a single gene (3 exons and 2 introns) and located at short arm of chromosome 11. In rat and mouse, insulin is encoded by two genes, insulin I where intron 1 is absent, and insulin II. While the rat insulin I and II are colocalized on chromosome 1, the mouse insulin I and II are located on two different chromosomes. Mouse insulin I is on chromosome 19 and mouse insulin II is on chromosome 7. In the presence of an appropriate stimulus, the insulin gene is transcribed to preproinsulin (Clark and docherty, 1992). The factors associated with the regulation of the transcription of the insulin gene are not completely understood but some transcription and growth factors have been implicated in the regulation. The transcription to preproinsulin is largely regulated by a highly conserved region approximately 36 bp upstream of the initiation start of transcription called the insulin promoter. This region is a target of many transcription factors including pancreatic/duodenal homeobox 1 (Pdx-1), MafA/L-Maf and beta2/NeuroD (B2) (Andrali *et al.*, 2008, Poitout *et al.*, 2006). These factors are also involved in normal pancreatic development because their total deletions result in pancreatic agenesis (Babu *et al.*, 2007). Although these factors have shown

to modulate the rate of insulin transcription and stability of insulin mRNA, the mechanisms underlying these actions are yet to be determined.

Species	A chain position			B chain position
	8	9	10	30
Human	Thr	Ser	Ile	Thr
Pig	Thr	Ser	Ile	Ala
Cattle, Goat	Ala	Ser	Val	Ala
Sheep	Ala	Gly	Val	Ala
Horse	Thr	Gly	Ile	Ala
Whale	Ala	Ser	Thr	Ala

Table 1.1: Insulin amino acids sequence of some species (Harris et al., 1956; Nicol and Smith, 1960)

1.4 Insulin synthesis

Insulin is 5.8 KDa protein consisting of two polypeptides, chain A and chain B, which are connected by two disulphide bonds at (A7-B7) and (A20-B-19) with one intra bond within A chain at (A6-11) (Goodman, 2003). The structure of insulin is shown in Figure 1.1. Insulin is produced by sequential proteolytic cleavage of its two precursors: preproinsulin and proinsulin. Preproinsulin is 11.5 KDa and has at its N-terminal a 24 aa signal peptide followed by B-chain of 30 aa, an Arg-Arg sequence, C-peptide of 31 aa, a lys-Arg sequence and finally A-chain of 21 aa. The major function of the signal peptide is to translocate preproinsulin to endoplasmic reticulum (ER). In ER, the signal peptide is cleaved by signal peptidase. Proinsulin is formed by the removal of the signal peptide and the appearance of disulphide bridges. Once proinsulin is formed, it is transported to Golgi apparatus and packed in Clatherin-rich vesicles which bud from the trans cisternae of Golgi. During maturation, the pH of the vesicle lumen becomes acidic triggering the activation of

endopeptidases which are involved in the final cleavage of proinsulin to insulin (Bailey *et al.*, 1992, Dodson and Steiner, 1998). Proinsulin conversion to insulin is triggered by the removal of C-peptide by the actions of two Ca^{2+}-dependent endopeptidases (PC 1/3 and PC 2). PC 1/3 and PC 2 cleave C-peptide at Arg 31-32 (B-C junction) and lys64-Arg 65 (C-A junction), respectively, generating insulin with flanking dibasic residues that are removed by zinc-dependent carboxypeptidase H (Smeekens *et al.*, 1992). In the presence of zinc, insulin forms hexamers and presents with equimolar concentration with C-peptide. Until recently, C-peptide had no known function and was used only as a marker for insulin release but accumulating evidence has showed that C-peptide is involved in enhancing glucose disposal and improving some of diabetes complications such as neuropathy and nephropathy in type 1 diabetes mellitus animal models and patients (Hills and Brunskill, 2008, Hills and Brunskill, 2009). In response to appropriate stimuli, insulin and C-peptide are released by exocytosis along with residual proinsulin, intermediate peptides and peptidases. Insulin is secreted into islet extracellular space before being drained into efferent arterioles and the portal vein. Insulin is rapidly cleared from the circulation by a specific enzyme called insulinase, which can be found in liver (major degradation site), kidney, muscle and other tissues, and hence its short half-life (4-5 minutes) (Dodson and Steiner, 1998, Bailey *et al.*, 1992).

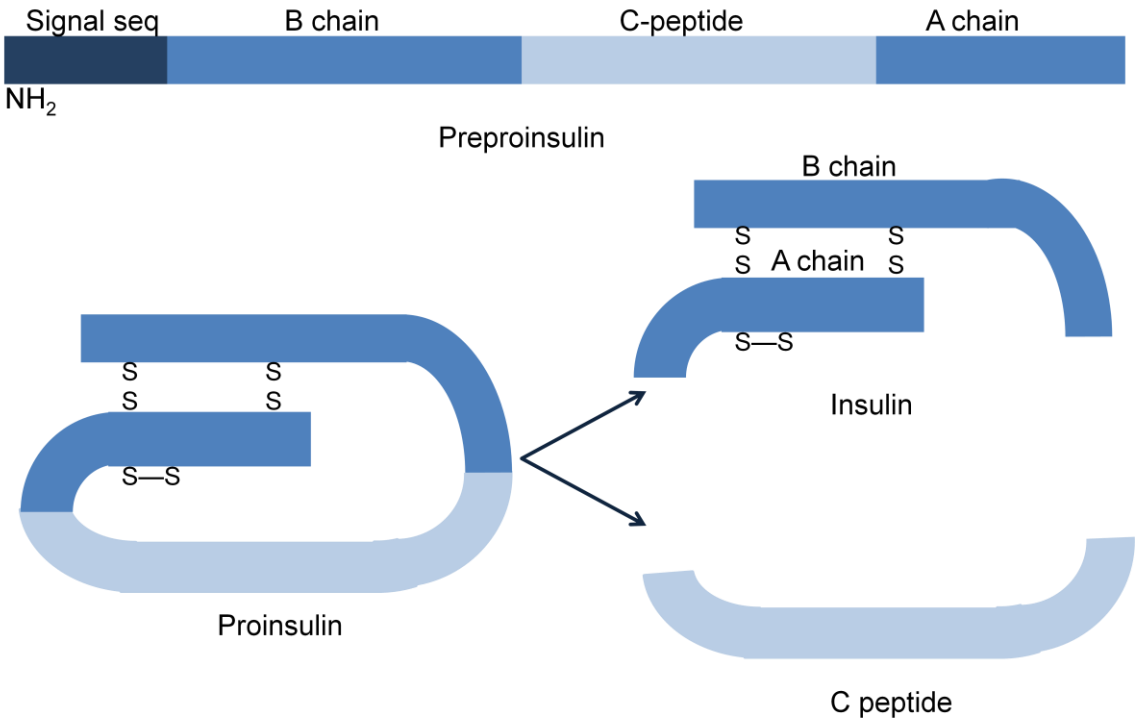

Figure 1.1: The posttranslational process of preproinsulin. Insulin is produced from its two precursors: preproinsulin and proinsulin. Preproinsulin is 11.5 KDa and has at its N-terminal a 24 aa signal peptide followed by B-chain of 30 aa, an Arg-Arg sequence, C-peptide of 31 aa, a lys-Arg sequence and finally A-chain of 21 aa. Proinsulin is formed by the removal of the signal peptide and the formation of disulphide bridges. Insulin is 5.8 KDa protein consisting of two chains of polypeptides, chain A and chain B which are connected by two disulphide bonds at (A7-B7) and (A20-B-19) with one intra bond within A chain at (A6-11) (Goodman, 2003).

1.5 Insulin actions

Insulin plays a very important role in maintaining energy homeostasis. It primarily affects carbohydrate, protein, and lipid metabolism in insulin-sensitive tissues such as liver, muscle and adipose tissue. Insulin stimulates glucose uptake into fat and muscle tissues via glucose transporter 4 (GLUT4) and promotes the storage of glucose and fatty acids as glycogen and triglycerides in muscle and adipose tissues. Furthermore, insulin enhances glycogen synthesis by enhancing glycogen synthase activity and suppresses the release and production of glucose from the liver via inhibiting glycogenolysis and gluconeogenesis (Newsholme *et al.*, 1992, Rang *et al.*, 2003). The physiological actions of insulin are summarized in Table 1.2. Insulin also promotes cell growth, differentiation and survival as part of its mitogenic activities.

Recently, insulin has been implicated in maintaining the function of various organs of the body including the CNS, heart and kidney (Bertrand *et al.*, 2008, Champe *et al.*, 2005, Plum *et al.*, 2006). For example in CNS, insulin regulates energy expenditure, peripheral glucose utilization, memory formation and information processing (Porte *et al.*, 2005, Plum *et al.*, 2006).

Type of metabolism	Liver cells	Fat cells	Muscle cells
Carbohydrate metabolism	↓ gluconeogenesis ↓ glycogenolysis ↑ glycolysis ↑ glycogenesis	↑ glucose uptake	↑ glucose uptake ↑ glycolysis ↑ glycogenosis
Fat metabolism	↑ lipogenesis ↓ lipolysis	↑ fatty acid synthesis ↓ lipolysis	-
Protein metabolism	↓ protein breakdown	-	↑ amino acid uptake ↑ protein synthesis

Table 1.2: The major metabolic effects of insulin (Rang et al., 2003).

1.6 Mechanism of insulin secretion

Insulin secretion is primarily regulated by nutrient secretagogues such as glucose, free fatty acids and some amino acids. However, it can be largely modified by non-nutrient secretagogues. The nutrient-induced pattern of insulin secretion consists of two phases. The peak of the first phase occurs within 2-5 minutes of glucose ingestion and lasts for approximately 10 minutes. This phase involves the release of readily releasable pool of secretory granules through the action of K_{ATP} channel-dependent pathway, also known as triggering pathway, in pancreatic β-cells. On the other hand, the second phase of insulin release starts shortly after glucose administration and is maintained for as long as the glucose level is elevated. This phase is associated with the translocation of secretory granules from reserve pools

to the readily releasable pool. Many of these granules contain newly synthesized insulin. This phase involves the action of K_{ATP} channel-independent pathway, also known as amplifying pathway (Henquin *et al.*, 2002, Gilon *et al.*, 2002, Bratanova-Tochkova *et al.*, 2002).

1.6.1 Nutrient metabolism by β-cells

Glucose is the major nutrient to stimulate insulin release and glucose metabolism within β-cells play a key role in initiating insulin secretion. Glucose enters β-cells by facilitated diffusion through specific glucose transporter, GLUT2 in rodents and GLUT1, 2 and 3 in human (Bailey *et al.*, 1992, MacDonald *et al.*, 2005). Once glucose enters the cells, it is converted to glucose-6-phosphate then to pyruvate by the process of glycolysis in nine enzymatic step reactions. Glucose phosphorylation in β-cells is governed by high affinity hexokinase (Km ~ 0.1 mM) and low affinity glucokinase (Km ~ 10 mM). Hexokinase (type 1) is fully saturated and therefore fully activated at all physiological glucose concentration, so it does not play an important role in glucose metabolism. Unlike hexokinases, glucokinase (formally known as hexokinase type 4) is highly specific and fully activated only at physiological concentrations of glucose (5-10mM) and thus represents the main glucose-sensing component and the rate-limiting step in glycolysis. Although ATP is generated at this point, the majority of energy is produced in the mitochondria by pyruvate oxidation. Pyruvate is converted to acetyl-CoA which is then oxidized to CoA by the citric acid cycle. The pyridine nucleotides, mainly NADH produced from citric acid cycle, are oxidized to ATP by the electron transport chain coupled to oxidative phosphorylation (Bailey *et al.*, 1992, MacDonald *et al.*, 2005). In addition to glucose, free fatty acids (FFAs) and some amino acids (aa) mainly arginine and

leucine, also stimulate insulin secretion. FFAs are generated as acetyl-CoA derivatives which in the mitochondria are converted to acetyl-CoA and normal citric acid cycle and oxidative phosphorylation ensue. On the other hand, amino acids undergo transamination to 2-keto acid which enters citric acid cycle to provide either precursors or intermediates for oxidation and generation of ATP (Bailey *et al.*, 1992, Van Schaftingen and Schuit, 1999).

1.6.2 β-Cell electrical activity

β-Cells are highly electrically excitable cells and an important feature of these cells is that their electrical activity is linked to the metabolic status of the cells. Electrophysiological measurements have specified that the resting membrane potential of β-cells is about $^{-}$70mV. At basal physiological glucose concentration (5mM), the resting membrane potential is predominantly dominated by K^+ efflux through the activity of K_{ATP}-channels and Na^+/K^+-ATPase. Increasing glucose concentration causes gradual depolarization to more positive potential ($^{-}$60-$^{-}$50mV). When glucose levels (~ 7mM) exceed the threshold potential, rapid depolarization occurs reaching a plateau potential of $^{-}$40-$^{-}$30mV. The plateau potential is characterized by an increase Ca^{2+} conductance mainly though voltage gated Ca^{2+} channels (VGCC). Repolarization of β-cells to resting potential is achieved by promoting K^+ efflux though voltage-gated K^+ channels and decreasing Ca^{2+} influx by two major ways: accelerating the uptake of Ca^{2+} into ER through the action of Ca^{2+}- pumps and increasing Ca^{2+} efflux in exchange for Na^+ or K^+ by the activity of Na^+/Ca^{2+} exchanger and Ca^{2+}-K^+ channels, respectively. The action potential of β-cells is characterized by two major aspects. First, once β-cells repolarize, they undergo a gradual depolarization forming recurrent cycles of depolarization and

repolarization which are better known as slow waves or bursts. Second, the plateau potential which is maintained by Ca^{2+} influx though VGCC superimpose the recurrent depolarization spikes that occur at $^{-}20$ to $^{-}10$mV (Ashcroft and Rorsman, 1989, Ashcroft and Ashcroft, 1992, Palti *et al.*, 1996).

1.6.3 Role of K_{ATP}-channels in insulin secretion

Glucose entry and metabolism within β-cells increase ATP concentration and ATP/ADP ratio. Changes in ATP/ADP ratio closes K_{ATP}-channels and causes depolarization of β-cell membranes. K_{ATP}-channels were firstly identified by Cook and Hales in 1984 (Cook and Hales, 1984). The functional K_{ATP}-channels consist of octamer of two different subunits, sulphonylurea receptor (SUR) and inward-rectifying K^+ channel (K_{IR}). SUR is a member of ATP-binding cassette (ABC) superfamily. It is encoded by two genes SUR1 and SUR2. SUR1 is mainly expressed in β-cells and brain while SUR2, which is further spliced to SUR2A and SUR2B, is found in cardiac, skeletal and vascular smooth muscle. The SUR1 represents the major site of action of sulphonylurea (SU) drugs. K_{IR} has two splice variant (6.1 and 6.2). In β-cells, $K_{IR\ 6.2}$ forms the ion transport pore (Miki *et al.*, 1999). Depolarization of β-cells following K_{ATP}-channels closure activates opening of VGCC and Ca^{2+} influx leading to insulin exocytosis and release. This pathway is known as the K_{ATP} channel-dependent pathway.

1.6.4 Role of intracellular Ca^{2+} in insulin secretion

Ca^{2+} is a key element in stimulus-secretion coupling in β-cells. The importance of Ca^{2+} stems from the fact that 1) removal of extracellular Ca^{2+} or blocking of Ca^{2+} channels abolishes glucose-induced insulin secretion; 2) increasing Ca^{2+}

concentration in the incubation medium of permeabilized islet cells is sufficient to induce exocytosis of insulin and 3) simultaneous measurement of intracellular Ca^{2+} concentration ($[Ca^{2+}]_i$) and insulin release shows spatial correlation. The basal $[Ca^{2+}]_i$ is about 50-100nM which increases to 10μM following metabolic activation of β-cells, opening of VGCC and entry of Ca^{2+} down its concentration gradient. Opening of VGCC is intermittent causing $[Ca^{2+}]_i$ oscillations and pulsatile insulin secretion (Ashcroft and Ashcroft, 1992). Five types of VGCC have been identified so far (L, T, R, N and P/Q) (Islam, 2010). The L-type VGCC is the major channel responsible for Ca^{2+} entry in both human and rodent while the P/Q-type VGCC is also involved in Ca^{2+}-induced exocytosis in human (Braun *et al.*, 2008). Ca^{2+} itself acts as a second messenger. Increasing $[Ca^{2+}]_i$ causes further Ca^{2+} release from ER and activation of protein kinases and lipases which largely modulate insulin secretion (Howell *et al.*, 1994).

1.6.5 Role of protein phosphorylation and insulin secretion

The modification of the availability and concentration of intracellular β-cell second messengers such as Ca^{2+}, cyclic nucleotide and products of phospholipids hydrolysis by nutrients and non-nutrients secretagogues can induce insulin secretion (Howell *et al.*, 1994). These mediators are involved in the activation of several intracellular transduction cascades such as Ca^{2+}-calmodulin-dependent kinases (CaMKs) (Figure 1.2), protein kinase C (PKC) (Figure 1.2), mitogen activated protein kinases (MAPKs) (Figure 1.2), protein kinase A (PKA) (Figure 1.3) and arachidonic acid (AA) (Figure 1.4) (Jones *et al.*, 1999).

1.6.5.1 Ca^{2+}-Calmodulin dependent kinases (CaMKs)

Ca^{2+}-calmodulin dependent kinases (CaMKs) are a 550 KDa protein composed of 8-10 subunits. Each subunit has regulatory and catalytic components. They are activated by Ca^{2+} in the presence of Ca^{2+}-binding protein (calmodulin) and represent a family of three types of kinases; myosin-light chain kinase (MLCK), CaMK II and CaMK III (Jones and Persaud, 1998). Accumulating evidence has indicated that CaMK II in particular has a role in initiating and potentiating insulin secretion (Figure 1.2). Increased CaMK II activity and phosphorylation of endogenous substrates correlate well with increased cytosolic Ca^{2+} and insulin secretion following β-cell exposure to either nutrient or non-nutrient secretagogues. Although the endogenous substrates of CaMK II involved in CaMK II-stimulated insulin secretion are not fully elucidated, CaMK II may trigger exocytosis by phosphorylating granule-associated synapsin protein (Easom, 1999, Tabuchi, 2000).

1.6.5.2 Protein kinase C

Protein kinase C (PKC) is found in all cell types and is widely involved in cell signaling. It is classified into three major classes according to their sensitivity to Ca^{2+} and diacylglycerol (DAG): 1) typical PKC (α, β, γ) are Ca^{2+} and DAG dependent, 2) novel PKC (δ, ε, η, θ) are Ca^{2+}-independent but DAG dependent and 3) atypical PKC (ζ, ι/λ, μ) are Ca^{2+} and DAG-independent (Zhang *et al.*, 2004). The expression profiling of PKC isoforms in β-cells has generated conflicting data. However, PKCα, βII, δ, ε, ζ, λ/ι and μ have been reported to be present in β-cell lines (Jones and Persaud, 1998). Under basal conditions, the typical isoforms of PKC are confined to the cytosol but following activation by either cytosolic Ca^{2+} or DAG levels or both,

PKC isoforms are translocated into the plasma membrane or membrane-associated organelles (Knutson and Hoenig, 1994). DAG is generated from the breakdown of phosphatidylinositol bis phosphate (PIP_2) by the action of phospholipase C_β (PLC_β) enzyme. Another by-product of PIP_2 is phosphatidylinositol tri-phosphate (IP3) which binds to IP3 receptors on ER causing Ca^{2+} release from intracellular stores which further increases cytosolic Ca^{2+} (Zawalich and Zawalich, 1996). The contribution of PKC in overall secretory response to either nutrients or non-nutrients is well established; however, the exact nature of which PKC isoform is involved is still debatable. Activation of PKC augments insulin secretion and the downstream effectors may include ion channels and secretory granules (Figure 1.2) (Jones and Persaud, 1998).

1.6.5.3 Mitogen-activated protein kinases (MAPKs)

MAPKs are ubiquitous enzymes and are activated by dual phosphorylation on threonine and tyrosine residues. As the name implies, they are mainly involved in mitogenesis and proliferation of cells; however, a non-mitogenic short term effect on insulin secretion has been reported. MAPKs are superfamily of kinases divided into 1) p42/44 MAPK or ERK, 2) p38 MAPK and 3) stress-activated protein kinase (SAP kinase) (Jones and Persaud, 1998). They are activated by a series of upstream kinases including Ras, Raf and MAPK kinase. MAPKs especially ERK play a permissive role in glucose-induced insulin secretion by phosphorylating certain proteins involved in exocytosis machinery (Figure 1.2) (Longuet *et al.*, 2005).

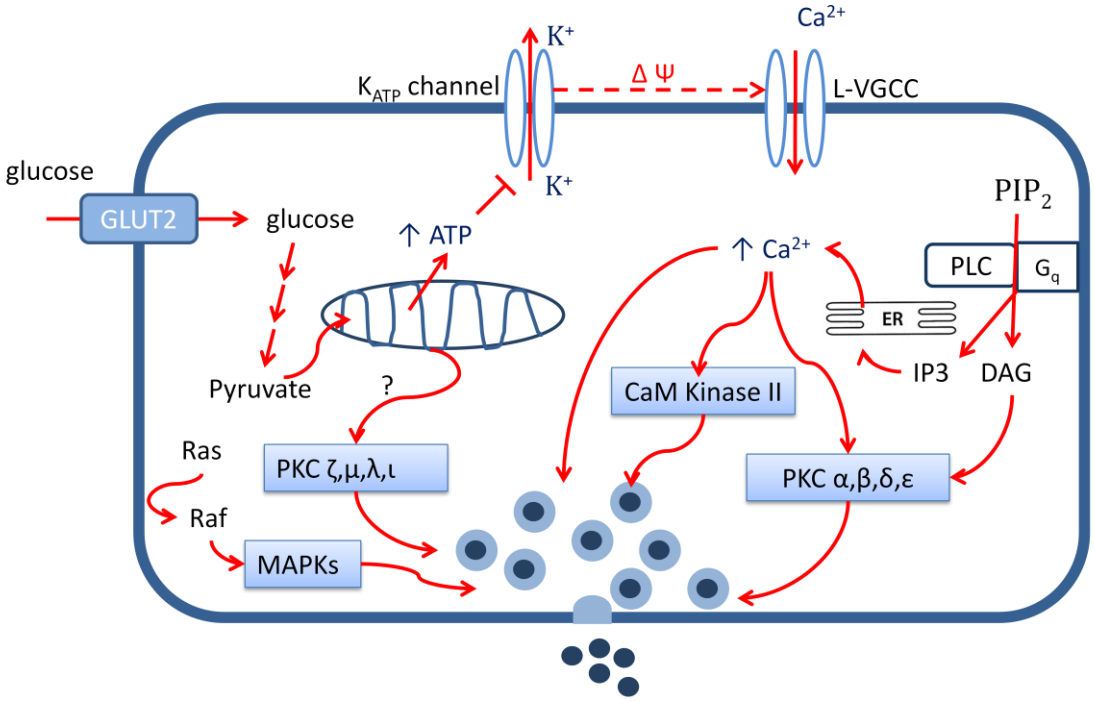

Figure 1.2: Role of protein kinases in insulin secretion. Entry of glucose through GLUT2 initiates its metabolism to pyruvate. Pyruvate enters the mitochondria and triggers oxidative phosphorylation. Increases in ATP concentration and ATP/ADP ratio block K_{ATP}-channels leading to depolarization and opening of L-voltage gated Ca^{2+} channels (VGCC). Elevations in intracellular Ca^{2+} concentration $[Ca^{2+}]_i$ initiate insulin exocytosis. Insulin secretion is largely augmented by the activation of protein kinases. Ca^{2+}/Calmodulin kinase II (CaM kinase II) is activated by increasing $[Ca^{2+}]_i$ and may trigger insulin release by acting at the late-stage of exocytosis. Phosphatidylinositol bis phosphate hydrolysis by phospholipase C (PLC_β) following activation of receptor operated agonist librates DAG and IP3. DAG acts directly to activate protein kinase C (PKC) while IP3 activates PKC indirectly by releasing Ca^{2+} from intracellular stores. Atypical PKC may also get activated upon glucose stimulation. PKC then potentiates glucose-induced insulin secretion. Activation of mitogen activated protein kinases (MAPKs) by a series of upstream kinases (Ras and Raf) can also be involved in glucose-induced insulin secretion.

1.6.6 Role of cyclic adenylate monophosphate (cAMP) in insulin secretion

cAMP is an important physiological regulator of β-cell function. It is generated from ATP by the action of adenylate cyclase (AC). To date, nine isoforms of AC have been identified (AC1-AC9), with type 2 and 3-7 being expressed in rat islets (Leech *et al.*, 1999). AC isoforms differ in their regulation by α and βγ subunit of GTP-binding protein, Ca^{2+}/calmodulin and protein kinases (Table 1.3) (Leech *et al.*, 1999, Simonds, 1999, Tian and Laychock, 2001). Elevation of cAMP following glucose or receptor operated agonists augments glucose-stimulated insulin secretion at several sites in the secretory pathways though protein kinase A (PKA)-dependent and independent signaling (Figure 1.3) (Ammala *et al.*, 1993, Christie and Ashcroft,

1984, Dachicourt *et al.*, 1996, Thams *et al.*, 2005). PKA is a serine/threonine kinase which has two regulatory and two catalytic domains. Two cAMP molecules are required to bind to each regulatory domain to release the catalytic activities of PKA. The targets of PKA include ion channels, enzymes and exocytosis machinery (Jones and Persaud, 1998). Apart from PKA-dependent actions of cAMP, PKA-independent activities though Epac molecules also contribute to the cAMP-induced insulin secretion. Epac (exchange proteins activated by cAMP) mediates the PKA-independent actions of cAMP (Shibasaki *et al.*, 2004). In mammals, two variants have been identified, Epac 1 and Epac 2, with the latter being the predominant isoform in pancreatic β-cells (Leech *et al.*, 2000). cAMP-activated Epac 2 enhances insulin secretion through 1) inhibition of K_{ATP}-channels leading to depolarization of β-cells, 2) activation and phosphorylation of IP3 receptors causing acceleration of Ca^{2+}-induced Ca^{2+} release, 3) stimulation of novel PLC (PLCε) triggering phospholipids hydrolysis and formation of DAG and IP3 and 4) activation of small GTPase proteins from Ras family (Rab 1 and Rab 2) resulting in exocytosis of insulin (Eliasson, 2003, Furman *et al.*, 2010, Hinke, 2009, Kang *et al.*, 2006, Kang *et al.*, 2008). In addition to the acute effects of cAMP on insulin secretion, cAMP also chronically promotes β-cell proliferation and survival mostly through activation of MAPKs (mainly ERK) and transcription factors such as cAMP-response element binding proteins (CREB) and cAMP-response element modulators (CREM) (Costes *et al.*, 2006, Rabinovitch *et al.*, 1980).

AC type	G_s	G_i	$G_{\beta\gamma}$	FSK	Ca^{2+}	PKC	CaM	PKA
AC 1	+	—	—	+			+	
AC 2	+	—	+	+		+		
AC 3	+	—		+			+	
AC 4	+		+	+				
AC 5	+	—		+	—	+		—
AC 6	+	—		+	—			—
AC 7	+		+	+		+		
AC 8	+		—	+			+	
AC 9	+			+				

Table 1.3: The regulation of adenylate cyclase (AC) subtypes by a number of agents listed in the table. There are at least 9 isoforms of AC identified to date. They all differ in their regulation by G protein subunits, foskolin (FSK), Ca^{2+}, protein kinase C (PKC), Ca^{2+}-calmodulin kinase (CaM) and protein kinase A (PKA). Positively regulated: +, negatively regulated: — (Leech *et al.*, 1999; Simonds 1999)

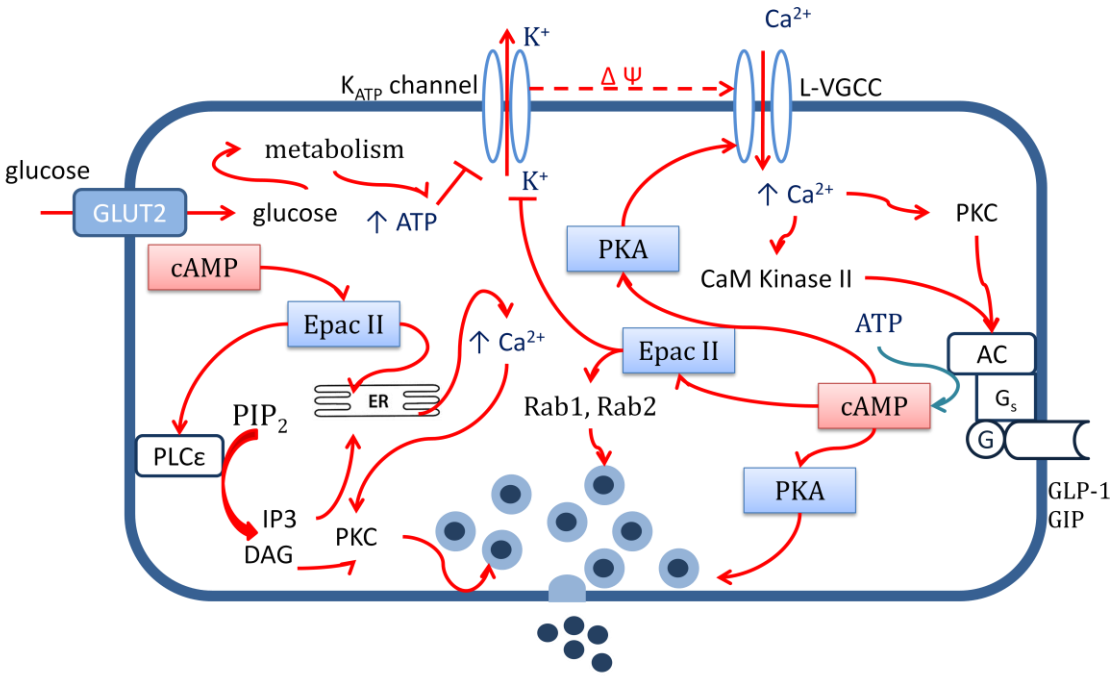

Figure 1.3: Role of cyclic adenosine monophosphate (cAMP) in insulin secretion. Entry of glucose through GLUT2 initiates its metabolism and causes increases in ATP concentration and ATP/ADP ratio. This step blocks K_{ATP}-channels which leads to membrane depolarization and opening of L-voltage gated Ca^{2+} channels (VGCC). Elevations in intracellular Ca^{2+} concentration $[Ca^{2+}]_i$ activate protein kinases. Activation of adenylate cyclase (AC) by protein kinases or G-protein coupled receptors increases intracellular cAMP concentration ($[cAMP]_i$). cAMP increases glucose-induced insulin secretion by either protein kinase A (PKA)-dependent or independent pathways. PKA-dependent signaling pathways involve ion channels and storage vesicles. PKA-independent pathway involves activation of Epac II. The downstreams of Epac II signaling involves K_{ATP}-channels, GTPases (Rab1 and Rab2), intracellular Ca^{2+} stores and PLCε.

1.6.7 Role of Arachidonic acid in insulin secretion

Arachidonic acid (AA) is a product of phospholipid hydrolysis and is generated by the action of phospholipase A_2 (PLA_2) and DAG lipase on phosphatidylcholine and DAG, respectively. The majority of AA is produced through PLA_2 pathway. There are at least three different types of PLA_2 expressed in islets: 1) cytosolic PLA_2 (type IV), Ca^{2+}-independent PLA_2 (type VI) and secretory PLA_2 (type I and II) (Persaud *et al.*, 2007). In addition to Ca^{2+}, AA may also act as a second messenger and thus regulates insulin secretion in response to nutrient or non-nutrient secretagogues. AA may increase insulin secretion by a combination of the following mechanisms (Figure 1.4): 1) increasing Ca^{2+} influx through VGCC, 2) mobilization of Ca^{2+} from intracellular stores and 3) activation of protein kinases, 4) facilitating secretory granules fusion and exocytosis (Jones and Persaud, 1993).

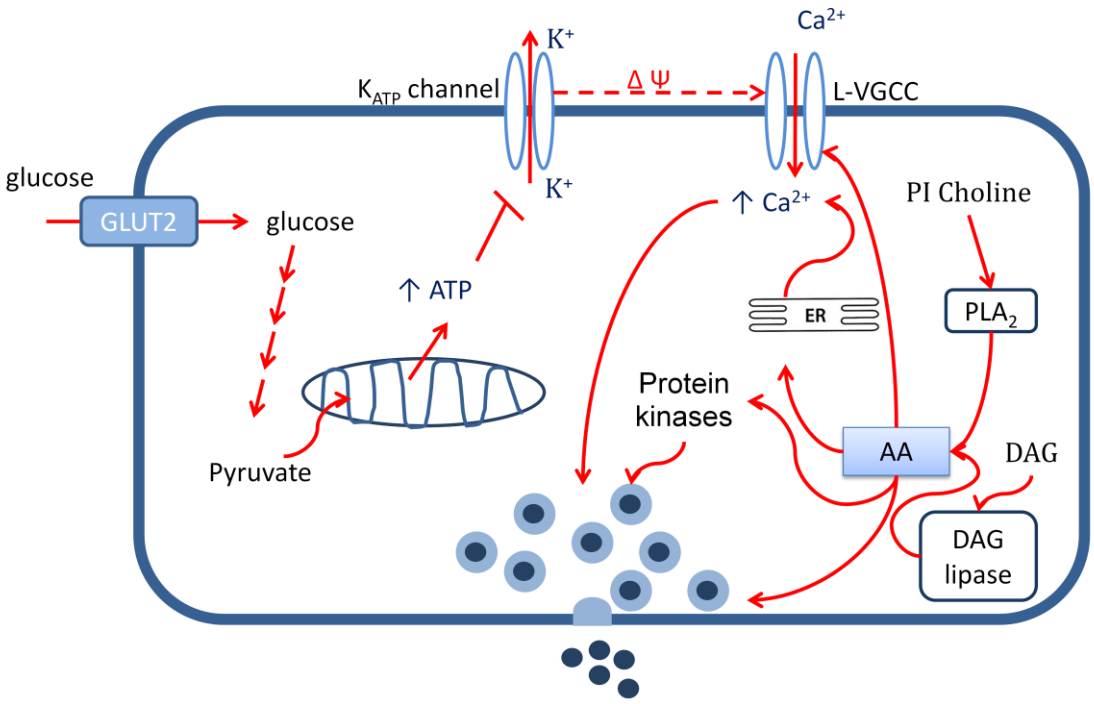

Figure 1.4: Role of arachidonic acid (AA) in insulin secretion. Entry of glucose through GLUT2 initiates its metabolism to pyruvate. Pyruvate enters the mitochondria and triggers oxidative phosphorylation. Increases in ATP concentration and ATP/ADP ratio block K_{ATP}-channels leading to depolarization and opening of L-voltage gated Ca^{2+} channels (VGCC). Elevations in intracellular Ca^{2+} concentration $[Ca^{2+}]_i$ initiate insulin exocytosis. Insulin secretion is largely augmented by the activation of AA. Phosphotidyl choline is hydrolyzed by PLA_2 to AA. AA is also liberated from DAG by the action of DAG lipase. AA increases insulin secretion by 1) opening L-type VGCC, 2) releasing Ca^{2+} from intracellular stores, 3) activating of protein kinases and 4) fusing insulin vesicles to the membrane.

1.6.8 Mechanism of exocytosis

Exocytosis is the end-stage of insulin secretion. The process of exocytosis includes docking, priming and fusion of secretory vesicles to the plasma membrane to release insulin molecules (Regazzi, 1999). Increasing glucose concentrations are associated with increased $[Ca^{2+}]_i$ and exocytosis of insulin granules. Each β-cell has 10,000-13,000 insulin-containing granules and each secretory granule contains approximately 10^6 molecules of insulin in addition to other polypeptides, low molecular weight molecules such as ATP, GABA, 5-HT and glutamate and high amounts of metal ions such as Zn^+ and Ca^{2+} (Eliasson *et al.*, 2008). The factors regulating exocytosis of secretory vesicles are not completely understood but may involve β-cell cytoskeleton, small GTPases and SNARE proteins (Wang and

Thurmond, 2009). These three elements interact to provide optimal responses to stimulus-induced insulin secretion. β-cells have dense web of actin filaments and microtubules. Glucose, for example, induces actin reorganization and microtubules remodeling allowing granules movement and mobilization. Granule docking is also enhanced by the action of small GTPases such as Rho, Rab and Ras families. However, the regulation of these GTPases is still unclear. Once the granules are docked by the action of cytoskeleton and small GTPases, the fusion of secretory vesicles to plasma membrane is facilitated by the interaction of vesicle-associated membrane protein (VAMP) or v-SNARE and plasma membrane-associated protein (SNAP-25 and syntaxin) or t-SNARE. This interaction allows the formation of the SNARE core complex and thus fusion pores are formed to release the content of the granules. The pores are of different sizes allowing differential release of the granule content (Eliasson *et al.*, 2008, Kasai *et al.*, 2010, Regazzi, 1999, Wang and Thurmond, 2009).

1.6.9 Regulation of insulin secretion

Insulin secretion is tightly regulated by complex of autocrine/paracrine, neurocrine and endocrine factors. These factors either potentiate or inhibit glucose-induced insulin secretion (Ahren, 1999). Table 1.4 and Figure 1.5 summarize the major modulators with their possible mechanism of actions on insulin secretion.

1.6.9.1 Autocrine/paracrine regulation

Autocrine regulation of insulin secretion involves insulin itself and polypeptides co-released with insulin. The released insulin provides a negative feedback mechanism and inhibits further insulin release (Persaud et al., 2002). Islet amyloid polypeptide (IAPP) and chromogranin A peptides are co-released with insulin from β-cells and

considered to be inhibitors of insulin secretion. Although the mechanism of action of these polypeptides is not fully elucidated, they may facilitate the opening of K_{ATP}-channels and the inactivation of VGCC (Ahren, 1999). In addition to autocrine regulation, paracrine modulation from neighbouring cells has been documented. Glucagon stimulates while somatostatin inhibits insulin release through activation of G-protein coupled receptor linked to either Gαs (glucagon) or Gαi (somatostatin) to increase or decrease cAMP levels, respectively (Porte *et al.*, 1976).

1.6.9.2 Neuronal regulation

Insulin secretion is largely modulated by neurotransmitters as islets are highly innervated by sympathetic, parasympathetic and sensory nerves (Ahren, 2000). Three major neurotransmitters are localized in the sympathetic nerves and are released upon activation. They are noradrenaline (NA), galanin and neuropeptide Y (NPY). In general, activation of sympathetic nerves inhibits glucose-induced insulin secretion. However, the action of noradrenaline on insulin release is species dependent. Insulin release is either inhibited (in rodent) or stimulated (in human) by noradrenaline acting on α_2 or β_2 adrenoceptors, respectively. Parasympathetic nerves release mainly four mediators upon the activation of the vagus nerve. They are acetylcholine (Ach), gastrin releasing peptide (GRP), vasoactive intestinal polypeptide (VIP) and pituitary adenylate cyclase-activating polypeptide (PACAP). Unlike the sympathetic nervous system, parasympathetic activation augments insulin secretion induced by glucose. The insulinotropic actions of these neurotransmitters are mediated by G-protein coupled receptors linked to either activation of phospholipid hydrolysis though PLC (Ach and GRP) and PLD (GRP) and elevation of cAMP levels (VIP and PACAP). Sensory neurons also secrete

neurotransmitters involved in insulin release modulation. Calcitonin gene-related polypeptide from sensory nerves has inhibitory action on insulin secretion through reduction of cAMP levels. Nerve fibers other than sympathetic, parasympathetic and sensory nerves have also been involved in islet function. The stimulatory action of cholecystokinin (CCK) released from islet nerves is mediated through CCK-A receptor linked to PLC and PLA_2 activation (Ahren, 1999, Ahren, 2000, Porte *et al.*, 1976).

1.6.9.3 Endocrine regulation

Endocrine regulation of insulin secretion is mediated by incretin family of gut hormones. The incretin effect is based on the observations that insulin responses following oral glucose loads are markedly elevated over the IV-administered glucose with similar effect on blood glucose levels. Glucagon-like peptide-1 (GLP-1), gastric inhibitory polypeptide (GIP) and CCK are gut hormones secreted from L, K and T-cells, respectively, located in the duodenum and jejunum. The potent stimulation of insulin secretion induced by these hormones is mediated by increased cAMP levels (GLP-1 and GIP) or phospholipid hydrolysis (CCK) (Ahren, 1999, Granner, 2000).

Name	Abbreviation	Source	Effect on insulin secretion	Receptor involved	Mode of influence
Islet amyloid polypeptide	IAPP	β-cells	Inhibitory	CTR/RAMP	Autocrine
Chromogranin A peptides	CgA	β-cells	Inhibitory	CgAR	Autocrine
Glucagon	-	α-cells	Stimulatory	GR	Paracrine
Peptide Y	PYY	α-cells	Inhibitory	PYY	Paracrine
Somatostatin	-	δ-cells	Inhibitory	SSTR2	Paracrine
Calcitonin gene-related polypeptide	CGRP	δ-cells and sensory nerves	Inhibitory	CRLR/RAMP 1	Paracrine and neurocrine
Pancreatic polypeptide	PP	γ-cells	Inhibitory	PPR	Paracrine
Noradrenaline	NA	Sympathetic nerves	Inhibitory or stimulatory	α_2R β_2R	Neurocrine
Galanin	-	Sympathetic nerves	Inhibitory	GalR	Neurocrine
Neuropeptide Y	NPY	Sympathetic nerves	Inhibitory	Y1R	Neurocrine
Acetylcholine	Ach	Parasympathetic nerves	Stimulatory	m3R	Neurocrine
Gastrin releasing peptide	GRP	Parasympathetic nerves	Stimulatory	GRPR	Nuerocrine
Vasoactive intestinal peptide	VIP	Parasympathetic nerves	Stimulatory	VPAC$_2$R	Nuerocrine
Pituitary adenylate cyclase-activating polypeptide	PACAP	Parasympathetic nerves	Stimulatory	PACAP1R	Neurocrine
Cholecystokinin	CCK	Nerves and T-cells in the gut	Stimulatory	CCK-AR	Nuerocrine and endocrine
Glucagon-like peptide-1	GLP-1	L-cells in the gut	Stimulatory	GLP-1R	Endocrine
Gastrin inhibitory polypeptide	GIP	K-cells in the gut	Stimulatory	GIPR	Endocrine

Table 1.4: Potentiators and inhibitors of insulin secretion (Ahrén 1999; Ahrén 2000)

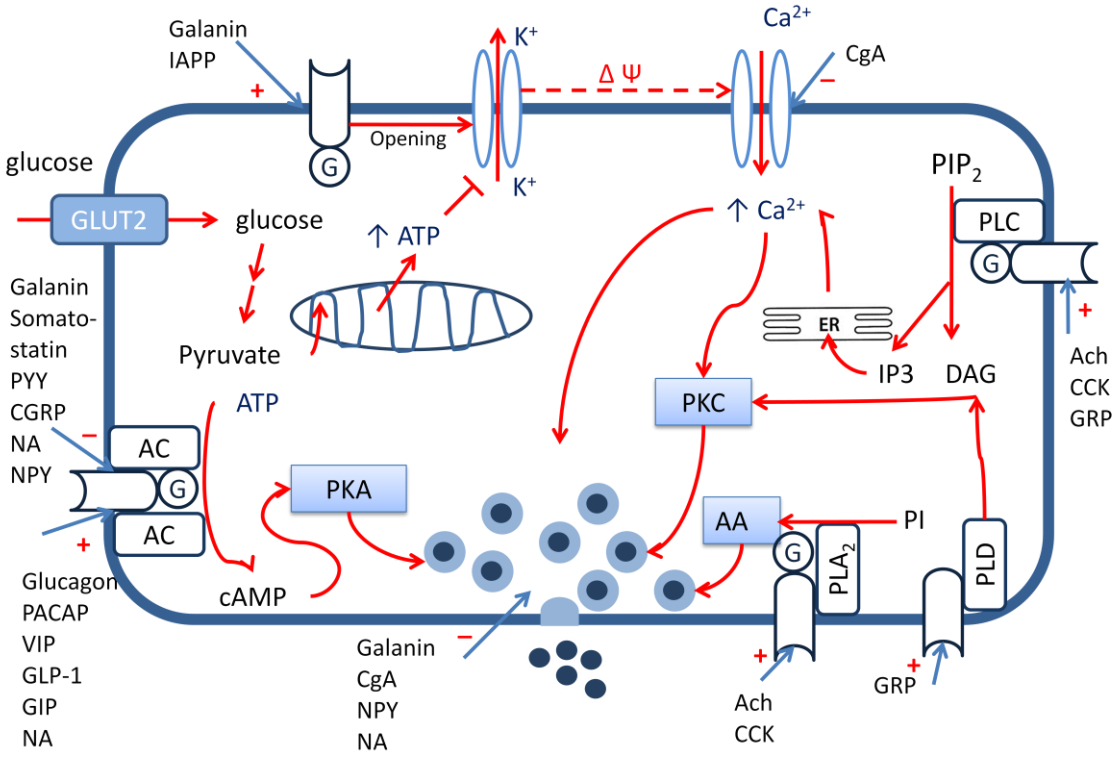

Figure 1.5: Regulation of insulin secretion by paracrine, neurocrine and endocrine mediators. These mediators modulate insulin secretion by the following mechanisms 1) Opening of K_{ATP}-channels (galanin and IAPP), 2) opening of VGCC (CgA), 3) activation of PLC (Ach, CCK and GRP), PLD (GRP) and PLA_2 (Ach and CCK) and 4) modifying cAMP levels by either decreasing (galanin, somatostatin, PYY, CGRP, NA and NPY) or increasing (glucagon, PACAP, GLP-1, GIP and NA) adenylate cyclase activity.

1.7 Diabetes mellitus

Diabetes mellitus (DM) is the fifth leading cause of death in the world (Roglic *et al.*, 2005). It is defined as a chronic metabolic disorder characterized by an elevated plasma glucose level due to either deficiency in insulin secretion or action or both (Williams and Pickup, 2004). The number of people with diabetes is increasing dramatically and it is estimated that by the year 2030, 440 million people will be affected by diabetes worldwide (Internaional Diabetes Federation, 2009). According to the World Health Organization (WHO), three clinical diagnostic criteria are recommended. These criteria are as follows: 1) symptoms of diabetes plus plasma glucose of 11.1 mmol/L or greater or 2) fasting plasma glucose of 7.0

mmol/L or greater or 3) plasma glucose of 11.1 mmol/L or greater at two hours following a 75-gram glucose load (World Health organization, 2006).

Diabetes is divided according to etiology, pathogenesis and treatment into two main types: type 1 diabetes mellitus and type 2 diabetes mellitus. Diabetes is a polygenic disease; however, monogenic diabetes can affect small percentage of people (Turner and Neil, 1992). Monogenic diabetes results from either dominant or recessive inheritance of mutation(s) in a single gene. The most well known forms of monogenic diabetes are neonatal diabetes and maturity onset diabetes of the young (MODY). Neonatal diabetes develops mainly from a mutation in K_{ATP}-channel subunit, $K_{IR\ 6.2}$ gene (KCNJ11), although recently other gene mutations have been identified (Nichols and Koster, 2002). On the other hand, the most common causes of MODY are mutations in either hepatic nuclear factor isoforms such as HNF-1α and HNF-4α or the metabolic enzyme glucokinase (Matschinsky *et al.*, 1993, Yamagata, 2003).

1.7.1 Type 1 diabetes mellitus

Type 1 diabetes mellitus (T1DM) results from an autoimmune destruction of insulin-producing cells leading to a massive reduction in β-cells and insulin deficiency. It occurs in 5-10% of all diabetic cases and usually affects children or adolescents (Gillespie, 2006). This disease is characterized by the presence of humoral (B-cells) and cellular (T-cells) responses against islet antigen (Ag). Thus, autoantibodies directed against insulin, glutamatic acid decarboxylase (GAD) and protein-tyrosine phosphatase-related molecules have been detected in patients with T1DM, in addition to infiltration of islets by $CD4^+$ and $CD8^+$ T-cells (Christie, 1992, Narendran *et al.*, 2005). T1DM affect people with genetic predisposition to

the disease. The major susceptibility genes lie within the human leukocyte Ag (HLA) region which is located on short arm of chromosome 6. HLA contributes to ~ 50% of genetic susceptibility to T1DM. These genes encode cell surface protein, major histocompatibility complex (MHC), which are responsible for Ag presentation and involved in interactions with other immune cells and activation of T-cells. 90% of children who develop T1DM early in life have two combinations of HLA genes (DR4-DQ8 or DR3-DQ2) (Dorman and Bunker, 2000, Wassmuth *et al.*, 1992). Another risk locus contributing to 10% of all genetic susceptibility to T1DM is in the insulin gene promoter (Knip, 2005, Narendran *et al.*, 2005).

Twin studies of mono and dizygotes have shown a concordance of 50% and 10%, respectively. Thus, environmental factors may also have an influential role in the development of the disease because a concordance of 100% would be expected if genetic factors were the solely causative factor (Wassmuth *et al.*, 1992). Viral infections, especially with rhino virus, may precipitate and aggravate autoimmune reaction in genetically susceptible individuals. Other environmental factors have been also reported, including cow's milk and other dietary supplements but the data are still not conclusive.(Achenbach *et al.*, 2005, Gillespie, 2006)

Unless insulin is given as a replacement therapy, patients with T1DM will develop severe hyperglycemia and ketoacidosis (Williams and Pickup, 2004). In the absence of insulin, glucose cannot enter the muscle and fat cells. As a result, the body starts to breakdown fat as a source of energy, producing ketone bodies, which accumulate in the blood leading to acidosis; ketoacidosis. Untreated ketoacidosis may lead to coma and death. Management of T1DM involves daily insulin therapy and/or islet transplantation. Table 1.5 shows the different types of insulin formulations with

their onset and duration of actions. Short acting insulin analogues are used to lower the immediate rise in postprandial glucose concentrations following ingestion of a meal while long acting ones are used to control the rise in glucose levels overnight (Knip, 2005, Williams and Pickup, 2004). Islet transplantation represents a novel way to cure diabetes. In this procedure, human islets isolated from brain-dead donors are infused into the portal vein of patients with T1DM. Unfortunately, scarcity of transplantable islets and the requirement for chronic immunosuppression make islet transplantation available to only a few people with T1DM. Therefore, alternative therapies such as gene therapy and β-cell development from stem cells are now being extensively investigated (Falqui, 2005, Knip, 2005, Jones *et al.*, 2008, Williams and Pickup, 2004).

Insulin class	Example	Trade name(s)	Route	Onset (h)	Peak (h)	Duration (h)
Regular insulin	Human insulin (regular)	Humulin R, Novolin R	Injection	0.2-0.5	1.0-3.0	4.0-8.0
Rapid-acting insulin analogues	Insulin lispro Insulin aspart Insulin glulisine	Humalog Novolog Apidra	Injection Injection Injection	< 0.5	0.5-2.5	3.0-4.5
Intermediate-acting insulin	Human insulin (NPH insulin) Lente	Humulin N, Novolin N Lente Humulin	Injection Injection	1.0-2.0	4.0-6.0	8.0-12.0
Long-acting insulin analogues	Insulin glargine Human ultralente	Lantus ultralente humulin	Injection Injection	0.75-1.5 2.0-3.0	- 4.0-8.0	>16.0 8.0-14
insulin combinations	Insulin regular and NPH insulin Insulin lispro protamine and insulin lispro Insulin aspart protamine and insulin aspart	Humulin 70/30 Humalog Mix 75/25 and 50/50 Novolog Mix 70/30	Injection Injection Injection	-	-	-

Table 1.5: Onset and duration of action and origin of different formulations of insulin available in the market (Williams and Pickup, 2004).

1.7.2 Type 2 diabetes mellitus

Type 2 diabetes mellitus (T2DM) is the most common form of the disorder affecting nearly 90-95% of overall incidence of diabetes. T2DM develops during adulthood around the age of 40 but recently the incidence is rapidly increasing in children due

mainly to increasing obesity (Deckelbaum and Williams, 2001, Williams and Pickup, 2004). It is characterized by a defect in β-cell function (decreased insulin secretion) and/or a reduction in insulin responsiveness in insulin-sensitive tissues such as liver, muscle and adipose tissue (Figure 1.6) (Cerasi, 1992, Weyer *et al.*, 1999).

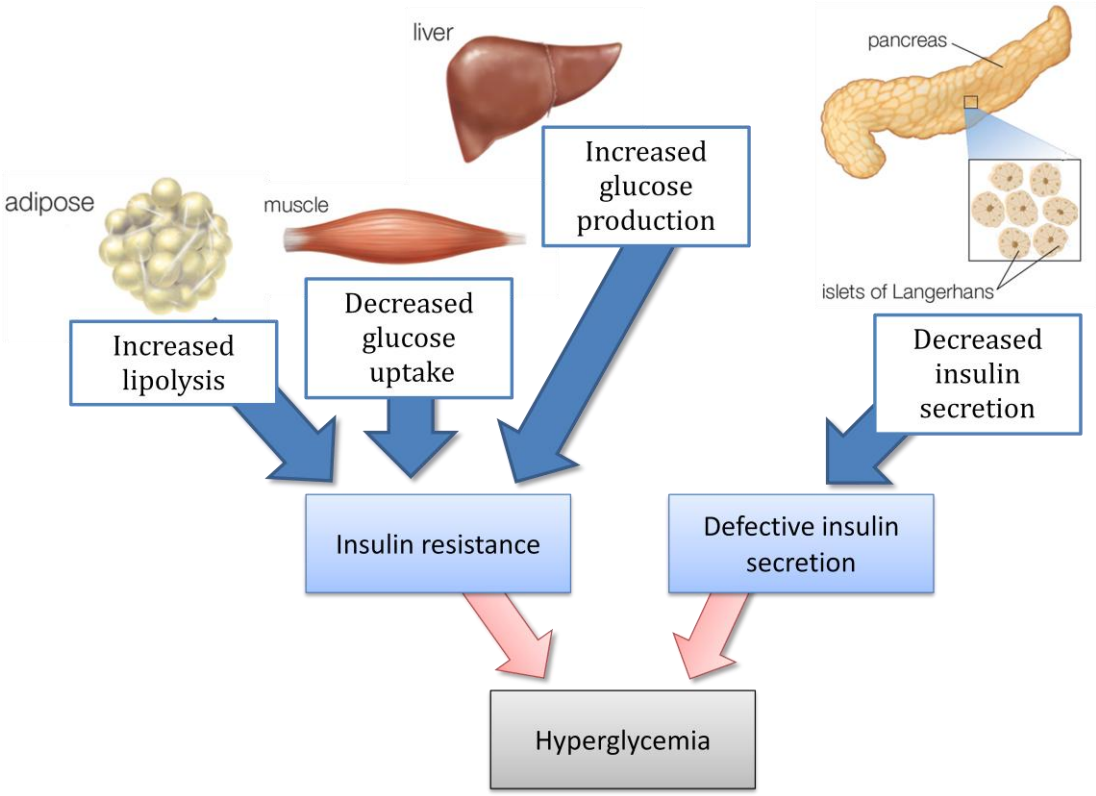

Figure 1.6: The major metabolic defects of type 2 diabetes mellitus.

T2DM is a multifactorial disease where both genetic and environmental factors play a very important role in its development. Environmental factors such as obesity, sedentary life style and hormone excess markedly influence the development of T2DM in genetically susceptible individuals (Cerasi, 1992). Recently, variations within several genetic loci were reported and were associated with an increased risk of T2DM as summarized in Table 1.6. The involvement of most genes (except of FTO and PPAR-γ genes) in β-cell function and insulin secretion further support the role of β-cell dysfunction in the development of T2DM (Frayling, 2007, Horikoshi *et*

al., 2007, Leroith and Accili, 2008, Lindgren and McCarthy, 2008, Sladek *et al.*, 2007, Staiger *et al.*, 2007, Zeggini *et al.*, 2008, Zeggini *et al.*, 2007).

Gene	Suggested function
PPARG	Nuclear hormone receptor transcription factor; adipocyte differentiation and function
KCNJ11	ATP-sensitive potassium channel; crucial for glucose-induced insulin secretion
TCF7L2	Wnt-signalling pathway in the islet; influences insulin and glucagon secretion
HHEX, IDE	HHEX (transcription factor with a key role in pancreatic development) and IDE (may affect insulin action, secretion)
SLC30A8	Zinc transporter, involved in islet insulin-granule function
FTO	Affects T2DM via obesity, but the pathway is unknown
CDKAL1	Possibly affects β-cell development, regeneration, function
CDKN2A, CDKN2B	Probable effect on β-cell development, regeneration, function
IGF2BP2	Involved in translation of insulin-like growth factor II
WFS1	Role in β-cell death and apoptosis

Table 1.6: T2DM susceptibility genes identified to date. Abbreviations: PPARG, peroxisome proliferator-activated receptor γ gene; KCNJ11, inwardly rectifying ATP-sensitive potassium channel subfamily J member 11 gene; TCF7L2, transcription factor 7-like 2 (T cell specific) gene; HHEX, haematopoietically expressed homoebox gene; IDE, insulin-degrading enzyme gene; SLC30A8, family 30 (zinc transporter) member 8 gene; FTO, fat mass and obesity associated gene; CDKAL1, CDK5 regulatory subunit associated protein 1 like 1 gene; CDKN2A, cyclin-dependent kinase inhibitor 2A gene; CDKN2B, cyclin-dependent kinase inhibitor 2B gene; IGF2BP2, insulin-like growth factor 2 mRNA binding protein 2 gene; WFS1, Wolfram syndrome 1 gene (Horikoshi et al., 2007; Sladek et al., 2007; Staiger et al., 2007; Zeggini et al., 2007; Frayling, 2007; Lindgren and McCarthy, 2008).

The symptoms of T2DM present gradually and patients may remain asymptomatic for many years. Symptoms such as polyuria, polydipsia and/or fatigue may be the only complaints that patients may suffer from. T2DM is often diagnosed due to an abnormal blood or urine glucose on routine physical examination or screening (Rang *et al.*, 2003, Steil, 1999).

1.7.2.1 Complications of T2DM

Untreated or poorly controlled diabetes mellitus type 2 increases the risk of developing macrovascular and microvascular complications, involving many different organs of the body (Steil, 1999). Macrovascular complications, which involve large vessels, can lead to coronary heart disease, stroke and peripheral vascular disease. It has been shown that such complications are responsible for

about 70-80% of the mortality among patients with T2DM (Steil, 1999). Microvascular complications, which affect small arteries and arterioles, are developed as a result of hyperglycemia and may lead to neuropathy, retinopathy and nephropathy. Lowering blood glucose reduces the risk of retinopathy, neuropathy and nephropathy by 73%, 60% and 54%, respectively (Rang *et al.*, 2003, Steil, 1999).

1.7.2.2 Management of T2DM

Management of T2DM consists of non-pharmacological and pharmacological therapies (Rang *et al.*, 2003). Non-pharmacological therapy involves life-style modifications such as healthy diet, physical activity, weight reduction and smoking and alcohol cessation. If these modifications fail to normalize blood glucose, pharmacological therapy should be initiated.

There are many classes of drugs that have been used to treat type 2 diabetes which can be classified as insulin secretagogues and non- insulin secretagogues (Table 1.7) (Blonde, 2009, Chen *et al.*, 2009). The insulin secretagogues increase the release of insulin from β–cells (Lebovitz, 2004, Rang *et al.*, 2003). Sulphonylureas and meglitinides are classes of insulin secretagougues drug (Rendell and Kirchain, 2000). Sulphonylureas enhance insulin secretion by binding to the SUR1 subunit of K_{ATP}-channel in β-cells, causing a closure of the K_{ATP}-channels. Closure of the K_{ATP}-channels is followed by opening of VGCC. Increased $[Ca^{2+}]_i$ triggers exocytosis of insulin from storage vesicles (Heine, 1996, Rang *et al.*, 2003, Rendell and Kirchain, 2000). Sulphonylureas are classified according to their potency, duration of action and incidence of side effects, into first generation sulphonylureas (tolbutamide, chlorpropamide, acetohexamide and tolazamide) and into second generation

sulphonylureas (glibenclamide, gliclazide, glipizide and glimepiride) (Lebovitz, 2004, Rang *et al.*, 2003, Rendell and Kirchain, 2000).

The other class of insulin secretagogues is meglitinide analogues. They include repaglinide and nateglinide and have no sulphonylurea moiety but have similar mechanism of action to sulphonylureas (Lebovitz, 2004, Rendell and Kirchain, 2000). They block SUR1/Kir6.2 channels and trigger insulin exocytosis from the storage vesicles (Chachin *et al.*, 2003, Hansen *et al.*, 2002, Hu *et al.*, 2000).

The non-insulin secretagogue drugs are biguanides (metformin), insulin sensitizers (thiazolidinediones), and α–glucosidase inhibitors. The mechanism of action of metformin involves activation of adenosine monophosphate-activated protein kinase (AMPK). Metformin reduces hepatic glucose production and thus improving fasting hyperglycemia (Bailey and Krentz, 2010, Lebovitz, 2004). The thiazolidinediones (rosiglitazone and pioglitazone) act as peroxisome proliferator-activated receptor gamma (PPARγ) agonists. PPARγ is part of a heterodimer that includes a retinoid X receptor (RXR). The drug-receptor complex binds to response elements within the promoter regions of specific genes involved in lipid metabolism resulting in either activation or inhibition of gene transcription leading to increased insulin sensitivity (Lebovitz and Banerji, 2001).

Other drugs which can be used are the starch blockers. These agents are α–glucosidase inhibitors, which inhibit the breakdown of carbohydrates to glucose resulting in a decrease in glucose absorption and a lower glycemic peak concentration. Examples of these agents are acarbose and miglitol (Lebovitz, 2004, Rendell and Kirchain, 2000).

Patients with progressive or uncontrolled T2DM may benefit from insulin treatment. Improvement in glycemic control has been seen in patients with uncontrolled T2DM on SUs or metformin when insulin was added as an add-on therapy.

Name of group	Example	MOA	Side effects
Sulphonylureas (SUs)	Tolbutamide Glibnclamide Glipizide Gliclazide Glimepiride	Increased Pancreatic insulin secretion	Hypoglycemia Weight gain Hyponatremia
Non-sulphonylureas (non-SUs)	Meglitinide Repaglinide Nateglinide	Increased Pancreatic insulin secretion	Hypoglycemia Weight gain
α-glucosidase inhibitors	Acarbose and Miglitol	Decreased gut carbohydrate absorption	Adverse gastrointestinal effects
Biguanides	Metformin	Decreased hepatic glucose production	Adverse gastrointestinal effects Lactic acidosis
Thiazolidinedione	Rosiglitazone Pioglitazone	Activation of PPAR-gamma Increased peripheral glucose disposal	Weight gain Edema

Table 1.7:Currently used classes of agents used to regulate glucose levels (Chen *et al.*, 2009)

1.7.2.3 New treatment for T2DM

New therapies for the treatment of T2DM have been introduced in the past few years. Some have been already available commercially while others are still in the developmental phase. One of the recently introduced class of compounds is the incretin-based therapy which involves GLP-1 analogues and dipeptidyl peptidase-4 (DPP-4) inhibitors (Table 1.8). GLP-1 acts though cAMP-coupled G-protein receptor located on β- and α-cells, CNS and GI tract to exert its actions. Binding of GLP-1 to its receptor on islet cells causes potentiation of glucose-induced insulin secretion

and suppression of glucagon release. It also increases and decreases β-cells survival and apoptosis, respectively, at least in studies using experimental animals. Through its action on GI tract, GLP-1 slows gastric emptying time leading to a reduction in post-prandial blood glucose level. GLP-1 reduces appetite and food intake through its action on CNS and thus contributes to weight loss. The therapeutic use of GLP-1 is limited due to its rapid degradation and inactivation by DPP-4 enzyme. Therefore, GLP-1 analogues that are resistant to the action of DPP-4 and DPP-4 inhibitors that inhibit the activity of the enzyme have been developed. GLP-1 mimetics include exendin-4, which is originally derived from the salivary secretion of the lizard *Heloderma suspectum* (the Gila moster), and its synthetic form exenatide. Another GLP-1 analogue which is yet to be approved by FDA is liraglitide. It is a long-acting once daily injection analogue to overcome the short half-life of exenatide ($t_{1/2}$= 3 hours). Sitaglibtin and saxagliptin are both DPP-4 inhibitors and result in 2-3 fold enhancements in endogenous levels of GLP-1. Clinically, GLP-1 analogues and DPP-1 inhibitors improve glycemia but only GLP-1 analogues are associated with weight loss and GI effects (Chen *et al.*, 2009, Triplitt, 2007).

Amylin analogues are a class of compounds that have been recently approved for the treatment of T2DM. Pramlintide (table 1.8) is the only synthetic amylin analogue available in the market. Amylin is a 37 amino acid peptide co-secreted with insulin from β-cells. The actions of amylin involve reduction in glucagon secretion in a glucose-dependent manner and delaying gastric emptying time. Both actions reduce post-prandial blood glucose concetrations without causing hypoglycemia (Chen *et al.*, 2009).

Name of the group	Example	Availability	Mode of administration	MOA	Side effects
Incretin mimetic	Exendin-4 Exenatide Liraglitide	Yes Yes No	Injection Injection Injection	Potentiating of insulin secretion Decreased glucagon secretion Decreased gastric emptying time Enhanced satiety	Adverse gastrointestinal effects Weight loss hypoglycemia
Amylin mimetic	Pramlintide	Yes	Injection	Decreased postprandial glucagon secretion Decreased gastric emptying Increased satiety	Adverse gastrointestinal effects
DDP-4 inhibitors	Sitaglibtin saxagliptin	Yes Yes	Oral Oral	Inhibition of incretin hormone metabolism	Adverse gastrointestinal effects Infection

Table 1.8: Recently added classes of glucose-lowering agents (Chen *et al.*, 2009; Triplitt 2007).

Two new classes of drugs, although waiting approval, have been identified as potential therapies for T2DM. The first class is type 2 sodium-glucose co-transporter (SGLT2) inhibitors. SGLT2 is located in the proximal tubule of the kidney and is responsible for renal glucose reabsorption. Blocking these co-transporter prevent reabsorption and increases excretion of glucose in the urine thus lowering blood glucose levels. A number of selective inhibitors of SGLT2 have been developed and are still in clinical trials (Table 1.9) (Boldys and Okopien, 2009). The other new class is glucokinase (GK) activators (Table 1.9). Activation of GK in β-cells and liver stimulates glucose-stimulated insulin secretion and augments hepatic glucose metabolism leading to improvement in glucose clearance from the blood stream (Al-Hasani *et al.*, 2003).

Name of the group	Example	Clinical development	Mode of administration	MOA
SGLT2 inhibitor	Dapagliflozin Remogliflozin Sergliflozin AVE – 2268 JNJ-28431754 ISIS 388626	III phase II phase II phase phase IIb II phase Preclinical	Oral Oral Oral Oral Oral Oral	Blocking reabsorption and increased excretion of glucose
GK activators	RO-28-1675 GKA1 GKA2 Compound A	Preclinical Preclinical Preclinical Preclinical	-	Activation of pancreatic and hepatic glucose metabolism

Table 1.9: Newly developed agents which are still in clinical and preclinical stages (Boldys *et al.*, 2009; AL-Hasani *et al.*, 2003).

1.8 Apoptosis pathway

Apoptosis, or programmed cell death, is a sequence of controlled processes that occurs in almost all types of cells leading to cell self-destruction. It is crucial in the removal of defective and potentially harmful cells. Impairment or excessive stimulation of the apoptotic pathway can lead to various types of diseases, including diabetes mellitus. Cells undergoing apoptosis manifest characteristic morphological changes such as shrinking of cells, condensation of chromatin, budding of plasma membrane and fragmentation of cells into membrane-bound structure called apoptotic bodies which contain cytosol, condensed chromatin and organelles fragments. These bodies are engulfed by macrophages and are removed without triggering inflammatory response. The molecular events underlying these changes are quite complex and require activation of certain proteolytic enzymes called caspases (Gewies, 2003).

1.8.1 Caspases: structure and function

Caspases are cysteine proteases derived from cysteine-dependent aspartate-specific proteases. The catalytic activities of these enzymes depend on cysteine

residue and their substrate cleavage site is after the aspartate residue. To date, there are 14 members of the caspase family in mammals with caspase-11 and -12 being only found in mouse. The caspase family is subdivided, according to their function, into two major groups 1) caspase-2, -3, -6, -7, -8, -9 and -10 which are activated during apoptosis or 2) caspases that are activated during inflammatory process (caspase-1, -4, -5, -11 and -12). In general, caspases are similar in their amino acid sequence, structure and substrate specificity. They are synthesized from their precursor procaspases which are composed of three domains: N-terminal prodomain, a large unit and a small unit. Proteolytic activation of procaspases releases the large and small subunits and the active caspase is formed as a heterodimer of two small and two large subunits (Creagh *et al.*, 2003).

The caspases involved in apoptosis (group 1) are further subdivided into two categories: 1) initiators (caspase-2, -8, -9, -10) which have long prodomains containing either death effector domain (DED) or caspase recruitment domain (CARD). They are primarily responsible for initiating the apoptotic cascades. The second category involves caspase-3, -6 and -7 which are called effector caspases. They have short or absent prodomains and are activated by the initiators. Their main function is to amplify the death signal and execute cell death (Creagh *et al.*, 2003, Gewies, 2003).

Apoptosis is triggered by various stimuli which activate caspases via several pathways: 1) the mitochondrial/apoptosome pathway (intrinsic pathway), 2) the death receptor pathway (extrinsic pathway), 3) the endoplasmic reticulum (ER) stress pathway and 4) granzyme B-mediated cell death. Although these pathways may be initially activated differently; cross-talk between them may occur (Araki *et*

al., 2003, Creagh *et al.*, 2003, Gewies, 2003, Hui *et al.*, 2004, Szegezdi *et al.*, 2006). Figure 1.7 shows a schematic representation of some major apoptotic signaling pathways.

1.8.2 Mitochondrial/apoptosome activation of caspases

The mitochondria play an integral part in both initiation and amplification of caspase activation. Cellular stimuli such as heat shock, oxidative stress, cytotoxic drugs and DNA damage can initiate caspase activation through permeabilization of the mitochondrial outer membrane. The disruption of the mitochondrial potential causes the release of cytochrome C and other mitochondrial factors into the cytosol. The permeability of mitochondrial outer membrane and the release of cytochrome C are largely regulated by pro-apoptotic and anti-apoptotic members of Bcl-2 family. The release of mitochondrial factors is inhibited by anti-apoptotic members of Bcl-2 such as Bcl-2 and Bcl-x_L, and promoted by pro-apoptotic Bcl-2 members such as Bax, Bak, Bad, Bim and Bid. The released cytochrome C binds to a monomeric cytosolic protein called Apaf-1 (apoptosin protease activating factor-1) which undergoes conformational changes and oligomerizes in the presence of dATP (deoxy adenosine triphosphate) with procaspase-9 forming an apoptosome, a heptomeric wheel-like structure. The activated apoptosome triggers the activation of caspase-9 which leads to subsequent stimulation of effector caspase-3 and -7. Caspase-3 further stimulates caspase-2 and -6 which indirectly activates caspase-8 and -10. Caspases affect several downstream effectors to execute cell death. One of the final targets of caspases is ICAD (inhibitor of caspase-activated DNase). Activation of caspases inactivates ICAD and cause the release of its DNase subunit (CAD). Caspase-activated DNase (CAD) enters the nucleus and fragments DNA

leading to the formation of "DNA ladder", a characteristic commonly seen in apoptotic cells (Creagh *et al.*, 2003, Gewies, 2003, Hui *et al.*, 2004).

1.8.3 Death receptor pathway

Death receptors are cell surface receptors that are involved in transducing the death signal and they belong to TNF receptor (TNFR) superfamily. The TNFR has a conserved sequence in the cytoplasmic part of the receptor called the death domain (DD). Upon binding of extracellular ligands such as TNF, Fas ligand (FasL/CD95L) or TNF-related apoptosis-inducing ligand (TRAIL) to the receptor, oligomerization and conformational changes occur in the receptor. Adaptor molecules such as Fas-associated death domain (FADD) proteins are recruited to the receptor by their own DD to form death-inducing signaling complex (DISC). FADD also possesses death effector domain (DED) and forms homotypic DED-DED interaction with DED-containing procaspase-8 leading to proteolytic activation and release of active caspase-8. The death signal generated upon the activation of caspase-8 can be transmitted by two mechanisms according to cell types. In type I cells, the stimulation of death receptor results in sufficient activation of caspase-8, which, in turn, activates downstream caspases which result in cell death. On the other hand, the signal generated from death receptor in type II cells is not strong enough to elicit a direct and full activation of caspase cascades; therefore, the signal is amplified by mitochondria-dependent activation of caspases. The active caspase-8 cleaves Bid of the Bcl-2 family. The truncated form of Bid is then translocated to the mitochondria where it activates Bax and Bak. These pro-apoptotic factors induce cytochrome C release, apoptosome assembly and activation of effector caspases (Creagh *et al.*, 2003, Gewies, 2003, Hui *et al.*, 2004).

1.8.4 ER stress mediated caspase activation

The ER is a vital organelle for post-translation modification, folding and assembly of proteins and storage of intracellular Ca^{2+}. Thus, defective folding, accumulation of misfolded protein and alteration in Ca^{2+} homeostasis can precipitate ER stress. ER stress triggers apoptosis by four major pathways. The first is through induction of transcription of CHOP (C/EBP homologous protein/GADD153), also known as growth arrest and DNA damage-inducible gene (GADD). Its major actions involve reduction in Bcl-2 protein expression and increased translocation of Bax into the mitochondria. The second is through activation of the JNK (c-Jun NH2-terminal kinase) pathway which in turn regulates gene expression of proteins associated with apoptosis and survival. The third is by activating caspase-12 especially in mice. The final pathway is through stimulation of pro-apoptotic Bcl-2 family (Araki *et al.*, 2003, Szegezdi *et al.*, 2006).

1.8.5 Granzyme B-mediated cell death

Activation of cytotoxic T-cells and natural killer cells can trigger the release of cytosolic granules which contain proteins responsible for initiating apoptosis. Perforin, one content of the granule, is a protein that functions by forming pores into the target cells to facilitate the entry of other granule components such as granzyme B. Granzyme B is a serine protease which cleaves aspartate-containing proteins involved in the apoptosis cascades. The major substrates of granzyme B are caspase-3, caspase-8 and Bid. Granzyme B-mediated Bid activation involves cleavage of Bid to produce a fragment, gtBid, which is then translocated into the mitochondria causing the release of cytochrome C and the assembly of apoptome (Creagh *et al.*, 2003, Hui *et al.*, 2004).

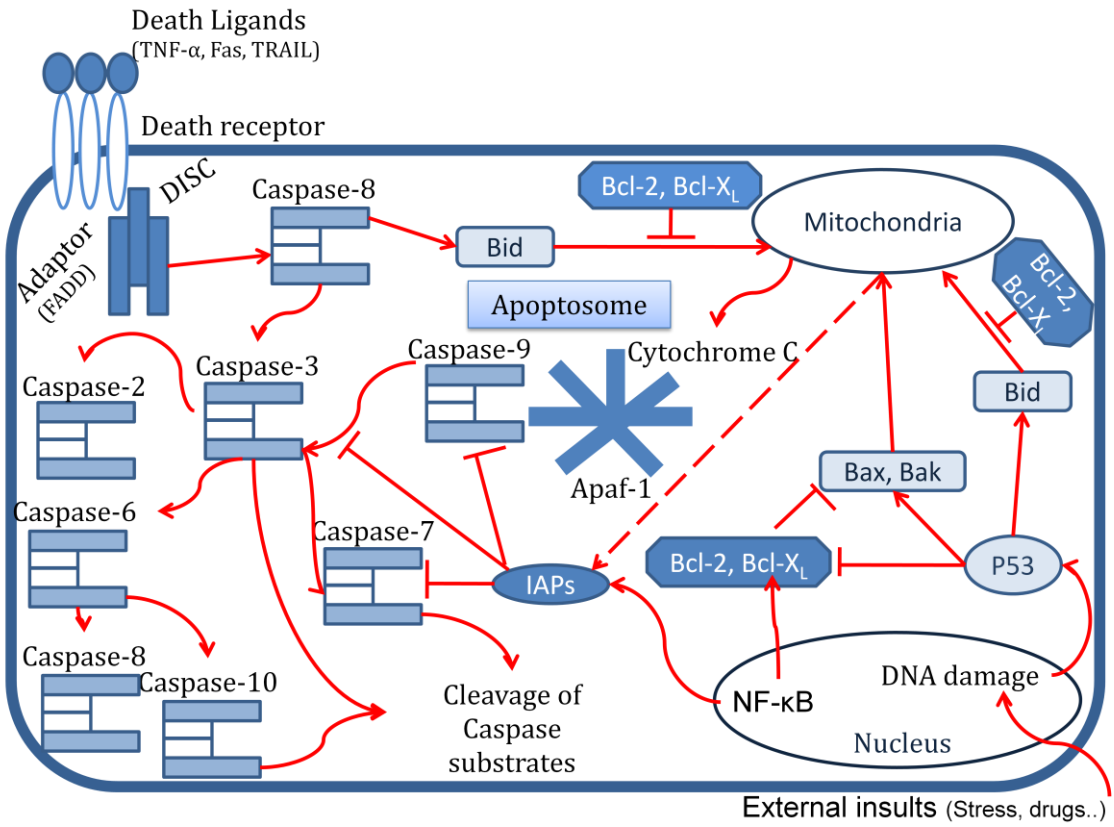

Figure 1.7: Schematic representation of some apoptotic pathways. Apoptosis can be induced either by activation of death receptor or by cellular stress. Activation of the death receptor liberates death inducing signaling complex (DISC) which cleaves procaspase-8 to caspase-8. The initiator caspase-8 activates caspase-3 which in turn activates caspase-2,-6,-7,-8,-10. The death signal may be amplified by the pro-apoptotic proteins (Bid). Bid increases mitochondria permeability and cytochrome C release. Cytochrome C contributes to the formation of apoptosome which also includes Apaf-1 and dATP. The apoptosome activates caspase-9 which then executes cell death through caspase-3. Induction of DNA damage by cellular stress promotes the activation of P35 transcription factor which activates pro-apoptotic proteins such as Bax and Bak. Apoptosis can be largely regulated by pro-survival signals. Anti-apoptotic proteins (Bcl-2 and Bcl-X_L) modulate the activities of pro-apoptotic proteins while IAPs inhibit caspase signaling. Both survival signals are induced by NF-κB transcription factor (from Gewies 2003).

1.8.6 Regulatory mechanisms in apoptosis

1.8.6.1 Bcl-2 family and IAPs

Apoptosis and caspase activation are tightly regulated by a set of various pro and anti-apoptotic molecules such as Bcl-2 family and inhibitors of apoptosis proteins (IAPs). Members of Bcl-2 family are proteins containing conserved sequence motifs known as Bcl-2 homology domains (BH1 to BH4). Bcl-2 family consists of approximately 30 members which can be divided into anti and pro-apoptotic subgroups. The anti-apoptotic group includes Bcl-2 and Bcl-xL and posses the

domain BH1,2,3,4 whereas the pro-apoptotic group includes two subdivisions 1) the Bax members such as Bax and Bak which contain the domain BH1,2,3 and 2) the BH3-only proteins such as Bid, PUMA, NOXA, Bim and Bad which have BH3 as the only domain. The function of the Bcl-2 family is to control mitochondrial outer membrane integrity and thus the release of cytochrome C and mitochondrial factors. The Bcl-2 family members interact and regulate the activity of each other. Under basal condition, the anti-apoptotic Bcl-2 members bind to the pro-apoptotic Bax-related members and thereby inhibit Bax or Bak activation. However, upon the arrival of an apoptotic stimulus, the BH3 only proteins interact with the anti-apoptotic members on the outer mitochondrial membrane to remove the inhibition of anti-apoptotic proteins imposed on the pro-apoptotic Bax members and thus promote their release. The Bax-related proteins integrate into the mitochondrial membrane contributing to the permeability of its outer membrane and the release of pro-apoptotic proteins (Gewies, 2003, Hui *et al.*, 2004).

The other group of proteins which are very important in caspase regulation are IAPs. IAPs are a family of anti-apoptotic proteins that are transactivated by nuclear factor κB (NF-κB). Eight members of IAPs have been identified in human. The function of XIAP, c-IAP I and c-IAP TT is to directly inhibit caspase-3,-7 and -9 (Gewies, 2003, Hui *et al.*, 2004).

1.8.6.2 PI3K/AKT pathway

Survival pathways are also activated to regulate apoptosis and one important pathway is the PI3K/AKT pathway. Activation of G-protein coupled receptors or tyrosine kinase receptors can recruit specific SH2-domain containing proteins including phosphotidyl inositol-3 kinase (PI3K). PI3Ks are heterodimeric proteins

that initiate signaling cascades through the phosphorylation of phosphotidyl inositol at the 3' position of the inositol ring to produce phosphatidylinositol 3-phosphate (PtdIns-3-P), phosphatidylinositol 3,4 bisphosphate (PtdIns-3,4-P2) and phosphatidylinositol 3,4,5 triphosphate (PtdIns-3,4,5-P3). These lipid products act as second messengers that activate several cellular target proteins such as AKT (Cantrell, 2001). AKT is a serine/threonine protein kinase and three isoforms (AKT 1, AKT 2, and AKT 3) have been identified in human to date. AKT exhibits its anti-apoptotic actions by modifying the activities of certain protein and transcription factors. AKT phosphorylates Bad and thus inhibits its activation. AKT also activates NF-κB-mediated expression of pro-survival genes by regulating IκB kinase (IκK) activity. Activation of AKT also affects transcription factors such as Forkhead transcription factors (FKHR). AKT phosphorylates three members of forkhead transcription factors namely FOX1 (previously known as FKHR), FOX3 (previously known as FKHRL1) and FOX4 (previously known as AFX). AKT-mediated phosphorylation of these transcription factors promotes transcription inactivation and nuclear exclusion. Forkhead transcription factors are involved in the regulation of cell apoptosis (Kim and Chung, 2002, Rena *et al.*, 1999).

1.9 β-cell death in diabetes mellitus

β-cell mass is tightly controlled by a balance between proliferation and neogenesis on one side and apoptosis and necrosis on the other side (Figure 1.8) (Lupi and Del Prato, 2008). Dysregulation of this balance can precipitate loss of β-cell mass and susequent diabetes. The reduction in β-cell mass is caused by either a decrease in proliferation or an increase in apoptosis with the latter being the most predominant factor. Increased apoptosis has been reported in both types of diabetes and it is

responsible for 80% and 50% loss of β-cells in T1DM and T2DM, respectively (Donath and Halban, 2004, Porte and Kahn, 2001). In general, there are three main factors that may initiate apoptosis and contribute to the loss of β-cell volume: 1) cytokines, 2) hyperglycemia and 3) dyslipidemia (Cnop *et al.*, 2005, Donath and Halban, 2004, Eizirik and Mandrup-Poulsen, 2001, Johnson and Luciani, 2010, Lupi and Del Prato, 2008, Mandrup-Poulsen, 2001, Robertson *et al.*, 2004).

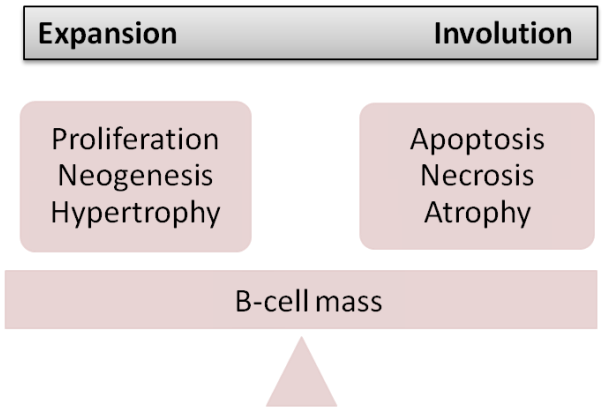

Figure 1.8: Mechanisms controlling β-cell mass (from Del Prato, 2008).

1.9.1 Cytokine-induced β-cell death

Several inflammatory cytokines such as interleukin-1β (IL-1β), tumor necrosis factor-α (TNF-α) and interferon-γ (INF-γ) are involved in mediating β-cell death. They are secreted by islet-infiltrating leucocytes (T-cells and macrophages) especially during the development of T1DM. An individual cytokine alone is not enough to elicit cell lysis but rather their combinations promote β-cell dysfunction and death. The susceptibility of β-cells to the cytotoxic effect of an individual cytokine is dramatically increased when two or more cytokines are combined together. The exact nature of the cytokine mixture that is able to produce the strongest death signal in T1DM is unclear, although a synergism of IL-1β + INF-γ,

TNF-α + INF-γ and IL-1β + TNF-α have been reported (Kim and Lee, 2009). Short term exposure of β-cells to cytokines impairs β-cell function due to downregulation of important genes involved in insulin secretion such as insulin, GLUT-2, glucokinase and PDX-1 (Cnop *et al.*, 2005, Donath *et al.*, 2010, Donath *et al.*, 2003, Eizirik and Mandrup-Poulsen, 2001, Johnson and Luciani, 2010).

The binding of IL-1β, TNF-α and INF-γ to their receptors on β-cells stimulate district signaling pathways leading to the activation of multiple transcription factors (Figure 1.9). IL-1β and TNF-α exert their action through activation of NF-κB pathway. NF-κB is a transcription factor involved in cellular stress response, cell growth, survival and apoptosis. It normally dimerizes with inhibitor of NF-κB (IκB) in the cytosol preventing its translocation into the nucleus. Upon cytokine activation, IκB kinase (IκK) phosphorylates IκB and facilitates its degradation by the proteasome. NF-κB is freed and translocated into the nucleus to regulate the promoter activity of genes encoding important proteins involved in the β-cell apoptosis pathway such as inducible nitric oxide synthase (iNOS), pro-apoptotic Bcl-2 family and Fas. Expression of iNOS and subsequent formation of nitric oxide (NO) disrupt β-cell mitochondrial glucose oxidation and deplete ER Ca^{2+} store leading to ER stress and destruction of β-cells. In addition to the activation of NF-κB pathway, IL-1β also activates members of MAPK family, namely p38, ERK and JNK. ERK and p38 pathways contribute to the production of nitric oxide (NO) while JNK signaling cascade negatively regulates the activity of pro-survival members of Bcl-2 family and thus promotes apoptosis (Cnop *et al.*, 2005, Donath *et al.*, 2003, Melloul, 2008).

INF-γ, on the other hand, stimulates mainly the action of JAK/STAT-1 pathway. JAK (Janus kinase) is a tyrosine kinase and following activation by INF-γ, it phosphorylates STAT (signal transducer and activator of transcription)-1 which dimerizes in the cytosol and is translocated into the nucleus to up-regulate the expression of major mediators in β-cell death such as INF-γ regulatory factors-1 (IRF-1), MHC class I and iNOS (Cnop *et al.*, 2005, Gysemans *et al.*, 2008). Although, the involvement of cytokines in the pathogenesis of T1DM is well defined, the role of cytokines especially IL-1β in β-cell death in T2DM is controversial. A group of researchers reported that glucose induced IL-1β production and contributed to β-cell death in T2DM (Maedler, 2002). However, this was challenged by others who reported that the IL-1β pathway was not activated in human islets following glucose challange (Welsh et al., 2005).

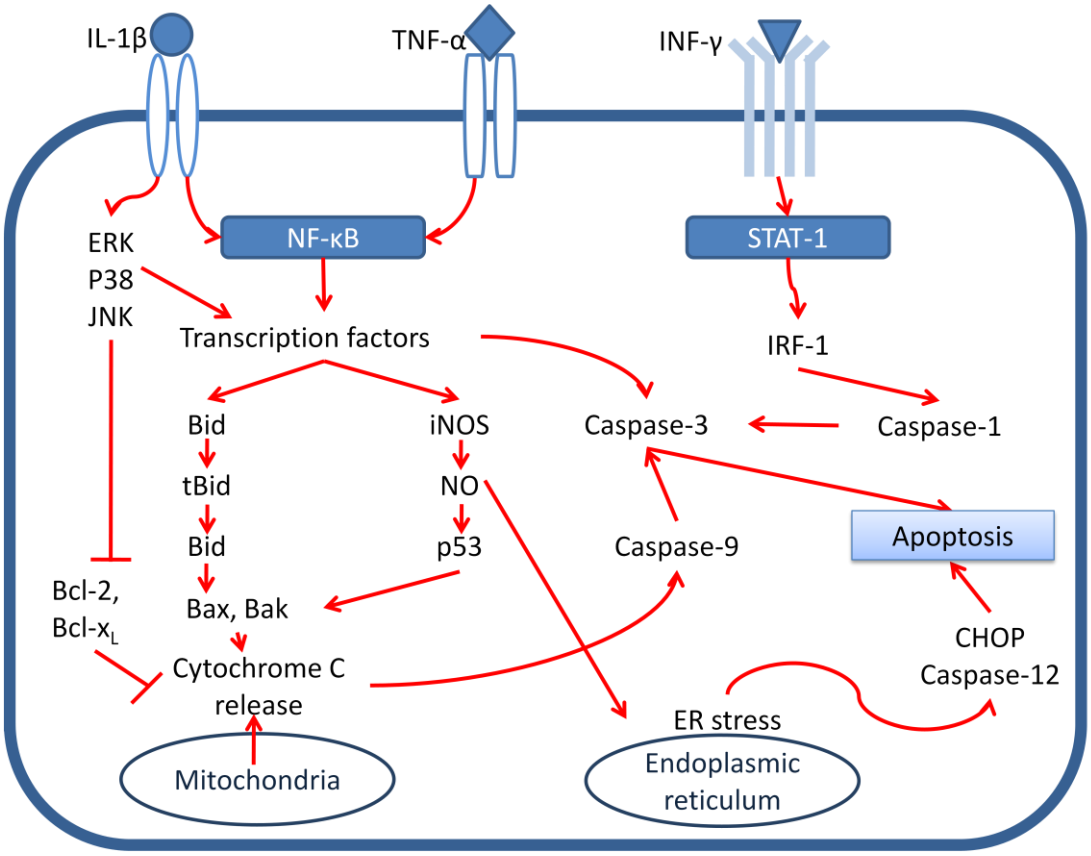

Figure 1.9: Schematic representation of the possible pathways involved in cytokines-induced β-cell death. Cytokines (IL-1β, TNF-α and INF-γ) activate several pathways leading to apoptosis of β-cells. These pathways involve activation of MAPKs, ER stress and liberation of pro-apoptotic proteins from the mitochondria (from Cnop *et al.*, 2005).

1.9.2 Hyperglycemia-induced β-cell death

Elevated levels of plasma glucose (hyperglycemia) are the major characteristic of T2DM. Glucotoxicity is a phenomenon where chronic elevations of glucose concentrations cause impairment of β-cell function and insulin sensitivity. Long term exposure of β-cells to high glucose levels has been associated with increased apoptotic rate though oxidative stress and mitochondrial activation of caspases. Activation and generation of reactive oxygen radicals (ROS) following excessive glucose metabolism blocks mitochondrial respiration, diminishes glucose-induced insulin secretion and activates apoptosis. Chronic hyperglycemia results in chronic stimulation of insulin biosynthesis. This will increase the metabolic demands on β-

cells as a result of an increased insulin output. Increased synthesis rate of proinsulin increase protein flux though ER precipitating ER stress and apoptosis (Donath and Halban, 2004, Evans, 2002, Johnson and Luciani, 2010, Maiese *et al.*, 2007, Poitout and Robertson, 2008, Robertson *et al.*, 2004).

1.9.3 Dyslipidemia-induced β-cell death

Obesity is a major risk factor of T2DM and is associated with increased circulating free fatty acid (FFA) levels. Chronic elevations in FFAs impair β-cell function and promote β-cell death by apoptosis. These deleterious effects of FFA are linked to saturated, but not unsaturated, fatty acids. This is due to the ability of unsaturated fat to form intracellular triglyceride (TG). The induction of β-cell death by FFA is mediated by a number of mechanisms including: 1) accumulation of lipid-derived metabolites, most importantly ceramide, 2) generation of ROS and subsequently oxidative stress and 3) increased NO production and ER stress. Increased ceramide synthesis is a key component of FA-induced β-cell apoptosis. In addition to the ability of ceramide to cause oxidative stress, it also inactivates pro-survival signals mediated by phosphotidylinositol 3-kinase/protein kinase B (PI3K/PKB). Ceramide blocks PKB activation thus removes the imposed inhibition on some of the pro-apoptotic effectors such as Bad and caspase-9 (Figure 1.10) (Donath and Halban, 2004, Evans, 2002, Poitout and Robertson, 2008, Robertson *et al.*, 2004).

FFAs have also been reported to modulate islet function through a number of lipid-binding GPCR including GPR40, GPR41, GPR43 and GPR119 in which GPR40 is the most extensively studied. It is thought that acute exposure of islets to FFAs potentiated glucose-induced insulin secretion via GPR40. However, chronic activation of GPR40 by FFAs in islets may lead to deterioration in islet function and

impairment in glucose-induced insulin secretion as reported in studies using genetically modified animals. It has been reported that glucose-induced insulin responses were restored in high fat fed GPR40 -/- knockout mice (Winzell and Ahren, 2007).

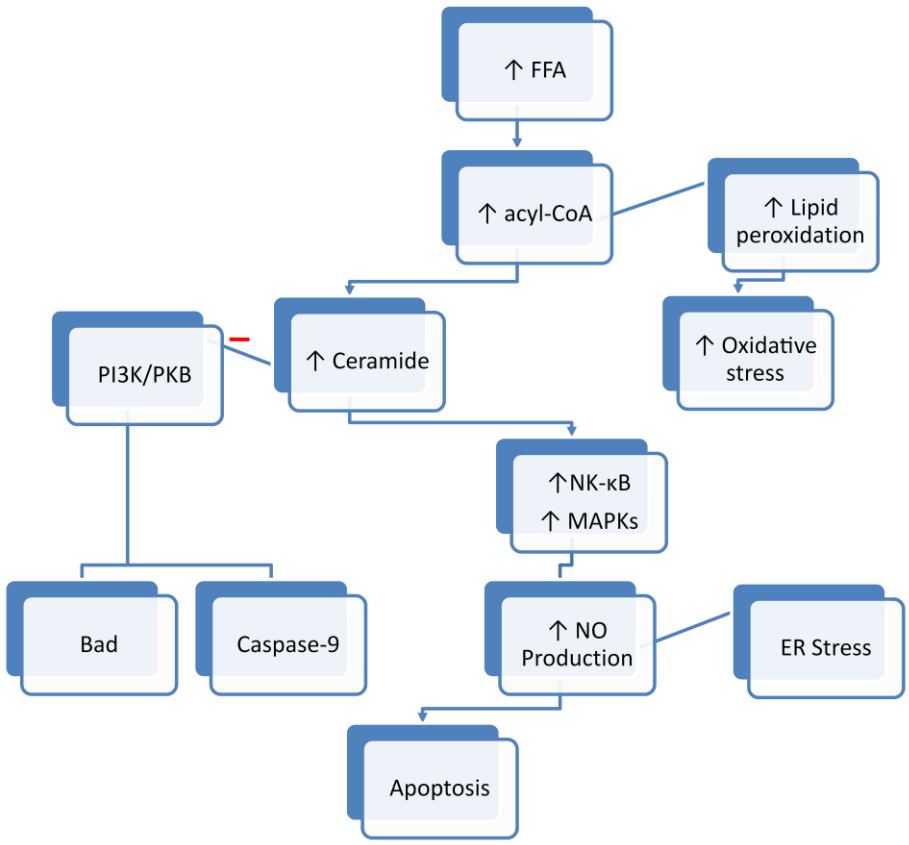

Figure 1.10: The possible pathways contributing to the lipotoxicity-induced apoptosis in β-cells (adapted from Evans *et al.*, 2002).

1.10 Phytochemicals as potential novel treatment for T2DM

Currently, there is a trend towards the development of new drugs for the management of T2DM. Currently available drugs reduce hyperglycemia either by increasing insulin secretion or reducing insulin resistance as detailed in section 1.7.2.2. Development in T2DM management techniques involves production of agents that target β-cell function. Among the available drugs used to manage T2DM, sulphonylureas and incretin-based therapy are the only classes that affect the

function of β-cells. The increased rate of failure with the use of sulphonylureas, up to 25% failure rate/year (Steil, 1999), and the deleterious effect of these drugs on cardiac and vascular functions during ischemia (Smits *et al.*, 1996) have limited their usage as a first-line therapy in patients with T2DM. Similarly, issues concerning long-term safety and cost of incretin-based therapies have also shadowed the use of these drugs in the treatment of T2DM. Incretin-based therapies mainly GLP-1 analogues are expensive and available in injection forms which may be inconvenient for patients with T2DM. In addition, they have been associated with incidence of acute pancreatitis *in vivo* and increase risk of tumor growth *in vitro* (Persaud and Jones, 2008). Therefore, identifying new or β-cell targeted drugs for the treatment of T2DM is an area of active research.

Herbal medicines have attracted attention as alternative therapeutic agents for treating T2DM because they are relatively inexpensive and many have been used for decades or centuries without deleterious side effects (Swanston-Flatt *et al.*, 1991). One successful example of plant-derived antidiabetic drug is metformin. Metformin, which was originally isolated from *Galega officinalis*, is now one of the standard treatment of T2DM.. A recent report has shown that 35-48% of patients with diabetes use alternative medicine (Garrow and Egede, 2006, Yeh *et al.*, 2003). Ethnopharmacological studies have reported that approximately 800 plants may have anti-diabetic activity (Alarcon-Aguilara *et al.*, 1998). Nevertheless, few have been shown to be effective in treating the symptoms of T2DM in rodents and humans, and their mechanisms of action are uncertain. Two of these promising plant extracts are *Gymnema sylvestre* and *Costus pictus*.

1.11 Gymnema sylvestre

Gymnema sylvestre (GS) is a large woody climber plant, from the Asclepiadaceae family, and is native to central and southern India, tropical Africa and Australia. A five year old plant is shown in Figure 1.11. This plant has been used as an ayurvedic medicine for the treatment of diabetes in India for centuries. It was also used in treating eye diseases, dental decay, rheumatic arthritis and gout (Kanetkar *et al.*, 2007, Leach, 2007).

The first scientific and experimental study of GS was started during the early 1930s by Mhaskar and Caius who found that the leaves of GS had the ability to reduce blood glucose levels in rabbits (Mhaskar and Caius, 1930). Since then, a lot of effort and work have been spent to identify the pharmacological actions and the chemical composition of this plant.

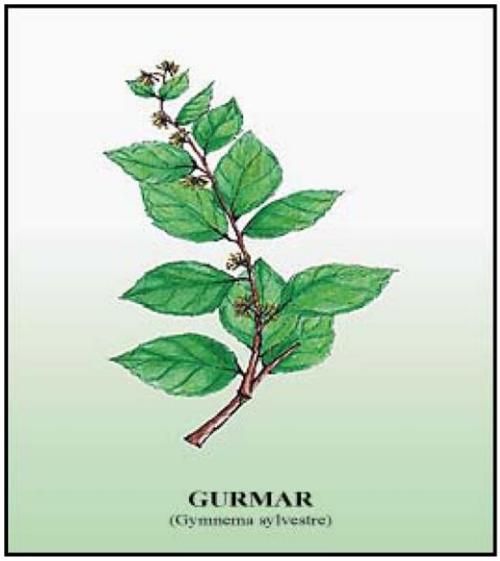

Figure 1.11: *Gymnema sylvestre* plant. 5-years old plant (Kanetkar *et al.*, 2007).

1.11.1 Chemical composition of *Gymnema sylvestre*

Different chemical constituents have been isolated and characterized from the leaves of GS during the past years. The GS leaves contain oleanane and dammarene classes of triterpene saponins. gymnemic acids and gymnemasaponins are Oleanane saponins. At least 17 different gymnemic acids and 7 different types of gymnemasaponins have been identified. Gymnemasides, components of GS, belong to the dammarene saponins group. There are 6 members of gymnemasides (A-F). In addition, a number of other constituents have also been reported in GS leaves (Arai *et al.*, 1995, Liu *et al.*, 2004, Manni and Sinsheimer, 1965, Murakami *et al.*, 1996, Rao and Sinsheimer, 1971, Sahu *et al.*, 1996, Sinsheimer and McIlhenny, 1967, Sinsheimer and Rao, 1970, Sinsheimer *et al.*, 1970, Ye *et al.*, 2000, Yoshikawa *et al.*, 1997a, Yoshikawa *et al.*, 1997b, Zhu *et al.*, 2008). Table 1.10 lists the components that have been isolated from the GS leaves.

GS leaves have been shown to have anti-diabetic, anti-sweetener, anti-dental caries and anti-viral activities. These actions are believed to be mostly mediated by gymnemic acids (GA), although contribution of the remaining isolates is also possible (Porchezhian and Dobriyal, 2003).

GS Chemical Constituents	Examples
Oleanane Saponins	- Gymnemic Acids - Gymnemasaponins
Dammarene Saponins	- Gymnemaside (A-F)
Other constituents	Flavones, Anthraquinones, Hentri-acontane, Pentatriacontane, α, β-Chorophylls, Phytin, Resins, d-quercitol, Tartaric acid, Formic acids, Butyric acids, Lupeol, β-Amyrin, Gymnamine, Conduritol (Alkaloid), Gymnemasin, Gumarin

Table 1.10: Chemical constituents of the leaves of *Gymnema sylvestre* (GS).

1.11.2 Pharmacological actions of *Gymnema sylvestre*

1.11.2.1 Effect on glucose homeostasis

GS dried leaves or aqueous alcoholic extracts have been shown to lower blood glucose levels in both animal and human studies. During the 1960s, Gupta and his co-workers reported that GS had an inhibitory effect on hyperglycemia induced by adrenaline, somatotropin and corticotrophin (Gupta, 1961, Gupta, 1963, Gupta and Variyar, 1961, Gupta and Variyar, 1964). In an attempt to identify the possible mechanism of actions of GS, several studies were conducted. The antihyperglycemic effect of GS was reported to be due, in part, to the ability of plant leaf extract to increase insulin secretion from β-cells of the islets of Langerhans. In a study done by Shanmugasundaram *et al.* 1981, the effect of chronic oral GS administration on glucose and insulin levels was assessed in alloxan-treated rabbits. The results showed that in fasting and post-prandial conditions there were reductions in blood glucose levels and elevations in insulin concentrations in GS-treated diabetic animals in comparison to control animals (Shanmugasundaram *et al.*, 1981). Other research groups reported that single or chronic ingestion of GS attenuated the increase in blood glucose levels and raised insulin levels during oral glucose or sucrose tolerance test in alloxan- or STZ- treated rats (Okabayashi *et al.*, 1990, Shanmugasundaram *et al.*, 1988, Srivastava *et al.*, 1985, Srivastava *et al.*, 1986)

The insulin-releasing effect of GS was further reported by subsequent studies. In a study done by Shanmugasundaram et al 1983, oral administration of a dried leaf powder of GS increased enzymes activities involved in glucose utilization by an insulin- dependent pathway (Shanmugasundaram *et al.*, 1983). A Japanese team led by Sugihara tested the effect of 4 gymnemic acids (GA I-IV). They found that GA-IV,

unlike the other fractions, caused a concentration-dependent fall in blood glucose levels correlated with a rise in insulin concentration in STZ diabetic mice (Sugihara *et al.*, 2000).

In addition to the insulin-releasing activity of GS, GS alcoholic extract may also protect β-cells from damage during the development of diabetes. Histological and morphological studies of pancreata from GS-treated STZ diabetic animals showed an increased number of β-cells compared to untreated diabetic rats. Regeneration or repair of islets of Langerhans may therefore be a possible effect of GS (Ahmed *et al.*, 2010, Shanmugasundaram *et al.*, 1990a).

Suppression of glucose absorption from the small intestine may also contribute to the antihyperglycemic effect of GS aqueous alcoholic extract. A study performed by Shimizu *et al*. (1997) showed that gymnemic acids from GS leaves inhibited glucose uptake through interfering with Na^+-glucose co-transport system (Shimizu *et al.*, 1997a). Similar results were obtained from other studies (Fushiki *et al.*, 1992, Shimizu *et al.*, 1997b, Shimizu *et al.*, 2001).

The effectiveness of GS in controlling hyperglycemia was also tested in patients with diabetes (Balasubramaniam *et al.*, 1988, Khare *et al.*, 1983, Shanmugasundaram *et al.*, 1981). Twenty two patients with T2DM and 27 patients with T1DM on conventional oral anti-hyperglycemic drugs and insulin therapy, respectively, were given 400mg/day GS alcoholic extract. In both groups, the patients showed a significant decrease in blood glucose level. In patients with T2DM, there was a reduction in their drug requirements. Similarly, in patients with T1DM, the insulin requirement came down after GS supplementation although the mechanism by which GS improved T1DM was not clear and may not be directly

mediated by insulin release (Baskaran *et al.*, 1990, Shanmugasundaram *et al.*, 1990b).

1.11.2.2 Effect on lipid metabolism

Alteration in lipid metabolism contributes to the development of T2DM and increased levels of fatty acids, triglyceride, and cholesterol are seen in patients with diabetes. The influence of GS on lipid metabolism has been investigated by a number of researchers. Shigematsu *et al.* (2001) studied the effect of ethanol/water extract of GS on liver lipids. Oral administration of GS to high fat fed rats markedly reduced liver cholesterol and triglyceride levels and prevented fat accumulation in peritoneal cavity (Shigematsu *et al.*, 2001). Furthermore, GS promoted fecal excretion of steroids in high fat fed animals as reported in a number of studies (Nakamura *et al.*, 1999, Terasawa *et al.*, 1994). Wang et al (1998) also reported that GS can alter lipid absorption by reversibly inhibiting oleic acid absorption in rat intestine, in a dose-dependent manner (Wang *et al.*, 1998).

1.11.2.3 Effect on sweet receptors

The leaves of GS were formally called "Gurmar", an Indian word that means sugar-destroying. GS extract reversibly suppressed the sweetness of sucrose, sodium saccharin, glycine and alanine (Meiselman and Halperin, 1970, Meiselman and Halpern, 1970, Warren *et al.*, 1969). The mechanism by which GS modulates sweet taste is not completely understood but may involve blockage of sweet taste receptors by either gurmarin, a peptide found in the GS leaves, or by GA, a triterpene saponin (Imoto *et al.*, 1991, Ninomiya and Imoto, 1995, Suttisri *et al.*, 1995, Yackzan, 1969, Ye *et al.*, 2001). It is postulated that this effect may reduce sugar craving contributing to the antidiabetic effect of GS.

1.12 Costus pictus

Costus pictus (CP), commonly known as spiral ginger, belongs to the Costaceae family and grows in gardens as an ornamental climbing plant. It was originated in Mexico and introduced recently into the southern states of India. CP has shown to have antidiabetic and antioxidant activities (Benny, 2004, Jayasri *et al.*, 2009b).

The first report examined the activities of CP showed that the leaves of this plant were responsible for the antidiabetic properties of CP (Benny, 2004) . The primary analysis of the CP leaves identified several chemical compounds including saponins, alkaloids, tannins, glycosides and flavonoids that may mediate the beneficial actions of CP on diabetes (George *et al.*, 2007).

Figure 1.12: *Costus pictus*, whole plant (Melendez-Camargo *et al.*, 2006).

1.12.1 Antidiabetic actions of CP

The glucose-lowering activity of CP leaves methanolic extract has been tested chronically in animals *in vivo*, where it was reported to reduce blood glucose levels in rats in which hyperglycemia had been induced by administering the β-cell toxins

alloxan or streptozotocin (STZ). Thus, 28 days oral administration of methanolic CP extract to hyperglycemic rats at 2 gm/kg body weight induced a significant ($p<0.001$) reduction in fasting blood glucose levels (Jayasri *et al.*, 2008). Similarly, Jothivel *et al.* also reported a reduction in blood glucose concentrations following a 21 day regime with methanolic extract of CP leaves in alloxan-treated rats (Jothivel *et al.*, 2007). The precise mechanism of the glucose-lowering effect of CP is not completely clear but it may be due, in part, to a direct stimulation of insulin secretion from pancreatic β-cells. Several studies have shown that the reduction of blood glucose in CP-treated animals was associated with increased in plasma insulin levels (Benny, 2004, Jayasri *et al.*, 2008, Jothivel *et al.*, 2007).

The antihyperglycemic activity of CP may also be due to a reduction in carbohydrate absorption. Jayasri *et al.* reported that aqueous CP extract inhibited the activities of α-amylase and α-glucosidase enzymes. Thus CP may prevent the breakdown of carbohydrates and suppress glucose absorption (Jayasri *et al.*, 2009a).

Improving insulin responsiveness in insulin-sensitive tissues may also contribute to the antidiabetic effect of CP. In a study done by Shilpa *et al.*, an extract of CP induced GLUT4 translocation and increased glucose uptake in insulin-responsive tissues (Shilpa *et al.*, 2009).

1.13 Aims and Objectives

Most biologically active compounds isolated from GS leaves have relatively low molecular weights (Murakami *et al.*, 1996, Sinsheimer and Rao, 1970, Sinsheimer *et al.*, 1970, Sugihara *et al.*, 2000), and the previously documented glucose-lowering

activities of GS have been attributed to these low molecular weight components. In this thesis I used a high molecular weight aqueous alcoholic GS extract (Chatterji, 2005a, Chatterji, 2005b) which was subsequently designated as the OmSantal Adivasi extract (OSA®) after the Santal tribe who first used GS leaves in Ayurvedic medicine. Therefore the main aim of this thesis was to examine the role of OSA® and on islet function and to compare OSA® profile to a methanolic extract of CP, another promising plant extract. The detailed objectives are listed below:

Thesis objectives were:

- To test the hypothesis that OSA® and methanolic extact of CP have a direct insulinotropic action on β-cells using MIN6 cells, a β-cell line, and primary islets in perfusion experiments.
- To test the dependence of OSA® and CP on intracellular Ca^{2+} concentrations in fura-2-loaded MIN6 cells and dispersed mouse islets using single cell Ca^{2+} microfluorimetry technique.
- To examine the chronic effect of OSA® on insulin gene expression and biosynthesis.
- To measure the effect of OSA® on intracellular cAMP levels in MIN6 cells and mouse islets.
- To explore the possible signaling pathways activated following OSA® exposure using pharmacological inhibitors of VGCC and protein kinases.
- To determine the effect of OSA® on glucagon secretion from mouse islets.

- To determine the effect of OSA® on β-cell mass and apoptosis by measuring caspase levels in MIN6 cells and mouse islets and identifying the possible underlying pathways of the cytoprotective effect of OSA® using microarray gene expression.

Chapter 2

Materials and Methods

2.1 Plant material and preparation

2.1.1 *Gymnema sylvestre* extract

The GS extract used in this study (OSA®) was prepared by extracting fresh GS leaves by aqueous alcohol according to the protocols described in the US Patents 6949261 and 6946151 (Chatterji, 2005a, Chatterji, 2005b). Briefly, GS leaves were soaked first in water for 18 hours (1 Kg/4 L) and then aqueous alcohol (40% ethanol) for 4 hours at room temperature. The solution was filtered and then treated with sulphoric acid to recrease the pH to 2. Any acid-insoluble salt that was precipitated was removed by filtration. The filtrate was neutralized with sodium hydroxide and seperated according to size using a membrane having a molecular weight cut-off of 3 KDa. The material retained by the membrane was collected and concetrated using a rotary flask in water bath (55-70C°). The final product was light brown powder.

GS leaves were identified by a botanist, and a voucher specimen (reference GS1-OSA1-G123/C) was deposited with Ayurvedic-Life International LLC (Neenah, WI 54946-0010, USA). The OSA® extract used in this study was a gift from Ayurvedic Life International LLC, Wisconsin, USA. OSA® solutions were freshly prepared for glucose tolerance test (GTT) as a 100 mg/ml stock in water for use in the *in vivo* animal study and 200 mg/ml stock in water and diluted in Gey & Gey buffer (Table 2.1) (Gey and Gey, 1936) for use in the *in vitro* experiments.

Reagents	Concentration (mM)
NaCl	111
$NaHCO_3$	27
KCl	5.0
$MgCl_2.6H_2O$	1.0
$MgSO_4.7H_2O$	0.28
KH_2PO_4	0.22

Table 2.1: Gey and Gey buffer

2.1.2 *Costus pictus* extract

Costus pictus (CP) leaves were collected from Kerala Agricultural University Mannuthy and a voucher specimen is deposited in the VIT University herbal garden, Vellore, Tamil Nadu (VIT/CP/G1). The leaves were processed as follows. Shade dried plant material was ground into powder and an extract was prepared by successive maceration of the powder (10 g) at room temperature with methanol for 48h in a shaker. The final extract was filtered and the filtrate was lyophilized to obtain a powdered extract. The powder was provided by M. A. Jayasri from VIT University. The extract was stored as a 100 mg/ml stock and diluted as appropriate in a physiological salt solution (Gey & Gey buffer) for use in experiments. The yield of the dry extract as a percentage weight of the starting fresh leaves of CP was 1.42%.

In vivo study

2.2 Studies using animals

2.2.1 Ob/ob mice

In 1949, an outbred colony at Roscoe B. Jackson Memorial lab was discovered and named ob/ob mice (OM). The OM has been used as a model of obesity and T2DM.

The major characteristic of the OM is that they are deficient in leptin. Leptin is a polypeptide hormone secreted from adipocytes and plays a key role in regulating food intake and energy expenditure. The lack of leptin in OM produces certain phenotypic features in these animals. They are infertile, hyperphagic, obese and insulin resistant. The hyperinsulinemia in OM develops after 2-weeks of birth while hyperglycemia is evident at the fourth week and peaks after 3-5 months. The pancreatic islets of OM are hyperplasic and have high number of β-cells (> 90% of cells are β-cells) (Ingalls *et al.*, 1950, Lindstrom, 2007, Lindstrom, 2010, Wolf, 2001).

2.2.2 Experimental Animals

Obese hyperglycemic male ob/ob mice (Harlan, UK) were used. They were produced by selective mutation of the Ob gene which encodes the hormone leptin. Insulin resistance and glucose intolerance was seen as soon as 2-4 weeks after birth. Lean male C57BL/6J mice (Charles River, Margate) served as controls to establish the obesity and hyperglycemia status of the ob/ob mice. The weight and fasting blood glucose of each mouse were measured before the start of experiment.

2.2.3 Glucose tolerance test

Glucose tolerance tests (GTT) were performed to evaluate the glucose intolerance status of the ob/ob mice. Before GTT, ob/ob or C57BL/6J mice were starved for at least 16 hours. 2 g/Kg body weight of 30% glucose was injected intraperitoneally (IP) and the glucose concentration was measured in blood samples taken from the tail vein at baseline and 15, 30, 60 and 120 minutes of glucose injection. Blood glucose measurements were performed using an Abbott glucometer (mediSence

opium 99765-15). To investigate the effect of a single oral dose of OSA® on blood glucose in ob/ob mice, 500mg/Kg of OSA® or vehicle was administered by gavage 30 minutes before performing the GTT. All experiments using animals were performed under UK Home Office License (PPL no. 70/5848).

Stduies using human subject examining the effect of OSA® in patients with T2DM was also carried out by our collegues in Burdwan Medical College clinic, West Bengal, India and is detailed in Appendix 1.

In Vitro studies

2.3 MIN cells

MIN cell lines are one of the insulinoma cell lines that have been developed by targeted expression of SV40 (Simian Virus) T antigen into pancreatic β-cells of transgenic mice. MIN6 cells have been used in our lab and considered to be a good and useful tool to study β-cell function. They rapidly transport and metabolize glucose by GLUT-2 and glucokinase, respectively. In addition, MIN6 cells have insulin secretory granules and secrete insulin in response to glucose. The glucose dependent increase in insulin secretion resembled that of isolated islets from rats and mice. The major disadvantage of MIN6 cells is that they have an unstable phenotype. Low passage cells respond to glucose in a concentration dependent manner but this ability is lost with high passage cells when they are kept in culture for prolonged period of time (Ishihara *et al.*, 1993, Persaud, 1999). Configuring the MIN6 cells as islet-like aggregates known as pseudoislet is one way of maintaining some glucose-dependent insulin secretion (Hauge-Evans *et al.*, 1999).

2.3.1 Cryopreservation and reconstitution of cells from frozen storage

The process by which cells or tissues are preserved by cooling to sub-zero temperature is called cryopreservation. Liquid nitrogen is used to achieve a temperature of -196C°, at which temperature any biological activity inside the cells is stopped. However, cells may die from sudden freezing. Therefore, slow programmable freezing is now widely used to avoid the freezing-induced rupture of intracellular compartment of cells. To cryopreserve MIN6 cells, 70-80% confluent MIN6 cells were trypsinized and resuspended in 10% DMSO containing DMEM. DMSO acts as cryoprotectant. Cells were homogenized by pipetting up and down and then transferred into 1ml cryovials. These vials were placed into a Nalgene® container and kept at -80C° overnight. Nalgene® contains a solution of 100% isopropyl alcohol and has the advantage of a controlled cooling rate of -1C°/minute. The vials were then transferred to liquid nitrogen for long-term storage.

MIN6 cells were reconstituted from frozen storage when needed for experiments. One cryovial ampoule containing MIN6 cells was defrosted quickly in water bath at 37C°. The cells were transferred into 15ml centrifuge tube, mixed with 10ml of DMEM and pelleted by centrifugation. The pellet was resuspended in DMEM and cultured in T-25 flask.

2.3.2 Maintenance of MIN6 cells

MIN6 cells (passage 28-44) were maintained as monolayers at 37C° (95% O_2/ 5% CO_2) in DMEM supplemented with 10% foetal calf serum (FCS), 2mM L-glutamine and 100 U/ml penicillin with 0.1 mg/ml streptomycin in tissue culture flask with 75cm^2 growing surface area (T-75). The medium contains vitamins and amino acids

and has a high glucose (25mM) content to meet the metabolic requirements for MIN6 cells growth. MIN6 cells form monolayers if cultured in negatively-charged tissue culture plastic which allows the adherence of MIN6 cells to their surface forming monolayers. Figure 2.1 shows the MIN6 cells growing as monolayers.

The medium was changed every 3-4 days and the MIN6 cells were detached and trypsinized when the flask confluency reached ≈ 70-80%. 0.1% trypsin/0.02% EDTA was used for trypsinization. Briefly, the medium was aspirated and the cells were washed with phosphate buffered saline (PBS). A T-75 flask containing MIN6 monolayers was incubated with 3 ml of trypsin/EDTA mixture at 37C° for 3-5 minutes to allow the detachment of MIN6 cells from the plastic surface. Seven ml of DMEM was added to inactivate trypsin since DMEM contains FCS which inhibits trypsin. The flask content was transferred to a sterile 15 ml falcon tube and centrifuged at 1000g for 3 minutes. The supernatant was discarded and the cell pellet was resuspended in 1ml DMEM. Ten µl of the resuspension was used for cell counting as described in section 2.7.

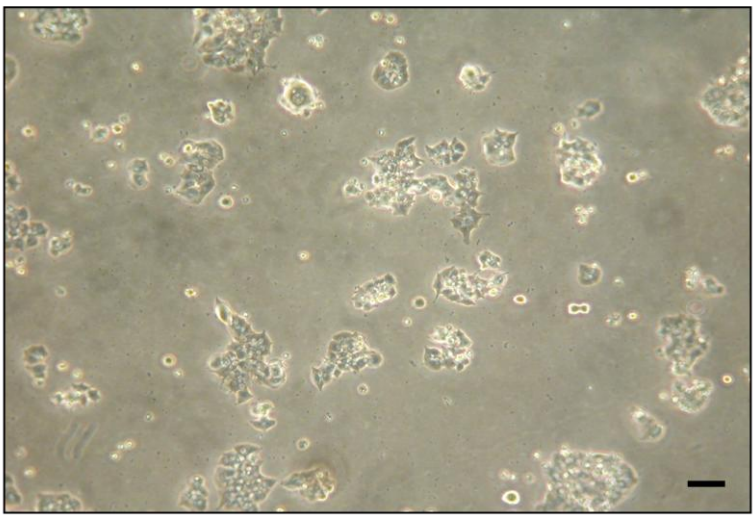

Figure 2.1: MIN6 cells (P 30) grow as monolayers. Bar shows 10µm.

2.3.3 Formation of MIN6 Pseudoislets (PIs)

To form PIs, MIN6 monolayers were trypsinized and cultured in 10 ml DMEM supplemented with 10% FCS, 2mM L-glutamine and 100 U/ml penicillin with 0.1 mg/ml streptomycin in 90mm bacterial Petri dishes at 37C° (95% O_2/ 5% CO_2). Incubation of MIN6 cells in bacterial Petri dishes prevents the adhesion of MIN6 cells to plastic surfaces and as a result MIN6 cells adhere to each other and form three-dimensional aggregates called pseudoislets (PIs). The medium was changed every 3-4 days and PIs were used in the experiments 7-10 days after subculturing of the MIN6 cells. Figure 2.2 shows the MIN6 cells growing as PIs.

Figure 2.2: MIN6 cells growing as pseudoislets. The micrograph shows the PIs 8 days after subculturing. Bar shows 50µm.

2.4 Isolation of mouse islets

The pancreata of outbred white albino ICR (Harlan, UK) mice were digested by collagenase as described previously (Papadimitriou *et al.*, 2007). Briefly, the mouse

was killed by neck dislocation and the abdominal area was opened. The common bile duct was exposed and clamped. Once collagenase (1 mg/ml) was injected, the pancreas was removed and digested at 37C°. The digested pancreas was washed with EMEM supplemented with 10% NCS (neonatal calf serum) and 100 U/ml penicillin with 0.1 mg/ml streptomycin and sieved into a sterile tube. The islets were purified on Histopaque® density gradients and cultured in 35mm bacterial dishes in RPMI medium supplemented with 10% FBS and 100 U/ml penicillin/0.1 mg/ml streptomycin.

2.5 Isolation of human islets

Human islets were provided by Dr. Guo Cai Huang, King's Human Islet Isolation Unit at King's College Hospital, UK. Briefly, pancreas was removed from non-diabetic heart-beating organ donor with permission from donor relatives and approval from Ethical Committee of King's College Hospital. Islets were isolated under aseptic conditions and cultured in Connaught Medical Research Laboratories (CMRL) medium at 37C° (95% O_2/ 5% CO_2). The islets were ≈ 90% viable and 70-80% pure (Brandhorst *et al.*, 1998, Huang *et al.*, 2004, Lakey *et al.*, 1997).

2.6 Counting of MIN6 cells

Cell counting was performed using a haemocytometer, consisting of 4 corner squares, each of which is composed of 16 smaller squares. It also contains centrally located square which has 25 smaller squares. All corner and centre squares have a total area of 1 mm^2. Placing a cover slip on the haemocytometer creates a chamber with a volume of 0.1 mm. Therefore, the total volume is 1 mm^2 x 0.1 mm or 0.1

mm^3. Since 1 cm^3 is equivalent to 1 ml, the cell number/ml is calculated as the average count of the 4 peripheral squares x dilution factor x 10^4.

2.7 Insulin secretion

2.7.1 Static incubation of MIN6 cells

MIN6 monolayer cells were seeded into a 96-well plate at a density of 20,000-30,000 cells/well and cultured in DMEM supplemented with 10% FCS, 2mM L-glutamine and 100 U/ml penicillin with 0.1 mg/ml streptomycin at 37C° for 2 days. Before the experiment, MIN6 cells were pre-incubated in 2mM glucose Gey & Gey buffer supplemented with 2mM $CaCl_2$ and 0.5 mg/ml BSA at 37C° for 120 minutes. The cells then were incubated with buffer containing either 2mM or 20mM glucose in the presence or absence of agents of interest for 30 minutes. At the end of the incubation period, 100µl of incubation medium was removed, added to 400µl borate buffer (Table 2.2) and stored at -20C° until insulin was measured by RIA.

Reagents	Concentration (mM)
Boric acid	133
EDTA	10
NaOH	67.5
BSA	1 mg/ml

Table 2.2: Borate buffer

2.7.2 Static incubation with mouse islets

Three or 5 mouse islets were transferred into 1.5 ml eppendorf tubes and preincubated for 2hrs, at 37C°, in RPMI supplemented with 2mM glucose. Following 2hrs incubation, the medium was replaced with the agent of interest for 30-60

minutes. The supernatant was removed and stored at -20C° until assayed for insulin content by RIA.

2.7.3 Perifusion with MIN6 PIs, mouse or human islets

The perifusion apparatus consists of 16 Swinnex chambers, each of which is lined with 1 μm pore-size nylon filter and connected by tubes to perifusion buffers and a peristaltic pump. The pumping of perifusion buffers occurs at a flow rate of 0.5 ml/min and perifusates are collected every 2 minutes. Since glucose metabolism is temperature-dependent, all perifusion experiments were done in a temperature-controlled room at 37C°. MIN6 PIs, mouse islets or human islets were aliquoted into perifusion chambers containing the nylon filter, and pre-perifused with 2mM glucose Gey & Gey buffer supplemented with 2mM $CaCl_2$ and 0.5 mg/ml BSA for 60 minutes at flow rate of 0.5 ml/min, during which the perifusate was discarded. At t=60 minutes, the tissues were perifused with Gey & Gey buffer supplemented with either 2mM or 20mM glucose in the presence or absence of agents of interest. The perifusion samples were collected every 2 minutes and stored at -20C° until insulin content was determined by RIA.

2.8 Total insulin content of mouse islets

Five mouse islets were transferred into 1.5 ml eppendorf tubes and incubated for 24hrs, under normal tissue culture conditions, with RPMI supplemented with 2mM glucose in the presence or absences of agent of interest. Following the 24hrs and 48 hrs incubation, the islets were washed with PBS, sonicated in acidified alcohol and stored at -20C° until assayed for insulin content by RIA.

2.9 Radioimmunoassay (RIA)

2.9.1 Background

Radioimmunoassay was developed by Yalow and Berson in 1960 and since then immunoassays represents the most popular method to measure insulin content in biological and non-biological fluids. The assay is based on competition between unlabelled insulin or antigen (standards or unknown samples) and a fixed amount of ^{125}I-labelled insulin (Tracer) for a limited number of insulin antibody binding sites (Ab). This reaction follows the law of mass action:

$$[AG] + [AG^*] + [Ab] \rightleftarrows [AG\ Ab] + [AG^*\ Ab] + [AG] + [AG^*]$$

From the above equation, the amount of labelled insulin bound to antibody [AG^* Ab] is inversely proportion to concentration of unlabelled insulin [AG] (standards or samples). Calculating the concentration of unlabelled insulin (unknown samples) can be done by measuring the radioactivity of labelled insulin [AG*] (Tracer) and extrapolating from a standard curve (Yalow and Berson, 1960).

2.9.2 Iodination and purification of insulin

A radioactive isotope of iodine ^{125}I (commercially available as Na^{125}I) was used in the labelling of insulin and the synthesis of the tracer. The high specific radioactivity, the absence of β radiation and the relatively long half-life ($t_{1/2}$=60 days) of ^{125}I make it preferable over other radio-isotopes. The iodination of insulin reaction involves two steps 1) oxidation of ^{125}I to iodous ion (I^+) by a mild oxidizing agent, Iodogen and 2) binding of the oxidized iodine ion into a tyrosine residue, an iodine receptor group, of insulin molecules. Iodogen, 1,3,4,6-tetrachloro-3a,ba-diphenylglycoluril, acts as oxidizing agent for ^{125}I. It is highly soluble in chloroform

but insoluble in water so when dispersed in chloroform Iodogen forms a coating layer surrounding the walls of a reaction tube after vaporization of the chloroform. The deposit formed is inaccessible to insulin but accessible to ^{125}I thus reducing the oxidation of insulin by Iodogen. Purification and separation of the iodinated-insulin is necessary to remove molecules other than iodinated-insulin and radio- active iodine not conjugated to insulin from the reaction mixture. Separation is done using gel filtration technique. This technique enables the use of a gel, Sephadex G-50, to separate the labelled insulin from the reaction by-products. Sephadex, or dextran gel, forms hydrophobic bonds with tyrosine moieties of insulin. Thus albumin-containing elution solutions are used in order to avoid adsorption and retention of insulin on the gel and column wells (Patrona and Peskar, 1987).

Pre-prepared 50µl of 200µg/ml of Iodogen in chloroform was dispensed in a reaction tube and the solvent left to evaporate to form Iodogen deposits. 1mg/ml of insulin in 10mM HCl was freshly prepared and diluted 8 times in 0.5M phosphate buffer. 40µl of insulin was mixed with 20µl of ^{125}I (activity 74 MBq) and incubated at room temperature for 30 minutes with occasional mixing every 5 minutes. The iodination reaction was stopped by adding 400µl of 50mM phosphate buffer. The sephadex beads were precoated with 50mM phosphate buffer supplemented with bovine serum albumin (BSA) to prevent insulin adherence to them. 50mM phosphate buffer was used as an elution solution and samples were collected every 2 minutes for 60 minutes. The radioactivity of each sample was measured using the γ-counter (Wizard) and samples with the highest counts/minute (cpm) were pooled and diluted to final concentration of $10x10^6$ cpm/ml. Figure 2.3 shows the iodination curve of insulin.

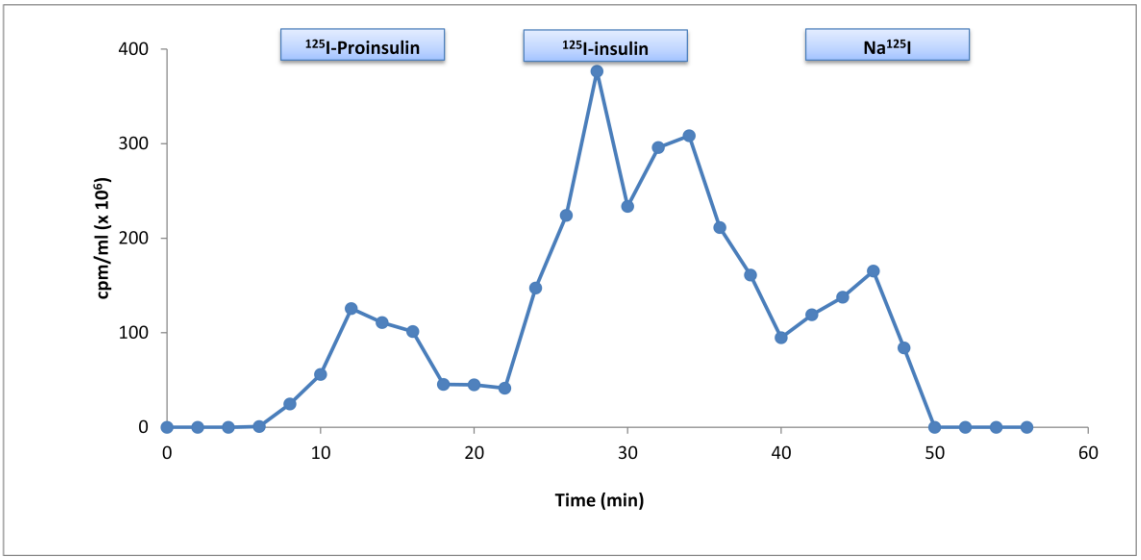

Figure 2.3: The iodination curve of Insulin. Iodinated insulin was separated using Sephadex G-50. The radioactivity of the collected samples was measured using a γ-counter. The first peak (12 min) represents fractions contained iodinated proinsulin which is followed by fractions that contained the highest amount of iodinated insulin (30 min). The last peak (45 min) separated contained the remaining radioactive isotope of iodine ($Na^{125}I$). Samples with the highest counts/minute (cpm) for ^{125}I-insulin were pooled, diluted to final concentration of $10x10^6$ cpm/ml and stored at 20C°.

2.9.3 RIA protocol

Standard tubes were prepared in triplicates from 10ng/ml insulin by serial dilution to give final concentration of 10, 5, 2.5, 1.25, 0.64, 0.32, 0.16, 0.08, 0.04 ng/ml. Reference tubes were made as the following: Total (T) contained only 100 µl of labelled insulin to measure the amount of radioactivity added to each tube. Non-specific binding (NSB) contained only 100 µl tracer and 200 µl borate buffer. It was used to correct for all the measurement in the assay. Maximum binding (MB) contained 100 µl of each of the following: tracer, antibody and borate buffer. The antibody aganist rat insulin was raised in guinea pigs. The samples were prepared in duplicates and contained 100µl of sample and 100 µl of both tracer and antibody. The insulin RIA protocol is given in Table 2.3 and the standard curve is shown in Figure 2.4.

The assay tubes were kept at 4C° for 48 hours to allow the binding and equilibrium between antibody and labelled and unlabelled insulin. The antibody bound antigen complexes were precipitated by adding 1 ml of polyethelenglycol (PEG) mixture containing 1 mg/ml γ-globulin, 15% PEG in PBS and 0.05% Tween to each tube except to the total (T) and centrifuged at 3000 rpm for 15 minutes. Supernatant was discarded and the radioactivity of the pellets containing the complexes was measured using the γ-Counter (Wizard).

	Buffer	AB	Tracer	Standard	sample
Total (T)	-	-	100 µl	-	-
Non-Specific Binding (NSB)	200 µl	-	100 µl	-	-
Maximum Binding (MB)	100 µl	100 µl	100 µl	-	-
Standard	-	100 µl	100 µl	100 µl	-
Samples	-	100 µl	100 µl	-	100 µl

Table 2.3: Protocol for Insulin RIA

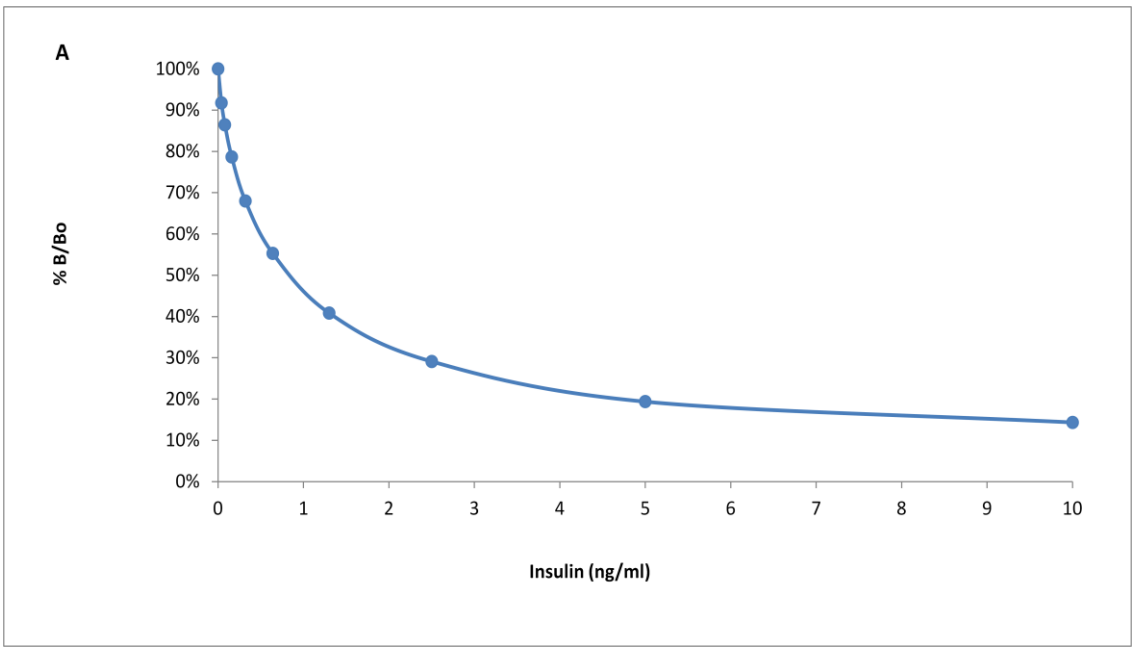

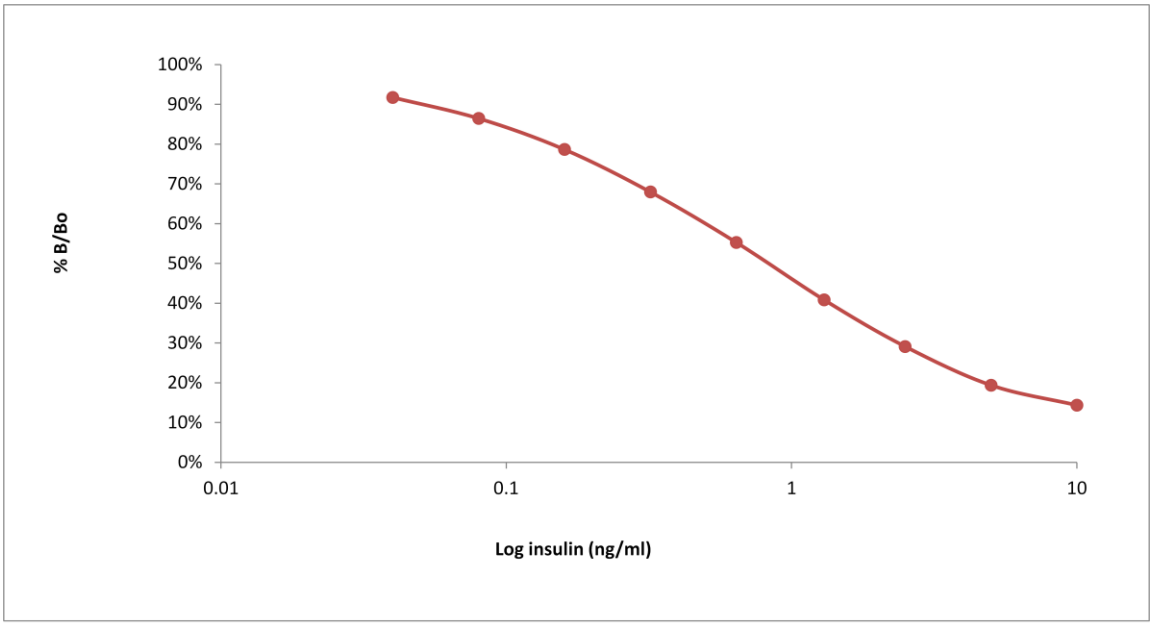

Figure 2.4: Insulin standard curve. (A) Insulin (ng/ml) is plotted against the percentage of antigen binding over maximum binding (B/Bo). (B) Log insulin (ng/ml) is plotted against the percentage of antigen binding over maximum binding (B/Bo).

2.10 Glucagon secretion

Measurement of glucagon secretion was carried out using perifusion experiments similar to section 2.7.3. 100 mouse islets were transferred into perifusion chambers containing the nylon filter. Islets were pre-perifused with 2mM glucose Gey & Gey buffer supplemented with 2mM $CaCl_2$ and 0.5 mg/ml BSA for 60 minutes to establish basal rate of glucagon secretion. Any perifusate collected during this time were discarded. Following 60 minutes, islets were perifused with 2mM glucose Gey & Gey buffer at a flow rate of 0.5 ml/min in the presence or absence of agent of interest. Perifusate samples were collected every 2 minutes and stored in -20C° until assayed for glucagon by RIA.

2.11 Cell viability

To estimate the proportion of viable and non-viable cells, the Trypan Blue exclusion test was used. This test depends on the fact that viable cells can be differentiated

from non-viable cells through the integrity of their membranes. Viable cells have intact cell membranes that prevent the entry of macromolecules such as Trypan Blue dye (MW ≈ 1000 Da) while non-viable cells have compromised plasma membranes therefore they become permeable to the dye, which has the ability to stain nuclear proteins. Hence non-viable cells appear blue under the light microscope (Johnson, 1995).

In our experiment, MIN6 cells or mouse islets, treated with the agent of interest, were stained and incubated with 0.1% (wt/vol) Trypan Blue dye in PBS for 15 minutes at 37C°. The cells were then washed with PBS and visualized under the light microscope. Images were captured using a Nikon Coolpix 4500 digital camera (Surrey, UK).

2.12 Calcium microfluorimetry

2.12.1 Background

Calcium microfluorimetry is an important technique in estimating intracellular Ca^{2+} concentration $[Ca^{2+}]_i$ in a single β-cells. It uses fluorescent Ca^{2+} indicators which emit light as a result of changes in $[Ca^{2+}]_i$. The fluorescent Ca^{2+} indicators are divided into two groups: single-wavelength dyes (single-wave length indicators) and dual wavelength ratiometric dyes (ratiometric indicators). The ratiometric indicators include Fura-2, Indo-1 and Rhod-2. The advantages of Fura-2 and ratiometric indicators in general over those of single wavelength include 1) the marked sensitivity of Fura-2 since the peaks of Ca^{2+}-free and Ca^{2+}-bound spectra arose at different wavelength and 2) Fura-2 is excited at two wavelengths allowing the estimation of a ratio which correlates well with changes in $[Ca^{2+}]_i$ thus

minimizing Ca^{2+}-unrelated artefacts. The major drawback of Fura-2 is its poor membrane permeability. Therefore, Fura-2 is provided as Fura-2/AM. The introduction of acetoxymethyl (AM) group masks the –ve charge on the carboxy group on Fura-2 molecule and facilitates the entry of Fura-2 into the cells. However, Fura-2/AM is inactive and enzymatic hydrolysis by esterases inside the cells is needed to liberate the active Fura-2, which then trapped inside the β-cells (Kao, 1994, Murchison and Griffith, 2007).

2.12.2 Preparation of coverslips

MIN6 cells were seeded on ethanol-washed glass coverslips which were first soaked in 2N acetic acid for 1hr at room temperature and then washed with deionised water. To disinfect the coverslips, they were soaked with 70% ethanol for 1hr. They were then washed with deionised water and left to dry in a sterile tissue culture hood for at least 1hr. The coverslips were sterilized by UV light for few seconds and stored at 4C° for further use in experiments.

To measure $[Ca^{2+}]_i$ in mouse islet cells, they were seeded on poly-D-lysine coated coverslips. One side of the acid-washed ethanol coverslips were covered with 0.1 mg/ml poly-D-lysine in PBS and left for 10 minutes. The coverslips were then washed with sterile water, left to dry in a tissue culture hood and stored at 4C° for further use in experiments

2.12.3 Seeding cells

MIN6 cells were trypsinized and resuspended in serum-free DMEM. The cells were placed on the coverslips and left to adhere for 2hrs at 37C°. Following 2hrs, DMEM supplemented with serum was added and cells were incubated for overnight. 300

islets were dissociated using EDTA, resuspended in serum-free RPMI and placed on poly-D-lysine coated coverslips and left to adhere for 1hr. The cells were maintained in culture for overnight RPMI supplemented with serum.

MIN6 cells were seeded on ethanol-washed glass coverslips at a density of 50,000 cell/coverslip while dispersed mouse islets were seeded on poly-D-lysine glass coverslips at a density of 160,000 cells/coverslip and allowed to adhere overnight under standard tissue culture conditions.

2.12.4 Procedure

The cells were loaded with 5μM of the Ca^{2+}-fluorophore Fura-2/AM for 30 minutes at 37C°. The coverslips were placed in a steel chamber which was mounted into a heating platform (37C°) on the stage of an Axiovert 135 Research Inverted Microscope. The cells were perifused with buffers containing the agents of interest at a flow rate of 1 ml/min. Cells were illuminated alternately at 340 and 380nm using an Axon Imaging Work-bench (Axon Instruments). Emitted light was filtered using a 510nm long pass barrier filter and detected using a Photonics Science ISIS camera. Data were collected every 3 seconds for multiple regions of interest in any one field of view and changes in the emission intensity of Fura-2 expressed as a ratio of dual excitation were used as an indicator of changes in $[Ca^{2+}]_i$.

2.13 Measurement of intracellular cAMP

Intracellular cAMP $[cAMP]_i$ in MIN6 cells or mouse islets was measured by enzyme immunoassay as stated by manufacturer's protocol. Briefly, MIN6 cells (30,000 cells/well) or mouse islets (5 islets/well) were incubated with Gey & Gey buffer in the presence or absence of agents of interest for 30 minutes at 37C°. The

supernatant was removed and stored at -20C° for estimation of insulin content. The cells were lysed and incubated with Rabbit anti-cAMP serum for 2 hrs at 3-5C°. cAMP-horseradish peroxidase conjugate was added to each well and incubated for an extra 1 hr. The wells were thoroughly washed with 0.01M phosphate buffer containing 0.05% tween 20 for at least 3 times. Enzyme substrate containing TBM (tetramethylbenzidine/1% hydrogen peroxide) was dispensed into each well and left for 30 min at room temperature. Once the blue color had developed, the reaction was stopped by addition of 1.0 M sulphuric acid. The concentration of $[cAMP]_i$ was determined relative to a standard curve by measuring the optical density at 450 nm. Figure 2.5 shows the standard curve of cAMP obtained in the experiment.

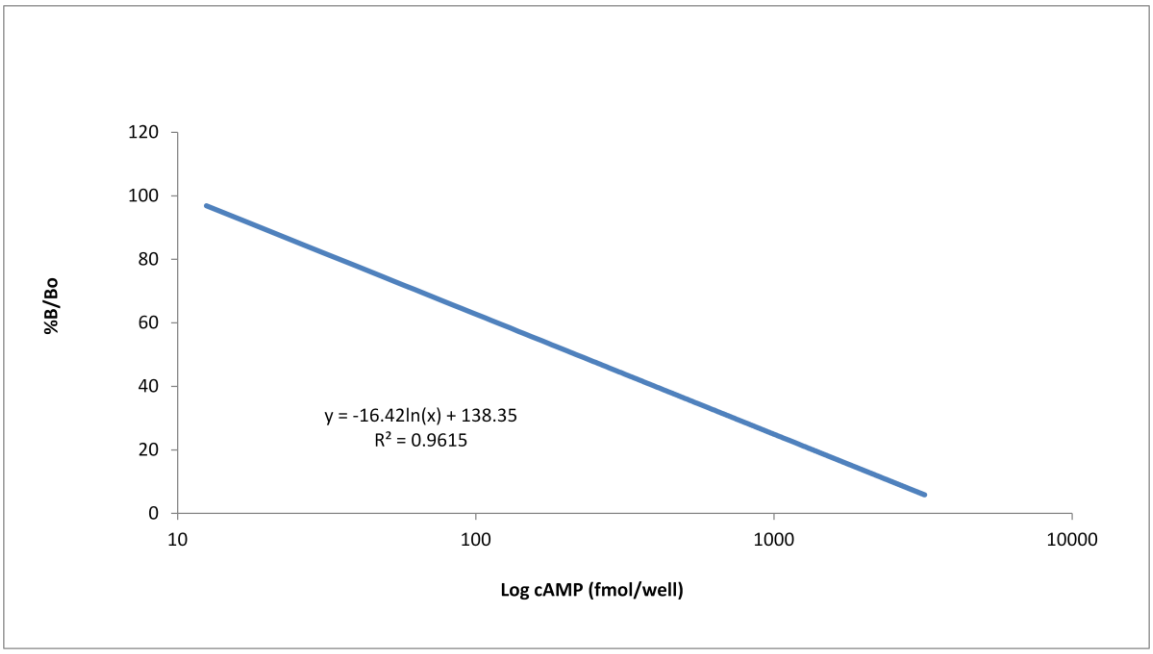

Figure 2.5: Standard curve of cAMP. Log cAMP (fmol/well) concentration is plotted against the percentage of antigen binding over maximum binding (B/Bo).

2.14 Measurement of apoptosis

2.14.1 Background

Caspases are the major proteolytic enzymes that are activated during apoptosis. In our experiments we measured caspases 3 and 7. The caspase 3/7 was measured using Caspase-Glo® 3/7 apoptosis assay kit (Promega, UK). The assay uses the luminogenic substrate (Z-DEVD-amino-luciferin) and a stable luciferase enzyme (Figure 2.6). Caspases cleaves the substrate liberating free amino-luciferin which can then be acted upon by luciferase to generate a luminescent signal which is directly proportional to caspase 3/7 activity (Promega, 2009) .

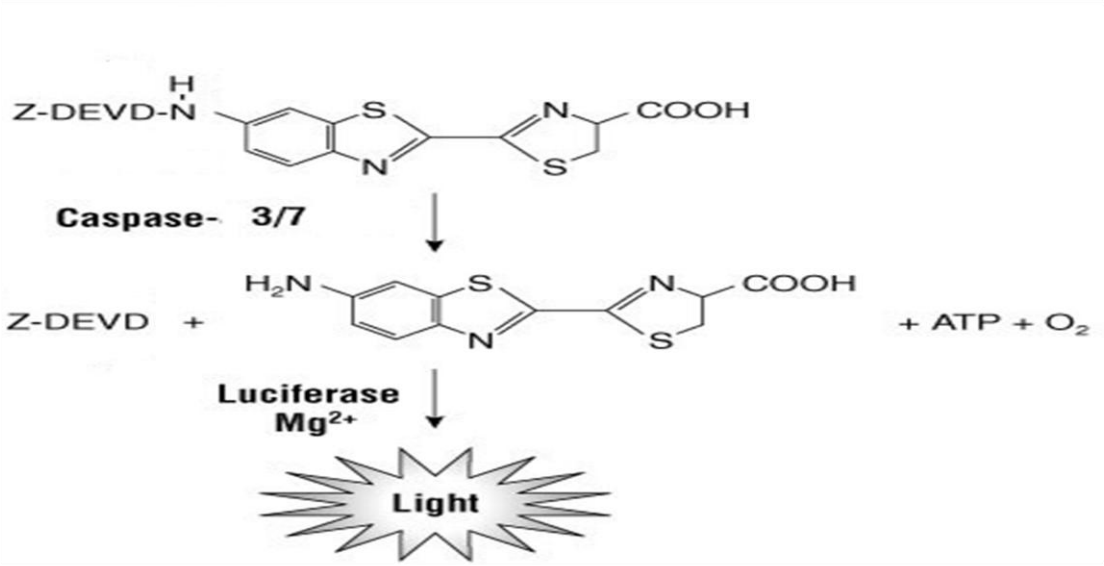

Figure 2.6: The reaction of caspase 3/7 and its luminogenic substrate containing Z-DEVD. Caspase 3/7 releases amino-luciferin. Luciferase acts on its substrate (amino-luciferin) and generates light (Promega 2009).

2.14.2 Assay protocol

MIN6 cells (10,000 cells/well) or mouse islets (5 islets/well) were seeded in white 96-well plates and left overnight under standard tissue culture conditions. On the day of the experiment, cells were preincubated with the agent of interest for 8 hrs before incubation with the agent of interest in the presence or absence of cytokines

for 16-18 hours. Caspase 3 and 7 activities were measured using Promega caspase-Glo® 3/7 assay kit (Promega Cat G8093) according to manufacturer procedure. Briefly, Caspase-Glo® 3/7 buffer was mixed with Caspase-Glo® substrate to form Caspase-Glo® reagent. Both Caspase-Glo® reagent and the cells were left to equilibrate at RT for 1 hr, after which, 50µl of Caspase-Glo® reagent was added to each well of the 96-well plate, mixed for 30 sec and incubated for 1 hr. The luminescent signal generated was measured using Veritas luminometer (Turner Biosystems) and the data were processed using Promega software

2.15 mRNA estimation

2.15.1 RNA extraction

Mouse RNA was extracted using Qiagen RNeasy mini kit according to the manufacturer's protocol. 150 islets treated with agents of interest were washed with PBS and lysed with RLT (a highly denaturing guanidine thiocyanate-containing buffer) supplemented with 14.3M β-mercaptoethanol, which immediately inactivates RNases to ensure purification of intact RNA. The lysed cells were transferred into RNase-free 1.5 eppendorf tube and homogenized by vortexing & passing the lysate 5 times through a 20-G needle fitted to an RNase-free syringe. One volume of 70% ethanol was added to the lysate and mixed by pipetting up and down to provide appropriate binding condition. The sample was applied to a RNeasy mini spin column, where the total RNA binds to the membrane. Each tube was centrifuged for 1 minute at 12,000 rpm and the flow-through was discarded. The column was washed with RW1 and the flow-through was discarded. Any residual DNA was removed by on-column DNase digestion using the RNase-Free DNase Set. The DNase-I stock was prepared by dissolving DNase-I stock with 550µl

RNase-free water. The DNase-I mix was prepared by mixing DNase-I with buffer RDD. 80µl of DNase-I mix was added to each column. The contaminants were washed with 350µl RW1 (ethanol-containing buffer) and then 500µl RPE (80% alcohol-containing buffer) and the flow-through was discarded. The column was centrifuged for an additional minute to dry it. The column was transferred into clean 1.5 RNase-free eppendorf tube and the RNA was eluted in 30µl RNase-free water.

2.15.2 RNA quantification

RNA concentrations were quantified spectrophotometrically, using 1 µl of RNA of each sample in the nanodrop-1000, by reading the absorbance at 260/280nm wave length. An efficacy ratio of ~ 2 indicated the purity of the RNA sample. The Concentration of each sample was calculated according to the following equation:

Concentration of RNA(ng/µl)= A_{260} x dilution factor x 40

2.15.3 cDNA synthesis

0.5 µg of RNA was converted to cDNA using Moloney Murine Leukemia Virus Reverse Transcriptase (mmLV-RT; Invitrogen 18080-044). The conversion was carried out according to the mmLV-RT manufacturer's procedures. Briefly, 0.5 µg of RNA of each sample was first mixed with 0.5µg/µl Oligo dT primer and 0.5µg/µl random primer. Each sample was incubated at 72C° for 5 minutes and then chilled on ice for 5 minutes. 18µl of Master Mix (Table 2.4) was added to each sample. The reaction was initiated by incubating the samples at 42C° for 50 minutes and inactivated by incubating the samples at 70 C° for 15 minutes. The samples were stored at -20 C° for quantitative PCR.

	For 40µl reaction	Final concentration
5 X RT buffer	8µl	1X
DTT (400mM)	1µl	10mM
Ribonuclease inhibitor (Rnasin 40U/µl)	4µl	160U
dNTP (10mM)	2µl	500µM
mmLV-RT (200U/µl)	2µl	400U
DNase/RNase-free H_2O	1µl	-

Table 2.4: The master mix content of reverse transcription reaction

2.16 Polymerase chain reaction (PCR)

The polymerase chain reaction (PCR) was discovered by Karry Mullis in 1983 and since then it has been widely used in molecular biology. PCR is an *in vitro* method for amplifying a defined sequence of DNA using a thermo-stable DNA polymerase enzyme. Real time PCR (RT-PCR) is a highly sensitive method for detection and quantification of mRNA as compared to conventional PCR methods. RT-PCR collects data by monitoring fluorescence emitted during the reaction in an exponential growth phase as the fluorescence signal generated corresponds to the amount of PCR products amplified in each cycle during the reaction, unlike traditional PCR where the PCR amplification products are measured at the end point (plateau). RT-PCR quantifies mRNA transcripts using fluorescent indicators. There are three major fluorescence systems for DNA amplification so far: 1) DNA-binding dyes (SYBR green), 2) hydrolysis probes (Taqman and scorpion) and 3) hybridizing probes (molecular beacons). SYBR green is a fluorescent intercalating agent that exhibits little fluorescence in solution but upon binding to double stranded DNA (ds DNA) it emits strong light (522nm) after excitation at 498nm. SYBR green is widely

used in RT-PCR due to the fact that it is cheap, simple to use, temperature stable and does not interfere with DNA polymerase. In addition, SYBR green can be used to monitor any gene since it does not discriminate between double-stranded DNA sequence. The non-specificity of SYBR green binding can result in binding of SYBR green to primer and non-specific amplification products. This can be overcome by performing melting curve analysis. The melting point of ds DNA is the temperature when 50% of DNA is singley stranded. Another potential drawback of SYBR green is the amplicon length which can be overcome by synthesizing primers that amplify short amplicons. Short amplicons (200-300 bp) can be amplified efficiently than the long ones because long amplicons generate strong fluorescence signals that can saturate the camera inside the thermocycler (Bustin, 2000, Nolan *et al.*, 2006).

The RT-PCR reaction and incorporation of SYBR green dye involve three major steps (Figure 2.7). In denaturation, DNA is unwound by heating the reaction tube to 94-95C°. At this step SYBR green is unbound therefore emitting little if any fluorescence. The temperature is reduced to 55-72C° (dependent on primer sequence) allowing annealing of the primer to the single stranded (ss) DNA to take place. Few molecules of SYBR green bind to the ds-primer/DNA and emit light upon excitation. During extension, DNA polymerase (at 72C°) adds new nucleotides to the free 3'-OH of the primers forming new templates of DNA. As the new synthesis of DNA continues, more molecules of the dye bind to the new strand and fluorescence is increased. The fluorescence is detected when it exceeds the threshold cycle (C_T point). CT is the cycle number at which fluorescence emission crosses the threshold (above baseline) and it reflects the amount of templates available at the start of the reaction. Thus the more templates present at the beginning of the reaction, the

lower the CT value and the fewer number of cycle needed for the fluorescence to exceed the baseline (Bustin, 2000).

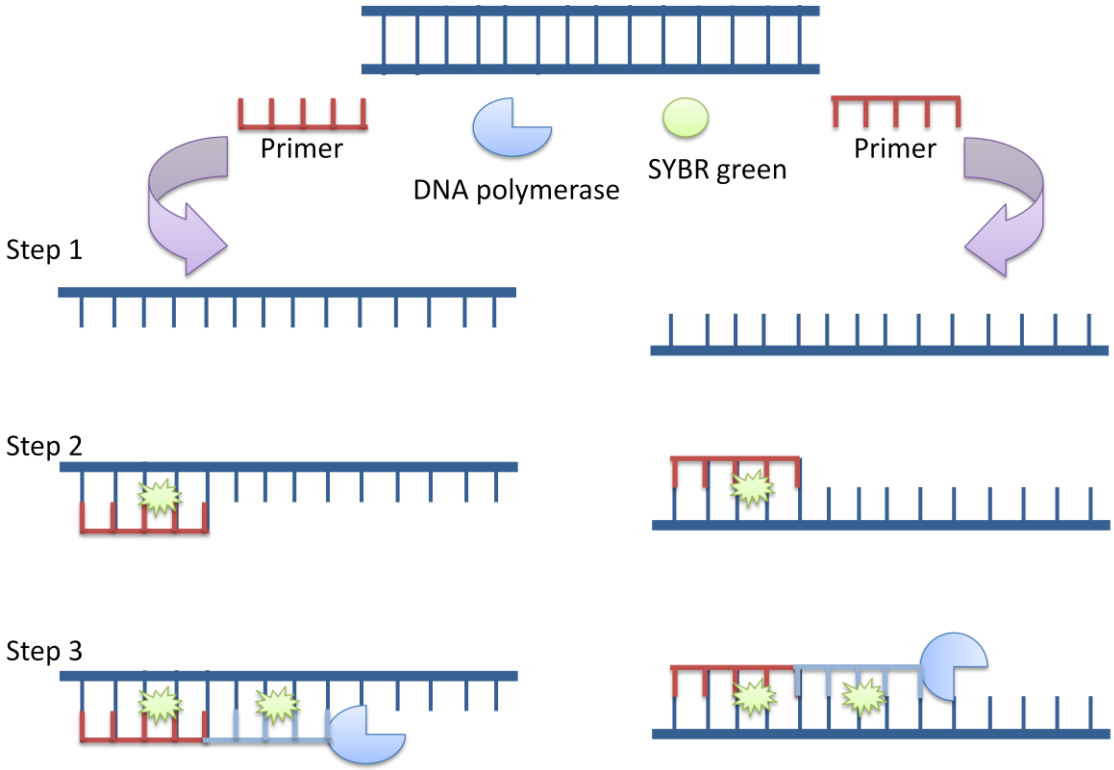

Figure 2.7: Schematic representation of SYBR green-based quantitative RT-PCR. 1) Denaturation (94-95C°): The cDNA is unwound first with few if any SYBR green bound to ss DNA. 2) Annealing (55-72C°): The primers bind to ds DNA. SYBR green then binds to DNA/primer complex and emits light upon excitation. 3) Extension (72C°): DNA polymerase enzyme synthesizes new templates of DNA. As the new synthesis of DNA continues, more molecules of the dye bind to the new strand and fluorescence is increased (Bustin, 2000)

Quantification of mRNA transcription can be either relative or absolute with the latter being more accurate then the former. Absolute quantification or standard curve method calculates the exact copy number/sample and is based on construction of an absolute standard curve for each amplicon. Extrapolation from the standard curve can be used to calculate the copy number of unknown sample.

2.16.1 Primer design and synthesis

The whole sequence of each gene was found on pubmed nucleotide network (http://www.ncbi.nlm.nih.gov/nuccore). The primers were designed using Primer

3 software (http://frodo.wi.mit.edu/primer3/). Primer 3 software was set to synthesize primers that have similar annealing temperature, amplify short amplicons (100-300 bp), and have GC contents of 40-60%. The specificity of primers was checked by nucleotide BLAST (Basic Local Alignment Search Tool; http://blast.ncbi.nlm.nih.gov/Blast.cgi). Mouse preproinsulin I and II cDNA sequences were used to design forward and reverse PCR primers that detected both preproinsulin mRNAs. The preproinsulin and actin were designed to amplify a 125 and 285 bp target PCR product, respectively, and their sequences are given in Appendix 2.

2.16.2 Gel electrophoresis

1.8% agarose gel was prepared for electrophoretic separation of the PCR products. 900mg of agarose was dissolved by microwaving for approximately 1 minute in 50ml 1x Tris-Base-EDTA (TBE, sigma, UK). Five µl of ethidium bromide (10mg/ml) was added to the dissolved agarose to give a final concentration of 1 µg/ml. The gel was poured in a comb-containing tank and left to solidify for 30-60 minutes. The gel was submerged with 1x TBE. The PCR products which were mixed with 5x loading dye (Qiagen) were loaded into the wells. The gel was developed at 75 volts for 30 minutes.

2.16.3 Preparation of standards

A standard curve of each gene of interest was prepared to allow for absolute quantification of the unknown samples. A PCR reaction for each gene was carried in duplicates. A gel electrophoresis was performed as described in section 2.17.2 and the product was visualized under UV light. A single band of the expected product

size was generated in all samples. The bands were excised, pooled and DNA was extracted using QIAquick® gel extraction kit (Qiagen). Briefly, the excised gels were weighed, mixed with 3 volumes of QG buffer (e.g 100mg ~ 300µl QG) and incubated at 50C° for 10 minutes until the slices were completely dissolved. The tubes were vortexed every 2-3 minutes during the incubation time to aid in solubilization. Isopropanol (v/v) was added to the dissolved gel slice which then were applied to the QIAquick® spin columns and centrifuged (13,000 rpm) for 1 minute. The flow-through was discarded and 0.5 ml of QG buffer was added to the column and centrifuged for 1 minute. The columns were washed with 0.75 ml of ethanol-containing PE buffer and centrifuged for 1 minute to remove any salts. The flow-through was discarded and any residual ethanol from the PE buffer was removed by centrifugation for an additional 1 minute. The columns were placed into clean 1.5 ml RNase-DNase tube and DNA was eluted in 30µl of RNase-DNase water. The DNA was quantified using NanoDrop-1000. The number of copies/µl was calculated as follows:

Number of molecules in 1 ng = (Avogadro no./ molecular weight of product) x 10^{-9}

The molecular weight of product is the average molecular weight of a base pair (660) multiplied by the length of the product.

Total number of copies/µl= concentration of the product (ng) x number of copies/ng

Serial dilutions were made to prepare standards ranging from 10^{9}-10^{1} in RNase-DNase water.

2.16.4 Quantitative PCR

Quantitative-PCR was carried using Roch® thermocycler (LightCycler 480) and LightCycler® FastStart DNA master^{PLUS} SYBR green I (Roch®, UK). At the start of the experiment, SYBR green mix was prepared by mixing 14µl of the enzyme with the dye. A master mix was prepared as detailed in Table 2.5. 16µl of master mix was added to either 4µl of cDNA or standard or water (Negative Control; NC) or RNA (not reverse transcribed, -RT).

	For 20µl reaction	Final concentration
Forward primer (10µM)	1µl	500nM
Reverse primer (10µM)	1µl	500nM
10X SYBR green I mix	2µl	1x
Water	12µl	-
Total	16µl	

Table 2.5: The master mix content of 20µl reaction for quantitative RT-PCR

Primer specificity was assessed by melt curve analysis followed by gel electrophoresis. mRNA accession number, cycling conditions, gel electrophoresis, melt curve analyses, assay efficiencies of standard curves series for each gene are described in Appendix 2.

2.17 Microarray

Applications of cDNA microarray in biological sciences are numerous and include measurement of mRNA expression levels, detection of single nucleotide polymorphisms (SNPs) and genotyping or resequencing part or whole genome. cDNA microarray consists of collection of short sequence of DNA (probes) that are

attached to a solid surface (silicone). Each probe is complimentary to a target sequence. The probe-target hybridization is detected optically by either fluorophore or chemiluminescence-labelled target. The labelled target generates a signal once they bind to the probes. The signal generated is directly proportional to the amount of target sample alreadu bound to the corresponding probes. In our experiment, Affymetrix chips (GeneChip® mouse genome 430 2.0 array) were used to measure the expression levels of mRNA. Each chip has 45,000 set of probes which detect the expression levels of more than 39,000 transcripts. The measurement of transcription level is based on the fact that each probe has 11 pairs which include a perfect match and a mismatch probe .

2.17.1 Measurement of RNA integrity

The quality of RNA samples was assessed using Agilent RNA 6000 Nano kit. Each kit contains four solutions: the ladder, dye concentrate, marker and gel matrix. The gel was prepared by pipetting 550µl of the gel matrix into a spin filter and centrifuging the mixture at 1500g for 10 minutes at room temperature. 65µl of the filtered gel was aliquoted into 0.5ml RNase-free tubes and used within 4 weeks of preparation. To prepare the gel-dye mix, the dye concentrate was left to equilibrate to room temperature for 30 minutes before mixing 0.5µl of the dye with 35µl of the filtered gel. This mix was vortexed well and centrifuged at 13000g for 10 minutes at room temperature. Before loading the gel-dye mix, the Nanochip was placed in the chip priming station. 9µl of the dye-gel mix was pipetted into the well marked (G). The chip priming station was closed and a plunger was pressed down until it was held by the clip. The clip was released after 30 seconds, the plunger was pulled back and the chip priming station was opened. 9µl of the gel-dye was pipetted into the

remaining wells marked (G). 5µl of the marker was loaded in all samples wells and in well marked #. 1µl of the ladder was pipetted into its corresponding well. The ladder was denatured by heating for 2 minutes at 70C°. 1µl of each sample was loaded into the 12 remaining wells. The chip was vortexed at 2400 rpm for 1 minutes and run in the Agilent 2100 bioanalyzer.

2.17.2 RNA amplification

Amplification and labelling of RNA samples for microarray analysis was carried out using the MassageAmp™ Premier RNA amplification kit. The protocol involves cDNA synthesis, *in vitro* transcription and aRNA (amplified RNA) purification. Figure 2.8 summarizes the RNA amplification process.

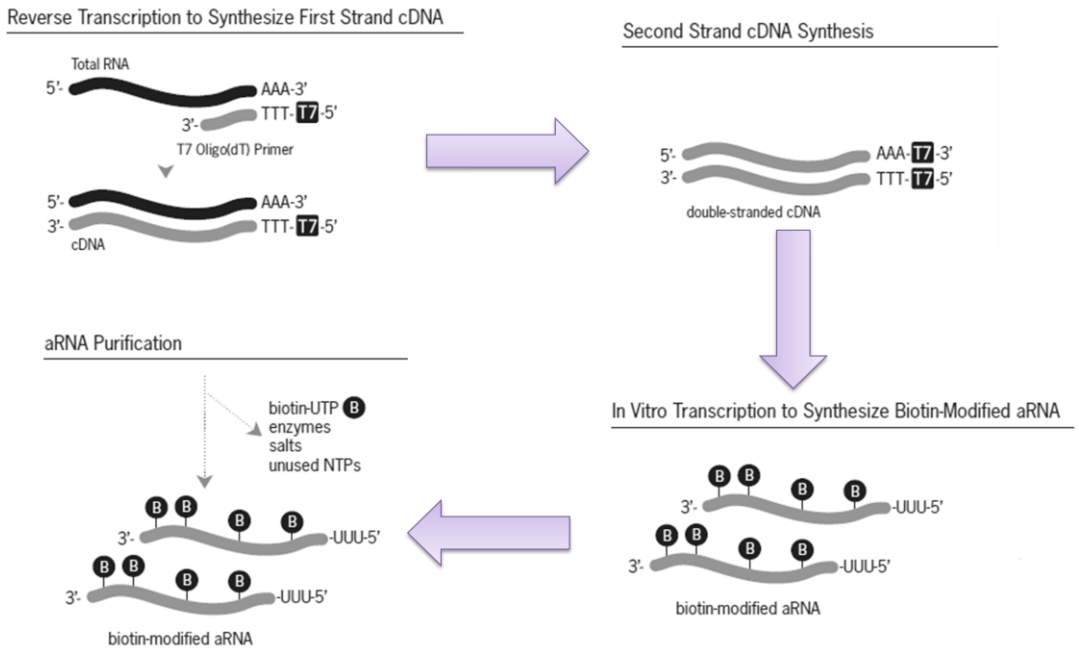

Figure 2.8: Schematic representation of MessageAmp™ Premier RNA amplification procedure. The reaction started by reverse transcribe RNA to first strand cDNA using T7 oligo(dT) primer. The second strand cDNA is synthesized using DNA polymerase The double stranded DNA is amplified and labelled with T7 Biotin. All the excess salts, enzymes and reagents from the previous reactions are removed during the purification process to improve the stability of biotin-modified aRNA.
(http://www3.appliedbiosystems.com/cms/groups/mcb_marketing/documents/generaldocuments/cms_055030.pdf).

2.17.2.1 cDNA synthesis

The First Strand cDNA was synthesized by mixing 500 ng of RNA with 5µl of First Strand Master Mix (Table 2.6). The mixture was incubated for 2 hours at 42C° in thermal cycler. The Second Strand cDNA was synthesized by incubating 10µl cDNA sample and 20µl of Second Strand Master Mix (Table 2.7) for 1 hour at 16C° and then 10 minutes at 65C°. The double stranded (ds) cDNA is ready for the *in vitro* transcription.

	Amount
First strand buffer Mix	4 µl
First strand enzyme Mix	1 µl
Final volume	5 µl

Table 2.6: First-Strand Master Mix for single reaction

	Amount
Second strand buffer Mix	5 µl
Second strand enzyme Mix	2 µl
Nuclease-free water	13 µl
Final volume	20 µl

Table 2.7: Second-Strand Master Mix for single reaction

2.17.2.2 *In vitro* transcription (IVT)

The RNA was amplified and labelled with biotin using oligo T7. 30µl of ds cDNA sample was mixed with 30µl T7 IVT Master Mix (Table 2.8). The reaction was incubated for at least 14 hours at 40C°.

	Amount
T7 Biotin IVT Mix	20 µl
T7 enzyme Mix	6 µl
Nuclease-free water	4 µl
Final volume	30 µ

Table 2.8: T7 IVT Master Mix for single reaction

2.17.2.3 aRNA purification and elution

To ensure the removal of salts and enzymes from the previous reactions, the aRNA was purified as follows. Each sample was mixed with 60µl of aRNA Binding Mix (Table 2.9) and then transferred to a U-bottom plate. 120µl of 100% ethanol was added to the wells and the plate was shaken for 2 minutes at 900 rpm. The RNA binding beads were captured by placing the plate on a magnetic stand for 5 minutes. The RNA binding beads will form a pellet in the bottom of the plate with a transparent supernatant. The supernatant was discarded. The plate was removed from the magnetic stand and the samples were washed twice with 100µl of aRNA wash solution. The plate was shaken for 1 minute at 1200 rpm and the beads were captured as previously described. The plate was shaken vigorously for 3 minutes at 4000 rpm to evaporate any residual ethanol. The purified aRNA was eluted from the RNA binding beads by adding 50µl of pre-heated (50-60C°) aRNA elution solution to each sample. The plate was shaken vigorously for 3 minutes at 4000 rpm and the RNA binding beads were captured as previously described. The aRNA- containing supernatant was transferred to RNase-free tubes.

	Amount
RNA Binding Beads	10 µl
aRNA Binding buffer concentrate	50 µl

Table 2.9: aRNA Binding Mix

2.17.3 Fragmentation of labelled aRNA

To hybridize the array chip, 15.5µg of biotinylated aRNA was fragmented by incubating the reaction with 5x array fragmentation buffer (Table 2.10) at 94C° for 35 minutes. 1µl of fragmented aRNA was removed to test the quality of the fragmentation reaction. The reaction should yield a profile of 25-500 nucleotides of aRNA fragments with a peak at approximately 200 nucleotides. The fragmented aRNA was used in the hybridization step.

	Concentration
Tris Acetate, pH 8.2	200 mM
Potassium Acetate	500 mM
Magnesium Acetate	150 mM

Table 2.10: 5x Array Fragmentation buffer composition

2.17.4 Hybridization of fragmented aRNA

30µl of each fragmented aRNA was transferred to 1.5 ml RNase-free screw tube. 270µl of hybridization cocktail Master Mix (Table 2.11) was added to each sample. The full cocktail mix was first denatured for 5 minutes at 99C° then for 5 minutes at 95C°. After denaturation, the mixture was centrifuged for 5 minutes at 14000 rpm. 200µl of the supernatant was used to hybridize the chip.

	Amount	Final concentration
Control Oligo B2 (3nM)	5.03 µl	50 pm
20x Eukaryotic hybridization control	14.96 µl	1 x
2x Hybridization buffer (100mM MES*, 1M sodium chloride, 0.01% Tween 20 and 0.M EDTA)	149.6 µl	1x
DMSO	20.94 µl	7%
Nuclease-free water	79.47 µl	-
Final volume	270 µl	
* MES: 2-(N-Morpholino) ethansulphonic acid		

Table 2.11: Hybridization Cocktail Master Mix composition

2.17.5 Chip hybridization

Mouse 430 2.0 Array Affymetrix Genechips® were used. The chips were pre-hybridized with pre-hybridization buffer for 10 minutes at 40C° in the oven. The pre-hybirdization buffer was removed from the chip and replaced with 200µl of the full hybridization cocktail. The chips were incubated in the oven at 45C° for at least 16 hours. After 16 hours, the full hybridization cocktail was removed and replaced with the array holding buffer. Now the chip is ready for the washing and staining steps.

2.17.6 Washing, staining and scanning of Affymetrix chips

The Fluidics station 450 was primed with Wash A for 15 minutes before placing the chips in their corresponding chambers. Each chip was stained with 600µl of two stain solutions: stain cocktail 1 (Table 2.12) and stain cocktail 2 (Table 2.13).

	Amount	Final concentration
2x Stain buffer (100mM MES, 1M Sodium chloride and 0.05% Tween 20)	600 µl	1x
Acetylated BSA (50 mg/ml)	48 µl	2 mg/ml
Streptavidin-phycoerythrin (1 mg/ml)	12 µl	10 µg/ml
Nuclease-free water	540 µl	
Final volume	1200 µl	

Table 2.12: Stain solution 1

	Amount	Final concentration
2x Stain buffer (100mM MES, 1M Sodium chloride and 0.05% Tween 20)	300 µl	1x
Acetylated BSA (50 mg/ml)	48 µl	2 mg/ml
Normal Goat IgG (10 mg/ml)	6 µl	100 µg/ml
Biotinylated antibody (0.5 mg/ml)	3.6 µl	3 µg/ml

Table 2.13: Stain solution 2

The wash/stain protocol is summarized in Table 2.14. The compositions of Wash A, Wash B and Array holding buffers are summarized in Table 2.15, 2.16 and 2.17, respectively. Acquisition of images was done using Affymetrix GeneChip® Command Console (AGCC). The Chips were scanned at 570nm using GeneChip® Scanner 3000 7G. The signal intensity was normalized and analyzed using Affymetrix Expression Console software and Affymetrix Microarray Suite (MAS 5.0). MAS 5.0 uses algorithm of the average of the differences in perfect match and mismatch probes. Mismatch probe is used to measure the background noise levels for each probe pair.

Protocol	Description
Post Hybridization wash #1	10 cycles of 2 mixes/cycle with Wash A at 25C°
Post Hybridization wash #2	4 cycles of 15 mixes/cycle with Wash B at 50C°
1st Stain	Stain the probe array for 10 min in Stain 1 at 25C°
Post Stain wash	10 cycles of 4 mixes/cycle with Wash A at 25C°
2nd Stain	Stain the probe array for 10 min in Stain 2 at 25C°
3rd Stain	Stain the probe array for 10 min in Stain 1 at 25C°
Final Wash	15 cycles of 4 mixes/cycle with Wash A at 30C°
Holding	1 cycle of 3 mixes/cycle with 1x array holding buffer at 25C°

Table 2.14: Fluidics wash/stain protocol for Affymetrix Genechip® mouse Genome 340 2.0 Array

	Final concentration
20x SSPE (3M NaCl, 0.2 M NH_2PO_4, 0.02 M EDTA)	6 X
Tween 20 (10%)	0.01 %

Table 2.15: Wash A buffer composition for 1000 ml

	Final concentration
MES	100 mM
Sodium chloride	0.1 M
Tween 20 (10%)	0.01 %

Table 2.16: Wash B buffer composition for 1000 ml

	Final concentration
MES	100 mM
Sodium chloride	1 M
Tween 20 (10%)	0.01 %

Table 2.17: 1x Array Holding buffer for 100 ml

2.17.7 Quality control of gene chip array

To assess the validity of the results of a microarray experiment, certain quality control measures were considered. These measures allow for direct comparison between chips and assure sample quality (illumina, 2010). The criteria for quality control included:

- Number of gene detected: all similar samples should have similar amount of transcript detected. A gene expression chip normally has 40-60% gene present. Low number of detected genes usually reflect high background or poor signal.
- Housekeeping genes and background: the expression of housekeeping genes should be fairly consistent among samples. The signals from housekeeping genes should be higher than that produced from the background. In Affymetrix chip, GAPDH, β-actin, transferring receptor and pyruvate carboxylase are the housekeeping genes used as control genes.
- Hybridization controls: Affymetrix chips have probes for eukaryotic RNA (bioB, bioC, bioD and cre). These probes are used as controls and their expression profile should produce a signal of low > intermediate > high.
- Measures of normality and correlation: histogram and box plot were used to determine the variation between arrays. Abnormal and dissimilar distribution of signal intensities between samples hinder direct comparison between samples. Pearson correlation was used to test the association between samples. Similar samples show strong correlation.

2.18 Data Analysis

Data are represented as mean ± SEM. In perifusion experiments with more than one treatment, the mean represents the area under the curve. Differences between treatments groups were assessed using analysis of variance (ANOVA), Student's t-test, and Bonferroni's multiple comparison test as appropriate and considered significant at $p < 0.05$.

Chapter 3

Gymnema sylvestre stimulates insulin secretion from mouse and human β-cells *in vivo*

3.1 Introduction

The prevalence of diabetes mellitus is growing worldwide and it has been estimated that by the year 2030, 440 million people will be suffering from this disease, with the vast majority having Type 2 diabetes mellitus (T2DM) (Internaional Diabetes Federation, 2009). The most common pharmacological treatments for T2DM, sulphonylureas and biguanides, tend to lose their effectiveness with prolonged treatment duration, so new pharmacological agents have been employed, including Peroxisome Proliferator-Activated Receptor-γ (PPARγ) agonists and agents that stimulate insulin secretion such as Glucagon-Like Peptide-1 (GLP-1) analogues and Dipeptidyl Peptidase IV (DPPIV) inhibitors (Persaud and Jones, 2008). However, the widespread application of these novel agents is limited by their cost and by concerns about their long-term safety (VanDeKoppel *et al.*, 2008, Persaud and Jones, 2008).

Some herbal medicines have been shown to have anti-diabetic activities (Alarcon-Aguilara et al., 1998, Swanston-Flatt et al., 1991, Yeh et al., 2003). Nevertheless, few have been shown to be effective in treating the symptoms of T2DM in rodents and humans, and their mechanisms of action are uncertain.

Crude or low molecular weight GS extracts have been reported to have anti-diabetic effects in alloxan- or streptozotocin-treated animals by raising plasma insulin levels and attenuating blood glucose responses during oral glucose/sucrose tolerance tests (Gupta, 1961, Gupta, 1963, Gupta and Variyar, 1961, Mhaskar and Caius, 1930, Okabayashi *et al.*, 1990, Shanmugasundaram *et al.*, 1983, Srivastava *et al.*, 1985, Srivastava *et al.*, 1986). Similarly, crude or low molecular weight GS extracts have been reported to have hypoglycemic effects in patients with hyperglycemic diabetes

(Baskaran *et al.*, 1990, Khare *et al.*, 1983, Shanmugasundaram *et al.*, 1981, Shanmugasundaram *et al.*, 1990b). The antihyperglycemic effect of GS extracts in these studies was postulated to be due, at least in part, to the ability of the plant leaves to increase insulin secretion from β-cells of the islets of Langerhans, although this was not directly demonstrated.

The studies described in this chapter investigated the effects of oral OSA® on glucose tolerance in an animal model of T2DM, as prelude to identifying the site and mechanism of action of OSA®.

3.2 Materials and Methods

3.2.1 Experimental Animals

Obese hyperglycemic male ob/ob mice (10 animals) were used, in which insulin resistance and glucose intolerance is seen as soon as 2-4 weeks after birth. Lean male C57BL/6J mice (10 animals) served as control to establish the obesity and hyperglycemia status of ob/ob mice. The weight and fasting blood glucose of each mouse were measured before the start of the experiment (Section 2.2.2).

3.2.2 Plant extract preparation

The GS extract used in this study (OSA®) was prepared by extracting fresh GS leaves by aqueous alcohol and fractionating it using molecular weight cut-off filtration (Chatterji, 2005a; 2005b). GS leaves were identified by a botanist, and a voucher specimen (reference GS1-OSA1-G123/C) was deposited with Ayurvedic-Life International LLC (Neenah, WI 54946-0010, USA). The OSA® extract used in this study was a gift from Ayurvedic Life International LLC, Wisconsin, USA. OSA®

solutions were freshly prepared for glucose tolerance test (GTT) as a 100 mg/ml stock in water (section 2.1.1).

3.2.3 Glucose tolerance test (GTT)

Glucose tolerance tests (GTT) were performed to test the glucose tolerance status of ob/ob mice as compared to their control (C57BL/6J) mice (section 2.2.3). Before GTT, the ob/ob mice or C57BL/6J mice were starved for at least 16 hours. 2 g/Kg body weight of 30% glucose was injected intraperitoneally (IP) and blood glucose level was measured in samples taken from the tail vein at baseline and 15, 30, 60 and 120 minutes of glucose injection. Blood glucose measurements were performed using an Abbot glucometer (mediSence opium 99765-15). To investigate the effect of a single oral dose of OSA® on blood glucose in ob/ob mice, 500mg/Kg of OSA® or vehicle was administered by gavage 30 minutes before performing the GTT. All experiments using animals were performed under UK Home Office License (PPL no. 70/5848).

3.2.4 Statistical analysis

Data are represented as mean ± SEM unless otherwise stated. Differences between treatment groups were assessed using analysis of variance (ANOVA) and Bonferroni's T test for multiple comparisons or Student's paired T test (two tailed), as appropriate. Differences between treatment groups were considered significant when $p < 0.05$.

3.3 Results

3.3.1 Effect of single OSA® administration in mouse model of diabetes

Table 3.1 summarizes the major characteristics of the experimental animals. In ob/ob mice, fasting blood glucose levels were markedly elevated as compared to their corresponding control values. In addition, the weights of ob/ob mice were significantly higher than those of the controls. During the glucose tolerance tests, ob/ob mice showed deterioration in glycemic control as presented by the elevation in circulating blood glucose at all time points when compared to their controls (Figure 3.1). A single oral administration of OSA® (500mg/Kg) to ob/ob mice 30 minutes prior to glucose challenge significantly ameliorated the glucose intolerance status of these mice (Figure 3.2) with OSA®-treated ob/ob mice showing a significant reduction in blood glucose levels and this effect was apparent at t=90 and 120 min. Vehicle-treated ob/ob mice remained glucose intolerant throughout the experiment.

Parameter	Control mice	ob/ob mice
Body weight (g)	23.3 ± 0.3	47.9 ± 1.06 ***
FBG (mM)	4.9 ± 0.2	12.0 ± 0.7 ***

Table 3.1: The major characteristics of the experimental animals. Following 16 hrs starvation, body weight and fasting blood glucose (FBG) were determined before the start of the experiment. Ob/ob mice had higher body weight and FBG as compared to their control mice (C57BL/6J mice), *** p<0.0001 versus controls. n= 10 mice

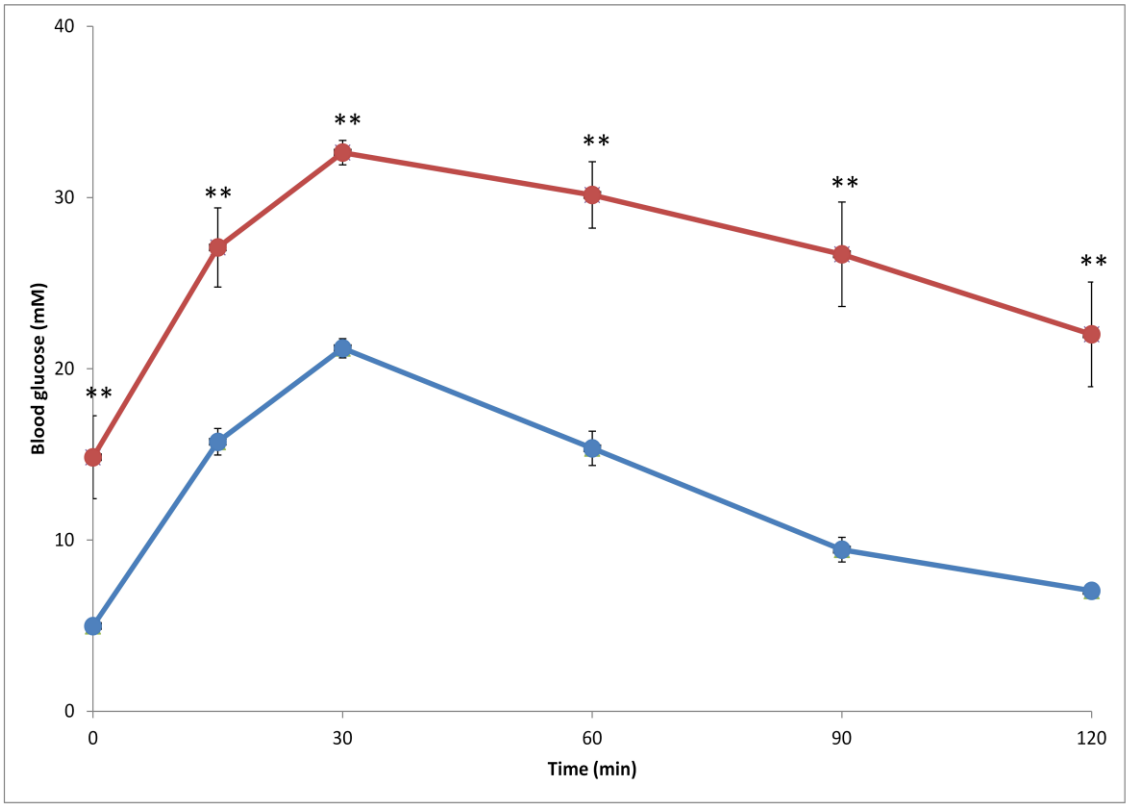

Figure 3.1: Glucose tolerance curves of ob/ob mice and C57BL/6J mice. Following 16 hrs starvation, blood glucose was measured before and 15, 30, 60 and 120 min after 2g/kg of 30% glucose load. Ob/ob mice (●) had an impaired glucose tolerance as compared to control mice (●). Blood glucose concentrations were significantly higher in ob/ob mice versus controls at all time points (p<0.01). Data are means ± SEM. n=10 mice.**

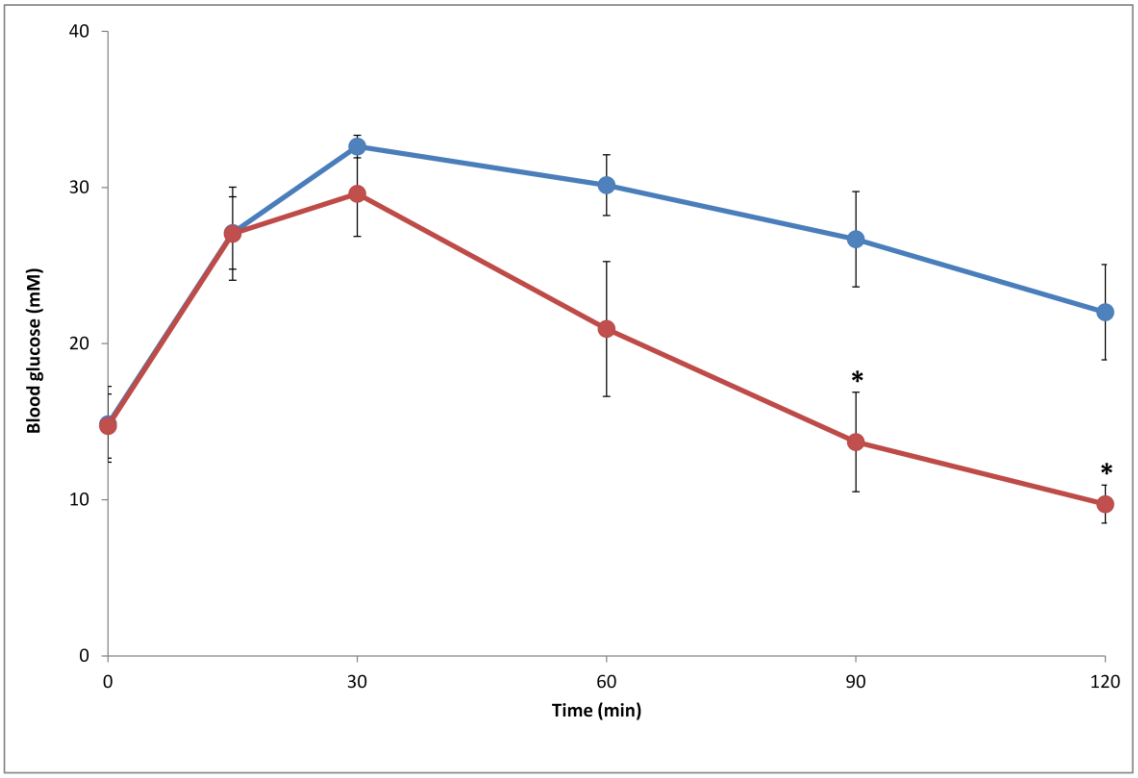

Figure 3.2: Effect of single OSA® administration on IP glucose tolerance in ob/ob mice. OSA® was administered orally 30 min prior to the glucose tolerance test. OSA® significantly improved glucose tolerance in ob/ob mice (●) as compared to ob/ob mice treated only with vehicle (●), * p<0.05 versus untreated ob/ob mice. Data are means ± SEM. n=10 mice.

3.4 Discussion

Crude extracts of GS leaves or low molecular weight isolates from GS extracts have been reported to reduce hyperglycemia in alloxan or streptozotocin-animal models of diabetes (Gupta, 1961, Gupta, 1963, Gupta and Variyar, 1961, Mhaskar and Caius, 1930, Okabayashi *et al.*, 1990, Shanmugasundaram *et al.*, 1983, Srivastava *et al.*, 1985, Srivastava *et al.*, 1986, Sugihara *et al.*, 2000). The GS extract used throughout the experiments was of a high molecular weight extract of >3000 Da, as determined by molecular weight cut-off filtration (Chatterji, 2005a, Chatterji, 2005b). To date, there have been relatively few reported studies of any GS extracts in humans (Baskaran *et al.*, 1990, Khare *et al.*, 1983, Shanmugasundaram *et al.*, 1981, Shanmugasundaram *et al.*, 1990b), and no reported studies in either animals or

humans using OSA® or other high molecular weight isolates. An essential pre-requisite for developing drugs as potential therapies for T2DM is to ensure that they are efficacious in animals and human subjects, therefore this chapter investigated whether this novel isolate from GS leaves had an effect on clinically relevant parameters such as glucose concentrations in a mouse model of T2DM and on insulin, C-peptide and glucose levels in a small cohort of patients with T2DM.

Ob/ob mice have been used as a model of obesity and T2DM in numerous experimental studies. They have a single mutation in leptin gene (ob) which code for the protein hormone, leptin, which plays a key role in energy expenditure and food intake. In comparison to control mice, ob/ob mice were hyperglycemic and obese, consistent with the reported phenotypic characteristics of these animals (Lindstrom, 2007, Lindstrom, 2010). As expected ob/ob mice had an impaired glucose tolerance but this was significantly improved upon administration of a single oral dose of OSA® prior to the glucose tolerance test. The dose of OSA® was chosen to mimic that used in the human study. The improvement of glucose tolerance started soon after glucose administration but did not achieve significance until 60 min after glucose injection. This may represent the time required for OSA® to reach its site of action and produce an effect after oral administration. The improvement of glucose tolerance could be due to either reduction in intestinal glucose absorption (especially if glucose load was given orally), alleviation of insulin resistance or increasing circulating plasma insulin levels. OSA® has shown previously to block glucose absorption in the intestine (Shimizu *et al.*, 1997a, Shimizu *et al.*, 1997b); however, this could not attribute to the improvement of glucose tolerance in our experiment because glucose was injected intraperitoneally

and thus intestinal glucose absorption was bypassed. OSA® is not likely to act by altering insulin resistance as reports have shown that crude GS extract attenuated hyperglycemia without altering insulin sensitivity in targets tissues (Tominaga *et al.*, 1995). Therefore, OSA® most likely improved glucose tolerance in ob/ob mice as a result of stimulation of insulin secretion. Although plasma insulin levels from ob/ob mice were not measured because of limitations in blood sample volumes, data from the human study support this notion.

The effect of OSA® was also investigated on plasma insulin, C-peptide and glucose in a small cohort of patients with T2DM (Appendix 1). This study was carried out by our collaborators from Burdwan Medical College clinic. The patients recruited to this study presented with both fasting and post-prandial hyperglycemia (Appendix 1: Figure 1 and 2) but with circulating insulin and C-peptide levels within the normal range. Oral treatment with OSA® for 60 days resulted in significant reductions in fasting and post-prandial plasma glucose levels to nearly normal values in 10 out of 11 patients (Appendix 1: Figure 1 and 2), although it is unclear why one member of the cohort did not respond to OSA® treatment. The effect of OSA® to decrease plasma glucose was not associated with changes in post-prandial glucose excursions nor in body weight, indicating that the effect of OSA® on glycemia was not secondary to a decrease in either glucose absorption or food intake, consistent with an effect via enhanced insulin secretion. Similarly, the lack of effect of OSA® on the extent of post-prandial glucose excursion suggests a lack of effect on the insulin sensitivity of target tissues, again consistent with a primary effect on insulin secretion. In accordance with this, measurements of plasma insulin and C-peptide levels demonstrated that OSA®-induced improvements in glycemic

control were accompanied by elevations in plasma insulin and C-peptide concentrations (Appendix 1: Figure 3 and 4) suggesting that OSA® has a direct stimulatory effect on β-cells in the islets of Langerhans.

In summary, OSA®, which is a high molecular weight fraction isolated from GS leaf extract, may provide a potential alternative therapy for the hyperglycemia associated with T2DM. I have shown in this chapter that OSA® is effective in alleviating glucose intolerance in ob/ob mice and in reducing blood glucose and increasing plasma insulin and C-peptide levels in humans. Our findings were therefore in consistent with the previously reported antidiabetic effect of GS *in vivo*. The reported antihyperglycemic action of GS was largely associated with elevations in plasma insulin levels suggesting a direct effect of GS on β-cells. Therefore I hypothesized that at least some of OSA® effects can be attributed to a direct stimulatory effect on insulin secretion from β-cells in the islets of Langerhans and this hypothesis was tested in the *in vitro* studies described in chapter 4.

Chapter 4

Gymnema sylvestre has a direct stimulatory effect on mouse and human islets *in vitro*

4.1 Introduction

Glucose homeostasis is controlled by the coordinated secretion of two opposing hormones: insulin and glucagon released from β- and α-cells, respectively, of the islets of Langerhans. Insulin is controlled by a range of stimulatory and inhibitory factors (Goodman, 2003). Glucose is the major stimulatory factor and the most important nutrient that plays the leading role in insulin release and synthesis in mammals (Van Schaftingen and Schuit, 1999). Under fasting conditions, blood glucose is normally maintained at around 5mM but this value could reach 10-12mM following ingestion of a meal rich in carbohydrates. β-Cells respond to the rise of plasma glucose concentrations by secreting insulin in a biphasic fashion. The first phase, which lasts a couple of minutes, involves a rapid increase in insulin secretion reaching a peak after 2-4 minutes before returning to a lower sustained phase of insulin output (phase 2) that lasts throughout glucose stimulation (Del Prato *et al.*, 2002, Henquin *et al.*, 2002). In rodent islets, glucose stimulation causes the release of 11-20 granules/cell/min from a readily available pool of 13,000 granules/cell (Ashcroft and Ashcroft, 1992, Eliasson *et al.*, 2008).

Regulation of insulin gene expression is complex and not completely understood. The total preproinsulin (PPI) cellular content is a balance between mRNA stability, mRNA gene expression and rate of translation of mRNA (Clark and docherty, 1992). Expression of insulin at both levels of mRNA and protein is regulated by glucose. During short-term exposure, glucose induces PPI mRNA translation but prolonged exposure to glucose causes an increase in PPI mRNA transcription and stability (Andrali *et al.*, 2008, Clark and docherty, 1992, Nielsen *et al.*, 1985, Welsh *et al.*, 1985). Generally, insulin gene expression is controlled by two major elements

upstream the transcription site 1) promoters, which initiate transcription and 2) enhancers, which do not initiate transcription by their own but rather enhance promoters' activities. Both promoters and enhancers are regulated by transcription factors. It has been shown that upon stimulation with glucose, several transcription factors are activated by either components or products of glucose metabolism or by elements of glucose signaling cascades such as kinases/phosphatases (Andrali *et al.*, 2008, Melloul *et al.*, 2002, Poitout *et al.*, 2006).

While insulin secretion is elevated during glucose stimulation, glucagon release is inhibited. Glucagon secretion is controlled by either direct nutrient metabolism in α-cell or by paracrine regulation from neighboring cells. Amino acids such as arginine and alanine are potent stimulators of glucagon secretion whereas insulin is a potent inhibitor. Unlike insulin, glucagon functions to counteract hypoglycemia by increasing hepatic output of glucose to maintain glucose supply to various part of the body, especially the CNS (Goodman, 2003, Gromada *et al.*, 2007, Quesada *et al.*, 2008).

Several plant extracts have been reported to stimulate insulin secretion *in vivo*. Leaves of GS plant extract have been shown to elevate plasma insulin levels and reduce blood glucose concentrations *in vivo* in animal models of type 2 and in human (Baskaran *et al.*, 1990, Gupta, 1961, Gupta, 1963, Gupta and Variyar, 1961, Khare *et al.*, 1983, Okabayashi *et al.*, 1990, Shanmugasundaram *et al.*, 1990b, Shanmugasundaram *et al.*, 1981, Shanmugasundaram *et al.*, 1983, Srivastava *et al.*, 1985, Srivastava *et al.*, 1986, Terasawa *et al.*, 1994). I have shown in chapter 3 that OSA® extract alleviated glucose intolerance in mice and raised insulin levels in patients with T2DM. It is difficult to explore the possible mechanism of action of any

plant extract in vivo, therefore in this chapter, I tested the effect of OSA® *in vitro* to determine whether OSA® has a direct insulinotropic activity in MIN6 cells and primary islets. I also examined the chronic effect of OSA® on insulin gene expression and total insulin content of mouse islets.

4.2 Materials and Methods

4.2.1 Maintenance of MIN6 cells

MIN6 cells (passage 28-44) were maintained as monolayers under standard tissue culture conditions as described in section 2.3.2. They were trypsinized and used in experiments when confluency reached 70-80%.

4.2.2 Formation of MIN6 Pseudoislets (PIs)

To form PIs, MIN6 cells were subcultered in bacterial dishes under standard tissue culture conditions as described in section 2.3.3. PIs were used in experiments following 7-10 days of culture.

4.2.3 Isolation of mouse and human islets

ICR mice were killed by cervical dislocation. The pancreata of these mice were digested by collagenase as described in section 2.4. The islets were purified using Histopaque gradient and incubated in RPMI at 37C° (95% O_2/ 5% CO_2). Human islets were isolated from non-diabetic donors as described in section 2.5 following obtaining appropriate ethical approval. Islets were cultured in CMRL under standard tissue culture conditions.

4.2.4 Plant material and preparation

OSA® leaves were extracted as described in section 2.1.1. High molecular weight GS extract, commercially available as OSA®, were isolated and provided as powder. Aqueous OSA® extract was prepared as 200mg/ml stock solution and further diluted in Gey & Gey buffer for use in experiments.

4.2.5 Insulin secretion

4.2.5.1 Static incubation with MIN6 cells

MIN6 monolayers cells were counted as described in section 2.6, seeded into 96-well plate at a density of 30,000 cells/well and cultured in DMEM supplemented with 10% FCS, 2mM L-glutamine and 100 U/ml penicillin with 0.1 mg/ml streptomycin at 37C° for 2 days (Section 2.7.1). MIN6 cells were pre-incubated with 2mM glucose Gey & Gey buffer supplemented with 2mM $CaCl_2$ and 0.5mg/ml BSA at 37C° for 2 hrs. The cells then were incubated with buffer containing 2mM glucose in the presence or absence of different concentrations of OSA® extract for 30 minutes at 37C°. Aqueous OSA® extract (200mg/ml stock solution) was used to prepare 0.06, 0.125, 0.25, 0.5, 1.0 mg/ml by serial dilution. Tolbutamide (100µM) and/or the protein kinase activator, phorbol 12-myristate 13-acetate (PMA: 500nM) were used as positive controls to stimulate insulin secretion. At the end of the incubation period, 100µl of incubation medium was removed and added to 400µl borate buffer and stored at -20C° until insulin was measured by RIA.

4.2.5.2 Perifusion with MIN6 PIs, mouse and human islets

To measure the reversibility of OSA® effects and the rate and pattern on insulin secretion, perifusions using MIN6 PIs, primary mouse and human islets were

performed, as described in section 2.7.3. MIN6 PIs or human islets were harvested and resuspended in DMEM medium and 100 µl was aliquoted into each perifusion chamber. For mouse islets perifusions, 60 ICR islets were dispensed into each chamber. PIs or islets were pre-perifused for 1 hr with buffer containing 2mM glucose and then with Gey & Gey buffer supplemented with either 2mM or 20mM glucose in the presence or absence of 0.125 or 0.25 mg/ml OSA®. To test the effect of OSA® at physiological glucose concentrations, human islets were perifused with either 5mM or 10mM in the presence or absence of 0.125 mg/ml OSA®. Perifusates were stored at -20C° until assayed for insulin by RIA as described in section 2.9.

4.2.6 Glucagon secretion

To investigate the effect of OSA® on glucagon secretion, perifusions with mouse islets were performed. As described in section 2.10, 100 ICR mouse islets were pre-perifused with Gey and Gey buffer supplemented with 2mM glucose for 1 hr. Collection of samples was started at t=60 minutes and islets were perifused with Gey & Gey buffer containing 2mM glucose or 20mM arginine in the presence or absence of 0.25 mg/ml OSA®. Samples were stored at -20C° until assayed for glucagon content by RIA (section 2.9).

4.2.7 Cell viability

The effect of OSA® on membrane permeability and cell viability was examined using the Trypan Blue exclusion test (section 2.11). MIN6 cells or mouse islets treated with different concentration of OSA® were stained with Trypan Blue due (0.1 mg/ml) for 15 minutes before being visualized under a light microscope.

4.2.8 Mouse Preproinsulin mRNA expression

Measurement of preproinsulin expression was performed to examine the chronic effect of OSA® on insulin gene expression. Mouse islets were isolated and incubated in RPMI (11.1mM glucose) overnight. 150 islets were preincubated with 2mM glucose and then treated with one of the following treatment: 2mM glucose, 20mM glucose (as positive control), 2mM glucose + 0.125 mg/ml OSA® for either 24 or 48 hrs. Islets were then washed with PBS and lysed using cell lysis solution (section 2.15.1). RNA from each treatment was extracted using Qiagen RNeasy mini kit (section 2.15.1). 0.5µg of RNA was reverse transcribed to cDNA using mmLV-RT (section 2.15.2). Negative (water only) and –RT controls were included to ensure the specificity of the reverse transcription process and the absence of any genomic contaminations. cDNA was further diluted 50 times to remove the influence of any remaining reagents from cDNA synthesis. Preproinsulin mRNA was quantified in real time using specific primers designed to amplify 125bp amplicon in the presence of SYBR green as the fluorescence indicator (section 2.16). Preproinsulin expression was normalized to actin, a house keeping gene. mRNA accession number, cycling conditions, gel electrophoresis, melt curve analyses, assay efficiencies and standard curves series for each gene are described in Appendix 2.

4.2.9 Total insulin content of mouse islets

Total insulin content of mouse islets (section 2.8) was determined by incubating 5 islets in 2mM glucose supplemented with either vehicle or 0.125 mg/ml OSA® for 24 and 48 hrs. 100µl of the medium was removed for insulin secretion measurement and islets were sonicated in acidified alcohol (200µl). Samples were stored at -20C° until assayed for insulin content by RIA.

4.2.10 Statistical analysis

Data are represented as mean ± SEM. For perifusion experiments with more than one treatment, mean was calculated as area under the curve. Differences between treatments groups were assessed using analysis of variance (ANOVA), Student's t-test, and Bonferroni's multiple comparison test as appropriate and considered significant at $p< 0.05$.

4.3 Results

4.3.1 Effect of OSA® on insulin secretion from MIN6 monolayers

The effect of OSA® on insulin secretion from MIN6 cell monolayers at basal glucose concentrations was assessed as described in Materials and Methods. Thirty minutes exposure of MIN6 cells to OSA® caused a concentration-dependent increase in insulin secretion at a substimulatory (2mM) glucose levels (Figure 4.1). OSA® significantly stimulated insulin release at a concentration of ≥ 0.125mg/ml and increasing OSA® concentration to 1.0 mg/ml resulted in a marked increase in insulin release from MIN6 cells (2mM glucose: 0.19 ± 0.02 pg/cell/hr; 2mM glucose + 1.0 mg/ml OSA®: 0.50 ± 0.02 pg/cell/hr). Both tolbutamide and/or PMA, insulin-releasing substances used as positive controls, augmented insulin secretion at 2 and 20mM glucose, respectively (Figure 4.1). Tolbutamide is a sulphonylurea and acts by blocking K_{ATP}-channels to increase insulin secretion; Whereas PMA augments insulin secretion by non-selectively activating typical PKC isoforms.

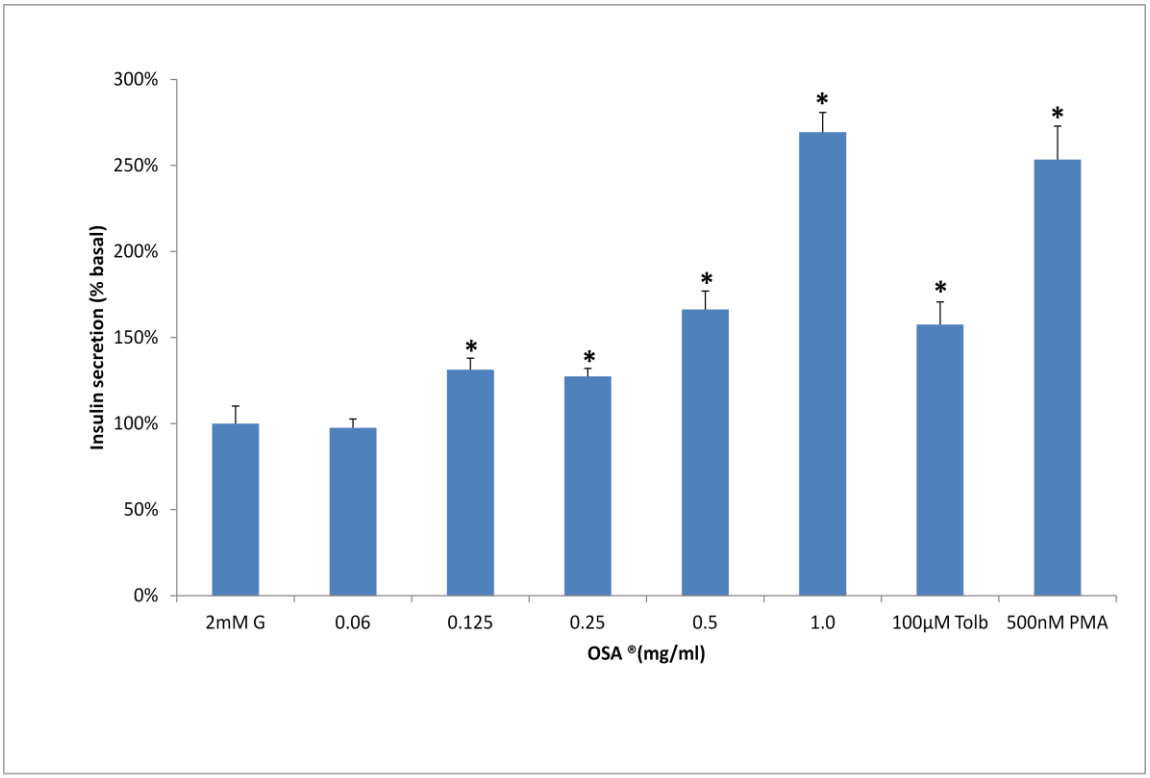

Figure 4.1: Effect of OSA® on insulin secretion from MIN6 cell monolayers at a substimulatory glucose concentration. MIN6 cells were incubated for 30 minutes at 37C° with (0.06 - 1.0 mg/ml) of OSA®. Insulin content of the supernatant was measured by RIA. Tolbutamide and PMA were used as positive controls. Data are means + SEM, n=12. * P<0.05 compared to 2mM glucose. G: glucose, Tol: Tolbutamide, PMA: phorbol 12-myristate 13-acetate

4.3.2 Effect of OSA® on membrane integrity and cell viability

The effect of OSA® on membrane integrity was assessed using the Trypan Blue exclusion test. Incubating MIN6 cells with 0.1% Trypan Blue dye for 15 minutes in the presence of different OSA® concentrations resulted in a dose-dependent increase in the uptake of the dye. The blue staining was evident at OSA® ≥ 0.5 mg/ml and 10-20% and 90-100% of MIN6 cells incubated in the presence of 0.5 and 1.0 mg/ml OSA®, respectively, showed an uptake of Trypan Blue dye indicating a loss of membrane integrity (Figure 4.2). In contrast, exposing MIN6 cells to 500nM PMA caused an increase in insulin secretion without compromising membrane integrity (Table 4.1). Similarly, Trypan Blue stained cells were apparent in mouse islets incubated with 1.0 mg/ml OSA® (Figure 4.2). Note however, OSA® at

concentrations of ≤ 0.25 mg/ml had no detectable effect on trypan blue uptake suggesting that OSA® was not toxic to β-cells at these concentrations.

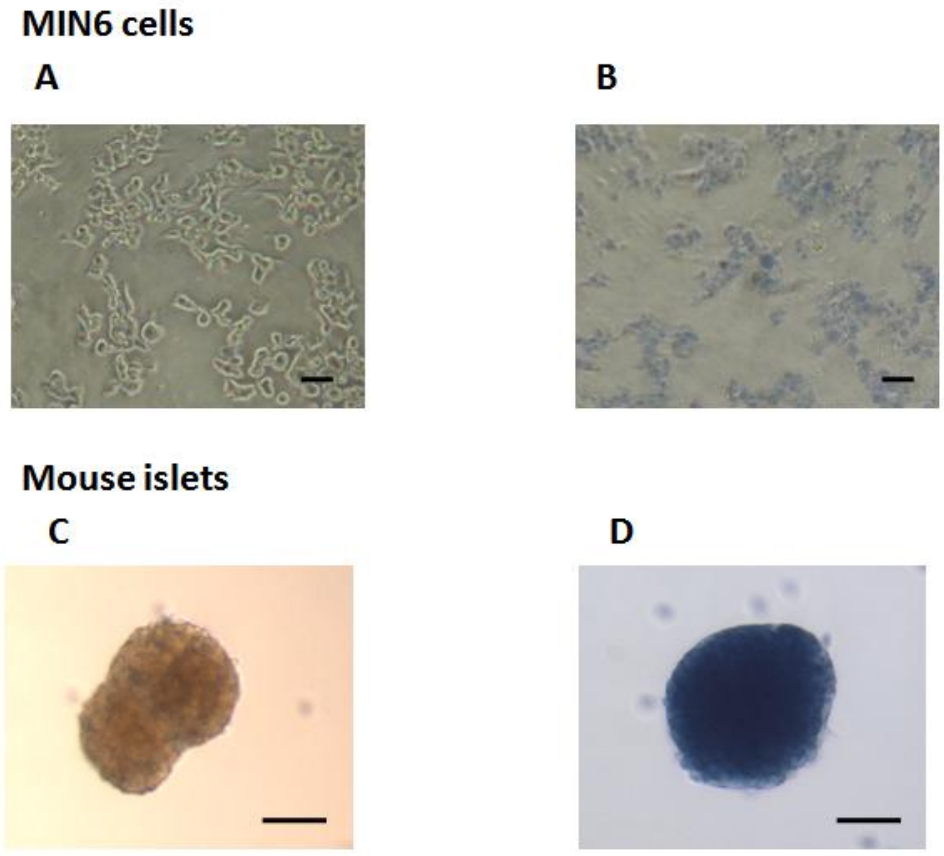

Figure 4.2: Effect of OSA® on membrane integrity using the Trypan Blue exclusion method. MIN6 cells and mouse islets were incubated in PBS supplemented with 0.1% Trypan Blue dye at 37C° for 15 minutes in the absence (A and C) or presence of 1.0 mg/ml OSA® (B and D). This concentration of OSA® caused widespread nuclear staining by trypan blue (B and D), indicative of membrane permeability induced by OSA®. Bar shows 10µm (A and B) and 50µm (C and D).

Treatment	Cells taking up Trypan Blue (% total)
2mM Glucose	0%
+ 0.06 mg/ml OSA	0%
+ 0.125 mg/ml OSA	0%
+ 0.25 mg/ml OSA	0%
+ 0.5 mg/ml OSA	10-20 %
+ 1.0 mg/ml OSA	90-100%
20mM Glucose + 500 nM PMA	0%

Table 4.1: Effect of OSA® on MIN6 cells membrane integrity. MIN6 cells were incubated with Gey and Gey buffer supplemented with agents shown in the table for 30 minutes at 37C°. The cells were further incubated with 0.1% trypan blue for 15 minutes at 37C°. Data represent the percentage of cells which have taken up the dye.

4.3.3 Effect of OSA® on the rate and pattern of insulin secretion from MIN6 PIs, mouse and human islets

The effects of OSA® on the pattern and rate of insulin secretion, and the reversibility of its effects, were tested using MIN6 PIs, mouse and human islets in *vitro*, as shown in Figure 4.3, 4.4 and 4.5, respectively. Perifusion of MIN6 PIs with buffer supplemented with 0.25 mg/ml OSA® at a substimulatory concentration (2mM) of glucose evoked an increase in insulin secretion as shown in Figure 4.3. The response to OSA® was rapid in onset, sustained for the duration of exposure to OSA®, and rapidly reversible upon its withdrawal. Subsequent exposure to 20mM glucose following OSA® treatment induced a further increase in insulin secretion (Figure 4.3). OSA® also mounted prompt, long-lived and reversible responses from mouse and human islets (Figure 4.4 and 4.5), with subsequent responses to 20mM glucose consistent with unimpaired secretory responses after exposure to OSA®.

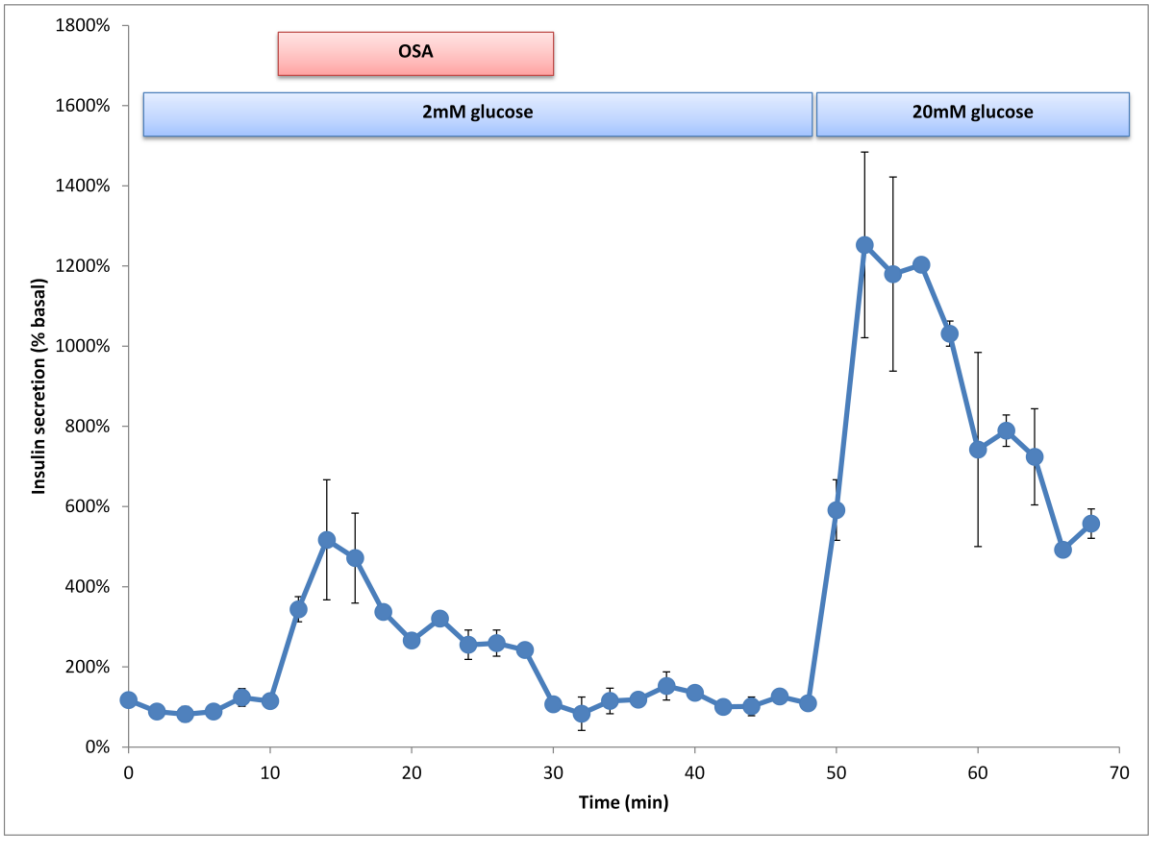

Figure 4.3: Effect of OSA® on insulin secretion from MIN6 PIs at a substimulatory glucose concentration. MIN6 PIs were perifused with buffer supplemented with 2mM glucose in the absence or presence of 0.25 mg/ml OSA®, as shown by the horizontal bar. Fractions were collected every 2 minutes and insulin content was determined by RIA. Data are expressed as % over basal (2mM glucose). Insulin secretion was significantly stimulated by the presence of OSA® at 2mM glucose ($p<0.001$). Points show mean ± SEM, n=4.

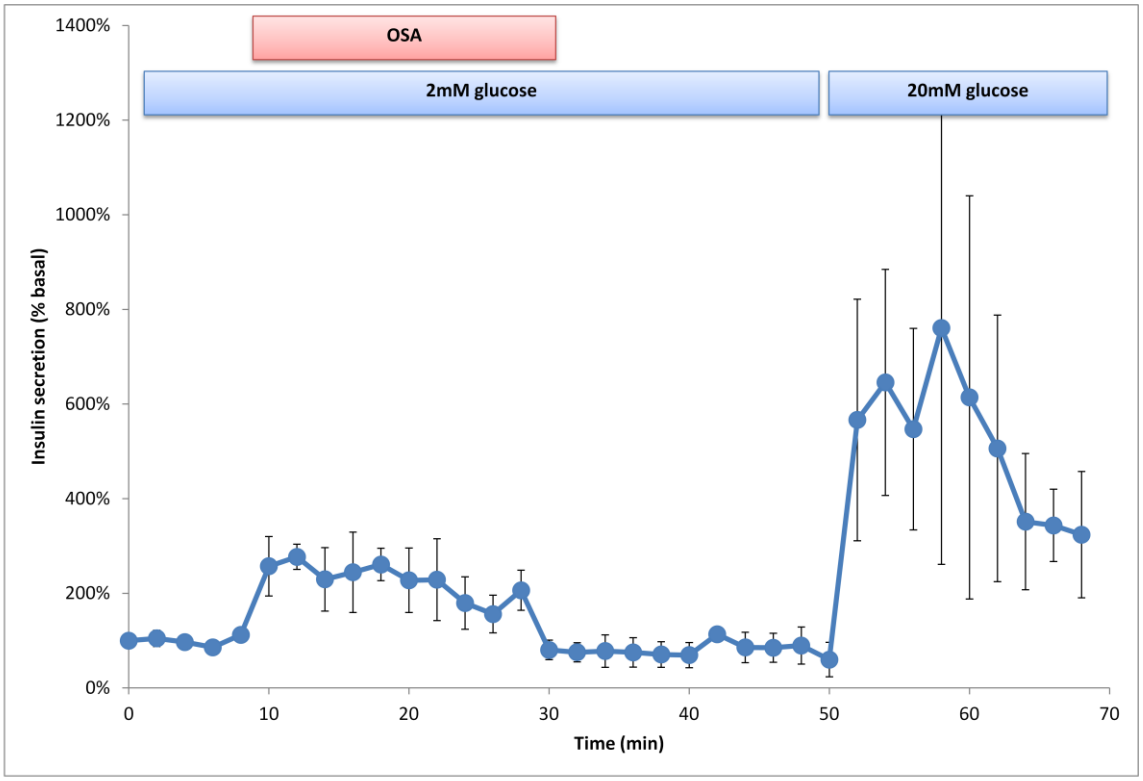

Figure 4.4: Effect of OSA® on insulin secretion from isolated mouse islets at a substimulatory glucose concentration. Mouse islets were perifused with buffer supplemented with 2mM glucose in the absence or presence of 0.25 mg/ml OSA®, as shown by the horizontal bar. Fractions were collected every 2 minutes and insulin content was determined by RIA. Data are expressed as % over basal (2mM glucose). Insulin secretion was significantly stimulated by the presence of OSA® at 2mM glucose ($p<0.001$). Points show mean ± SEM, n=4.

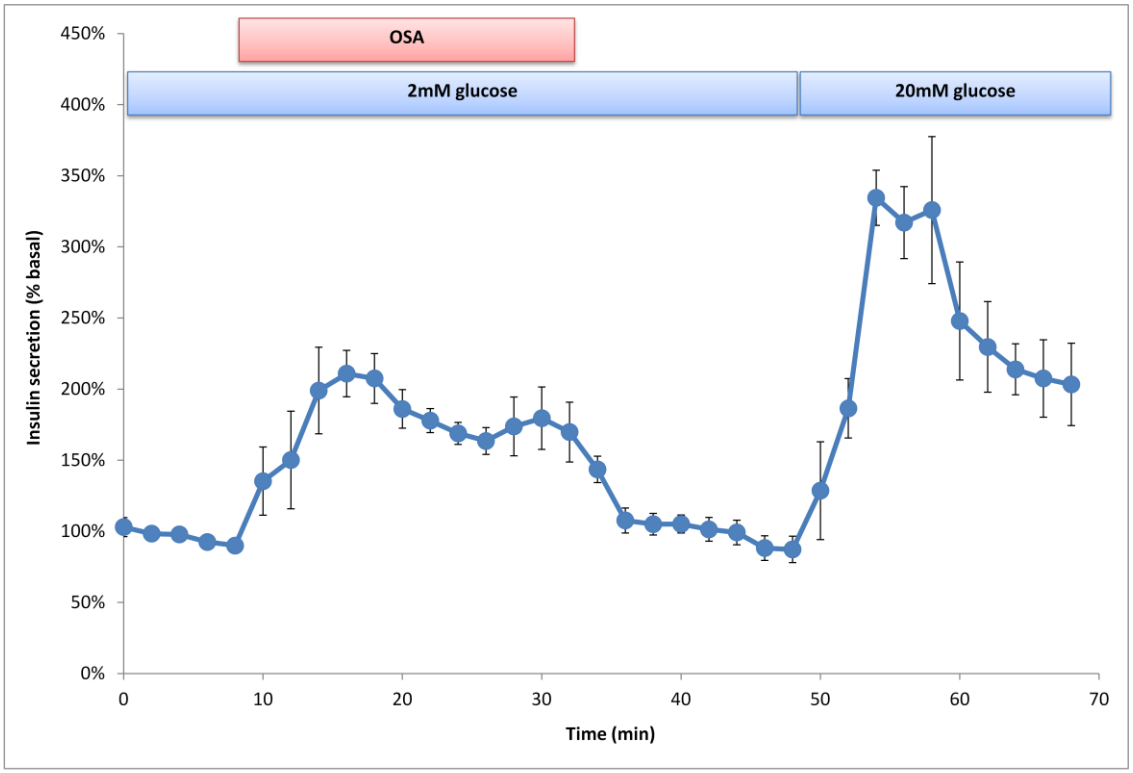

Figure 4.5: Effect of OSA® on insulin secretion from human islets at a substimulatory glucose concentration. Human islets were perifused with buffer supplemented with 2mM glucose in the absence or presence of 0.125 mg/ml OSA®, as shown by the horizontal bar. Fractions were collected every 2 minutes and insulin content was determined by RIA. Data are expressed as % over basal (2mM glucose). Insulin secretion was significantly stimulated by the presence of OSA® at 2mM glucose ($p<0.001$). Points show mean ± SEM, n=4.

In addition to initiating an insulin secretory response, OSA® (0.25 mg/ml) potentiated glucose-induced insulin secretion from MIN6 PIs, as shown in Figure 4.6. Thus, increasing the glucose concentration from 2 to 20mM (10-30 min) resulted in the expected biphasic pattern of glucose-induced insulin secretion. The first phase was rapid and transient, reaching a peak within 4 minutes followed by a sustained second phase of insulin secretion of a lower magnitude. Exposure to OSA® (0.25 mg/ml) in the continued presence of 20mM glucose (30-50 min) further potentiated the glucose-induced secretory response, with enhanced rates of insulin secretion being maintained for the duration of exposure to OSA®. Similarly, 20mM glucose caused a biphasic increase in insulin secretion from mouse and

human islets. Again, glucose-induced insulin secretion was significantly augmented upon exposure to OSA® (Figure 4.7 and 4.8).

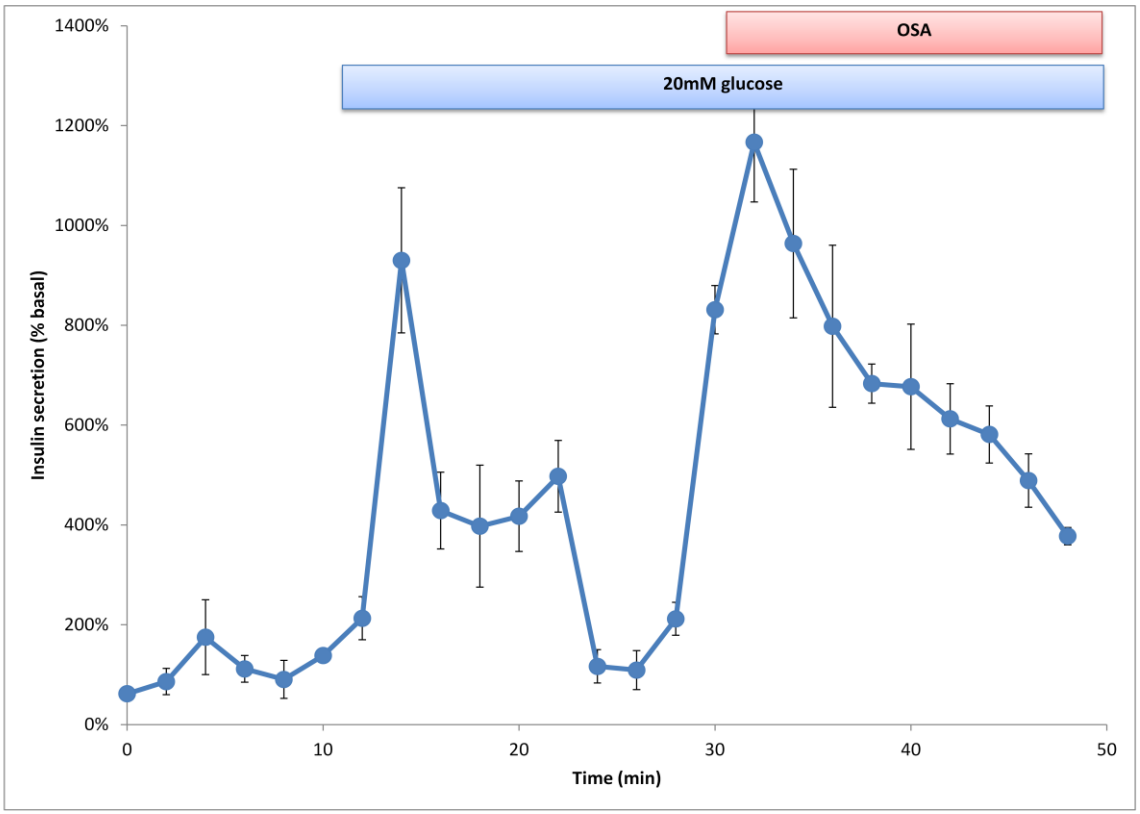

Figure 4.6: Effect of OSA® on insulin secretion from MIN6 PIs at a stimulatory glucose concentration. MIN6 PIs were perifused first with 2mM glucose for 10 minutes then perifused with buffer supplemented with 20mM glucose in the absence or presence of 0.25 mg/ml OSA®, as shown by the horizontal bar. Fractions were collected every 2 minutes and insulin content was determined by RIA. Data are expressed as % over basal (2mM glucose). Insulin secretion was significantly stimulated by the presence of OSA® at 20mM glucose ($p<0.05$). Points show mean ± SEM, n=4.

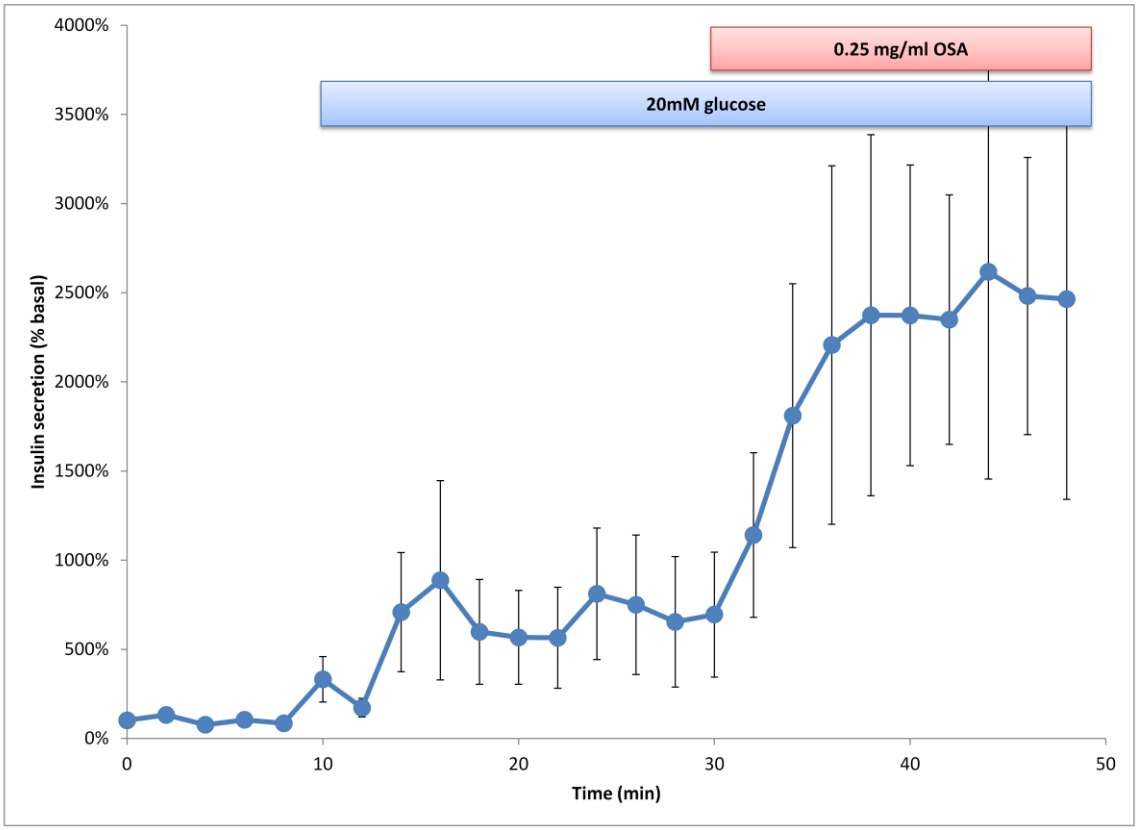

Figure 4.7: Effect of OSA® on insulin secretion from isolated mouse islets at a stimulatory glucose concentration. Mouse islets were perifused first with 2mM glucose for 10 minutes then perifused with buffer supplemented with 20mM glucose in the absence or presence of 0.25 mg/ml OSA®, as shown by the horizontal bar. Fractions were collected every 2 minutes and insulin content was determined by RIA. Data are expressed as % over basal (2mM glucose). Insulin secretion was significantly stimulated by the presence of OSA® at 20mM glucose ($p<0.05$). Points show mean ± SEM, n=4.

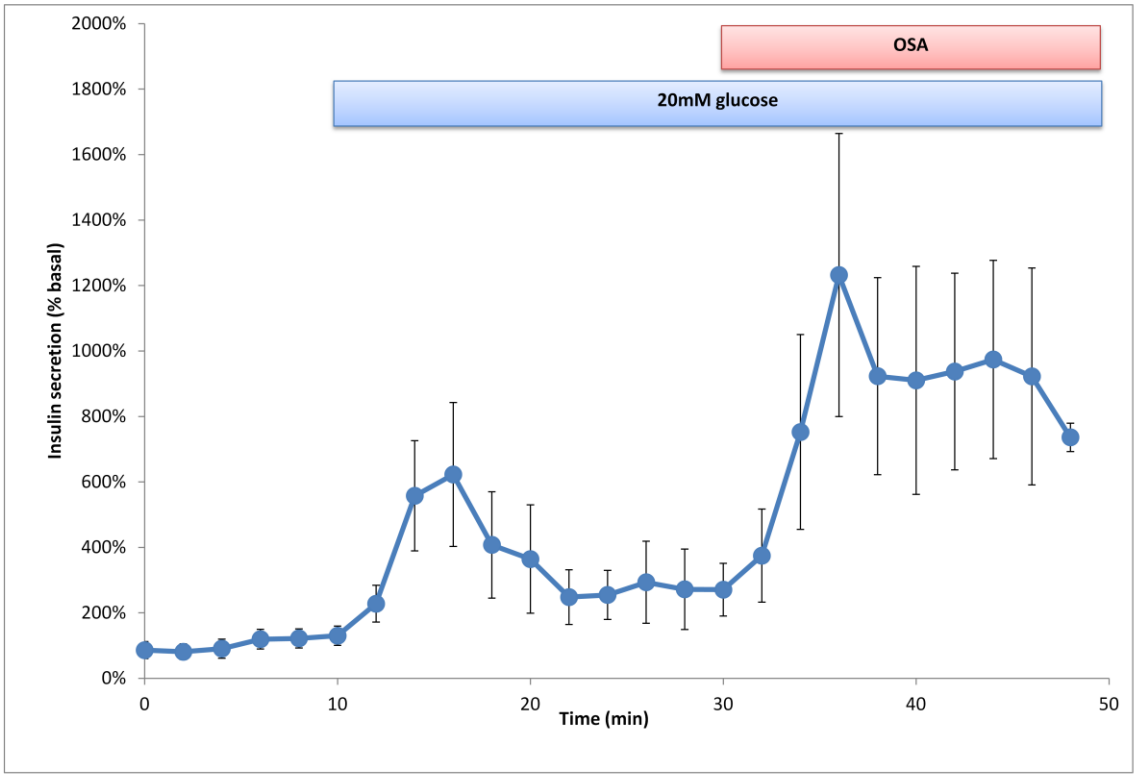

Figure 4.8: Effect of OSA® on insulin secretion from human islets at a stimulatory glucose concentration. Human islets were perifused first with 2mM glucose for 10 minutes then perifused with buffer supplemented with 20mM glucose in the absence or presence of 0.125 mg/ml OSA®, as shown by the horizontal bar. Fractions were collected every 2 minutes and insulin content was determined by RIA. Data are expressed as % over basal (2mM glucose). Insulin secretion was significantly stimulated by the presence of OSA® at 20mM glucose ($p<0.05$). Points show mean ± SEM, n=4.

4.3.4 Effect of OSA® on insulin secretion from human islets at physiological glucose concentrations

The effect of OSA® at more intermediate glucose concentrations was also examined using perifusion experiments with human islets. Human islets were perifused with either 5mM (Figure 4.9) or 10mM glucose (Figure 5.10) in the presence of 0.125mg/ml OSA®. Both glucose concentrations caused stimulation in insulin secretion which was further potentiated upon exposure to OSA®. The increase in OSA®-induced insulin secretion at 5mM and 10mM glucose was similar in profile to that seen at 2mM and 20mM glucose. The insulin secretion induced by OSA® was rapid and remained elevated throughout the presence of OSA®.

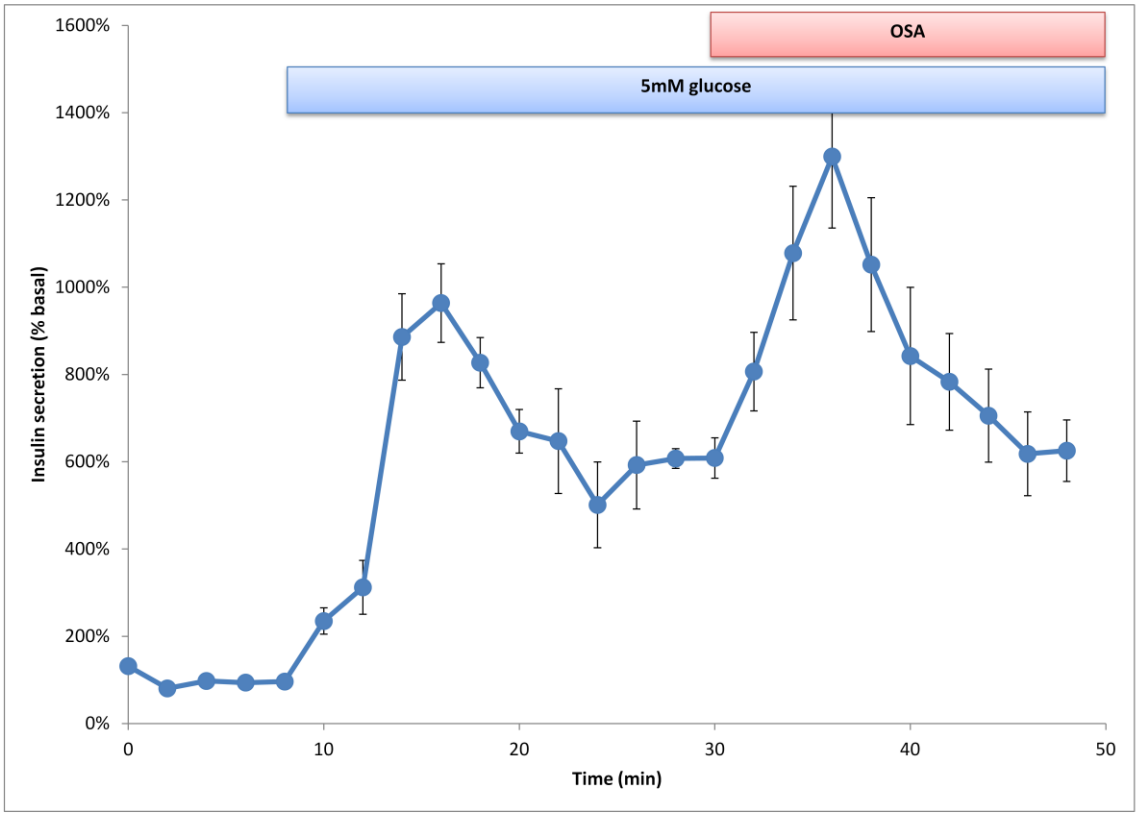

Figure 4.9: Effect of OSA® on insulin secretion from human islets at physiological glucose concentrations (5mM). Human islets were perifused with buffer supplemented with 5mM glucose in the absence or presence of OSA®, as shown by the horizontal bar. Fractions were collected every 2 minutes and insulin content was determined by RIA. Data are expressed as % over basal (2mM glucose). Insulin secretion was significantly stimulated by the presence of OSA® at 5mM glucose ($p < 0.01$). Points show mean ± SEM, n=4.

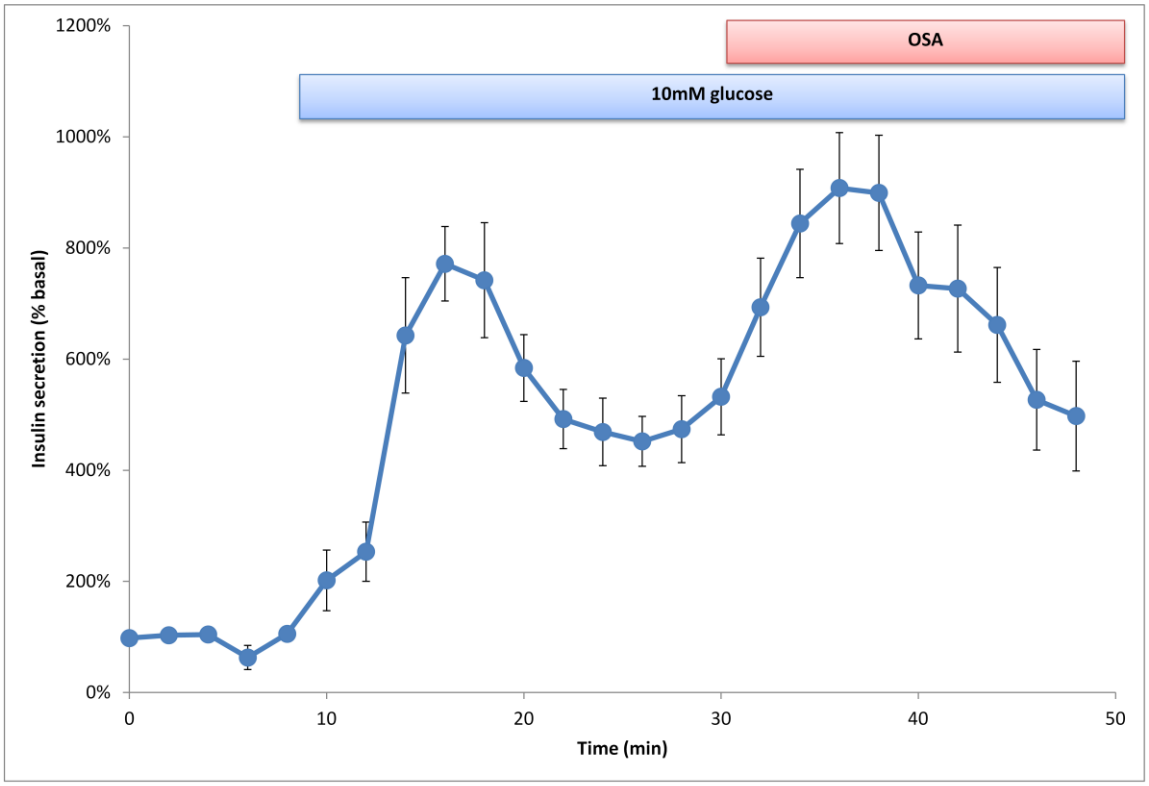

Figure 4.10: Effect of OSA® on insulin secretion from human islets at physiological glucose concentrations (10mM). Human islets were perifused with buffer supplemented with 10mM glucose in the absence or presence of OSA®, as shown by the horizontal bar. Fractions were collected every 2 minutes and insulin content was determined by RIA. Data are expressed as % over basal (2mM glucose). Insulin secretion was significantly stimulated by the presence of OSA® at 10mM glucose ($p<0.01$). Points show mean ± SEM, n=4.

4.3.5 Effect of OSA® on glucagon secretion from mouse islets

The possible contribution of α-cells to the overall effect of OSA® was assessed by measuring glucagon release in perifusion experiment using mouse islets. Exposure of mouse islets to 0.25 mg/ml OSA® at 2mM glucose initiated a small increase in glucagon secretion (Figure 4.11). The glucagon secretory response to OSA® was rapid reaching its peak within approximately 2 minutes of the onset of stimulation. However, the elevations in glucagon output returned almost to basal despite the continuous presence of OSA®. Glucagon secretion was further increased upon subsequent exposure to 20mM arginine (Figure 4.11). Under maximum stimulation of glucagon secretion (induced by 20mM arginine), OSA® further potentiated arginine-induced glucagon secretion (Figure 4.12).

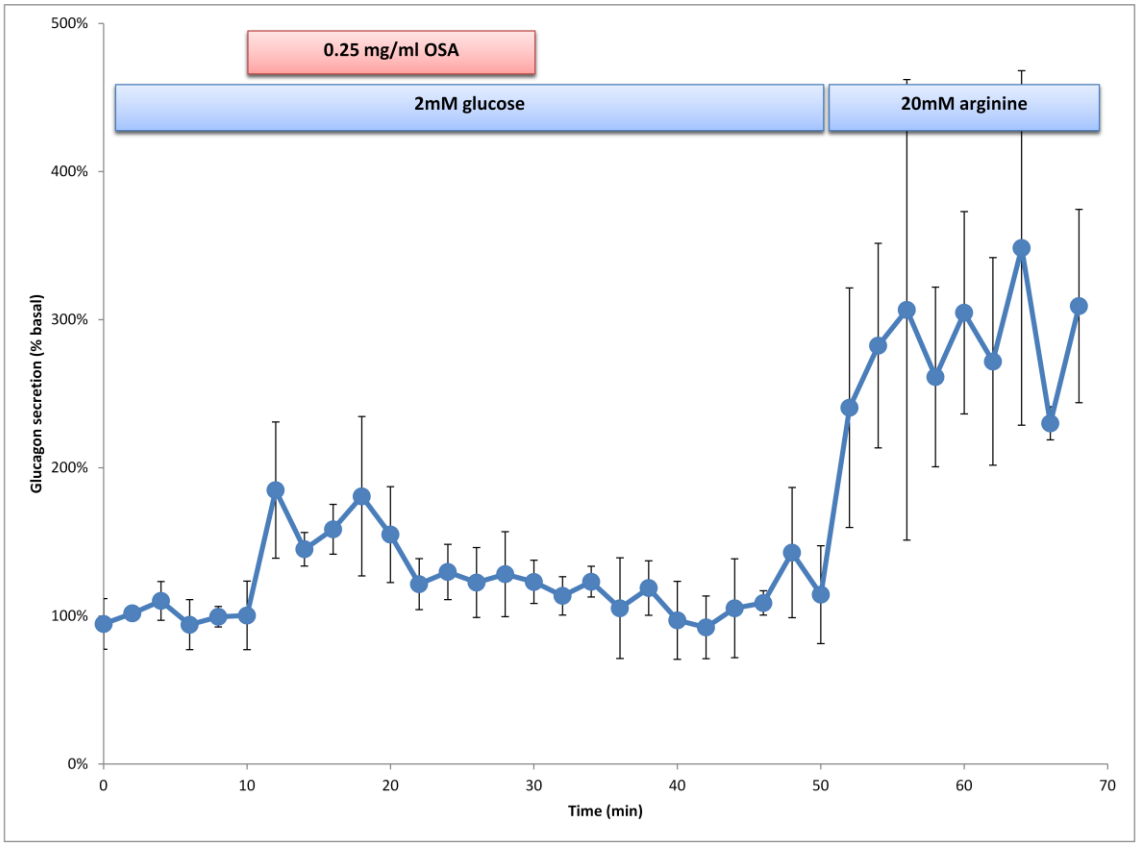

Figure 4.11: Effect of OSA® on glucagon secretion from mouse islets at a substimulatory glucose concentration. Mouse islets were perifused throughout with buffer supplemented with 2mM glucose in the absence or presence of 0.25 mg/ml OSA®, as shown by the horizontal bar. Samples were collected every 2 min and glucagon content was measured by RIA. Data are expressed as % of basal (2mM glucose). Glucagon secretion was significantly stimulated by the presence of 0.25 mg/ml OSA® at 2mM glucose ($p<0.001$). Points show mean ± SEM, n=4.

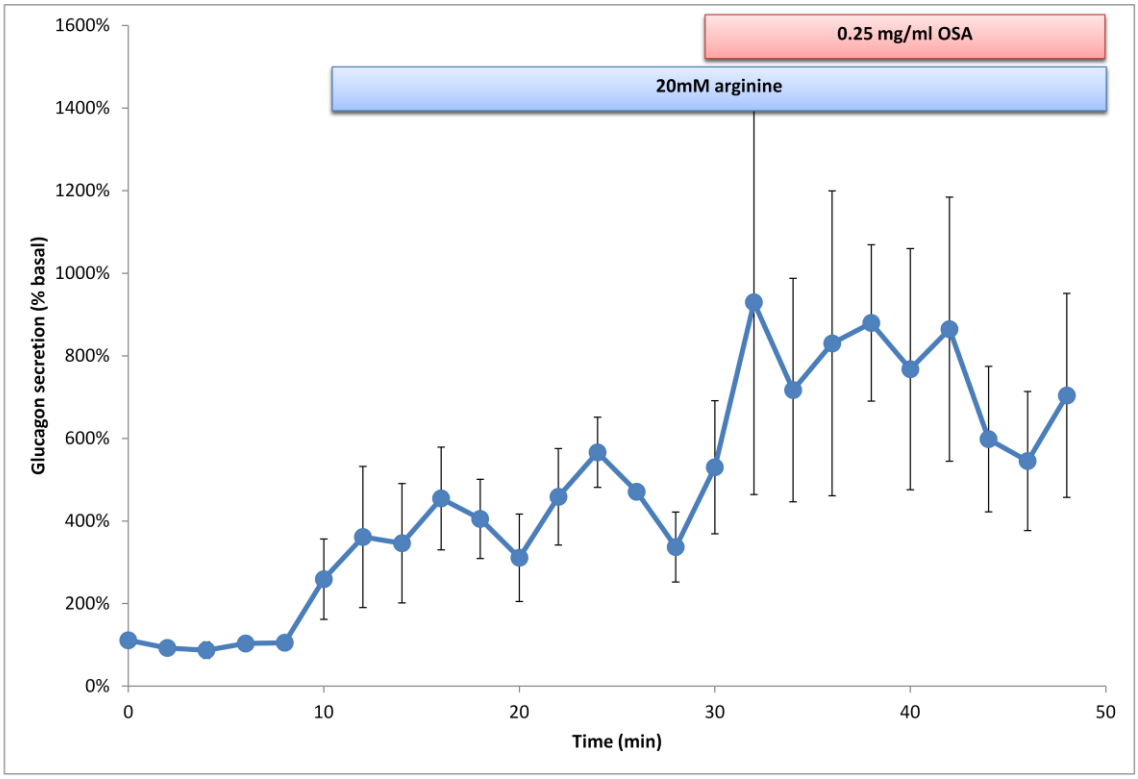

Figure 4.12: Effect of OSA® on glucagon secretion from mouse islets at a stimulatory arginine concentration. Mouse islets were perifused throughout with buffer supplemented with 20mM arginine in the absence or presence of 0.25 mg/ml OSA®, as shown by the horizontal bar. Samples were collected every 2 min and glucagon content was measured by RIA. Data are expressed as % of basal (2mM glucose). Glucagon secretion was significantly stimulated by the presence of 0.25 mg/ml OSA® at 20mM arginine ($p<0.001$) . Points show mean ± SEM, n=4.

4.3.6 Effect of OSA® on preproinsulin mRNA expression

The possible effect of OSA® on insulin gene transcription was determined by measuring preproinsulin (PPI) mRNA expression using quantitative PCR (Figure 4.13 and 4.14). Stimulatory concentrations of glucose (20mM) caused a 2.5 fold increase in PPI mRNA levels following 24 hrs exposure. The PPI mRNA levels induced by 20mM glucose remained elevated after 48 hrs. Similarly, 0.125mg/ml OSA® at 2mM glucose resulted in a significant increase in PPI expression (approximately 1.5 fold increase) at 24 hrs (Figure 4.13) which was also sustained after 48 hrs (Figure 4.14). However, the extent of OSA®-induced increase in PPI mRNA levels was lower than that of 20mM glucose.

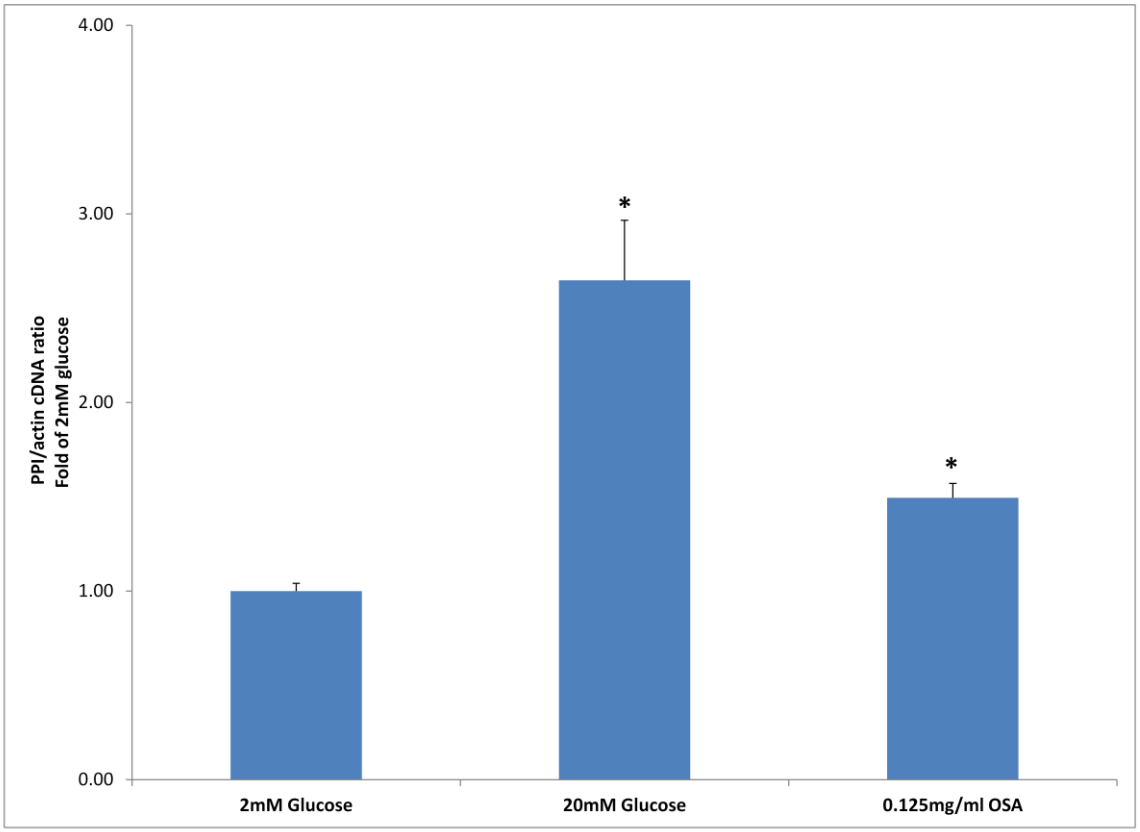

Figure 4.13: Effect of OSA® on preproinsulin mRNA expression from mouse islets following 24 hrs exposure. 150 mouse islets were preincubated with 2mM glucose and then incubated with 20mM glucose or 2mM glucose supplemented with either vehicle or 0.125 mg/ml OSA for 24 hrs. Quantification of PPI was carried out as desrciped in Materials and Methods. PPI mRNA levels were normalized to actin mRNA. OSA® and 20mM glucose caused a significant (* p<0.05) increase in PPI expression at 24 hrs. Data show mean + SEM, n=3.

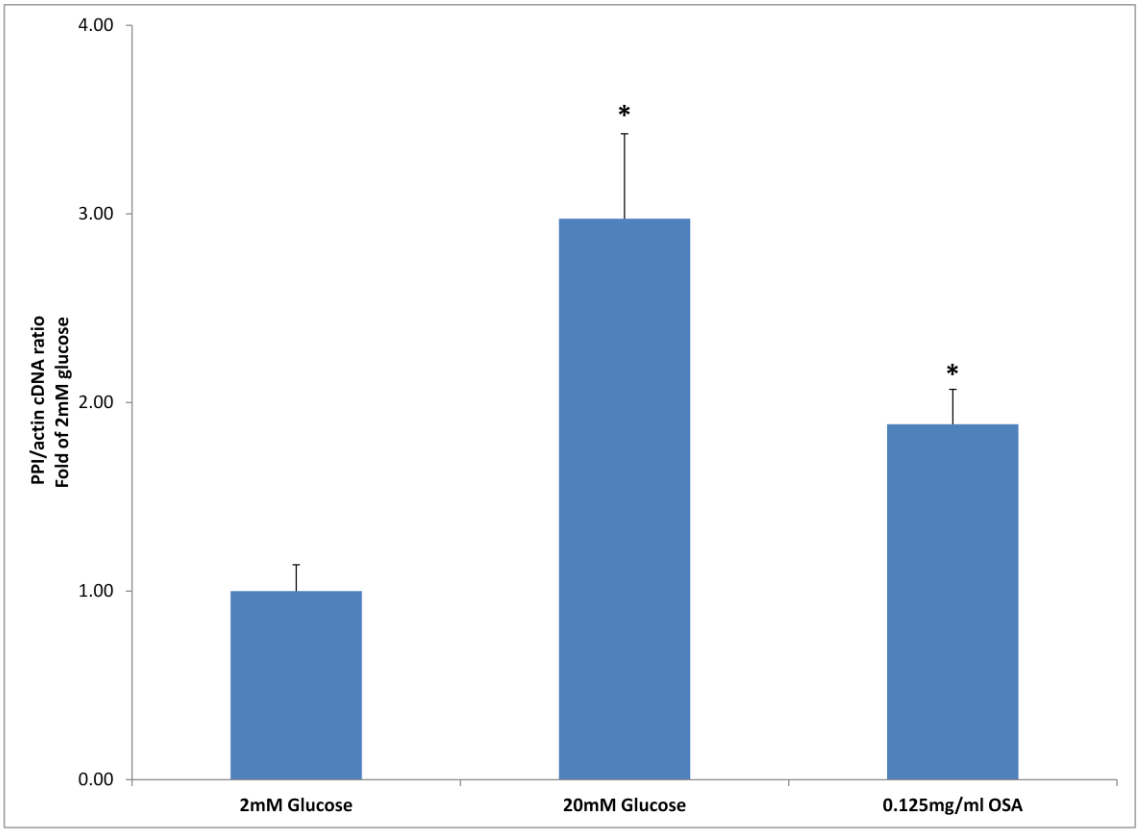

Figure 4.14: Effect of OSA® on preproinsulin mRNA expression from mouse islets following 48 hrs exposure. 150 mouse islets were preincubated with 2mM glucose and then incubated with 20mM glucose or 2mM glucose supplemented with either vehicle or 0.125 mg/ml OSA for 48 hrs. Quantification of PPI was carried out as described in Materials and Methods. PPI mRNA levels were normalized to actin mRNA. OSA® and 20mM glucose caused a significant (* p<0.05) increase in PPI expression at 48 hrs. Data show mean + SEM, n=3

4.3.7 Effect of OSA® on mouse total insulin content

Chronic exposure of mouse islets to either 0.125 mg/ml OSA® or 20mM glucose for 24 (Figure 4.15) or 48 (Figure 4.16) hrs was not accompanied with any increases in total insulin content in response to the increase in PPI mRNA levels (Figure 4.13 and 4.14). However, simultaneous measurement of insulin in the supernatants from OSA® or 20mM glucose-treated islets showed a dramatic stimulation in insulin secretion (2mM glucose: 1.7 ± 0.12, 2mM glucose + OSA®: 2.9 ±0.08 and 20mM glucose: 4.03 ± 0.7 ng/islet) as expected. The increases in insulin secretion induced by 20mM glucose or OSA® with no changes in insulin content were consistent with maintaining insulin stores by elevating PPI mRNA levels.

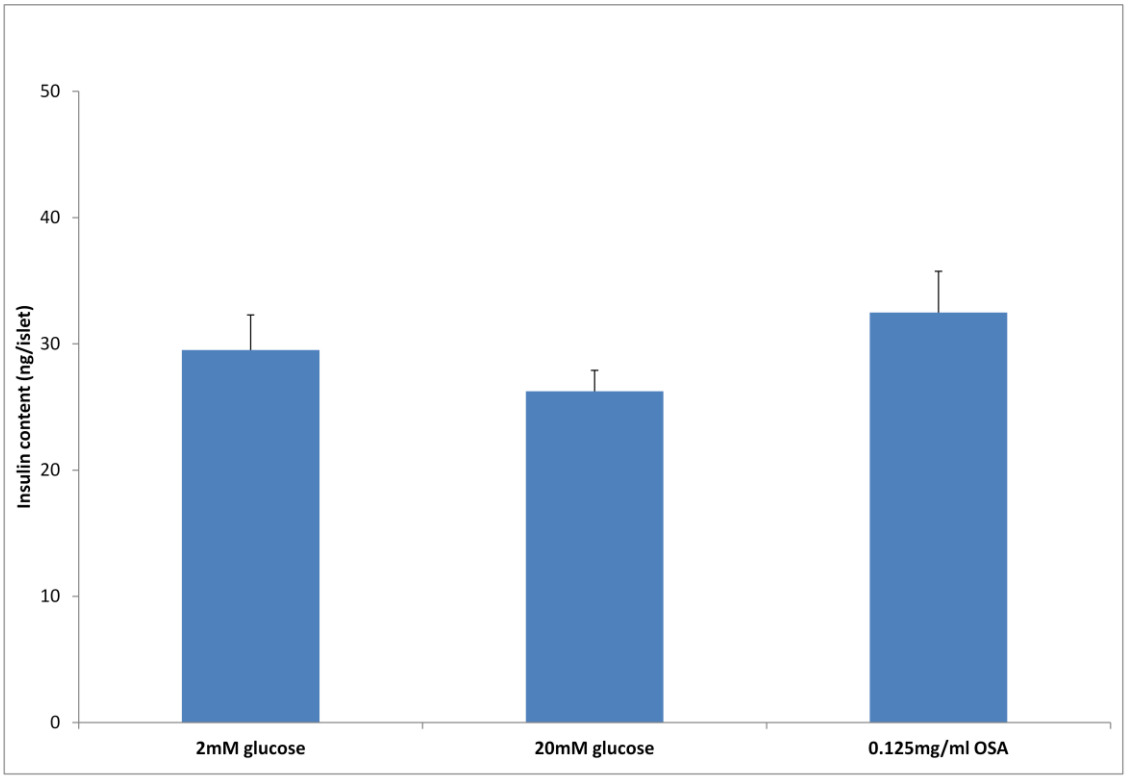

Figure 4.15: Effect of OSA® on mouse total insulin content following 24 hrs exposure. Five mouse islets were incubated with 2mM glucose supplemented with either vehicle or 0.125 mg/ml OSA or 20mM glucose for 24 hrs. Islets were sonicated in acidified alcohol and insulin content were determined by RIA. Neither 0.125 mg/ml OSA® nor 20mM glucose caused a significant change in islet total insulin content. Data are mean + SEM, n=6.

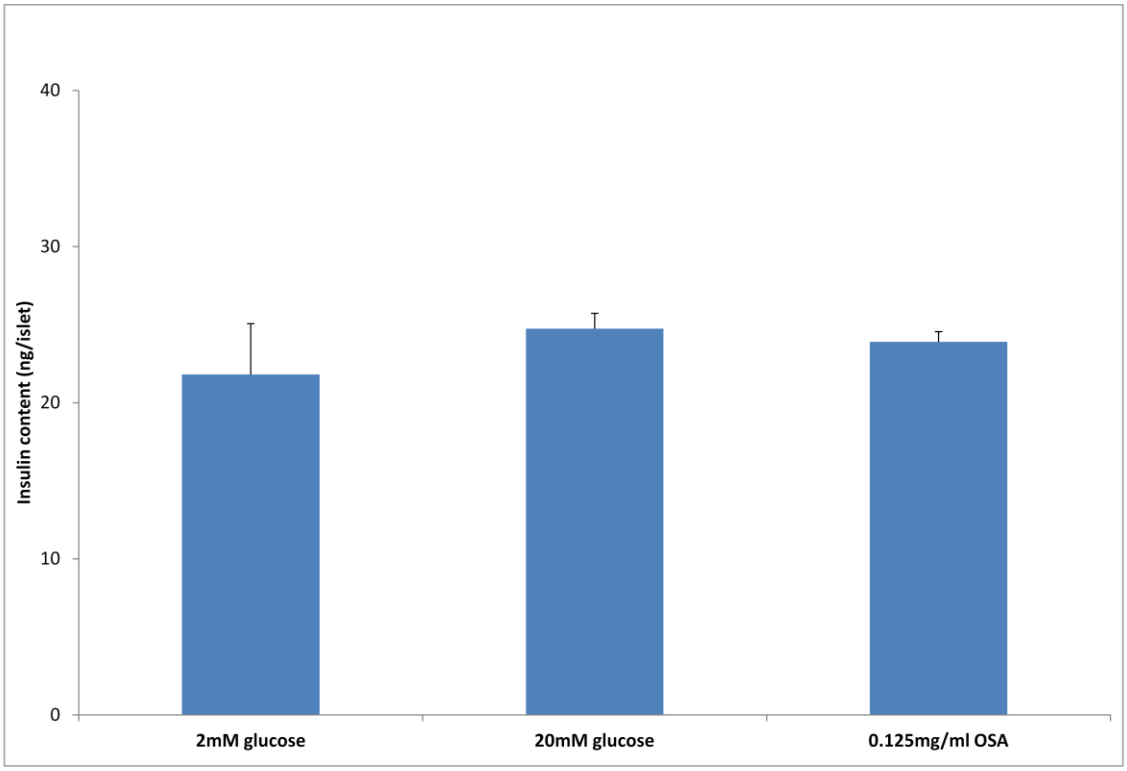

Figure 4.16: Effect of OSA® on mouse total insulin content following 48 hrs exposure. Five mouse islets were incubated with 2mM glucose supplemented with either vehicle or 0.125 mg/ml OSA or 20mM glucose for 48 hrs. Islets were sonicated in acidified alcohol and insulin content were determined by RIA. Neither 0.125 mg/ml OSA® nor 20mM glucose caused a significant change in islet total insulin content. Data are mean + SEM n=6.

4.4 Discussion

It has been established in chapter 3 that OSA® markedly increased plasma insulin levels in human with T2DM and improved glycemic control in an animal model of diabetes (ob/ob mice) *in vivo*. This effect may be due in part to the ability of OSA® to directly modulate hormone secretion and synthesis in islets of Langerhans. To test this hypothesis, I examined the acute effects of OSA® on insulin and glucagon secretion and the chronic effects of OSA® on insulin synthesis *in vitro*. The insulinotropic activity of OSA® was first investigated using MIN6 cells and primary β-cells (mouse and human islets).

The MIN6 cell-line is a β-cell line derived from a mouse insulinoma. It was established by targeted expression of SV40 (Simian virus 40) T antigen in

transgenic mice. SV40 T antigen is a protein which functions to inhibit growth-suppressing proteins allowing the cells to proliferate indefinitely. The advantages of MIN6 cell-line over other β-cell-lines include high insulin content and glucose responsiveness (especially at low passage) (Ishihara *et al.*, 1993, Persaud, 1999). I used MIN6 cells as a rapid screening tool for establishing the effective OSA® concentrations range and static experiments with MIN6 monolayers showed a concentration-dependent increase in insulin secretion at basal glucose levels. In all our experiments, the basal glucose concentration was maintained at 2mM, a sub-stimulatory concentration of glucose, to eliminate the possible contribution of glucose to the secretory response. The elevation in insulin levels was significant at OSA® concentration of ≥ 0.125 mg/ml.

MIN6 cells used in static experiments were grown as monolayers thus they had a minimal cell-cell contact and were less responsive to secretagogues. Nevertheless, this was restored when MIN6 cells were configured as three-dimensional islets like structure (Pseudoislets: PIs). MIN6 PIs have an improved secretory responsiveness due to enhanced β-cell to β-cell contact and communication (Hauge-Evans *et al.*, 1999) so in our subsequent perifusion experiments MIN6 cells were configured as PIs. Perifusion experiments allow the rate and pattern of insulin secretion to be determined. In our experiments, OSA® initiated insulin secretion at a substimulatory concentration (2mM) of glucose suggesting a nutrient- and metabolism-independent mechanism of action on MIN6 cells. This was further confirmed by our observations that OSA® also potentiated the maximum glucose-induced (20mM) secretory responses, indicating that OSA® does not act as a nutrient itself, nor as an enhancer of glucose metabolism, but has an effect

independent of nutrient metabolism. A 20mM concentration of glucose was chosen to eliminate the contribution of metabolism-induced ATP in OSA®-induced insulin secretion. OSA® also initiated and potentiated insulin secretion from mouse and human islets supporting a direct effect of OSA® on primary β-cells. Perifusion with more physiological concentrations of glucose demonstrated that OSA® stimulated insulin secretory responses from human islets at both 5mM (fasting blood concentration) and 10mM glucose (post-prandial glucose level).

Extracts of GS leaves contain a mixture of saponin compounds (Liu *et al.*, 2004, Manni and Sinsheimer, 1965, Murakami *et al.*, 1996, Sinsheimer and McIlhenny, 1967, Sinsheimer and Rao, 1970, Sinsheimer *et al.*, 1970, Sugihara *et al.*, 2000, Ye *et al.*, 2000, Yoshikawa *et al.*, 1997b, Zhu *et al.*, 2008). The presence of these compounds may be detrimental to membrane integrity and cell viability (Schulz, 1990), causing pathological and unregulated release of insulin from damaged β-cells (Persaud *et al.*, 1999) because these saponins are normally used experimentally as permeation agents in a number of studies (Ahnert-Hilger and Gratzl, 1988, Schulz, 1990). There are a number of reasons why this is unlikely to account for the insulin-releasing properties of OSA®. Firstly, OSA® does not damage β-cell membranes at a concentration of ≤ 0.25 mg/ml OSA® from MIN6 cells and islets as assessed by Trypan Blue exclusion test. OSA® concentration of ≥ 0.5 m/ml caused a marked uptake of the Trypan Blue dye into MIN6 cells and mouse islets in a concentration-dependent manner. The Trypan Blue uptake to virtually all cells was seen when a concentration of 1.0 mg/ml OSA® was used, consistent with a previously reported study (Persaud *et al.*, 1999). Secondly, insulin secretory responses induced by ≤ 0.25 mg/ml OSA® were sustained and readily

reversible following its removal, consistent with the activation of a regulated secretory response. Finally, MIN6 cell or primary islets which had been exposed to OSA® alone were capable of mounting a normal secretory response to glucose following OSA® treatment, confirming that OSA® treatment was not associated with β-cell damage because the cells were subsequently able to metabolize glucose and trigger membrane depolarization in response to glucose.

Nutrients such as glucose have been documented to have a stimulatory effect on insulin biosynthesis, which involves transcription and translation of PPI mRNA (Andrali *et al.*, 2008, Poitout *et al.*, 2006) which is processed to proinsulin and then insulin. Our measurements of mouse PPI mRNA levels indicated that exposure to OSA® alone also caused a significant increase in PPI gene expression which was apparent at both incubations time (24 and 48 hrs) similar to the effect of 20mM glucose on insulin gene expression. 20mM glucose resulted in an approximately 2.5 fold increase in PPI expression throughout the two time points of the experiment. The increase in PPI mRNA levels induced by 20mM glucose have been reported previously to be likely due to an autocrine effect of insulin on insulin gene transcription in addition to a direct effect of glucose on insulin promoter and stabilization of PPI insulin mRNA (Leibiger *et al.*, 2000, Nielsen *et al.*, 1985, Welsh *et al.*, 1985). Our results were consistent with other groups who reported a stimulation of PPI gene expression by glucose in β-cell lines (da Silva Xavier *et al.*, 2000, Nielsen *et al.*, 1985), rat (Giddings *et al.*, 1985, Philippe *et al.*, 1994) and human islets (Evans-Molina *et al.*, 2007). The reported effect was noticeable during prolonged exposure to glucose (most likely after 24-48 hrs), similar to our results. OSA® may also increase mRNA levels of PPI in a mechanism partially similar to

glucose. Our data using mouse islets demonstrated that OSA® had a sustained effect on insulin output during both acute and chronic incubation periods. The insulin secretion induced by OSA® may reach sufficient concentrations in the vicinity of β-cells to act locally on insulin receptor to promote insulin gene expression.

The elevated levels of PPI mRNA were not associated with increases in insulin content from mouse islets exposed to OSA®. Our results showed that following 24 and 48 hrs mouse islets treated with OSA® secreted only less than 5% of their total insulin content, in agreement with published reports that showed islets released about 10% of total insulin content even after prolonged stimulation with 20mM glucose (Bailey *et al.*, 1992). These observations are consistent with a physiological effect of OSA® to compensate for the released insulin by increasing production without overloading the β-cell. This is crucial to maintain stores of insulin and to prevent β-cell insulin depletion.

The stimulatory effect of OSA® was not only confined to β-cells only but also applied to α-cells. OSA® stimulated glucagon secretion at both basal glucose and stimulatory arginine concentrations supporting our observations that OSA® did not act as a nutrient nor via enhanced nutrient metabolism. The ability of insulin secretagogues to modulate glucagon secretion is not uncommon. Sulphonylureas have been shown to increase glucagon secretion in mouse α-cells (MacDonald *et al.*, 2007) and in patients with T1DM (Bohannon *et al.*, 1982). This may possibly reflect some similarities in the mechanism of action between sulphonylurea and OSA®.

In conclusion, OSA® has a direct insulinotropic activity on a β-cell line and on primary islets. It modulates islet function by initiating and potentiating insulin and

glucagon secretion. The secretory responses of OSA® were further supported by the elevations of preproinsulin mRNA and thus maintenance of insulin stores. The ability of OSA® to preserve insulin stores is consistent with therapeutic usefulness in patients with T2DM. Unfortunately, the therapeutic use of OSA® may be hindered by the obscurity of the signalling pathways underlying OSA® actions. Therefore, in chapter 5 the possible molecular mechanisms of actions of OSA® were investigated.

Chapter 5

Gymnema sylvestre-induced insulin secretion: role of extracellular Ca^{2+} and protein kinases

5.1 Introduction

Increasing cytosolic Ca^{2+} and protein kinase activation play important roles in insulin-stimulus secretion coupling. Glucose and other nutrients stimulate insulin secretion primarily through a K_{ATP} channels-sensitive pathway. When glucose enters β-cells, it gets metabolized rapidly generating ATP. Increases in ATP concentration and ATP/ADP ratio cause closure of K_{ATP} channels, depolarization of β-cells and opening of voltage gated Ca^{2+} channels (VGCC). Opening of VGCC results in Ca^{2+} influx, elevation of intracellular Ca^{2+} concentration ($[Ca^{2+}]_i$) and insulin exocytosis (Ashcroft and Ashcroft, 1992, Howell, 1984). Non-nutrients potentiate insulin secretion through receptor-mediated activation of second messengers and protein kinases. Activation of G-protein coupled receptors linked to either αq and αs leads to activation of PLC and AC, respectively. PLC generates IP3 and DAG which increases Ca^{2+} release from intracellular stores and activates DAG-sensitive PKC, respectively. On the other hand, AC generates cAMP from ATP which in turn amplifies the stimulus signal through PKA-dependent and PKA-independent pathways (Howell *et al.*, 1994). PLA_2 also has been reported to influence insulin secretion by librating arachidonic acid (AA) from phosphatidylcholine. PLA_2 has been categorized into three major groups: cytosolic PLA_2 ($cPLA_2$), Ca^{2+}-independent PLA_2 ($iPLA_2$)and secretory PLA_2 ($sPLA_2$) (Persaud *et al.*, 2007). While $cPLA_2$ and $iPLA_2$ can be activated by glucose (Jones *et al.*, 2004), $sPLA_2$ is mainly activated under inflammatory conditions (Sun *et al.*, 2004). Although the mechanism of action of AA-induced insulin secretion is not completely understood, it may involve 1) facilitating Ca^{2+} entry through VGCC, 2) increasing Ca^{2+} release from intracellular

stores, 3) activating protein kinases and 4) stimulating fusion of insulin vesicles and exocytosis (Jones and Persaud, 1993).

I have established in chapter 4 that OSA® directly initiated and potentiated insulin secretion from the MIN6 cell line and from mouse and human islets. It is important to understand the molecular mechanism of action(s) of OSA® if OSA® is to be used therapeutically but the intracellular signaling pathway by which OSA® increases insulin secretion is currently unknown. Therefore, in this chapter I investigated whether the stimulatory action of OSA® on insulin secretion from MIN6 cells and mouse islets is dependent on extracellular Ca^{2+} and indentified the possible intracellular signaling components(s) of OSA®-induced insulin secretion from mouse and human islets.

5.2 Materials and Methods

5.2.1 Plant material and preparation

OSA® was prepared by extracting the fresh GS leaves as mentioned in section 2.1.1. The OSA® powder was a gift from Dr. Arun Chatterji (Ayurvedic Life International, Wisconsin, USA). Aqueous stock (200 mg/ml) of OSA® was freshly prepared and diluted in physiological solution for experiments.

5.2.2 Maintenance of MIN6 cells

MIN6 cells (passage 30-37) were maintained as monolayers in DMEM supplemented with 10% fetal bovine serum (FBS), 2mM glutamine and 100U/ml penicillin/0.1mg/ml streptomycin under standard tissue culture conditions (section 2.3.2). The cells were harvested and used in experiments when the cell confluency reached 70-80%.

5.2.3 Isolation of mouse and human islets

Islets from male ICR mice and non-diabetic humans were isolated as described in section 2.4 and 2.5. The isolated mouse islets were cultured in RPMI supplemented with 10% newborn calf serum (NCS) and 100U/ml penicillin/0.1mg/ml streptomycin while the human islets were kept in CMRL supplemented with 10% NCS and 100U/ml penicillin/0.1mg/ml streptomycin in humidified (5% CO_2, 95% O_2) incubator.

5.2.4 Insulin secretion

5.2.4.1 Static and perifusion secretion with MIN6 cells, mouse and human islets

The effect of various inhibitors on OSA®-induced insulin secretion from MIN6 cells, mouse and human islets were assessed using either static secretion experiments or temperature-controlled perifusion apparatus, essentially as described previously in section 2.7. In static incubations, MIN6 cells (20,000 cells/well), section 2.7.1, or mouse islets (3 islets/300µl), section 2.7.2, were pre-treated with 2mM glucose medium for 2 hrs. MIN6 cells and mouse islets were treated for 30 minutes and 1 hr, respectively, with OSA® in the presence or absence of agents mentioned in the corresponding figure legends. 100µl of supernatant was removed and stored at -20C° until assayed for insulin content by RIA.

In perifusion experiments (section 2.7.3), groups of 60 mouse islets or 100µl of the suspended human islets were perifused with buffer containing 2mM glucose, 2mM $CaCl_2$ and 0.5 mg/ml BSA and supplemented with 0.25 mg/ml OSA® in the

presence or absence of various pharmacological inhibitors. The perifusate was collected every 2 min and stored at -20C° until assayed for insulin content by RIA.

5.2.5 Measurement of intracellular Ca^{2+} levels ($[Ca^{2+}]_i$)

MIN6 cells (50,000 cells/coverslip) or dispersed mouse islets (160,000 cells/coverslip) were seeded on ethanol-washed and poly-D-lysine coated glass cover slips, respectively. Cells were allowed to adhere overnight under standard tissue culture conditions. The effect of OSA® on $[Ca^{2+}]_i$ were measured by Ca^{2+} microfluorimetry as described in section 2.12. Cells were loaded by Fura-2/AM for 30 min at 37C° and then perifused with 2mM glucose supplemented with OSA® (flow rate 1ml/min) in the presence or absence of either 0.1mM EGTA or 10μM nifedipine. Cells were excited at 340 and 380nm and the emitted light was captured by a CCD camera. Changes in $[Ca^{2+}]_i$ were expressed as a 340:380 ratio.

5.2.6 Measurement of intracellular cAMP levels

MIN6 cells (30,000 cells/well) or mouse islets (5 islets/well) were treated for 30 minutes at 37C° with treatments shown in the corresponding Figure legends. 100μl of supernatant was removed and assayed for insulin content by RIA while the cells were lysed and intracellular cAMP levels $[cAMP]_i$ was quantified by enzyme immunoassay as described in section 2.13.

5.2.7 Statistical analysis

Data were expressed as mean ± SEM. The mean for some perifusion expreriments represents the area under the curve was. Differences between treatment groups were assessed using one way analysis of variance (ANOVA), Student's t-test, or

Bonferroni's multiple comparison test as appropriate, and differences between treatments were considered significant at $p< 0.05$.

5.3 Results

5.3.1 Effect of OSA® on mouse β-cell $[Ca^{2+}]_i$

Addition of OSA® caused a marked elevation in $[Ca^{2+}]_i$ in MIN6 cells even at a concentration as low as 0.03 mg/ml (Figure 5.1). This increase in $[Ca^{2+}]_i$ was completely abolished by the removal of extracellular Ca^{2+} using 0.1mM EGTA or by blocking VGCC by 10μM nifedipine. The response to OSA® had a lag time of approximately 3 min and persisted even after washing the cells with 2mM glucose buffer solution creating a new higher basal $[Ca^{2+}]_i$. Further elevation of $[Ca^{2+}]_i$, above the new baseline, was observed after addition of 0.06 mg/ml OSA®. In addition, The cells were able to further elevate $[Ca^{2+}]_i$ after exposure to 500μM Carbachol. Similar to MIN6 cells, dispersed mouse islets responded to 0.06 mg/ml OSA® in a similar fashion to that seen with MIN6 cells (Figure 5.2). Exposing mouse islets to OSA® resulted in a delayed (onset of approximately 3 minutes) and a sustained (even after the removal of OSA®) increase in $[Ca^{2+}]_i$. This response was also completely inhibited by the presence of EGTA and nifedipine.

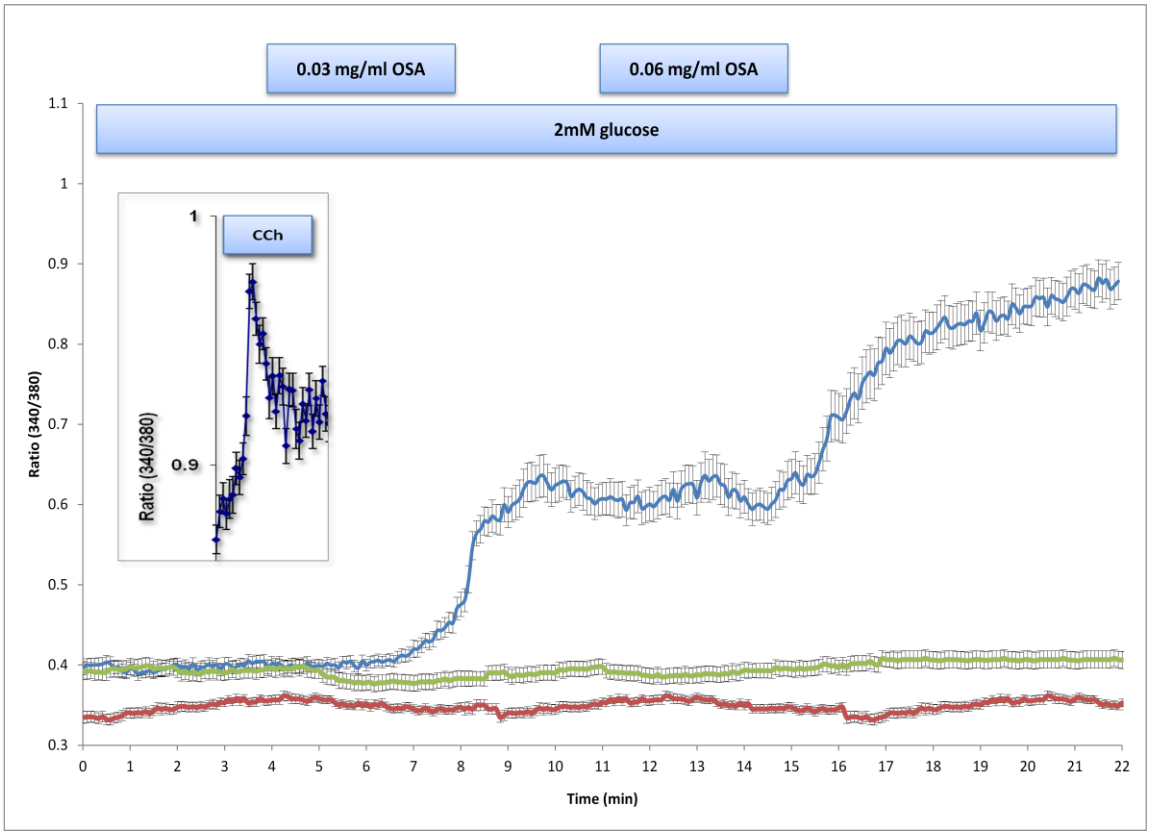

Figure 5.1: Effect of OSA® extract on intracellular Ca^{2+} levels in MIN6 β-cells. Fura-2-loaded MIN6 cells were perifused throughout with a buffer containing 2mM glucose and supplemented with OSA® extract for 3 min, as shown by the horizontal bar, in the presence (—) or absence (—) of extracellular Ca^{2+} or in the presence of nifedipine (—) . Changes in $[Ca^{2+}]_i$ were determined by single cell microfluorimetry and expressed as 340/380nm ratiometric data. OSA® significantly (P<0.01) elevated $[Ca^{2+}]_i$ which was completely abolished in the absence of extracellular Ca^{2+} or in the presence of nifedipine (P<0.01). Carbachol (CCh) further elevated $[Ca^{2+}]_i$ from cells which had been exposed to OSA® (inset) Data are mean ± SEM, n=30-34 cells for each experimental treatment.

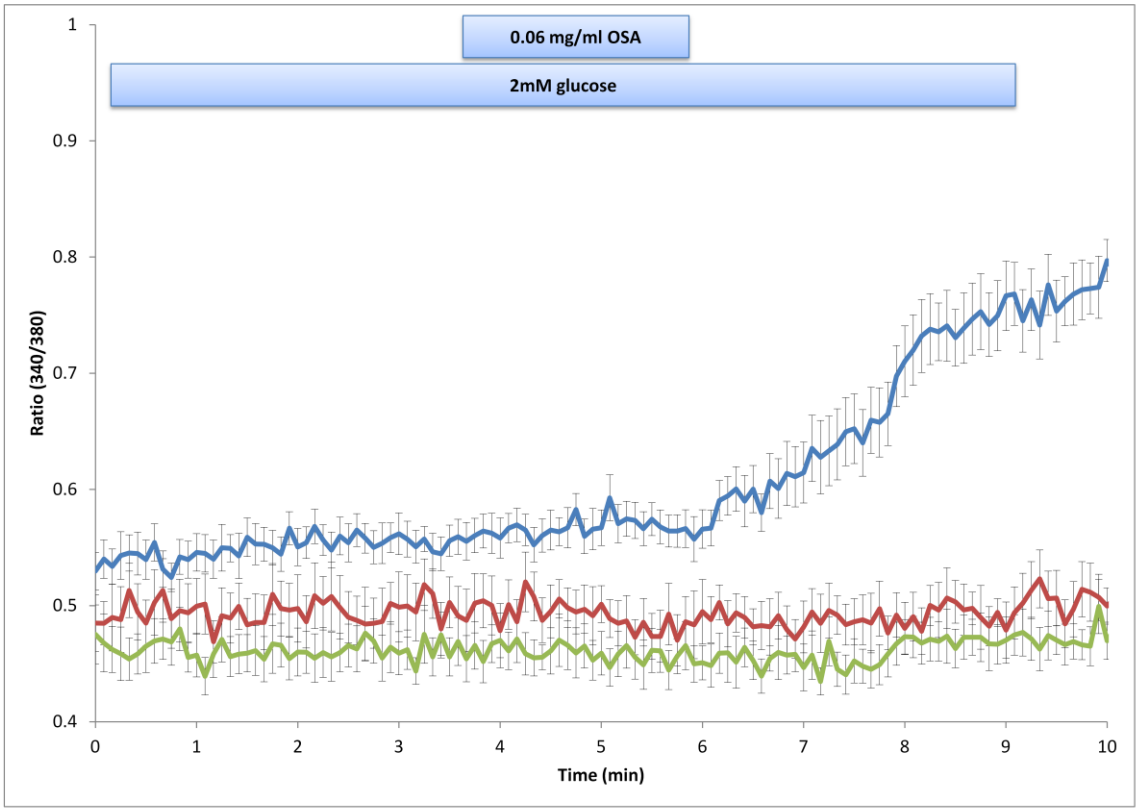

Figure 5.2: Effect of OSA® extract on intracellular Ca^{2+} levels in mouse islet β-cells. Fura-2-loaded dispersed mouse islets were perifused throughout with a buffer containing 2mM glucose and supplemented with OSA® extract for 3 min, as shown by the horizontal bar, in the presence (—) or absence (—) of extracellular Ca^{2+} or in the presence of nifedipine (—) . Changes in $[Ca^{2+}]_i$ were determined by single cell microfluorimetry and expressed as 340/380nm ratiometric data. OSA® significantly (P<0.01) elevated $[Ca^{2+}]_i$ which was completely abolished in the absence of extracellular Ca^{2+} or in the presence of nifedipine (P<0.01). Data are mean ± SEM, n=30-34 cells for each experimental treatment.

5.3.2 Effect of K_{ATP} channel opening on OSA®-induced insulin secretion from mouse islets

One hour incubation of mouse islets with 0.25 mg/ml OSA® caused a significant increase in insulin secretion as shown in Figure 5.4. Addition of 250μM diazoxide, a K_{ATP} channel opener, completely blocked glucose-induced insulin secretion (Figure 5.3) but did not alter the OSA® effect on insulin secretion (Figure 5.4).

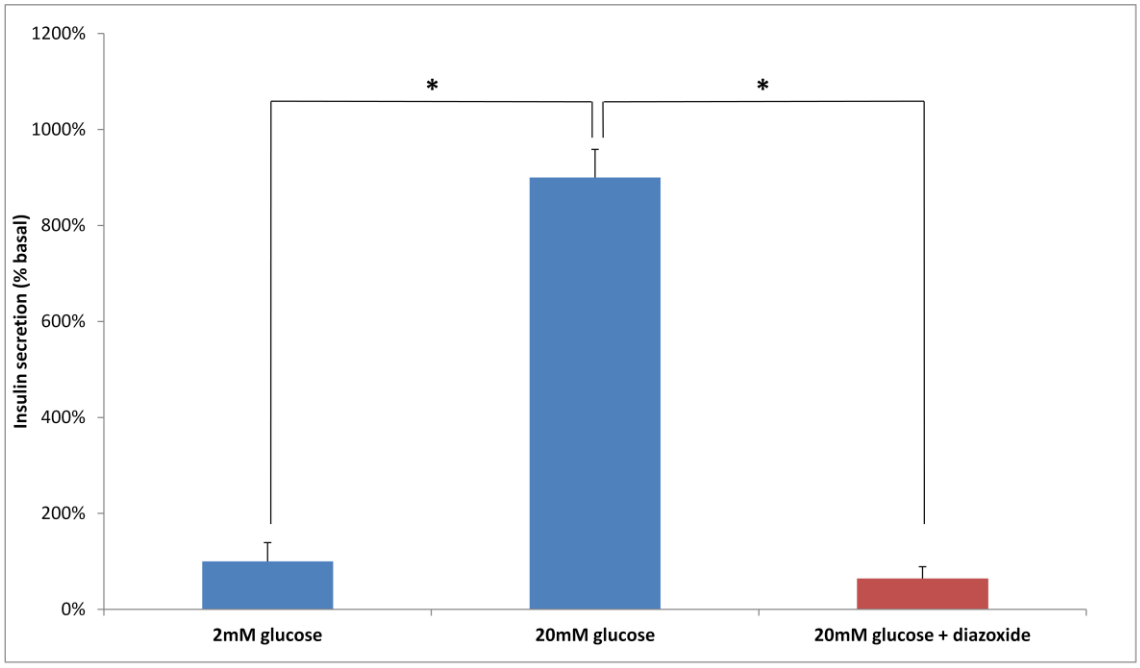

Figure 5.3: Effect of diazoxide on glucose-induced insulin secretion from mouse islets. Mouse islets were preincubated with buffer supplemented with 2mM glucose for 2 hrs before incubating them with Gey & Gey buffer supplemented with 2mM glucose alone or with 20mM glucose in the presence (▪) or absence (▪) of diazoxide. Data show mean + SEM, n=10 for each treatment. Diazoxide completely blocked insulin secretion induced by 20mM glucose (* $p < 0.05$).

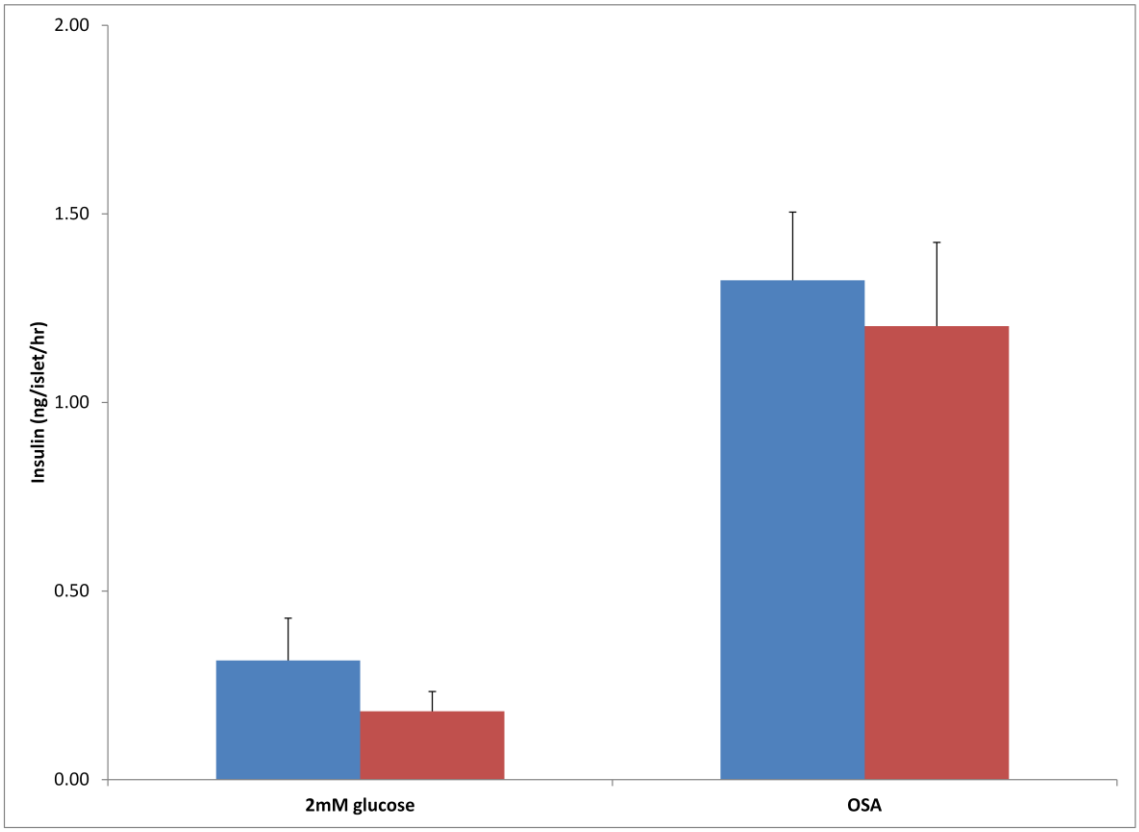

Figure 5.4: Effect of K_{ATP} channel opening on OSA®-induced insulin secretion from mouse islets. Three islets were preincubated with buffer supplemented with 2mM glucose for 2 hrs before incubating them with buffer supplemented with either 2mM glucose or 0.25mg/ml OSA® in the presence (▪) or absence (▪) of diazoxide. Data show mean + SEM, n=10 for each treatment. Diazoxide did not alter the insulin secretory effect of OSA®.

5.3.3 Effect of extracellular Ca^{2+} removal and VGCC blockade on OSA®-induced insulin secretion from MIN6 cell monolayers

Thirty minutes exposure of MIN6 cell monolayers to OSA® (0.25 and 1.0 mg/ml) caused an increase in insulin secretion. Removal of extracellular Ca^{2+} (+ 0.1mM EGTA) or addition of nifedipine reduced the increases in insulin output in the presence of 0.25 mg/ml but not 1.0 mg/ml OSA®-treated cells (Figure 5.5 and 5.6, respectively).

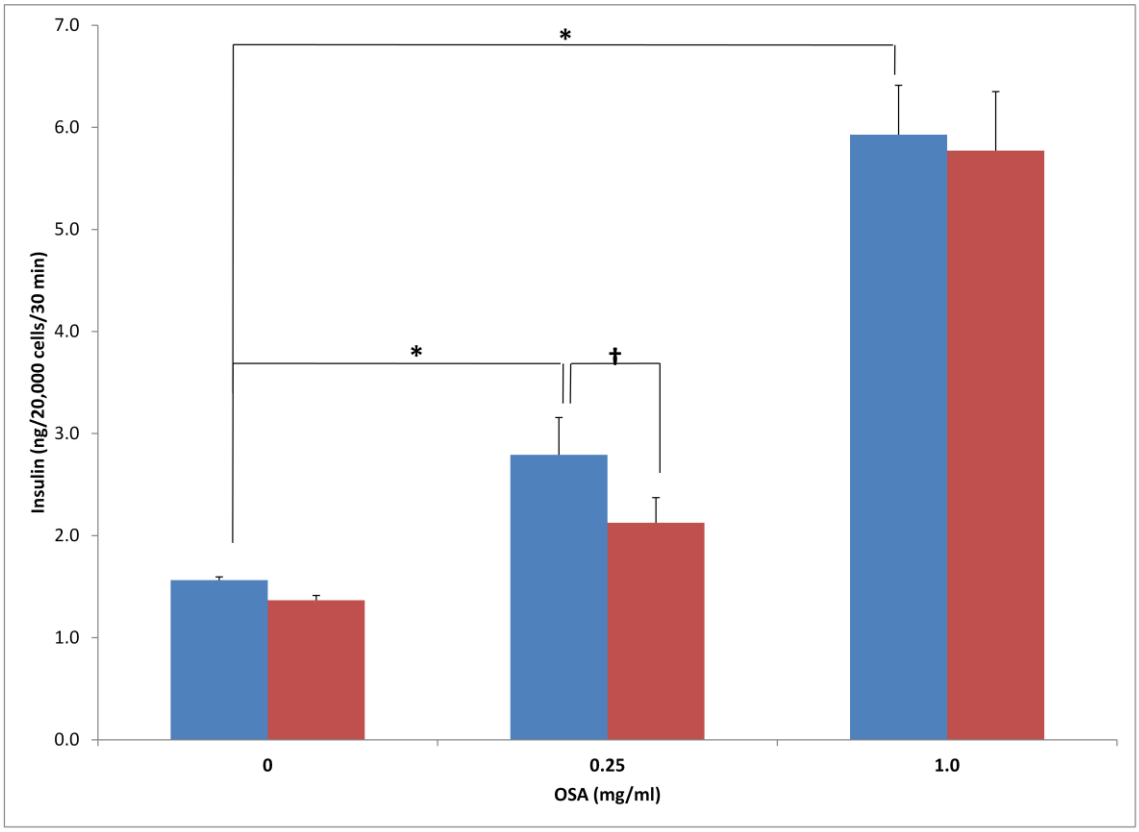

Figure 5.5: Effect of Ca^{2+} removal on OSA®-induced insulin secretion from MIN6 cells monolayers. MIN6 cells were preincubated with buffer supplemented with 2mM glucose for 2 hrs before incubating them with 2mM glucose Gey & Gey buffer supplemented with either 0.25 mg/ml or 1.0 mg/ml OSA® in the presence (▪) or absence (▪) of 0.1mM EGTA. Data show mean + SEM, n=10 for each treatment group. Addition of OSA® (0.25 or 1.0 mg/ml) significantly increase insulin secretion (*p<0.05 when compared to 0 mg/ml OSA® within the same group). However, the removal of extracellular Ca^{2+} reduced insulin secretion in the presence of 0.25 mg/ml but not 1.0 mg/ml OSA® (†p<0.05 when compared to the same treatment in the absence of EGTA).

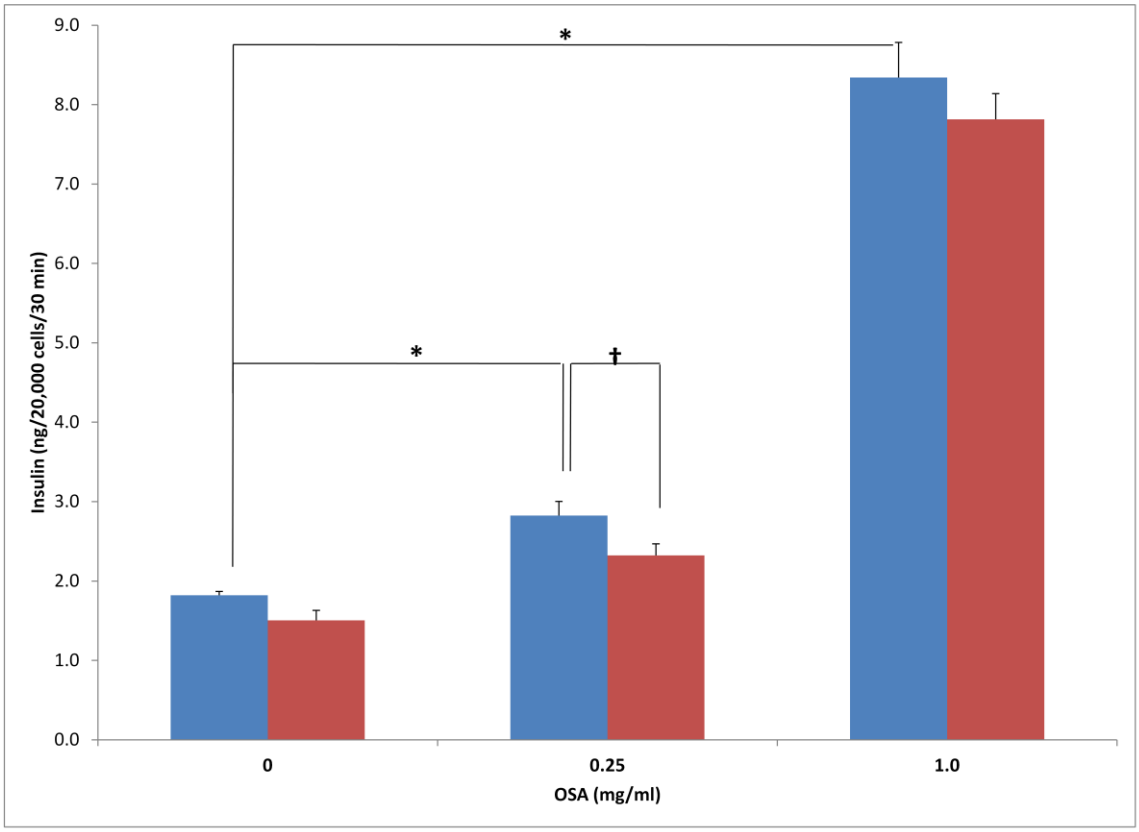

Figure 5.6: Effect of VGCC blockade on OSA®-induced insulin secretion from MIN6 cell monolayers. MIN6 cells were preincubated with buffer supplemented with 2mM glucose for 2 hrs before incubating them with 2mM glucose Gey & Gey buffer supplemented with either 0.25 mg/ml or 1.0 mg/ml OSA® in the presence (▪) or absence (▪) of 10µM nifedipine. Data show mean + SEM, n=10 for each treatment group. Addition of OSA® (0.25 or 1.0 mg/ml) significantly increased insulin secretion (*p<0.05 when compared to 0 mg/ml OSA® within the same group). However, blocking VGCC did significantly reduce insulin secretion in the presence of 0.25 mg/ml but not 1.0 mg/ml OSA® (†p<0.05 when compared with the same treatment in the absence of nifedipine)

5.3.4 Effect of VGCC blockade on OSA®-induced insulin secretion from mouse and human islets

Perifusing either mouse (Figure 5.8) or human islets (Figure 5.9) with buffer containing 0.25 mg/ml OSA® for 20 minutes induced a rapid and sustained insulin secretion at 2mM glucose. The sustained increase in insulin secretion caused by OSA® was significantly decreased but not completely abolished when VGCC were blocked with 10µM nifedipine, a concentration that showed to be effective in blocking glucose-induced insulin secretion (Figure 5.7). These results were consistent with the partial inhibitory effect seen in static incubations of MIN6 cell monolayers.

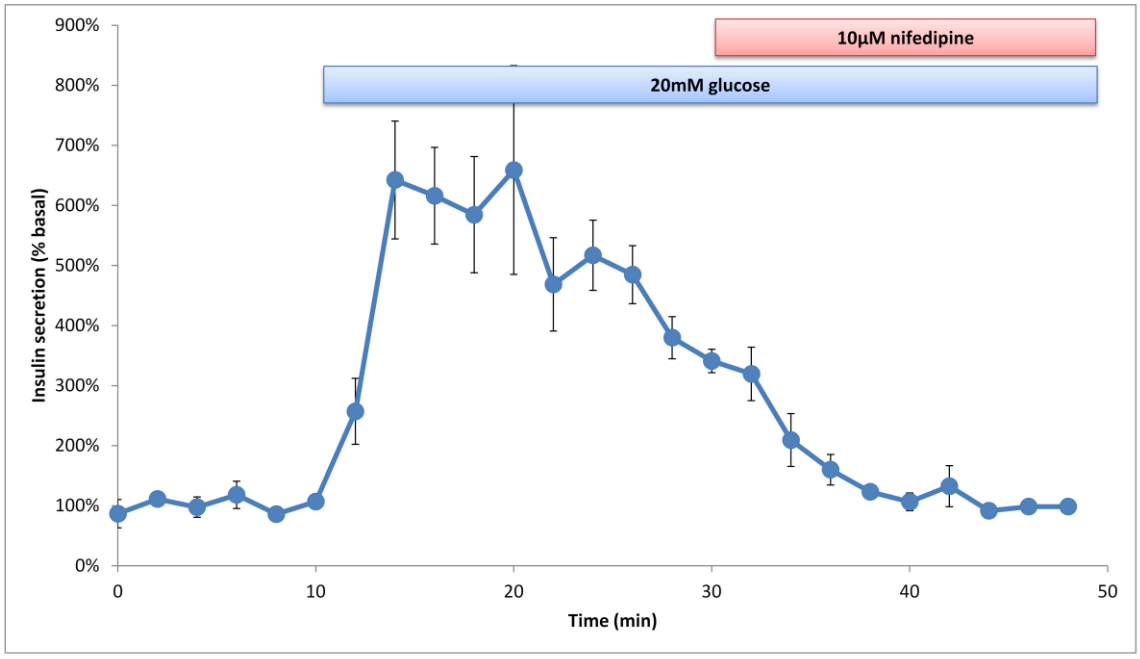

Figure 5.7: Effect of nifedipine on glucose-induced insulin secretion from human islets. Human islets were preperifused with buffer supplemented with 2mM glucose for 2 hrs before perifusing them with Gey & Gey buffer supplemented with 20mM glucose throughout and then in the presence 10µM nifedipine (30-50 min) as shown by the horizontal bar. Data show mean ± SEM, n=4 for each treatment. Nifedipine blocked insulin secretion induced by 20mM glucose ($p<0.05$).

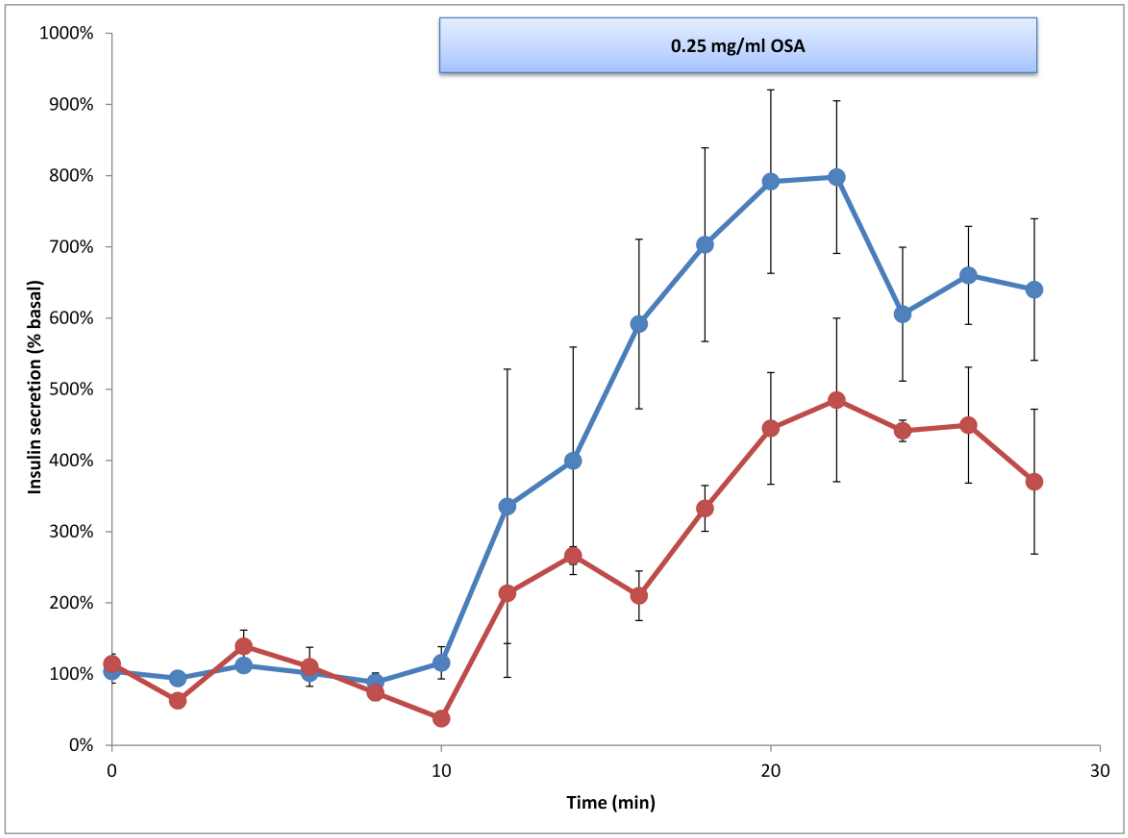

Figure 5.8: Effect of VGCC blockade on OSA®-induced insulin secretion from mouse islets. Mouse islets were perifused with buffer supplemented with 2mM glucose for 10 minutes first and then with OSA® in the presence (●) or absence (●) of 10µM nifedipine. Results are expressed as percentage of basal (2mM glucose). Points show mean ± SEM, n=4. Nifedipine reduced but not completely abolished OSA®-induced insulin secretion ($p<0.01$).

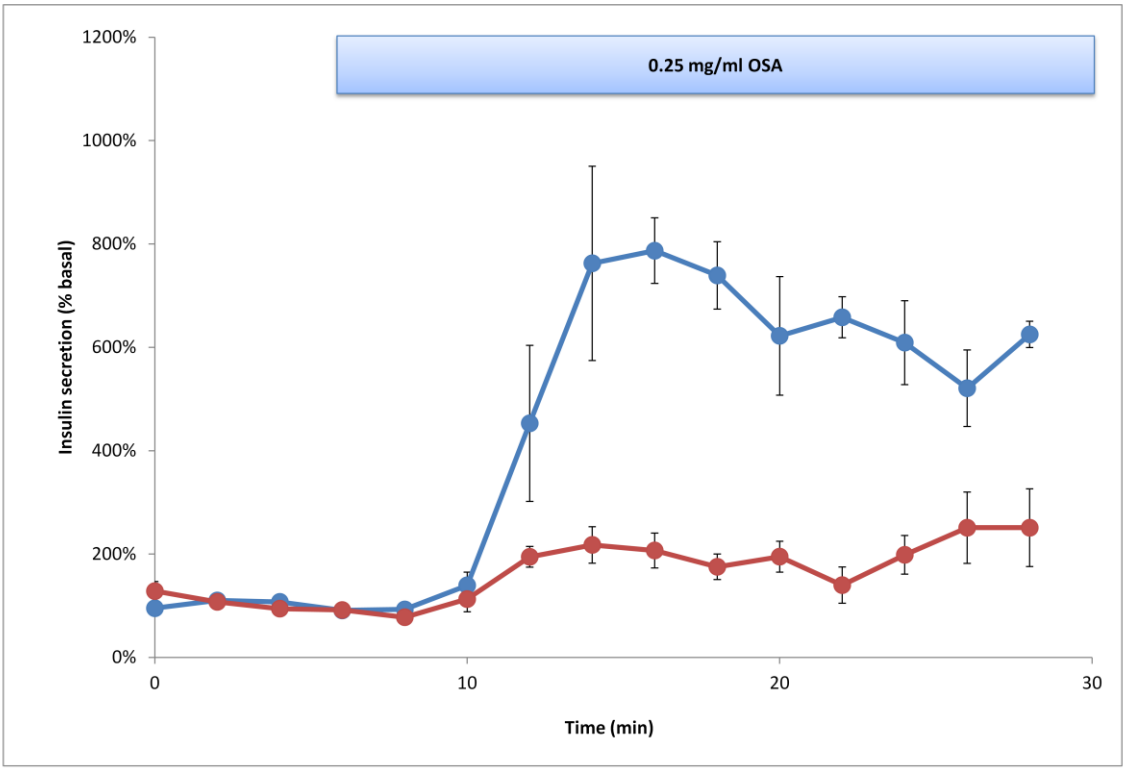

Figure 5.9: Effect of VGCC blockade on OSA®-induced insulin secretion from human islets. Human islets were perifused with buffer supplemented with 2mM glucose for 10 minutes first and then with OSA® in the presence (●) or absence (●) of 10μM nifedipine. Results are expressed as percentage of basal insulin secretion (2mM glucose). Points show mean ± SEM, n=4. Nifedipine reduced but not completely abolished OSA®-induced insulin secretion ($p<0.01$).

5.3.5 Effect of protein kinase inhibition on OSA®-induced insulin secretion from mouse and human islets

The involvement of protein kinases in the signaling of OSA®-induced insulin secretion was assessed using pharmacological inhibitors of protein kinases known to be involved in insulin-secretion coupling. Staurosporine, a non-selective ATP site general protein kinase inhibitor, inhibited carbachol-induced insulin secretion (Figure 5.10). However, it partially but not completely inhibited the stimulatory effect of OSA® on insulin secretion from mouse (Figure 5.11) and human (Figure 5.12) islets, consistent with the involvement of protein kinase activation in OSA-induced insulin secretory responses.

The possible contributions of diacylglycerol (DAG)-sensitive protein kinase C and Ca^{2+}/calmodulin kinase II (CaMK II) were further investigated by perifusing OSA®-treated islets with buffers containing selective inhibitors of DAG-dependent isoforms (α and β) of protein kinase C (Gö 6976) and CaMK II (KN62). Interestingly, neither 1μM Gö 6976 (Figure 5.14 and 5.15) nor 10μM KN62 (Figure 5.17 and 5.18) inhibited the insulin secretory profile from either mouse or human islets exposed to OSA®, although both compounds have shown to be effective at the concentrations used in these experiments (Harris *et al.*, 1997, Li *et al.*, 1992) (Figure 5.13 and 5.16).

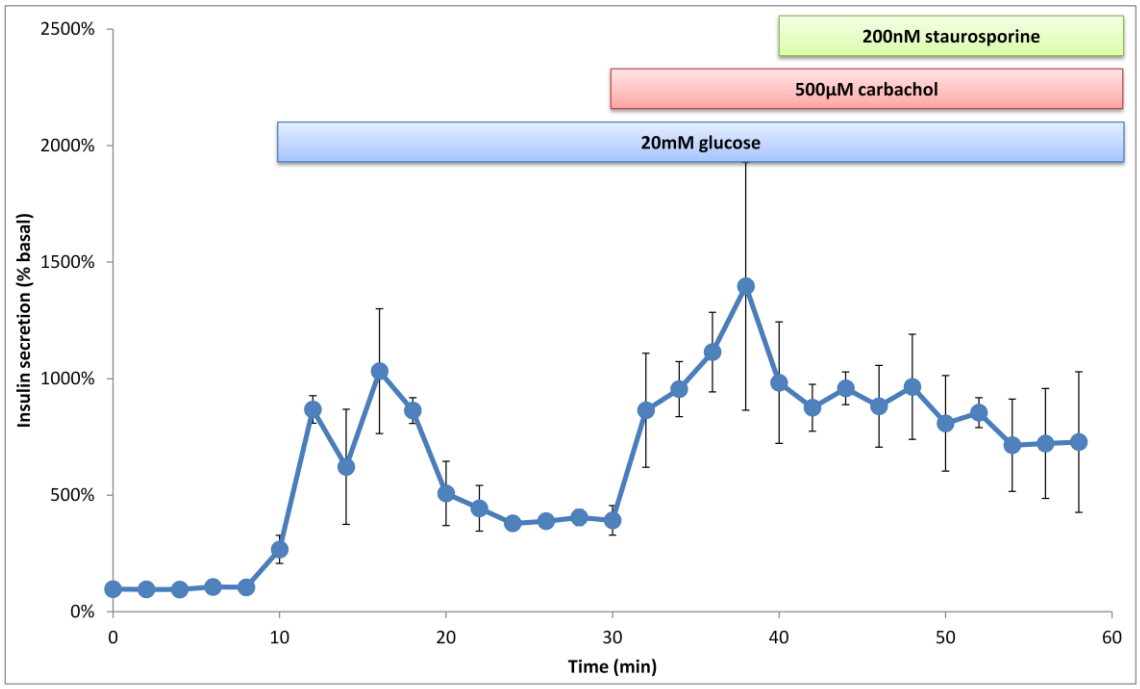

Figure 5.10: Effect of staurosporine on carbachol-induced insulin secretion from human islets. Human islets were preperifused with buffer supplemented with 2mM glucose for 1 hrs before perifusing them with Gey & Gey buffer supplemented with 20mM glucose throughout and then in the presence of 500μM carbachol alone (30-40 min) or with 500μM carbachol + 200nM staurosporine (40-60 min). Data show mean ± SEM, n=2 for each treatment. Staurosporine blocked insulin secretion induced by carbachol ($p<0.05$).

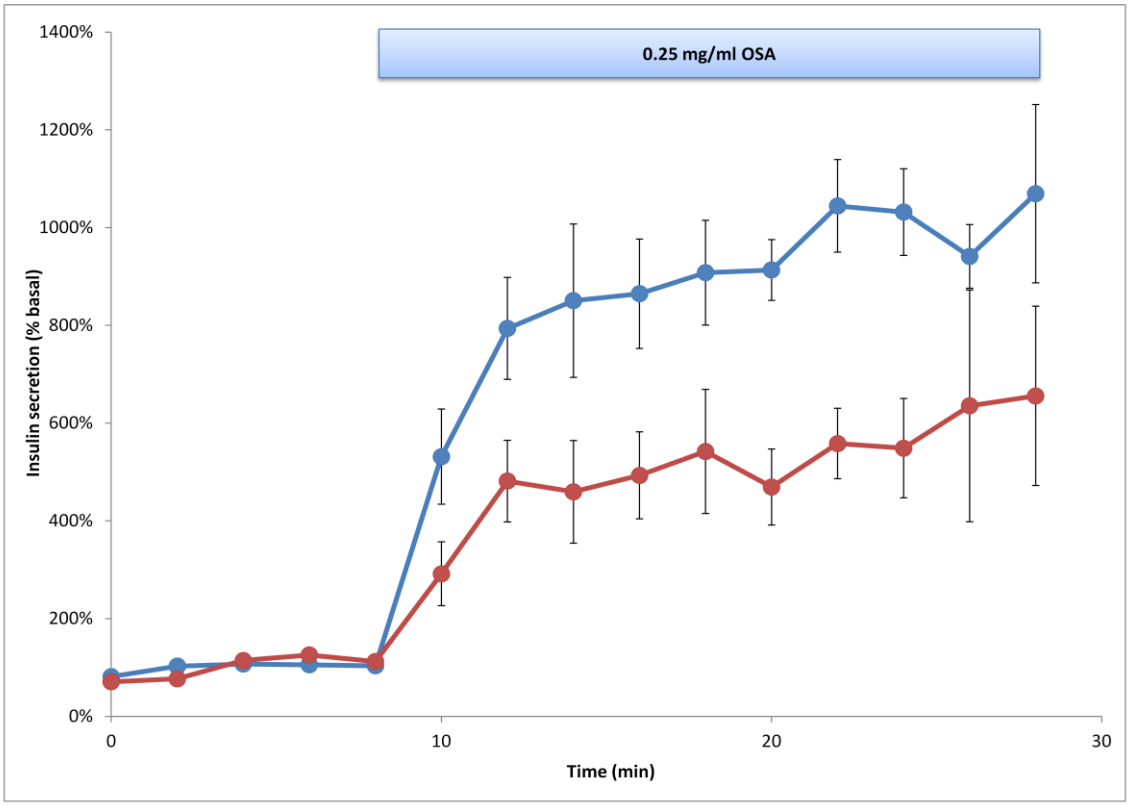

Figure 5.11: Effect of staurosporine on OSA®-induced insulin secretion from mouse islets. Mouse islets were perifused with buffer supplemented with 2mM glucose then with 0.25 mg/ml OSA® in the presence (●) or absence (●) of 200nM staurosporine. Results are expressed as percentage of basal insulin secretion (2mM glucose). Points show mean ± SEM, n=4. Staurosporine reduced but not completely abolished OSA®-induced insulin secretion ($p<0.01$).

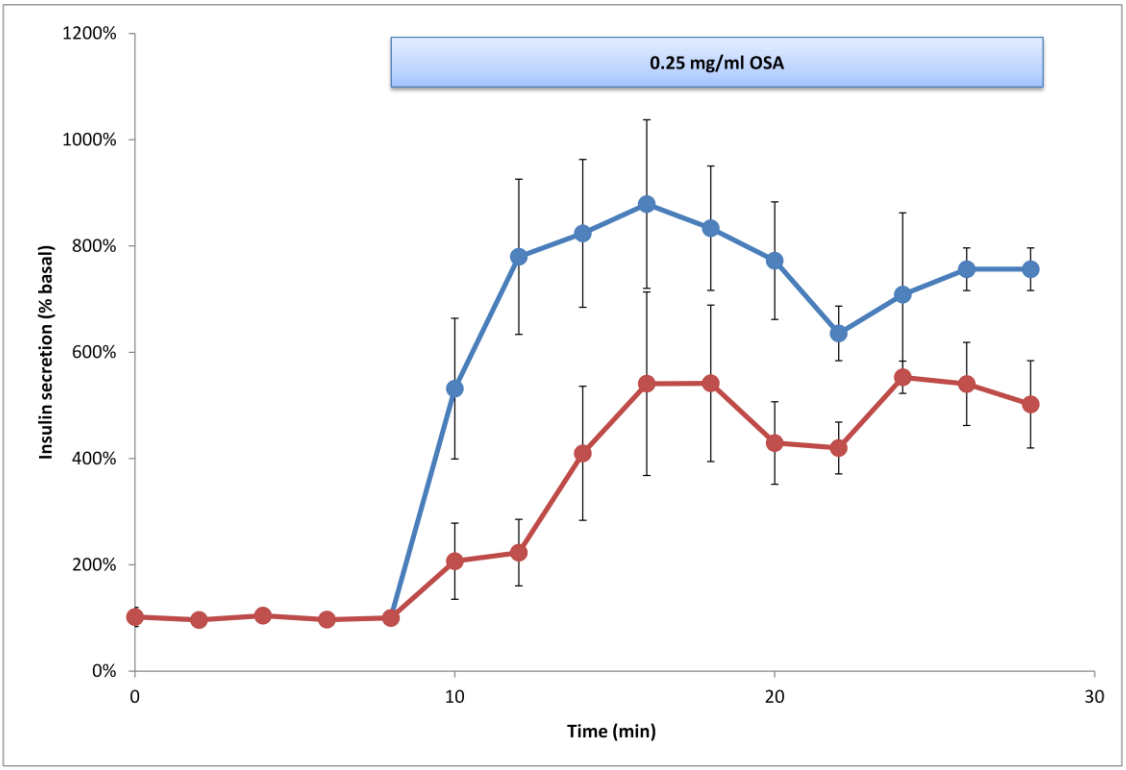

Figure 5.12: Effect of staurosporine on OSA®-induced insulin secretion from human islets. Human islets were perifused with buffer supplemented with 2mM glucose then with 0.25 mg/ml OSA® in the presence (●) or absence (●) of 200nM staurosporine. Results are expressed as percentage of basal insulin secretion (2mM glucose). Points show mean ± SEM, n=4. Staurosporine reduced but not completely abolished OSA®-induced insulin secretion (p<0.01).

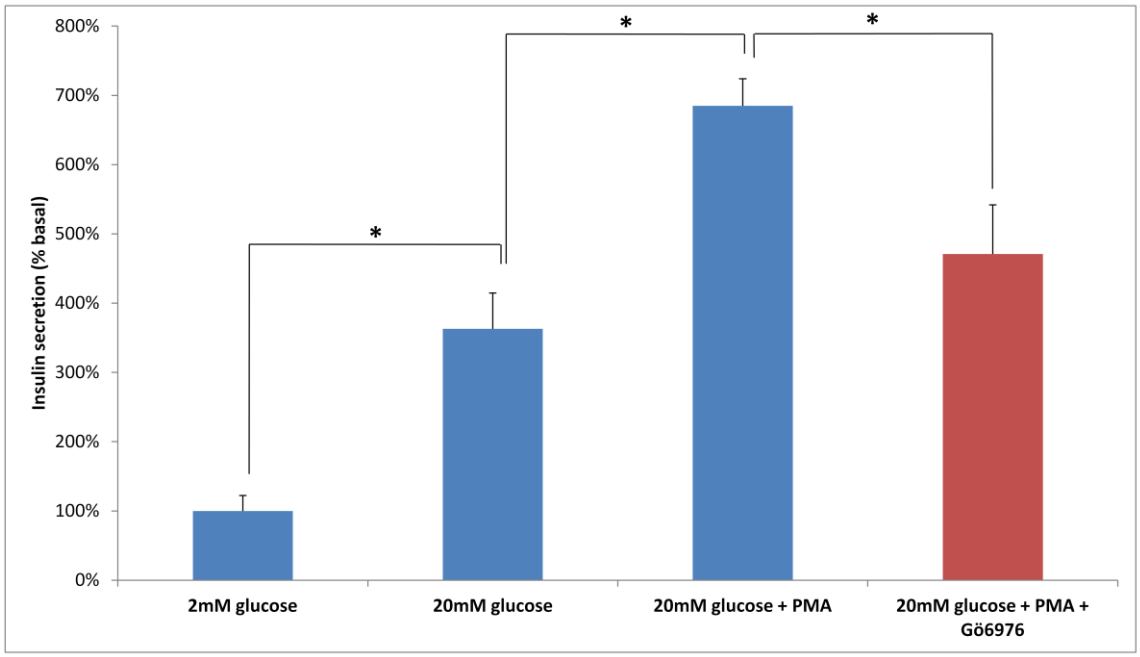

Figure 5.13: Effect of Gö 6976 on PMA-induced insulin secretion from mouse islets. Mouse islets were preincubated with buffer supplemented with 2mM glucose for 2 hrs before incubating them with Gey & Gey buffer supplemented with 2mM glucose alone or 20mM glucose alone or 20mM glucose + 500nM PMA or 20mM glucose + 500nM PMA + 1µM Gö 6976. Data shows mean + SEM, n=6-8 for each treatment. Gö 6976 reduced insulin secretion induced by 20mM glucose + PMA (*p<0.05).

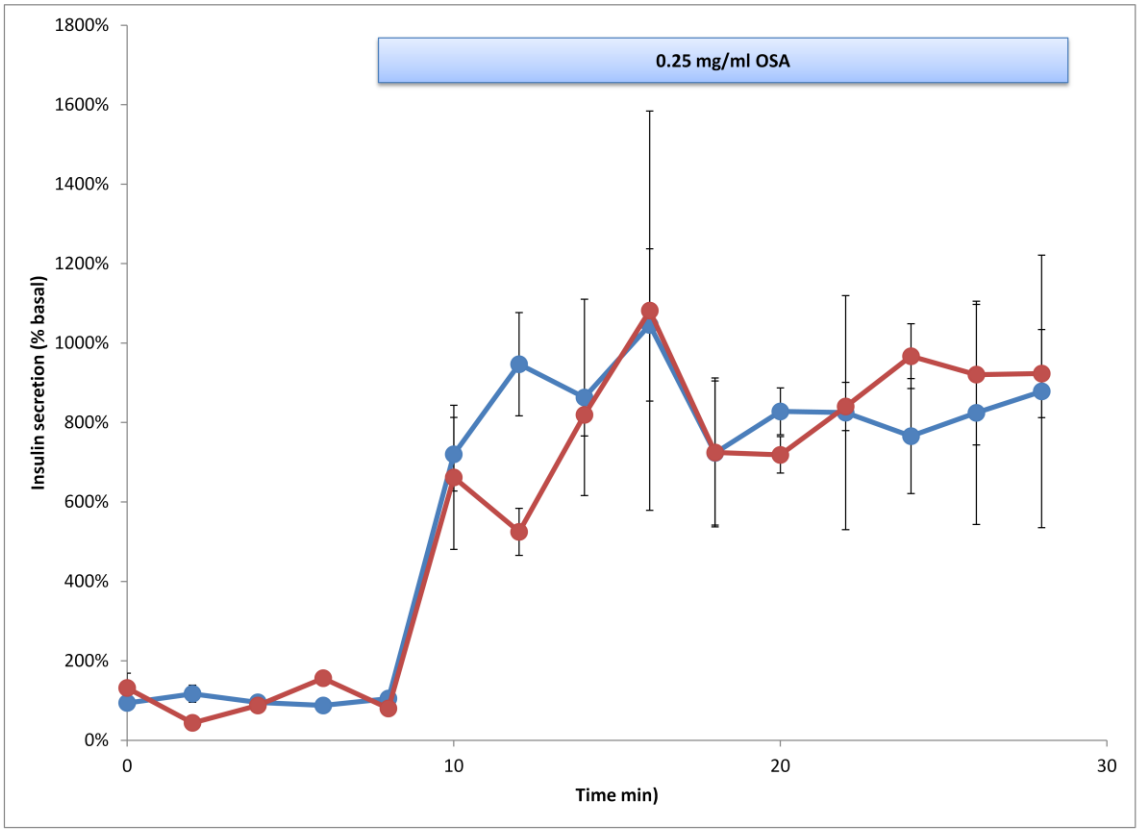

Figure 5.14: Effect of PKCαβ inhibition on OSA®-induced insulin secretion from mouse islets. Mouse islets were perifused with buffer supplemented with 2mM glucose then with 0.25 mg/ml OSA® in the presence (●) or absence (●) of 1μM Gö 6976. Results are expressed as percentage of basal insulin secretion (2mM glucose). Points show mean ± SEM, n=4. PKCαβ inhibition did not alter the insulin output induced by OSA®.

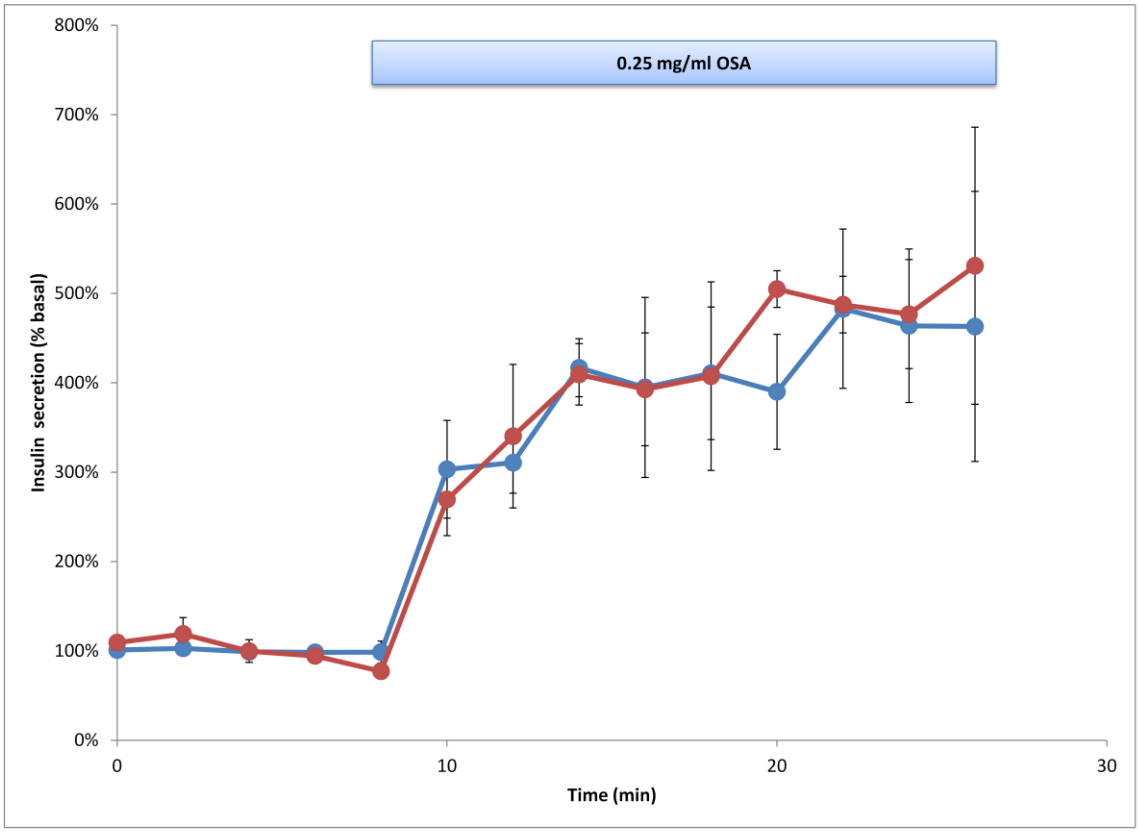

Figure 5.15: Effect of PKCαβ inhibition on OSA®-induced insulin secretion from human islets. Human islets were perifused with buffer supplemented with 2mM glucose then with 0.25 mg/ml OSA® in the presence (●) or absence (●) of 1μM Gö 6976. Results are expressed as percentage of basal insulin secretion (2mM glucose). Points show mean ± SEM, n=4. PKCαβ inhibition did not alter the insulin output induced by OSA®.

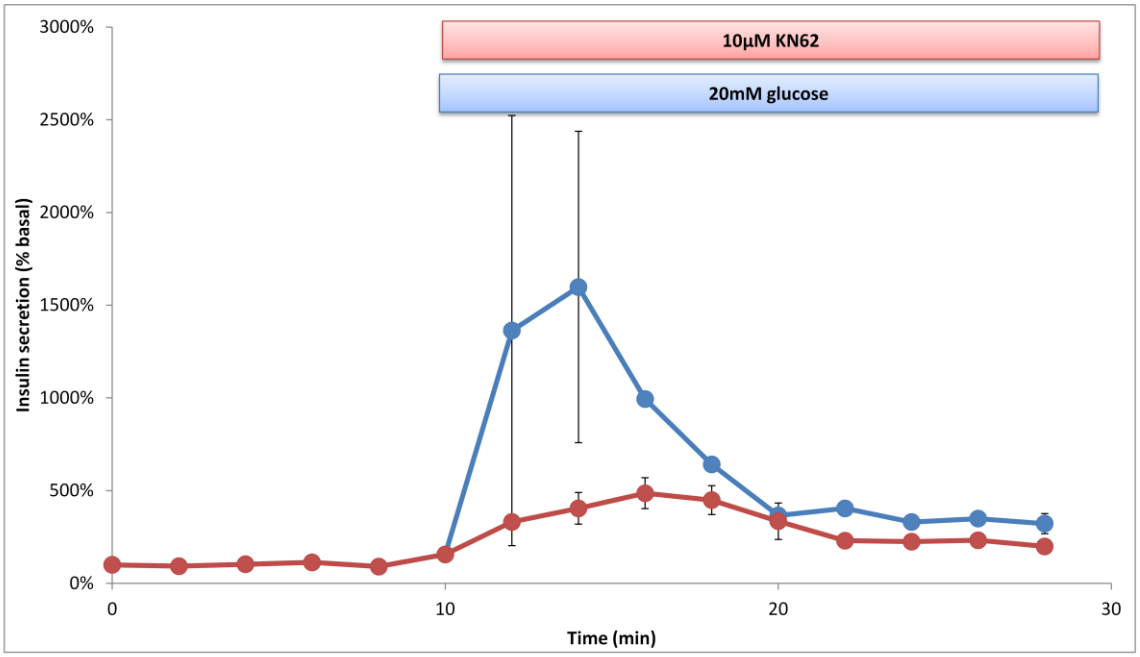

Figure 5.16: Effect of KN62 on glucose-induced insulin secretion from human islets. Human islets were preperifused with buffer supplemented with 2mM glucose for 1 hrs before perifusing them with Gey & Gey buffer supplemented with 20mM glucose in the presence (●) or absence (●) of 10μM KN62. Data show mean ± SEM, n=4 for each treatment. KN62 reduced insulin secretion induced by 20mM glucose ($p<0.05$).

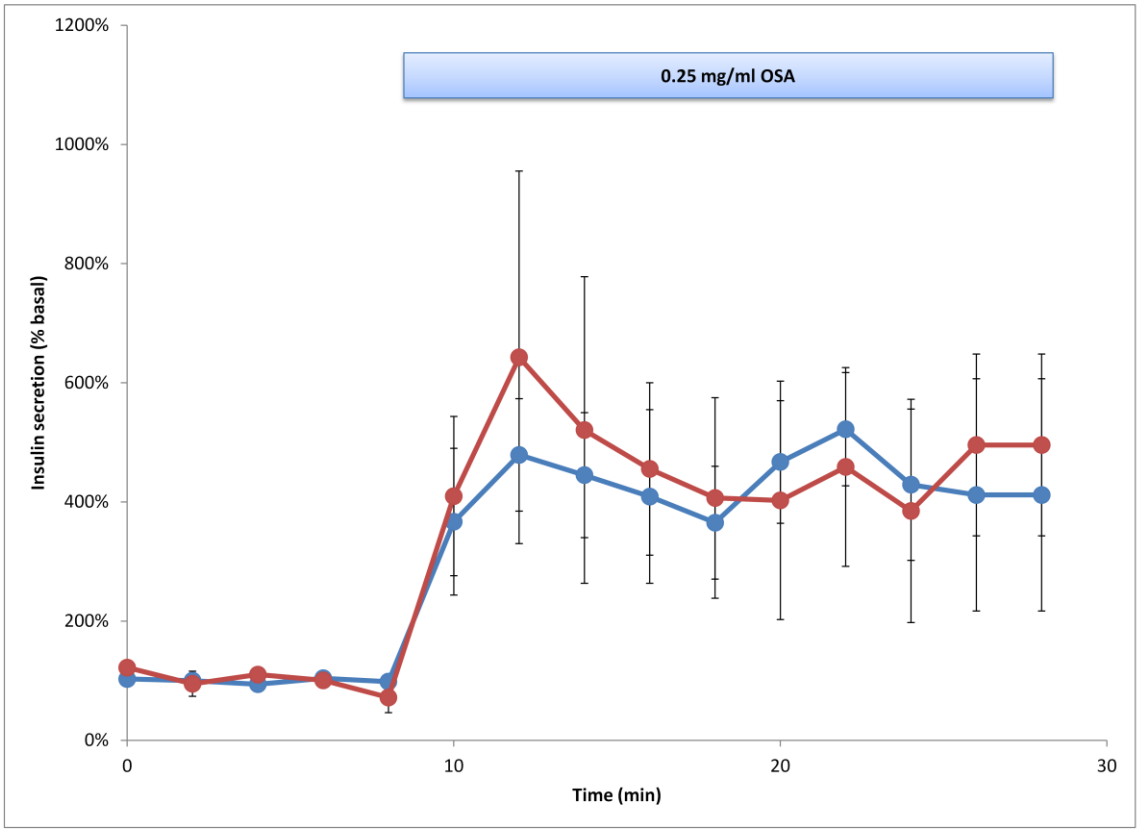

Figure 5.17: Effect of CAMK II inhibition on OSA®-induced insulin secretion from mouse islets. Mouse islets were perifused with buffer supplemented with 2mM glucose then with 0.25 mg/ml OSA® in the presence (●) or absence (●) of 10µM KN62. Results are expressed as percentage of basal insulin secretion (2mM glucose). Points show mean ± SEM, n=4. OSA®-induced insulin secretion was not inhibited by KN62.

5.3.6 Effect of OSA® on mouse β-cells $[cAMP]_i$

The possible role of cAMP in mediating the effect of OSA® on insulin secretion was also investigated. MIN6 cells or mouse islets were treated with buffer containing 2mM or 20mM glucose in the presence of 0.25 mg/ml OSA® or 10µM noradrenaline. The treated cells were incubated throughout the experiments with the non-selective phosphodiesterases inhibitor, 3-isobutyl-1-methylxanthine (IBMX) or IBMX plus forskolin (FSK), an activator of adenylate cyclase, to allow for $[cAMP]_i$ measurements. Thirty minutes exposure of MIN6 cells to 20mM glucose in the presence of 0.25 mg/ml OSA® significantly reduced glucose-induced $[cAMP]_i$ in cells treated with IBMX (Figure 5.19). This effect was further manifested when the cells were incubated with FSK. OSA® completely attenuated FSK-induced elevation

in $[cAMP]_i$ stimulated by glucose (Figure 5.20). Noradrenaline, which is α2 agonist, reduced $[cAMP]_i$ and thus decreased glucose-stimulated insulin secretion and is used as a positive control. Similarly, OSA® blocked the increase in $[cAMP]_i$-induced by glucose in IBMX or FSK-treated mouse islets (Figure 5.23 and 5.24). Despite the reductions of $[cAMP]_i$ in MIN6 cells and mouse islets, concurrent measurement of insulin showed a stimulation of insulin secretion by OSA® (Figure 5.21, 5.22, 5.25 and 5.26).

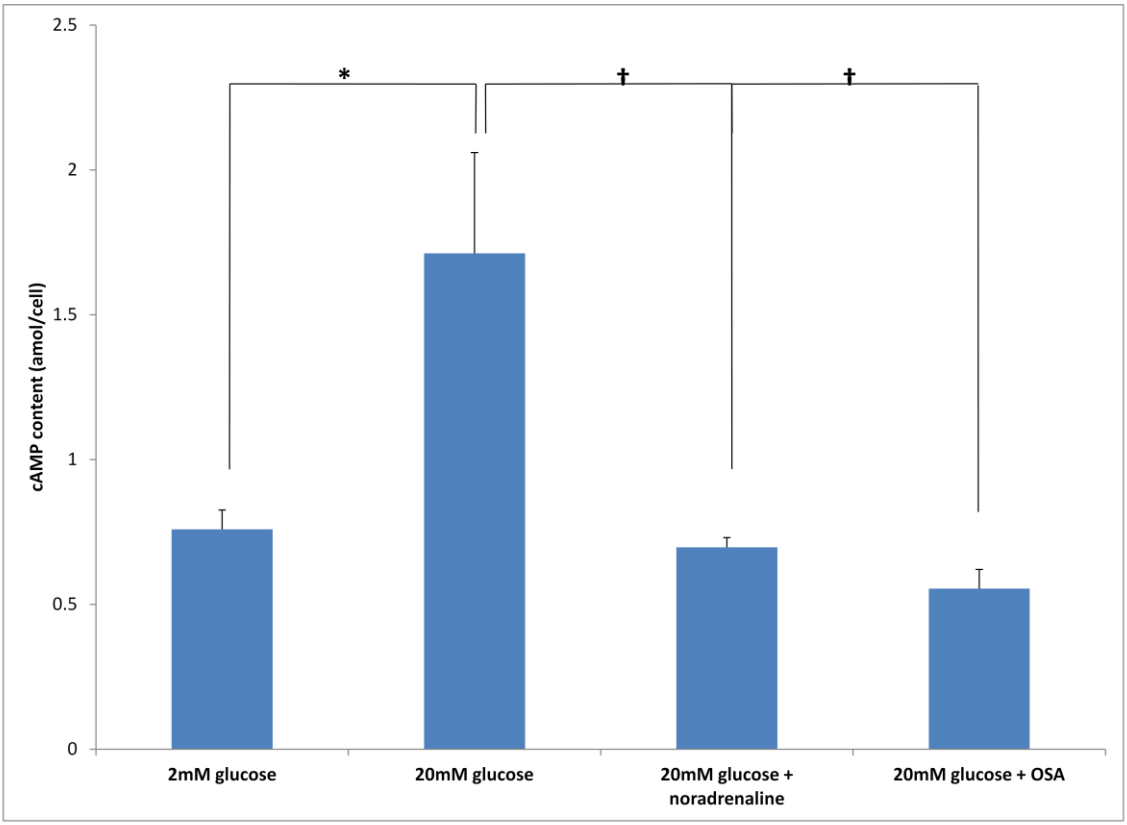

Figure 5.19: Effect of OSA® extract on intracellular cAMP levels in IBMX-treated MIN6 β-cells. MIN6 cells were preincubated with 2mM glucose for 2 hrs and then incubated for 30 minutes with 2mM glucose Gey & Gey buffer alone or supplemented with 20mM glucose in the presence or absence of 10μM noradrenaline (as positive control) or 0.25 mg/ml OSA® in the presence of IBMX (▪). Cells were lysed and intracellular cAMP levels ($[cAMP]_i$) were determined by ELISA. Glucose induced accumulation of $[cAMP]_i$ (* $p<0.05$ versus 2mM glucose) which was reduced by noradrenaline and OSA® in IBMX-treated cells (†$p<0.05$ versus 20mM glucose alone). Data show mean + SEM, n=8.

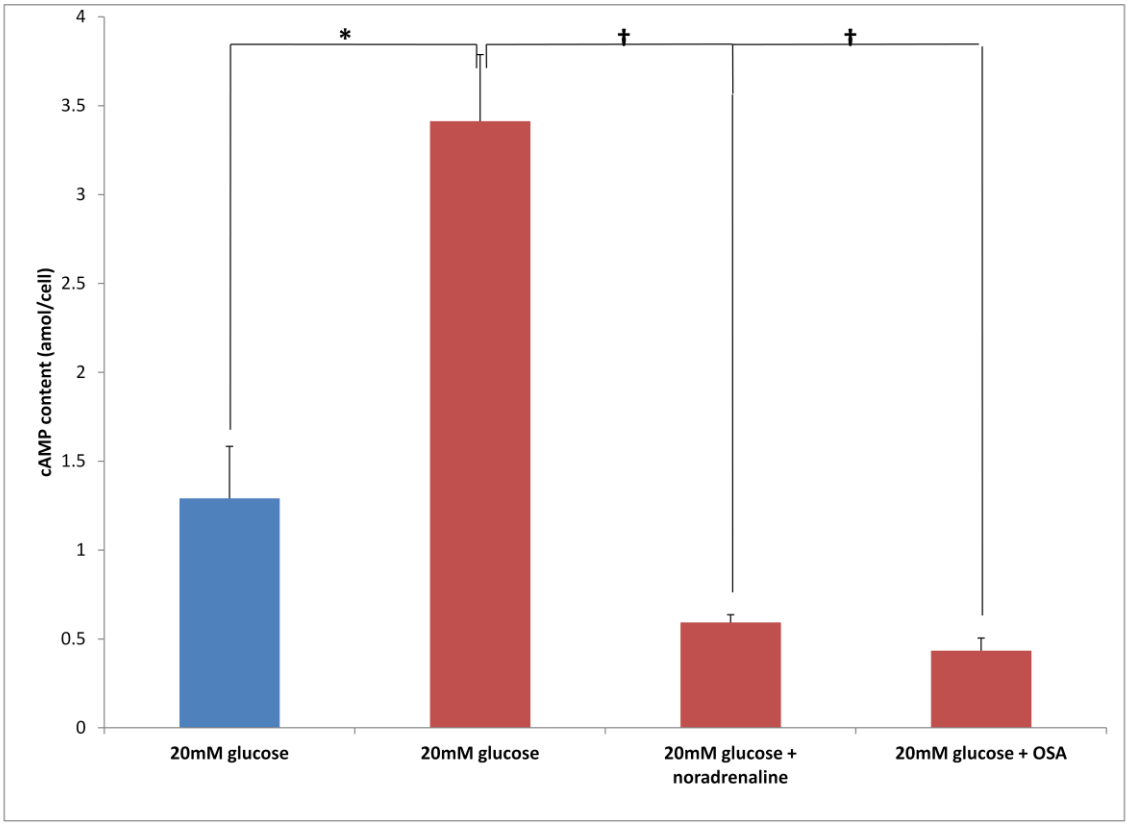

Figure 5.20: Effect of OSA® extract on intracellular cAMP levels in FSK-treated MIN6 β-cells. MIN6 cells were preincubated with 2mM glucose for 2 hrs and then incubated for 30 minutes with buffer supplemented with 20mM glucose in the presence or absence of 10μM noradrenaline (as positive control) or 0.25 mg/ml OSA® in the presence of IBMX (▪) or FSK (▪). Cells were lysed and intracellular cAMP levels ($[cAMP]_i$) were determined by ELISA. FSK caused further elevations in $[cAMP]_i$ over glucose-induced $[cAMP]_i$ in IBMX-treated cells (*p<0.05 versus 20mM glucose in the absence of FSK). However, the glucose induced accumulation of $[cAMP]_i$ which was reduced by noradrenaline and OSA® in FSK -treated cells (†p<0.05 versus 20mM glucose in the presence of FSK). Data show mean + SEM, n=8 .

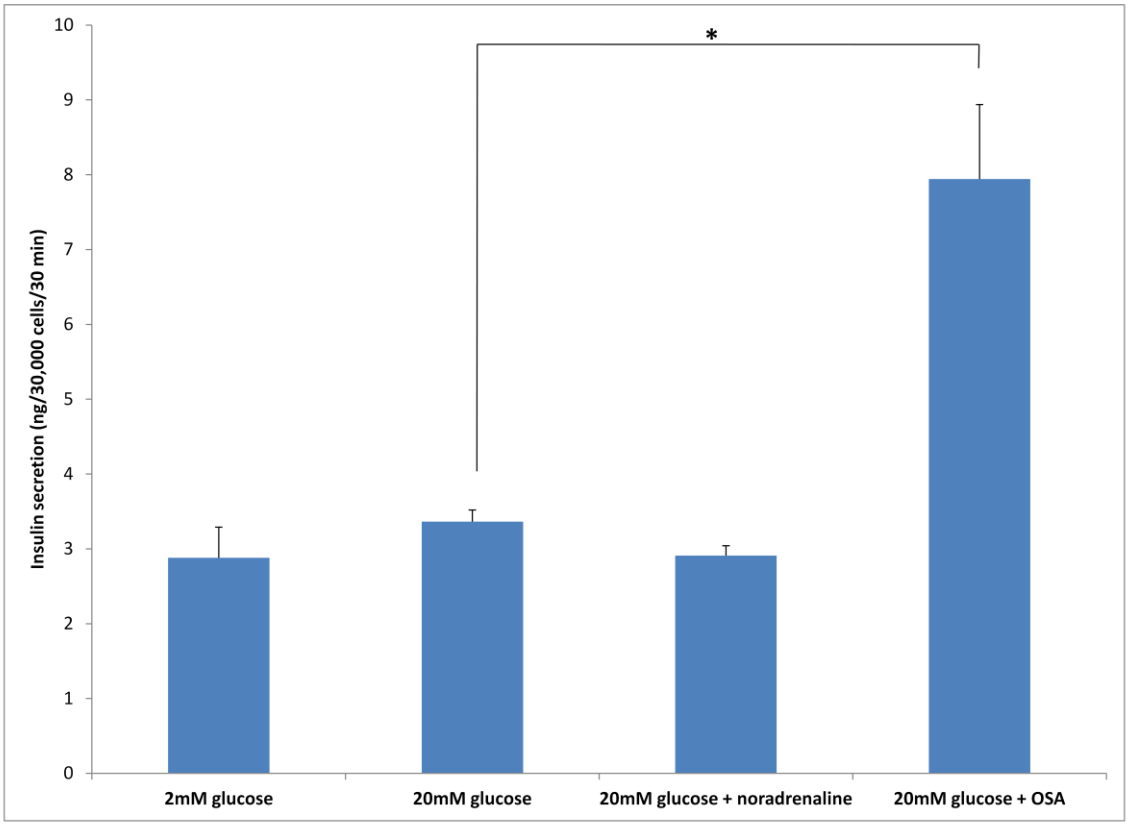

Figure 5.21: Effect of OSA® extract on insulin secretion from IBMX-treated MIN6 β-cells. MIN6 cells were preincubated with 2mM glucose for 2 hrs and then incubated for 30 minutes with 2mM glucose Gey & Gey buffer alone or supplemented with 20mM glucose in the presence or absence of 10µM noradrenaline (as positive control) or 0.25 mg/ml OSA® in the presence of IBMX (▪). The supernatant was removed and insulin content was measured by RIA. OSA® caused increases in glucose-induced insulin secretion from IBMX-treated cells (*p<0.05 versus 20mM glucose alone). Data show mean + SEM, n=8.

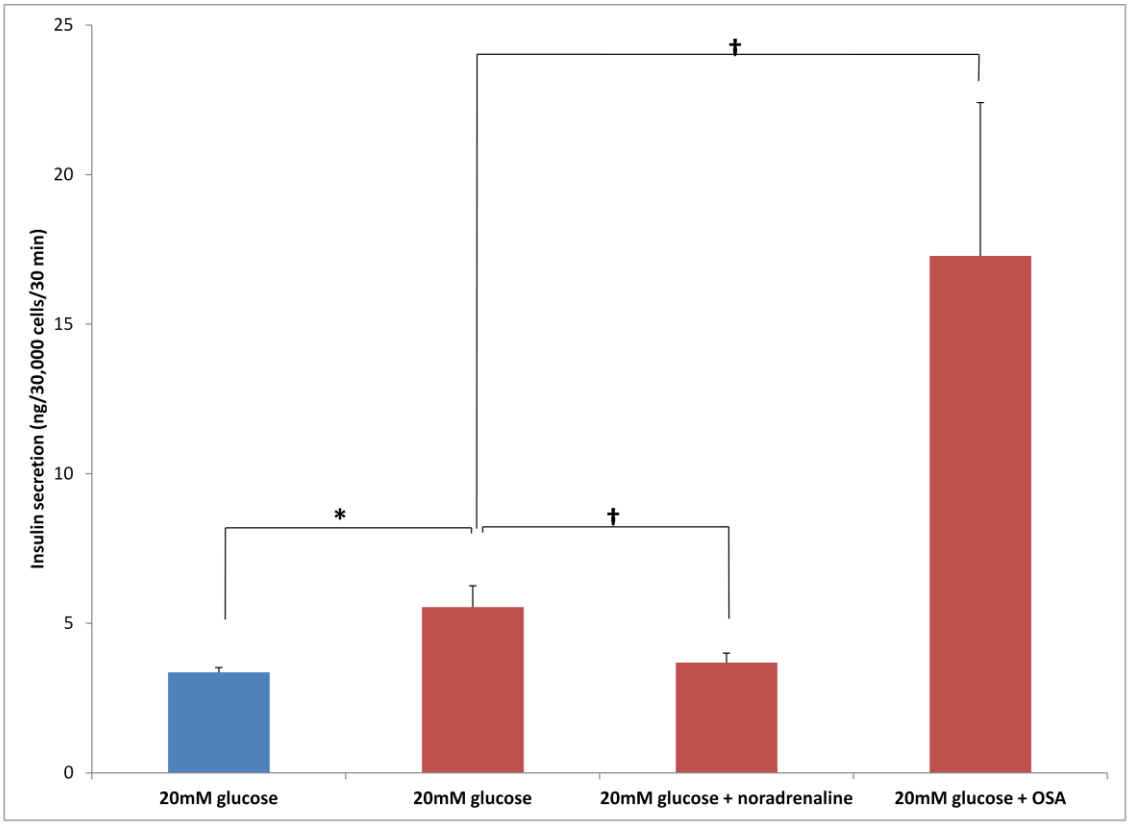

Figure 5.22: Effect of OSA® extract on insulin secretion from FSK-treated MIN6 β-cells. MIN6 cells were preincubated with 2mM glucose for 2 hrs and then incubated for 30 minutes with 2mM glucose Gey & Gey buffer alone or supplemented with 20mM glucose in the presence or absence of 10µM noradrenaline (as positive control) or 0.25 mg/ml OSA® in the presence of IBMX (▪) or FSK (▪). The supernatant was removed and insulin content was measured by RIA. FSK caused further increase in insulin secretion over glucose-induced insulin secretion in IBMX-treated cells (*p<0.05 versus 20mM glucose in the absence of FSK). The glucose-induced insulin secretion was reduced by noradrenaline but augmented by OSA® in FSK -treated cells (†p<0.05 versus 20mM glucose in the presence of FSK). Data show mean + SEM, n=8 .

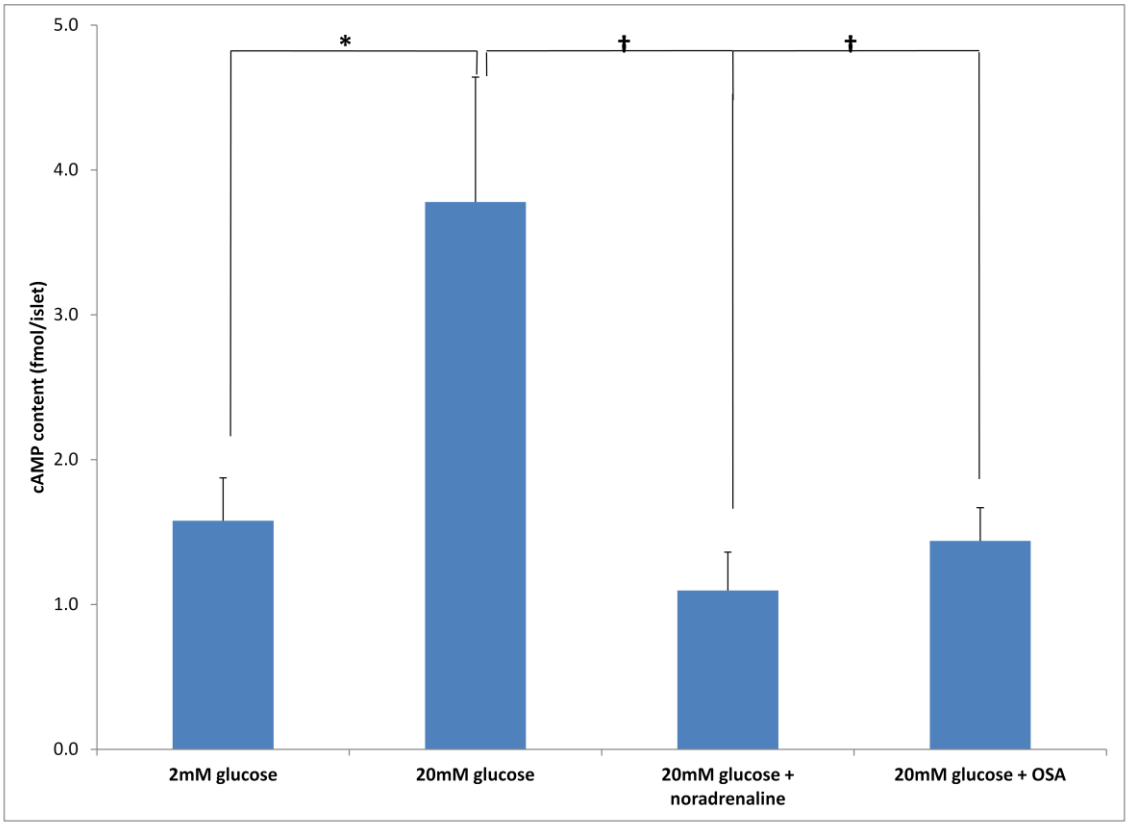

Figure 5.23: Effect of OSA® extract on intracellular cAMP levels in IBMX- treated mouse islets. Mouse islets were preincubated with 2mM glucose for 2 hrs and then incubated for 30 minutes with 2mM glucose Gey & Gey buffer alone or supplemented with 20mM glucose in the presence or absence of 10µM noradrenaline (as positive control) or 0.25 mg/ml OSA® in the presence of IBMX (▪). Cells were lysed and intracellular cAMP levels ($[cAMP]_i$) were determined by ELISA. Glucose induced accumulation of $[cAMP]_i$ (*p<0.05 versus 2mM glucose) which was reduced by noradrenaline and OSA® in IBMX-treated cells (†p<0.05 versus 20mM glucose) . Data show mean + SEM, n=8.

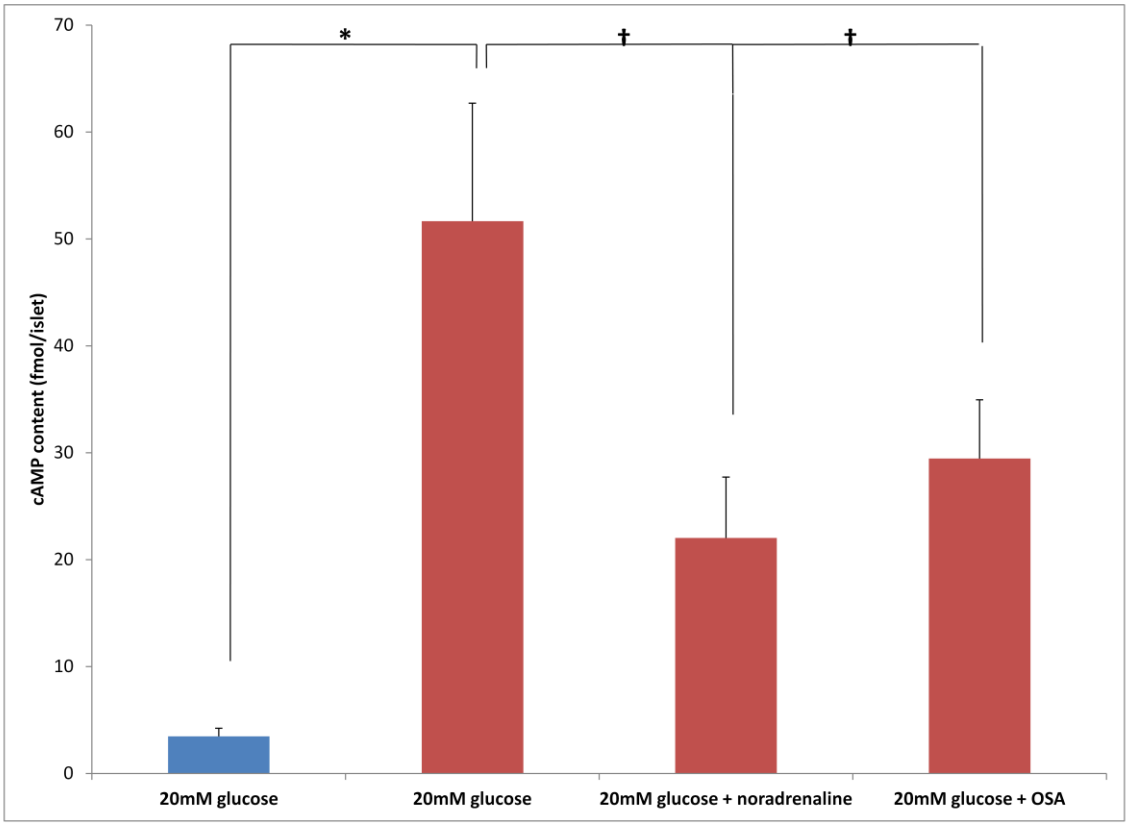

Figure 5.24: Effect of OSA® extract on intracellular cAMP levels in FSK-treated mouse islets. Mouse islets were preincubated with 2mM glucose for 2 hrs and then incubated for 30 minutes with buffer supplemented with 20mM glucose in the presence or absence of 10µM noradrenaline (as positive control) or 0.25 mg/ml OSA® in the presence of IBMX (▪) or FSK (▪). Cells were lysed and intracellular cAMP levels ($[cAMP]_i$) were determined by ELISA. FSK caused further elevations in $[cAMP]_i$ over glucose-induced $[cAMP]_i$ in IBMX-treated cells (*p<0.05 versus 20mM glucose in the absence of FSK). However, the glucose-induced accumulation of $[cAMP]_i$ was reduced by noradrenaline and OSA® in FSK -treated cells (†p<0.05 versus 20mM glucose in the presence of FSK). Data show mean + SEM, n=8.

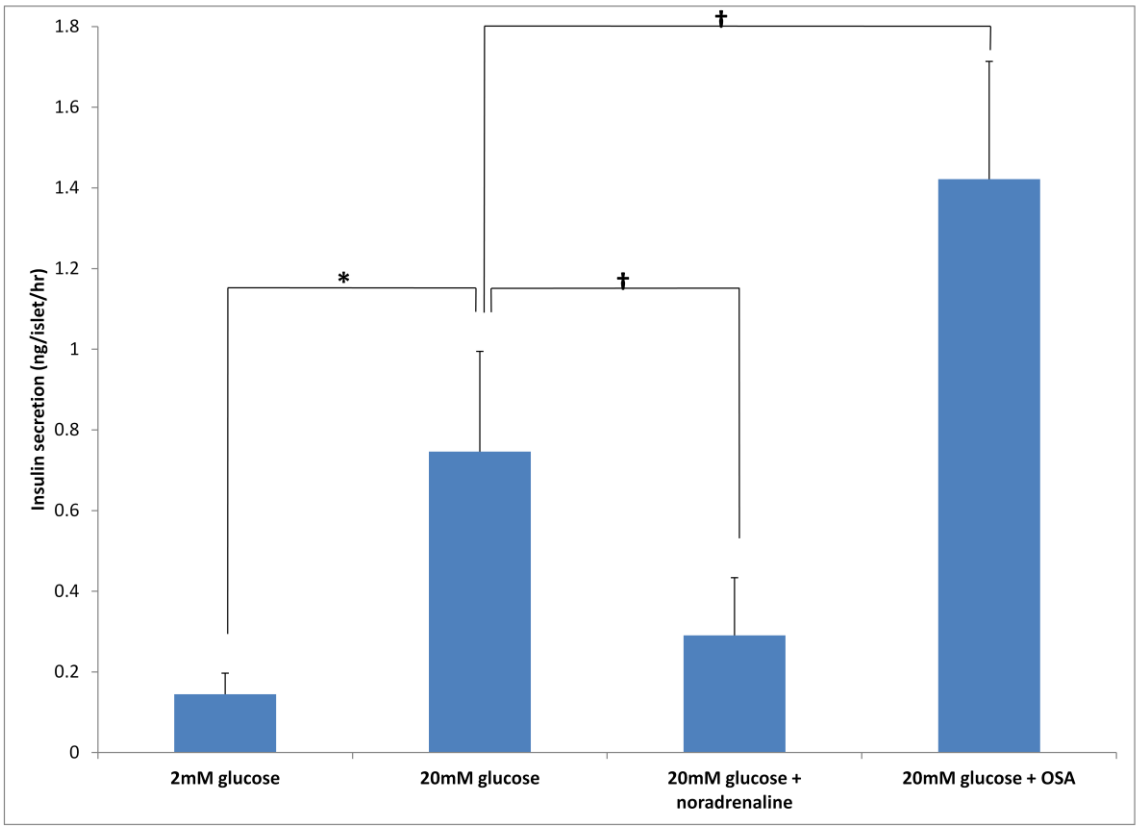

Figure 5.25: Effect of OSA® extract on insulin secretion from IBMX-treated mouse islets. Mouse islets were preincubated with 2mM glucose for 2 hrs and then incubated for 30 minutes with 2mM glucose Gey & Gey buffer alone or supplemented with 20mM glucose in the presence or absence of 10µM noradrenaline (as positive control) or 0.25 mg/ml OSA® in the presence of IBMX (▪). The supernatant was removed and insulin content was measured by RIA. Glucose caused an increase in insulin secretion (*p<0.05 versus 2mM glucose) which was further potentiated by OSA® but reduced by noradrenaline in IBMX-treated cells (†p<0.05 versus 20mM glucose). Data show mean + SEM, n=8.

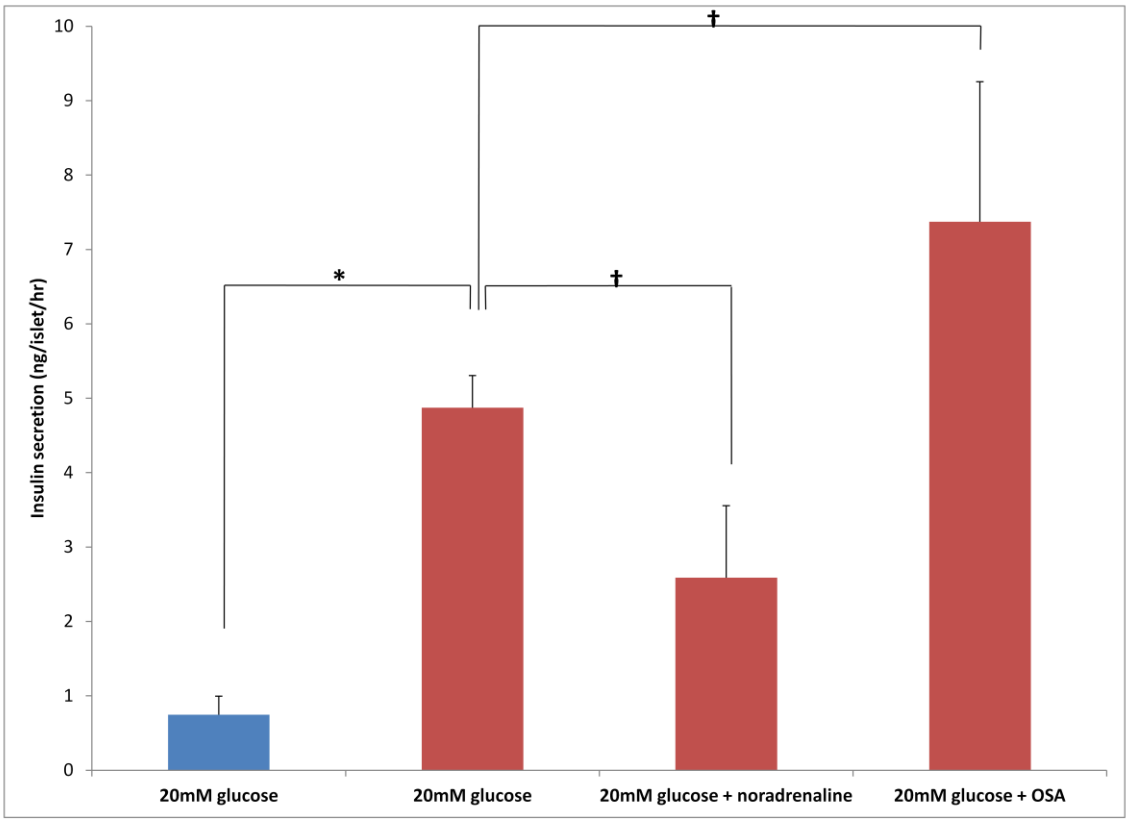

Figure 5.26: Effect of OSA® extract on insulin secretion from FSK-treated mouse islets. Mouse islets were preincubated with 2mM glucose for 2 hrs and then incubated for 30 minutes with buffer supplemented with 20mM glucose in the presence or absence of 10μM noradrenaline (as positive control) or 0.25 mg/ml OSA® in the presence of IBMX (▪) or FSK (▪). The supernatant was removed and insulin content was measured by RIA. FSK caused further increase in insulin secretion over glucose-induced insulin secretion in IBMX-treated cells (*p<0.05 versus 20mM glucose in the absence of FSK). The glucose-induced insulin secretion was reduced by noradrenaline but augmented by OSA® in FSK -treated cells (†p<0.05 versus 20mM glucose in the presence of FSK). Data show mean + SEM, n=8.

5.4 Discussion

In the previous chapter, I have established that OSA® initiated insulin secretion at 2mM glucose by direct effects on β-cells. The concentration of OSA® used was not associated with any damage to the β-cell plasma membrane, as evident by the Trypan Blue exclusion test, suggesting that OSA® stimulates insulin secretion by interacting with a regulated secretory pathway.

The classic insulin secretion pathway is mainly initiated by glucose and other nutrients which when they are metabolized within pancreatic β-cells trigger closure of K_{ATP}-channels, depolarization of β-cells and opening of VGCC leading to

elevations of $[Ca^{2+}]_i$ and insulin exocytosis. Several reports have shown that $[Ca^{2+}]_i$ alone can induce insulin release. This pathway is largely modulated by hormones and neurotransmitters through activation of second messengers such as DAG, IP3 and cAMP and subsequent stimulation of various mediators such as PKC, CaMKs, PKA, and AA.

Insulin secretagogues such as sulphonylurea induce insulin secretion by blocking K_{ATP}-channels leading to β-cells depolarization, opening of L-type VGCC and subsequent increases in $[Ca^{2+}]_i$ thus bypassing glucose metabolism. Since OSA® also induced insulin secretion at a substimulatory glucose concentration the effect of OSA® on K_{ATP}-channels and $[Ca^{2+}]_i$ was tested. Maintaining K_{ATP}-channels in the open state by diazoxide was not associated with a reduction in OSA®-induced insulin secretion from mouse islets implying that OSA® acts beyond K_{ATP}-channels closure and subsequent depolarization of β-cells. In our study, exposing MIN6 cells or mouse β-cells to OSA® significantly elevated $[Ca^{2+}]_i$ which was completely abolished when extracellular Ca^{2+} was removed or VGCCs were blocked by nifedipine, indicating that OSA®-induced elevation of $[Ca^{2+}]_i$ occurs solely because of Ca^{2+} entry though L-type VGCC and may contribute to the stimulatory action of OSA® on insulin secretion. Furthermore, depletion of extracellular Ca^{2+} or blockade of VGCC by nifedipine also resulted in reductions in insulin secretion from MIN6 cells treated with 0.25 mg/ml but not 1.0 mg/ml OSA®. This was in agreement with our data using Trypan Blue exclusion tests (chapter 2) which demonstrated that OSA® at a concentration of ≥ 0.5 mg/ml caused a massive release of insulin in a Ca^{2+}-unregulated manner due to extensive damage to plasma membrane and effective permeabilization of the cells. Blocking VGCC with nifedipine also affected

OSA®-induced insulin secretion from primary islets. Our results from perifusion experiments of mouse and human islets with OSA® in the presence and absence of nifedipine showed a partial inhibition in the increase in insulin secretion caused by OSA®. These data suggest that the secretory responses to OSA® were dependent, at least in part, on the ability of OSA® to increase cytosolic Ca^{2+} by facilitating Ca^{2+} entry through VGCC.

The involvement of protein kinases in stimulating insulin secretion is well documented. Glucose and other receptor-operated agonists stimulate insulin secretion through activation of second messengers and protein kinase signaling cascades (Howell *et al.*, 1994). Thus I tested the possible contribution of protein kinases in the stimulatory effect of OSA® on insulin secretion. Our experiments showed that staurosporine did not completely block OSA®-induced insulin secretion in either mouse or human islets even when it was used at a concentration that has been shown previously to inhibit islet PKC, PKA and Ca^{2+}-sensitive protein kinases (Persaud *et al.*, 1993). These observations are consistent with a partial involvement of kinase activation in the stimulatory effect of OSA® on insulin secretion. To identify the possible kinases involved in β-cell secretory responses to OSA®, I assessed the contribution of islets DAG-sensitive PKC, CaMKII and PKA, in OSA®-induced insulin secretion.

DAG-sensitive PKC isoforms and CaMKII are Ca^{2+}-sensitive protein kinases and their role in mediating the effect of some receptor-operated agonists such as acetylcholine and carbachol is well established. PLC activation leads to the generation of DAG which subsequently activates DAG-sensitive PKC. PLC also liberates Inositol trisphosphate (IP3) which causes Ca^{2+} release from intracellular

stores. The released Ca^{2+} is associated with calmodulin to activate CaMKII which plays an important role in mobilizing insulin vesicles and insulin exocytosis (Howell *et al.*, 1994). Both kinases (DAG-sensitive PKC and CaMKII) are also stimulated following Ca^{2+} influx into β-cells. However, our data do not support a role for these two kinases in the β-cell secretory responses to OSA®. The inhibitors of DAG-sensitive PKC (Gö6976) and CaMKII (KN62) had no effect on OSA® stimulation of insulin secretion. The involvement of other Ca^{2+}-dependent kinases or lipases is still possible and identification of these mediators merits further investigation.

Protein kinase A has been reported to have an important role in β-cell responses to cAMP-elevating agents such as glucagon and glucagon-like peptide (GLP-1). Activation of AC through G-protein coupled receptors generates the second messenger cAMP which activates PKA and thus potentiates insulin secretion as well as having PKA-independent effects (Furman *et al.*, 2010). Activators (such as FSK) or inhibitors (such as noradrenaline) of AC can largely modulate the levels of cAMP so I assessed whether cAMP was involved in OSA®-induced insulin secretion by directly measuring the effect of OSA® on $[cAMP]_i$. cAMP is rapidly inactivated by phosphodiesterases (PDEs) (Shafiee-Nick *et al.*, 1995) so I used a PDE inhibitor, IBMX to allow for accurate measurement of intracellular cAMP ($[cAMP]_i$). Our results showed that OSA®, unexpectedly, inhibited $[cAMP]_i$ accumulation in IBMX-treated MIN6 cells and mouse islets. Stimulation of AC by FSK led to enhanced production of $[cAMP]_i$ which was again reduced by the presence of OSA®. The reduction in $[cAMP]_i$ by OSA® presumably reflects a G-protein-mediated effect linked to $G\alpha_{i/o}$. Although OSA® decreased $[cAMP]_i$ levels from MIN6 cells and mouse islets, concomitant measurement of insulin output from these cells showed

that insulin secretion was significantly stimulated by OSA®, as expected, suggesting a dissociation of the insulin secretory response to OSA® from its cAMP-reducing effect. In accordance with our results, carbachol, a muscarinic receptor agonist known to stimulate secretion, has been previously reported to lower cAMP levels while increasing $[Ca^{2+}]_i$ in a number of cell types including β-cells (Dai *et al.*, 1991, Madison and Yamaguchi, 1996, Nakagawa *et al.*, 2009, Watson *et al.*, 1993).

Our results also demonstrated that OSA® stimulated insulin secretion independently of Ca^{2+} influx and protein kinase activation as shown by the persistent activity of OSA® on insulin secretion even when the cells were incubated with nifedipine, a VGCC blocker, or staurosporine, a general protein kinase inhibitor. This may suggest that OSA® acts at least in part at a late stage of the secretory cascade distal to VGCC and protein kinase activation. In this context, OSA® may share some similarities with arachidonic acid (AA). Similar to OSA®, AA induced insulin secretion at substimulatory concentrations of glucose (Persaud *et al.*, 2007). In addition, neither OSA®- nor AA-induced insulin secretion was fully blocked by closing VGCC or inhibiting protein kinase activation (Band *et al.*, 1992, Basudev *et al.*, 1993), suggesting an effect on the exocytotic process to directly release insulin (Band *et al.*, 1993). These similarities between OSA® and AA may indicate that OSA® mediates some of its effects either through the generation of AA, or through a similar mechanism to AA.

In summary, a proposed mechanism of action of OSA® on insulin secretion is shown in Figure 5.27 in which OSA® may increase $[Ca^{2+}]_i$ through VGCC either directly or through activation of a $G\alpha_{i/o}$ protein coupled receptor. Association of OSA® with the receptor librates Gαi which acts on AC to inhibit cAMP formation.

The beta gamma (βγ) subunit of the G protein may act as stimulatory subunits to activate PLA_2 to liberate AA. It has been reported in the literature that PLA_2 can be activated by the βγ subunit in a number of cell types including platelets and retinal rod cell (Jelsema and Axelrod, 1987, Murayama *et al.*, 1990). AA can then initiates insulin secretion as described in the Figure.

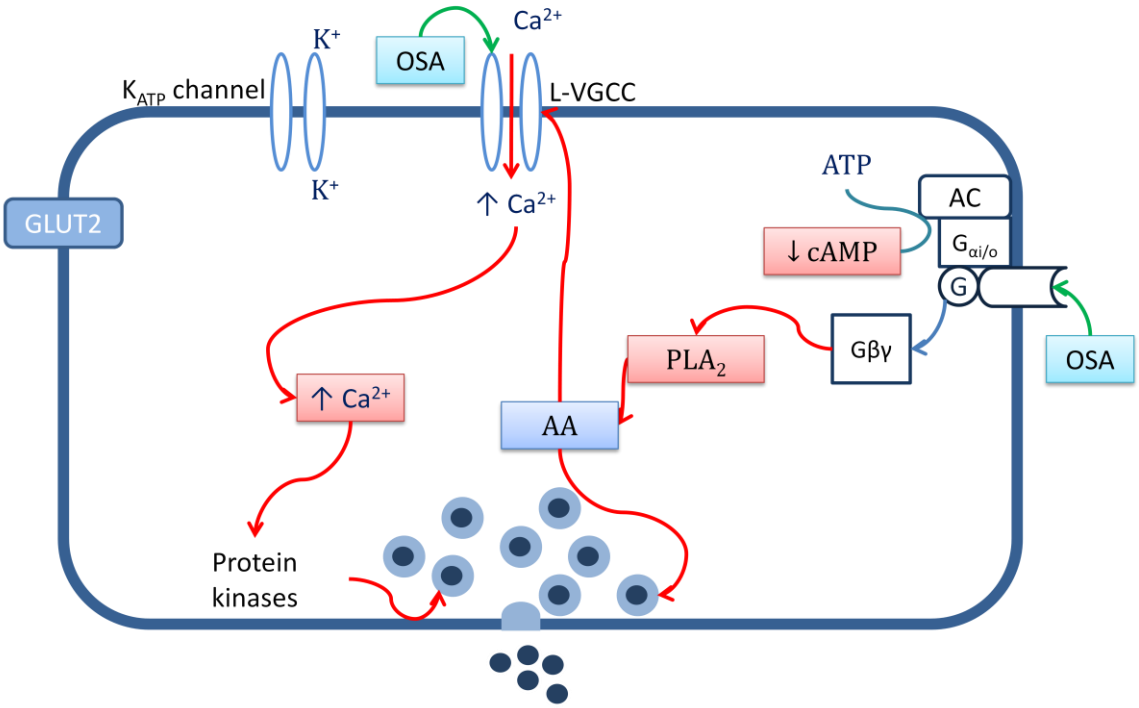

Figure 5.27: Model of OSA®-induced insulin secretion from β-cells. OSA® may activate $G_{\alpha i/o}$-coupled receptor. The Gβγ subunits may then be released to activate PLA_2. This enzyme may liberate arachidonic acid (AA). AA stimulates insulin secretion by one of these mechanisms: 1) facilitating Ca^{2+} entry through VGCC, 2) activating protein kinases and 3) stimulating fusion of insulin vesicles and exocytosis. OSA® may also act directly on VGCC to increase $[Ca^{2+}]_i$.

Chapter 6

Gymnema sylvestre protects β-cells from cytokine-induced apoptosis

6.1 Introduction

DM has been associated with reductions in β-cell volume and mass, mainly due to excessive induction of apoptosis (Donath and Halban, 2004, Johnson and Luciani, 2010, Lupi and Del Prato, 2008). In T1DM, for example, β-cell death can be precipitated by the release of pro-inflammatory cytokines from activated macrophages and T-cells. Cytokines (IL-1β, TNF-α and INF-γ) acting through their receptors activate several signaling pathways which are involved in apoptosis and β-cell survival (Cnop *et al.*, 2005). The NF-κB pathway is one of the major pathways induced by cytokines. In unstimulated cells, NF-κB is bound to its inhibitory protein IκB in the cytosol. Upon activation, NF-κB is released from its regulatory protein and translocated into the nucleus where it acts as transcription factor to directly regulate the expression of numerous pro and anti-apoptotic genes (Melloul, 2008). It has been previously reported that NF-κB-responsive genes encode proteins that can promote either β-cell apoptosis - such as iNOS, pro-apoptotic Bcl2-family and Fas - or β-cell survival - such as MnSOD and IAPs (Cnop *et al.*, 2005, Melloul, 2008). NF-κB-independent signaling pathways are also involved in triggering apoptosis, including signaling through MAPKs, JAK/STAT and granzyme B (Cnop *et al.*, 2005, Eizirik and Mandrup-Poulsen, 2001, Gysemans *et al.*, 2008, Hui *et al.*, 2004, Mandrup-Poulsen, 2001). In addition, cross talk with other crucial pathways involved in cell survival has been observed and down regulation of these pathways may augment cell death and apoptosis. PKA-CREB signaling is one of these pathways. Activation of AC causes enzymatic cleavage of ATP to cAMP which activates PKA. Activation of PKA stimulates the induction of certain transcription factors involved in cell survival through CREB-CREM interaction (Costes *et al.*,

2006). AKT signaling has also been involved in cell survival. AKT exerts its anti-apoptotic actions by 1) phosphorylating and thus inactivating BAD, a pro-apoptotic member of Bcl2 family, 2) preventing the cleavage of pro-caspase-9 to caspase-9 leading to the inhibition of caspase signaling, 3) stimulating IκK activity to positively regulate NF-κB-induced anti-apoptotic genes, 4) inactivating FOXO-stimulated pro-apoptotic genes and 5) blocking DNA fragmentation by increasing the activity of ICAD and thus preventing the nuclease action of CAD (Kim and Chung, 2002).

Prevention of β-cell death has been the ultimate therapeutic target for DM treatment. Unfortunately, none of the commonly-used existing therapies have shown to affect the deterioration of β-cells in humans. Recently, exendin-4, a GLP-1 agonist, has been shown to protect β-cell from apoptosis in insulin-secreting cells and in primary islets (Ferdaoussi *et al.*, 2008). However, the cost, route of administration and possible side-effect of acute pancreatitis have limited the use of exendin-4 as one of the ideal/first-line therapies (Persaud and Jones, 2008). Therefore, the search for an affordable, orally administered and safe drug which protects the β-cell mass continues. I have shown in previous chapters that OSA®, a GS extract, is effective in improving β-cell secretory function without any deleterious effect. Other GS extracts have been reported to preserve β-cell mass in STZ- or alloxan-treated rodents (Ahmed *et al.*, 2010, Shanmugasundaram *et al.*, 1990a). However, the molecular signaling underlying this effect is unknown. Therefore, the aim of this chapter was to investigate whether OSA® has a protective effect in β-cells which have been challenged with cytokines and to

determine the possible components/pathways which contribute to the mechanism(s) by which OSA® exerts its action.

6.2 Materials and Methods

6.2.1 Plant material and preparation

OSA® which contains GS leave was extracted as described in section 2.1.1 and provided as powder. Aqueous stock (200 mg/ml) was prepared in physiological solution for use in experiments.

6.2.2 Maintenance of MIN6 cells

MIN6 cells (passage 40-44) were maintained as monolayers in DMEM supplemented with 10% fetal bovine serum (FBS), 2mM glutamine and 100U/ml penicillin/0.1mg/ml streptomycin under standard tissue culture conditions (section 2.3.2). The cells were harvested and used in experiments when the cell confluency reached 70-80%.

6.2.3 Isolation of mouse islets

Islets from male ICR mice were isolated as described in section 2.4. The isolated mouse islets were cultured in RPMI supplemented with 10% newborn calf serum (NCS) and 100U/ml penicillin/0.1mg/ml streptomycin under standard tissue culture conditions.

6.2.4 Apoptosis assay

6.2.4.1 Measurement of caspase 3/7 activity in MIN6 cells and mouse islets following chronic cytokines exposure

The effect of mixed cytokines on apoptosis in MIN6 cells and mouse islets was assessed using Promega Caspase Glo® 3/7 apoptosis assay, following the manufacturer's protocol (section 2.14.2). Briefly, MIN6 cells (10,000 cells/well) or mouse islets (5 islets/well) were seeded in white 96-well plate overnight under standard tissue culture condition. MIN6 cells were treated with either IL-1β (50 U/ml) or TNF-α (1000 U/ml) or INF-γ (1000 U/ml) in combination of two or more cytokines, as indicated in the figure legends, for 16-18 hours. Mouse islets were treated with a mixture of cytokines (IL-1β, TNF-α and INF-γ) for 16-18 hours. Caspase Glo® reagent was prepared as described in section 2.14.2 and added to each well. Following 1 hr, luminescence was measured using Veritas luminometer.

6.2.4.2 Measurement of caspase 3/7 activity in MIN6 cells and mouse islets following OSA® exposure

The protective effect of OSA® on apoptosis was assessed as described in section 2.14.2. MIN6 cells (10,000 cells/well) or mouse islets (5 islets/well) were seeded in white 96-well plate and incubated overnight under standard tissue culture conditions. MIN6 cells or mouse islets were pretreated with OSA® for 8 hrs before incubating them with cytokines mixture as indicated in the figure legends. Luminescence from each well was measured using Veritas luminometer after 1 hr incubation with caspase Glo® reagent.

6.2.5 Microarray

6.2.5.1 Experimental design

Mouse islets were grouped into the following groups: control, control + 0.125 mg/ml OSA®, cytokines (50U/ml IL-1β, 1000U/ml TNF-α and 1000U/ml INF-γ) and cytokines + 0.125 mg/ml OSA®. 290 islets were picked in triplicates into these groups. In OSA® treated groups, the islets were preincubated with OSA® for 8 hours before treating them with their corresponding treatment for 16-18 hours. The islets were washed with ice-cold PBS and RNA was extracted as described in section 2.15. The RNA integrity of each sample was assessed as described in section 2.17.1. The RNA integrity number and the gel electrophoresis of each sample are shown in Appendix 3 (Figure 1).

6.2.5.2 Gene expression profiling

RNA of each sample was amplified, labeled and purified according to section 2.17.2. Fragmentation of each aRNA was carried as section 2.17.3. The expected profile of the aRNA fragments is shown in Appendix 3 (Figure 2). Each fragmented sample was mixed with hybridization cocktail (section 2.17.4) and the mixture was hybridized to a mouse genome 430 2.0 array chip (section 2.17.5). The chips were washed, stained and scanned as described in section 2.17.6. The normalized signal intensities were generated using MAS 5.0. Signal distribution (in normal and log scale) and Pearson's correlation of all samples are listed in Appendix 3 (Figure 3).

6.2.6 Statistical analysis

Data were expressed as mean ± SEM. Differences between treatment groups were assessed using one way analysis of variance (ANOVA), Student's t-test, or

Bonferroni's multiple comparison test as appropriate, and differences between treatments were considered significant at $p<0.05$. The signal intensities, in microarray experiment, were calculated using MAS 5.0. The Qlucore software was used to determine and to calculate the ratio and fold changes of genes between two different treatment groups in which one group acted as basal. A false discovery rate of at least 40% and a $p<0.05$ were used to filter genes that are differently expressed. The possible signaling pathways and networks were generated using GeneGo® software, a pathway analysis tool.

6.3 Results

6.3.1 Effect of cytokines on apoptosis in MIN6 cells and mouse islets

Chronic exposure of MIN6 cells to a combination of two or more cytokines induced apoptosis as assessed by elevations in caspase-3 and -7 activities. A mixture of IL-1β + TNF-α with or without INF-γ caused the highest elevations in caspase-3 and -7 levels (Figure 6.1). Similarly, chronic exposure of mouse islets to a mixture of cytokines resulted in increases in caspase-3 and -7 concentrations (Figure 6.2).

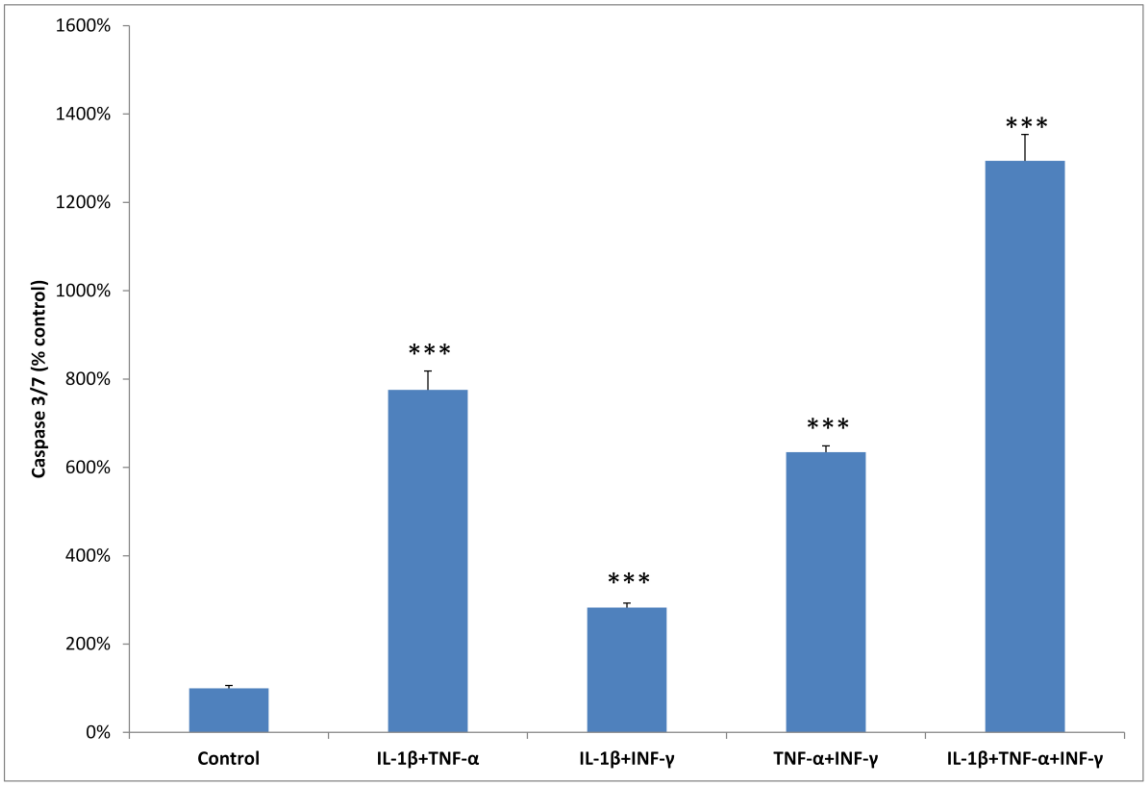

Figure 6.1: The effect of cytokines on caspase 3/7 from MIN6 cells. MIN6 cells were seeded in white 96-well plate at a density of 10,000 cell/well and incubated overnight at 37C°. They were incubated with IL-1β (50 U/ml), TNF-α (1000 U/ml) and INF-γ (1000 U/ml) in a combination of two or more for 16-18 hrs. Caspase 3/7 was measured as described in Materials and Methods. All combinations significantly increased caspase 3/7 levels (*p<0.001). Data are mean + SEM, n=6.**

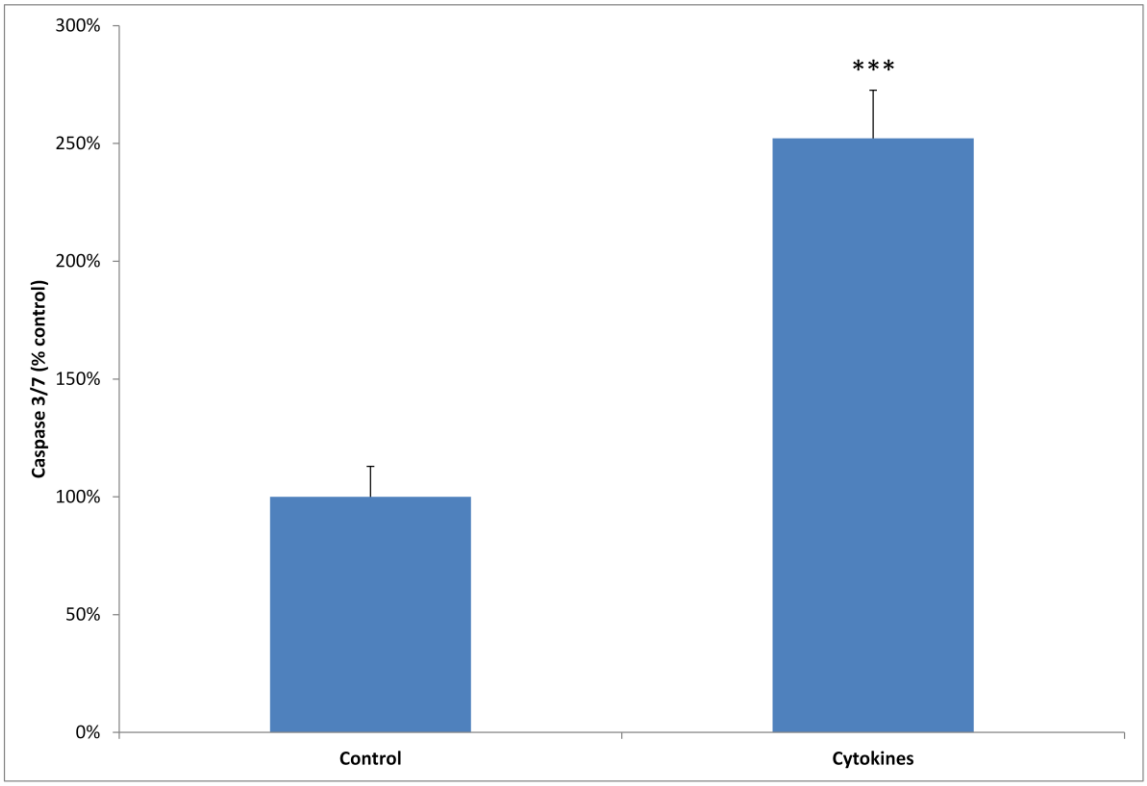

Figure 6.2: The effect of cytokines on caspase 3/7 from mouse islets. Mouse islets were seeded in white 96-well plate at a density of 5 islets/well and incubated overnight at 37C°. They were incubated with a mixture of IL-1β (50 U/ml), TNF-α (1000 U/ml) and INF-γ (1000 U/ml) for 16 hrs. Caspase 3/7 was measured as described in Material and Methods. Cytokines significantly increased caspase 3/7 levels (*p <0.001). Data are means+ SEM, n=6.**

6.3.2 Effect of OSA® on cytokine-induced apoptosis in MIN6 cells and mouse islets

In MIN6 cells, OSA® (0.03-0.125mg/ml) or exendin (1μM) alone did not increase basal levels of cell apoptosis. Addition of two or more cytokines significantly increased caspases activities, indicative of increased apoptosis. Pre-incubation with OSA® reduced apoptosis induced by IL-1β+ TNFα (Figure 6.4) and IL-1β+ TNFα + INFγ(Figure 6.3)combinations but not by TNFα + INFγ mix (Figure 6.4). Exendin was used as a positive control and shown to decrease caspase-3 and -7 levels in the same fashion as OSA®. Pre-treatment of MIN6 cells with exendin for 8 hrs also protected them from apoptosis induced by cytokines mix.

Similar to MIN6 cells, mouse islets incubated with OSA® or exendin alone did not show any detectable changes in apoptosis, as assessed by changes in caspase-3 and -7 levels. However, pre-treating mouse islets with either OSA® or exendin for 8 hrs caused a reduction in cytokine-induced caspase-3 and -7 levels (Figure 6.5).

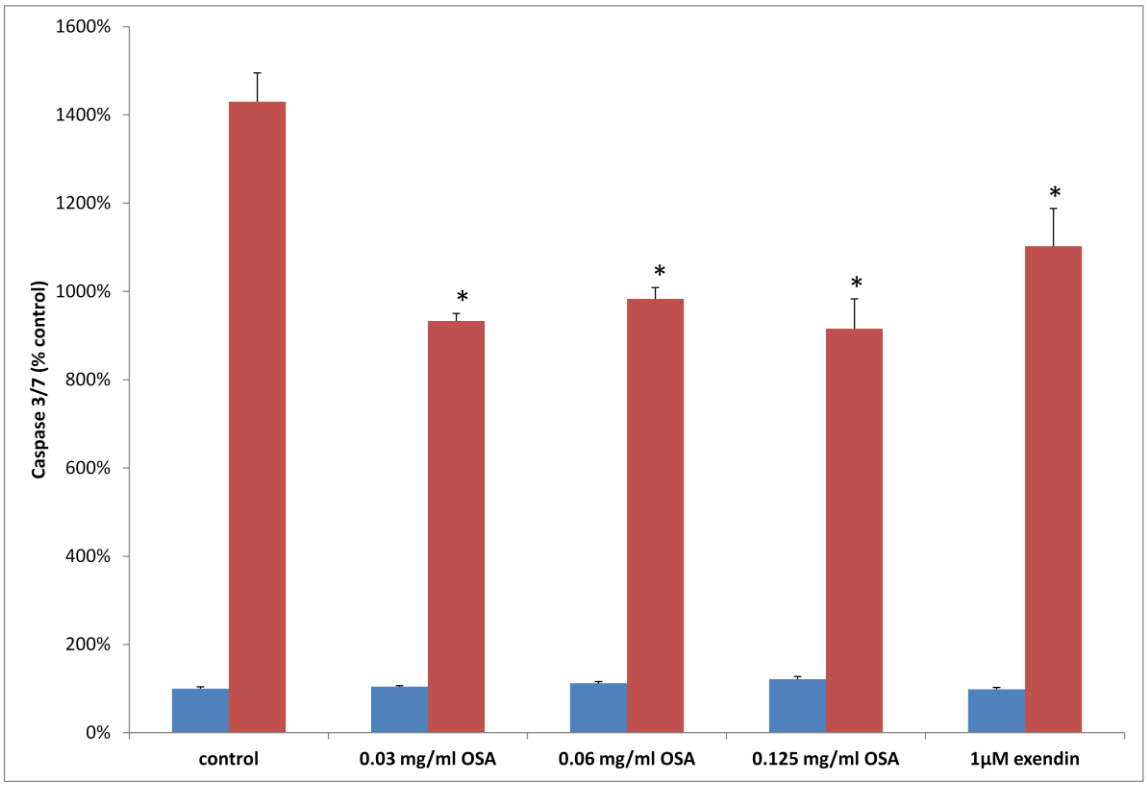

Figure 6.3: The effect of OSA® on cytokine-induced apoptosis from MIN6 cells. MIN6 cells were seeded in white 96-well plate at a density of 10,000 cells/well and incubated overnight at 37C°. They were pre-treated with OSA® (0.03-0.125 mg/ml) or exendin (1μM) for 8 hrs before incubating them with OSA® (0.03-0.125 mg/ml) or exendin (1μM) in the presence (▪) or absence (▪) of cytokines (IL-1β, TNF-α and INF-γ) for 16 hrs. Caspase 3/7 was measured as described in Materials and Methods. OSA® and exendin partially protected MIN6 cell from cytokines-induced apoptosis (*p <0.05). Data are mean + SEM, n=6.

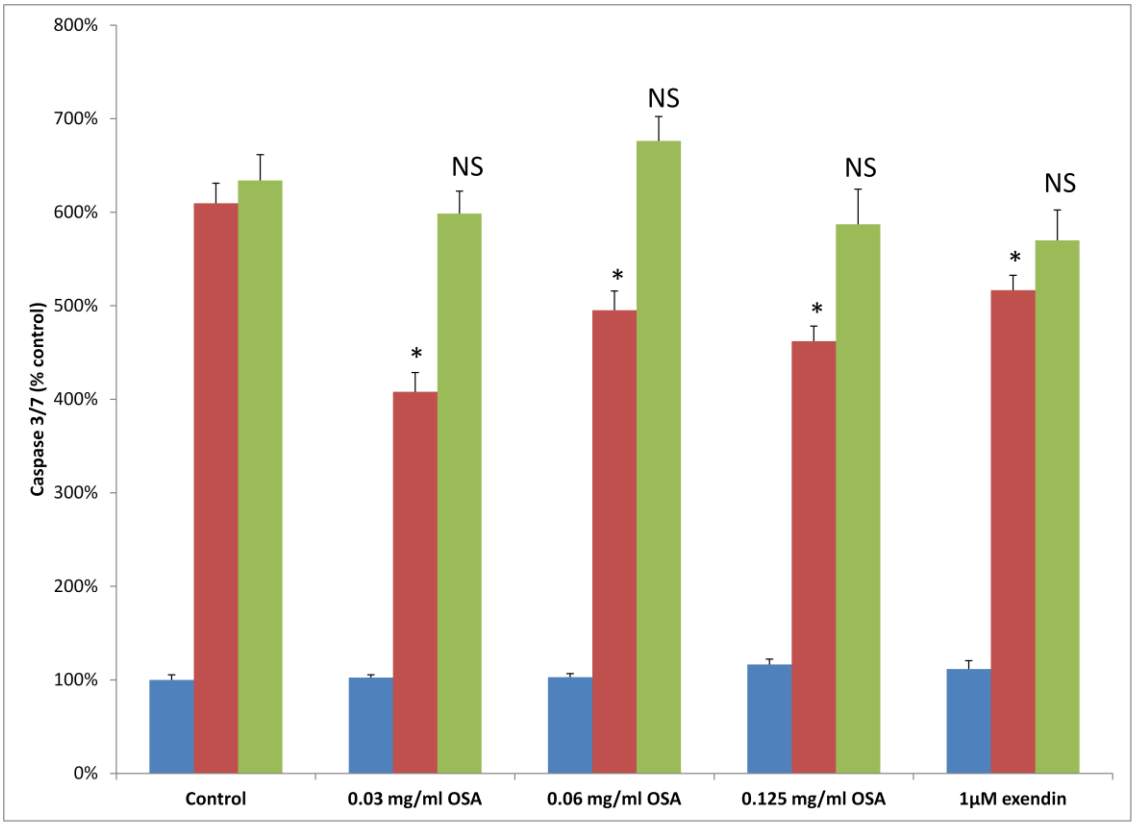

Figure 6.4: The effect of OSA® on two mixture combination of cytokine-induced apoptosis from MIN6 cells. MIN6 cells were seeded in white 96-well plate at a density of 10,000 cells/well and incubated overnight at 37C°. They were pre-treated with OSA® (0.03-0.125 mg/ml) or exendin (1µM) for 8 hrs before incubating them with OSA® (0.03-0.125 mg/ml) or exendin (1µM) in either the presence (▪) or absence (▪) of IL-1β + TNF-α or in the presence (▪) or absence (▪) of TNF-α +INF-γ for 16 hrs. Caspase 3/7 was measured as described in Materials and Methods. OSA® and exendin partially protected MIN6 cell from IL-1β + TNF-α mix (*p<0.05) but not from TNF-α + INF-γ - induced apoptosis. Data are mean + SEM, n=6, NS= not significant.

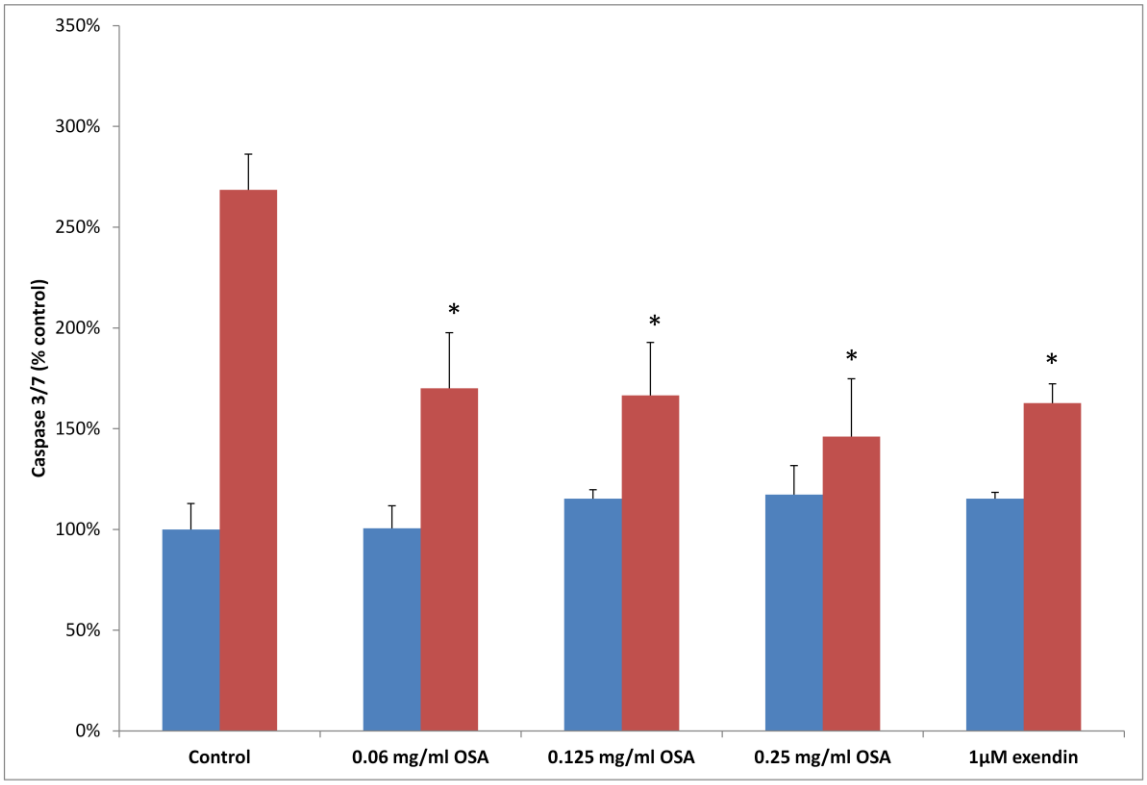

Figure 6.5: The effect of OSA® on cytokines-induced apoptosis from mouse islets. Mouse islets were seeded in white 96-well plate at a density of 5 islets/well and incubated overnight at 37C°. They were pre-treated with OSA® (0.06-0.25 mg/ml) or exendin (1μM) for 8 hrs before incubating them with OSA® (0.06-0.25 mg/ml) or exendin (1μM) in the presence (▪) or absence (▫) of cytokines (IL-1β + TNF-α + INF-γ) for 16 hrs. Caspase 3/7 was measured as described in Material sand Methods. OSA® and exendin partially protected mouse islets from cytokines-induced apoptosis (*p<0.05). Data are mean + SEM, n=8.

6.3.3 Microarray analysis of effect of OSA® on apoptosis-induced gene expression in mouse islets

Microarray analysis was used to investigate the genes responsible for the protective effect of OSA® against cytokine-induced apoptosis. Chronic (16-18 hrs) incubation of islets in the presence of cytokines modified the mRNA expression of approximately 200 genes related to apoptosis and cell survival. Selected genes that were modified by cytokines are listed in Table 6.1. A number of pro-apoptotic genes were upregulated including casp3, Fasl, FADD, JAK2 and XAF1. In addition, expression of anti-apoptotic genes including Bcl-2, XIAP, TNFAIPs and TRAFs was concomitantly increased. The pathways modulated by cytokines were analyzed

using GeneGo® software. Enrichment analysis showed upregulation in pathways and networks involved in DNA damage and apoptosis. Several gene pathways including the p-53-dependent pathway (p-53, Bard1, E2F1), ER stress-dependent pathway (GRP78, ire1, Mek3, MAPK-14/p-38, JNK/jun), mitochondrial stress pathway (NOXA, mcl-1, granzymes), NF-κB-dependent pathway (Rela, IκB, IκK, NF-κB, Bcl-xL, Bcl-2, Bim, cIAP) and metabolic pathways (PI3K, AKT, FOXO, AC, PKA, creb1) were altered. GeneGo process networks of cytokine-induced genes are listed in Appendix 3.

Pre-incubation in the presence of OSA® before exposure of the islets to cytokines was associated with down regulation in casp3 gene expression, consistent with our Promega Caspase Glo® 3/7 data (Fig 6.5). Furthermore, OSA® caused the upregulation in mRNA transcripts of protective, anti-apoptotic genes including AKT-2 (2.1 fold increase), ICAD (3.9 fold increase) and MnSOD (1.4 fold increase).

Probe set ID	Gene symbol	Gene title	Function	Fold change
TNF superfamily				
1417865_at	Tnfaip1	tumor necrosis factor, alpha-induced protein 1 (endothelial)	Anti-apoptotic	-1.66786
1419607_at	Tnf	tumor necrosis factor	Pro-apoptotic	-1.78881
1429117_at	Tradd	TNFRSF1A-associated via death domain	Pro-apoptotic	-2.23958
1418309_at	Tnfrsf11b	tumor necrosis factor receptor superfamily, member 11b	Pro-apoptotic	-3.68407
1460251_at	Fas	Fas (TNF receptor superfamily member 6)	Pro-apoptotic	-5.33013
1457918_at	Tnfaip2*	Tumor necrosis factor, alpha-induced protein 2	Anti-apoptotic	-7.43241
1427689_a_at	Tnip1	TNFAIP3 interacting protein 1	Anti-apoptotic	-15.5226
1445452_at	Traf1*	TNF receptor-associated factor 1	Anti-apoptotic	-61.0534
1418424_at	Tnfaip6*	tumor necrosis factor alpha induced protein 6	Anti-apoptotic	6.62016
1426095_a_at	Tnfrsf22	tumor necrosis factor receptor superfamily, member 22	Pro-apoptotic	4.71958
1420412_at	Tnfsf10	tumor necrosis factor (ligand) superfamily, member 10	Pro-apoptotic	3.67048
1446499_at	Fadd*	Fas (TNFRSF6)-associated via death domain	Pro-apoptotic	3.55389
1418803_a_at	Fasl*	Fas ligand (TNF superfamily, member 6)	Pro-apoptotic	2.4673
1430259_at	Tnfrsf11a	tumor necrosis factor receptor superfamily, member 11a	Pro-apoptotic	2.05552
1423182_at	Tnfrsf13b	tumor necrosis factor receptor superfamily, member 13b	Pro-apoptotic	1.77002
1416170_at	Trap1	TNF receptor-associated protein 1	Pro-apoptotic	1.72337
1416888_at	Fadd*	Fas (TNFRSF6)-associated via death domain	Pro-apoptotic	1.44346
1416571_at	Traf4*	TNF receptor associated factor 4	Pro-apoptotic	2.31386
1443288_at	Traf6*	TNF receptor-associated factor 6	Anti-apoptotic	-1.68039
1438857_x_at	Irak1	interleukin-1 receptor-associated kinase 1	Pro-apoptotic	3.49106
1436507_at	Irak2	interleukin-1 receptor-associated kinase 2	Pro-apoptotic	1.9292
Caspases				
1430192_at	Casp3*	caspase 3	Pro-apoptotic	2.46673
1424552_at	Casp8	caspase 8	Pro-apoptotic	-2.42548

Continued next page

Probe set ID	Gene symbol	Gene title	Function	Fold change
Bcl-2 family				
1423572_at	Bcl2l2	BCL2-like 2	Anti-apoptotic	2.28111
1457687_at	Bcl2*	B-cell leukemia/lymphoma 2	Anti-apoptotic	2.19735
1437913_at	Bcl2a1a /// Bcl2a1b /// Bcl2a1d	B-cell leukemia/lymphoma 2 related protein A1a ,A1b, A1d	Anti-apoptotic	1.97552
1426191_a_at	Bcl2l1*	BCL2-like 1/Bcl-xL	Anti-apoptotic	1.95283
1429347_at	Bcl2l14	BCL2-like 14 (apoptosis facilitator)	Pro-apoptotic	1.89781
1418991_at	Bak1	BCL2-antagonist/killer 1	Pro-apoptotic	1.71162
1437122_at	Bcl2*	B-cell leukemia/lymphoma 2	Anti-apoptotic	1.64619
1443524_x_at	Bcl10	B-cell leukemia/lymphoma 10	Pro-apoptotic	1.58184
1418970_a_at	Bcl10	B-cell leukemia/lymphoma 10	Pro-apoptotic	1.561
1426050_at	Bcl2l1*	BCL2-like 1/Bcl-xL	Anti-apoptotic	1.49336
1424814_a_at	Bcl2l14	BCL2-like 14 (apoptosis facilitator)	Pro-apoptotic	1.47969
1416837_at	Bax	BCL2-associated X protein	Pro-apoptotic	-1.55287
1418971_x_at	Bcl10	B-cell leukemia/lymphoma 10	Pro-apoptotic	-1.58997
1420887_a_at	Bcl2l1*	BCL2-like 1/Bcl-xL	Anti-apoptotic	-2.75618
1456006_at	Bcl2l11*	BCL2-like 11 (apoptosis facilitator)/Bim	Pro-apoptotic	-2.96549
1438089_a_at	Bclaf1	BCL2-associated transcription factor 1	Pro-apoptotic	-3.36289
1420363_at	Bik	BCL2-interacting killer	Pro-apoptotic	-3.88908
1431731_at	Bnip2	BCL2/adenovirus E1B interacting protein 2	Anti-apoptotic	4.74136
1422491_a_at	Bnip2	BCL2/adenovirus E1B interacting protein 2	Anti-apoptotic	4.68776
1437913_at	Bcl2a1a /// Bcl2a1b /// Bcl2a1d	B-cell leukemia/lymphoma 2 related protein A1a , A1b, A1d	Anti-apoptotic	1.97552
1448560_at	Bid	BH3 interacting domain death agonist	Pro-apoptotic	-5.61673
Inhibitor of apoptosis family				
1443698_at	Xaf1*	XIAP associated factor 1	Pro-apoptotic	7.06048
1437533_at	Xiap*	X-linked inhibitor of apoptosis	Anti-apoptotic	1.54896
1421392_a_at	Birc3/cIAP*	baculoviral IAP repeat-containing 3	Anti-apoptotic	-11.5244
NF-κB associated family				
1446718_at	Nfkbib/I-κB*	nuclear factor of kappa light polypeptide gene inhibitor, beta	Pro-apoptotic/anti-apoptotic	3.44674
1417483_at	Nfkbiz/I-κB*	nuclear factor of kappa light polypeptide gene enhancer in B-cells inhibitor, zeta	Pro-apoptotic/anti-apoptotic	1.69435
1429128_x_at	Nfkb2*	nuclear factor of kappa light polypeptide gene enhancer in B-cells 2, p49/p100	Pro-apoptotic/anti-apoptotic	-2.50255
1432275_at	Ikbkb*	inhibitor of kappaB kinase beta	Pro-apoptotic/anti-apoptotic	1.86434
1419536_a_at	Rela*	v-rel reticuloendotheliosis viral oncogene homolog A (avian)	Pro-apoptotic/anti-apoptotic	-1.49623

Continued next page

Probe set ID	Gene symbol	Gene title	Function	Fold change
MAPK family				
1416703_at	Mapk14/p-38*	mitogen-activated protein kinase 14	Pro-apoptotic	5.04271
1422999_at	Map3k14/NIK	mitogen-activated protein kinase kinase kinase 14	Pro-apoptotic	2.45332
1419168_at	Mapk6/Erk3	mitogen-activated protein kinase 6	Pro-apoptotic	2.73492
1419169_at	Mapk6/Erk3	mitogen-activated protein kinase 6	Pro-apoptotic	2.44754
1451714_a_at	Map2k3/Mek3*	mitogen-activated protein kinase kinase 3	Pro-apoptotic	2.32581
1426585_s_at	Mapk1/Erk2*	mitogen-activated protein kinase 1	Pro-apoptotic	2.12903
1418060_a_at	Mapk7/Erk5	mitogen-activated protein kinase 7	Pro-apoptotic	2.03755
1425456_a_at	Map2k3/Mek3*	mitogen-activated protein kinase kinase 3	Pro-apoptotic	1.8943
1440442_at	Map2k7/Mek7	mitogen-activated protein kinase kinase 7	Pro-apoptotic	1.86374
1436522_at	Map3k3/Mekk3	mitogen-activated protein kinase kinase kinase 3	Pro-apoptotic	1.86305
1415974_at	Map2k2/Mek2	mitogen-activated protein kinase kinase 2	Pro-apoptotic	1.67458
1426233_at	Map2k4/Mek4	mitogen-activated protein kinase kinase 4	Pro-apoptotic	1.6606
1437045_at	Mapk8/JNK*	mitogen-activated protein kinase 8	Pro-apoptotic	1.65405
1438719_at	Map3k2Mekk2	mitogen-activated protein kinase kinase kinase 2	Pro-apoptotic	-1.4787
1420932_at	Mapk8/JNK*	mitogen-activated protein kinase 8	Pro-apoptotic	-2.37644
1426686_s_at	Map3k3/Mekk3	mitogen-activated protein kinase kinase kinase 3	Pro-apoptotic	-2.49938
1426104_at	Mapk14/p-38*	mitogen-activated protein kinase 14	Pro-apoptotic	-2.70219
1442364_at	Mapk14/p-38*	Mitogen-activated protein kinase 14	Pro-apoptotic	-2.8479
1448694_at	Jun*	Jun oncogene	Pro-apoptotic	-3.26723
1423403_at	Mapkbp1	mitogen-activated protein kinase binding protein 1	Pro-apoptotic	-4.29504
1457936_at	Mapk8/JNK*	mitogen-activated protein kinase 8	Pro-apoptotic	-5.04387
1460636_at	Map2k2	mitogen-activated protein kinase kinase 2	Pro-apoptotic	-6.96117
1422853_at	Shc1	src homology 2 domain-containing transforming protein C1	Pro-apoptotic	-2.48928
1418508_a_at	Grb2	growth factor receptor bound protein 2	Pro-apoptotic	-1.60956
1419823_s_at	Ksr1	kinase suppressor of ras 1	Pro-apoptotic	-3.23021
1415974_at	Map2k2/Mek2	mitogen-activated protein kinase kinase 2	Pro-apoptotic	1.67458

Continued next page

Probe set ID	Gene symbol	Gene title	Function	Fold change
JAK/STAT Pathway				
1421065_at	Jak2*	Janus kinase 2	Pro-apoptotic	2.4657
1423021_s_at	Insl3 /// Jak3	insulin-like 3 /// Janus kinase 3	Pro-apoptotic	-1.43774
1433804_at	Jak1	Janus kinase 1	Pro-apoptotic	-1.67133
1433803_at	Jak1	Janus kinase 1	Pro-apoptotic	-3.47393
1433805_at	Jak1	Janus kinase 1	Pro-apoptotic	-47.4873
1424272_at	Stat3	signal transducer and activator of transcription 3	Pro-apoptotic	1.39933
1426353_at	Stat6	signal transducer and activator of transcription 6	Pro-apoptotic	-1.47053
1422102_a_at	Stat5b	signal transducer and activator of transcription 5B	Pro-apoptotic	-1.50497
1421469_a_at	Stat5a	signal transducer and activator of transcription 5A	Pro-apoptotic	-2.60425
1448713_at	Stat4	signal transducer and activator of transcription 4	Pro-apoptotic	-6.1894
Mitochondria associated factors				
1419060_at	Gzmb*	granzyme B	Pro-apoptotic	2.81032
1417898_a_at	Gzma	granzyme A	Pro-apoptotic	1.53819
1448787_at	LOC100233175 /// Moap1	hypothetical protein LOC100233175 /// modulator of apoptosis 1	Pro-apoptotic	-4.0138
1418203_at	Pmaip1/NOXA*	phorbol-12-myristate-13-acetate-induced protein 1	Pro-apoptotic	6.67546
1456381_x_at	Mcl1*	myeloid cell leukemia sequence 1	Pro-apoptotic/Anti-apoptotic	1.97908
P-53 pathway and DNA damage				
1438542_at	Trp53*	Transformation related protein 53	Pro-apoptotic	2.31092
1420594_at	Bard1*	BRCA1 associated RING domain 1	Anti-apoptotic	2.09309
1452325_at	Trp73*	transformation related protein 73	Pro-apoptotic	1.8321
1449519_at	Gadd45a	growth arrest and DNA-damage-inducible 45 alpha	Pro-apoptotic	-2.10964
1418404_at	Rad9	RAD9 homolog (S. pombe)	Anti-apoptotic	-1.72923
1431875_a_at	E2f1*	E2F transcription factor 1	Pro-apoptotic	2.41351
1450885_at	Dffa/ICAD*	DNA fragmentation factor, alpha subunit	Anti-apoptotic	-5.46386
ER protein folding and ER stress				
1427464_s_at	Hspa5/Gpr78*	heat shock protein 5	Anti-apoptotic	-11.4759
1419163_s_at	Dnajc3*	DnaJ (Hsp40) homolog, subfamily C, member 3	Pro-apoptotic/Anti-apoptotic	-22.666
1430371_x_at	Eif2ak3	eukaryotic translation initiation factor 2 alpha kinase 3	Pro-apoptotic/Anti-apoptotic	1.73873
1431886_at	Ern1/ire1*	endoplasmic reticulum (ER) to nucleus signalling 1	Pro-apoptotic/Anti-apoptotic	2.247

Continued next page

Probe set ID	Gene symbol	Gene title	Function	Fold change
AKT pathway				
1442759_at	Akt1*	Thymoma viral proto-oncogene 1	Anti-apoptotic	1.56157
1424480_s_at	Akt2*	thymoma viral proto-oncogene 2	Anti-apoptotic	-1.63811
1435260_at	Akt3*	thymoma viral proto-oncogene 3	Anti-apoptotic	-2.60967
1435879_at	Akt3*	thymoma viral proto-oncogene 3	Anti-apoptotic	-2.85733
1416981_at	Foxo1*	forkhead box O1	Pro-apoptotic	2.24965
1444226_at	Foxo3*	forkhead box O3	Pro-apoptotic	2.06833
1416982_at	Foxo1*	forkhead box O1	Pro-apoptotic	2.02244
1443798_at	Pik3cd*	phosphatidylinositol 3-kinase catalytic delta polypeptide	Anti-apoptotic	3.4528
1422992_s_at	Pik3cd*	phosphatidylinositol 3-kinase catalytic delta polypeptide	Anti-apoptotic	3.33526
1422707_at	Pik3cg*	phosphoinositide-3-kinase, catalytic, gamma polypeptide	Anti-apoptotic	1.57961
1418463_at	Pik3r2*	phosphatidylinositol 3-kinase, regulatory subunit, polypeptide 2 (p85 beta)	Anti-apoptotic	1.73981
CREB pathway				
1427414_at	Prkar2a*	protein kinase, cAMP dependent regulatory, type II alpha	anti-apoptotic	-1.48141
1440133_x_at	Prkar1b*	protein kinase, cAMP dependent regulatory, type I beta	anti-apoptotic	-3.14864
1416754_at	Prkar1b*	protein kinase, cAMP dependent regulatory, type I beta	anti-apoptotic	-3.29962
1455462_at	Adcy2*	adenylate cyclase 2	anti-apoptotic	-2.79496
1418098_at	Adcy4*	adenylate cyclase 4	anti-apoptotic	-1.39297
1456307_s_at	Adcy7*	adenylate cyclase 7	anti-apoptotic	-5.64773
1418754_at	Adcy8*	adenylate cyclase 8	anti-apoptotic	-4.09899
1430847_a_at	Crem	cAMP responsive element modulator	anti-apoptotic	-1.74682
1423402_at	Creb1*	cAMP responsive element binding protein 1	anti-apoptotic	-1.42899
1452529_a_at	Creb1*	cAMP responsive element binding protein 1	anti-apoptotic	-2.55916
1448135_at	Atf4/Creb2	activating transcription factor 4	Anti-apoptotic	-4.57499

Table 6.1: Effect of cytokines on selected genes involved in apoptosis/survival in mouse islets. Mouse islets were treated with cytokines (IL-β + TNF-α + INF-γ) for 16-18 hrs. Microarray analysis was performed and the gene expression was assessed as described in Materials and Methods. Genes mentioned in the text were asterisked.

6.4 Discussion

It is well known that reduction in β-cell mass is a major contributor of DM pathogenesis. In principle a decrease in the β-cell mass could be caused by either a decrease in the rate of proliferation or an increase in cell loss through apoptosis. Inappropriate activation of apoptosis is thought to be the main mode of β-cell loss in DM (Donath and Halban, 2004, Johnson and Luciani, 2010, Lupi and Del Prato,

2008). Pro-inflammatory cytokines (IL-1β, TNF-α and INF-γ) have been reported to play important roles in β-cell death in DM (Cnop *et al.*, 2005), especially in T1DM although there is now accumulating evidence that T2DM is an inflammatory condition associated with inappropriate levels of circulating cytokines (Donath *et al.*, 2003). Cytokine-induced NF-κB-dependent and -independent pathways lead to apoptosis by acting on various steps in both intrinsic and extrinsic pathways of apoptosis. In the intrinsic pathway, the permeabilization of mitochondrial membrane, cytochrome C release and caspase activation are upregulated by pro-apoptotic members of the Bcl2 family such as Bax, Bak, Bad and Bim, and downregulated by anti-apoptotic members of Bcl2 family such as Bcl2 and Bcl-x_L. In the extrinsic pathway, ligand-activated death receptors, including the TNFR superfamily, recruit FADD which subsequently activates caspase-8. Both pathways are inhibited by IAPs, a family of caspase inhibitors (Creagh *et al.*, 2003, Gewies, 2003, Hui *et al.*, 2004, Mandrup-Poulsen, 2001). NF-κB plays a pivotal role in the regulation of apoptosis, because it induces the expression of both pro- and anti-apoptotic genes (Melloul, 2008). Cytokine-induced NF-κB- independent pathways are mainly activated by MAPKs and JAK/STAT pathways (Gysemans *et al.*, 2008, Mandrup-Poulsen, 2001). JAK/STAT activation via the INF-γ receptor causes upregulation of gene expression of major mediators involved in β-cell death such as IRF-1 and iNOS (Gysemans *et al.*, 2008).

In our experiments, chronic exposure of MIN6 cells to cytokines induced apoptosis as assessed by our measurements of caspase 3/7 levels. As expected, elevated levels of caspase 3/7 were evident in MIN6 cells treated with a mixture of two or more cytokines. These observations were consistent with published data that showed

activation of caspase-3 was noticeable by 18 to 24 hrs in MIN6 cells (Sarkar *et al.*, 2009). In the present study the increases in caspase 3/7 levels were markedly reduced in cells pretreated with OSA®. This effect of OSA® was comparable to that seen with exendin, which was reported to protect β-cells from apoptosis *in vitro* (Ferdaoussi *et al.*, 2008). Similarly, prolonged incubation of mouse islets with cytokines also prompted caspase 3/7 production which again was significantly inhibited by pretreatment with OSA®. The increase in caspase-3 levels in mouse islets was also confirmed using microarray analysis of mRNA expression. Consistent with previously published data (Sarkar *et al.*, 2009), cytokines induced a 2.4 fold increase in caspase-3 levels, which was significantly reduced by approximately 50% by OSA® treatment. Therefore, OSA® may have a protective effect on β-cells from cytokine-induced apoptosis. To explore the possible molecular pathways by which OSA® inhibited caspase 3/7, microarray analysis of cytokine-treated mouse islets in the presence or absence of OSA® was performed.

Our microarray data, as well as other published microarray data (Cardozo *et al.*, 2001a, Cardozo *et al.*, 2001b, Sarkar *et al.*, 2009), showed that exposing mouse islets to cytokines caused general modifications in the expression of genes involved in cell metabolism, cell adhesion, antigen presentation, cell cycle, ion channel formation, cytokine processing, DNA repair, apoptosis and cell defense. Changes in mRNA levels of some of these genes may precipitate β-cell death. Our microarray results showed complex changes in the expression of genes involved in apoptosis. Cytokines caused the upregulation of both pro- and anti-apoptotic genes. The complex nature of cytokine-mediated signaling makes it difficult to ascertain which key factor is responsible for the changes in mRNA expression seen in microarray

analysis. Activation of NF-κB could contribute to these changes but interestingly our data showed a cytokine-induced reduction in the expression of mRNA levels of both NF-κB and most of the up- and down-stream effectors of NF-κB with the exception of IκB, suggesting a down-regulation of this pathway. NF-κB target genes may exert a negative feedback mechanism on NF-κB. The NF-κB expression in our study was associated with an increase in IκB expression, which may be explained by the fact that the IκB expression was elevated to provide negative feedback mechanism to regulate and reduce NF-κB activity. It seems that the newly synthesized IκB acts by binding to the nuclear-localized NF-κB and then exporting it to the cytoplasm causing a temporary switch off in NF-κB gene expression. The reduction in NF-κB expression seen in our microarray data may be explained by this oscillatory nature of NF-κB expression following cytokine exposure.

Our observations were in contrast to previously published data which showed activation of NF-κB expression following cytokines exposure (Cardozo *et al.*, 2001a, Cardozo *et al.*, 2001b, Sarkar *et al.*, 2009). These discrepancies in the results may reflect differences in cell preparation and in the time-course of cytokine treatment. In our study, I used whole islets preparation while the other report used FACS-purified β-cells. In addition, the total exposure time to cytokines in our study was shorter that the one used in the published report.

Other possible key regulators of the changes in the gene expression seen in our experiments may include augmentation of the death signal through activation of MAPKs, via the NF-κB-independent pathway, or through reducing expression of the survival pathways such as the AKT and PKA pathways. It was previously demonstrated that IL-1β induced apoptosis through activation of ERK and p-38

MAPK in whole islets and purified β-cells (Larsen *et al.*, 1998, Pavlovic *et al.*, 2000). In agreement with this, our results also showed that cytokines treatment upregulated ERK and p-38 MAPK expression. It has been reported that AC-cAMP-PKA-CREB pathway is involved in the transcription of anti-apoptotic genes and thus in cell survival (Furman *et al.*, 2010). Our measurement of the genes encoding these elements showed a reduction in the expression of all of them, suggesting impairment in cell defenses and repair. Similarly, it is well known that AKT exerts anti-apoptotic effects by a number of different mechanisms involving activation of IκK and ICAD and inactivation of BAD, caspases and some transcription factor including FOXO (Kim and Chung, 2002). Our results demonstrated that the expression of AKT and subsequently ICAD genes was reduced and FOXO expression was increased in response to cytokines. This may suggest that stimulation of MAPKs pathways or inhibition of PKA and AKT signaling may account for the cytokine-induced modification of gene expression seen in our study.

In addition to the activation of these pathways, signs of mitochondrial stress, ER stress and DNA damage were evident in the cytokine-treated islets. The mRNA levels of granzyme B which stimulates mitochondrial ROS production and caspase signaling was significantly upregulated. Similarly, genes involved in the regulation of protein folding such as GPR78 and Dnajc3 were compromised, which can lead to ER stress. Our data also showed elevations in genes involved in DNA fragmentation and cleavage such as p-53, Trp73 and ICAD, consistent with increased levels of apoptosis.

It has been demonstrated that islets are equipped with free radical scavenging systems. During normal oxidative phosphorylation, a small percentage of ROS are

produced but are quickly detoxified by MnSOD to H_2O_2 which is converted to H_2O and O_2 by catalase in the cytosol (Evans, 2002). Our microarray analysis of OSA-treated mouse islets in the presence of cytokines indicated an upregulation in the expression of a key member of the free radical scavengers. Thus, OSA® increased the expression levels of MnSOD which may contribute to the reduction in caspase-3 levels, consistent with a possible role for OSA® as an anti-oxidant. These results were in agreement with previously published reports showing that aqueous extract of GS leaves elevated SOD activity in rat islets (Diwan *et al.*, 1995, Ohmori *et al.*, 2005).

Enrichment analysis of pathways using GeneGo® software indicated that the anti-oxidant and anti-apoptotic activity of OSA® may be mediated through activation of pathways involved in call survival, most notably the PI3K/AKT signaling pathway. Our observations showed that islets treated with OSA® in the presence of cytokines showed increased AKT mRNA levels, especially the AKT-2 isoform, when compared to cytokine-treated islets. The mRNA expression of down-steam effectors of AKT were also increased by OSA®. Therefore, it is possible that OSA® activates PI3K which generates numerous second messengers including phosphotidyl inositol (3,4,5) tri phosphate (PIP_3). This lipid product activates AKT-2 which mediates the activation and transcription of survival genes such as MnSOD and ICAD. However, further confirmation of these results with quantitative RT-PCR is required.

In conclusion, a heightened state of oxidative and ER stresses, apoptotic-based cell death and impairment of PI3K/AKT signaling contributes to β-cell deterioration and death seen in T2DM. Chronic OSA® treatment partially protected a β-cell line and primary islets from cytokine-induced apoptotic cell death suggesting that

OSA® may have important therapeutic actions as a potential therapy in the treatment of T2DM in addition to the insulin-releasing effects described in previous chapters. The anti-apoptotic effect of OSA® may be mediated through the PI3K/AKT pathway and further experiments using pharmacological inhibitors and/or genetic knock down of PI3K or AKT are required to validate the involvement of PI3K/AKT elements in the cytoprotective activity of OSA®.

Chapter 7

Costus pictus stimulates insulin secretion from mouse and human islets *in vitro*

7.1 Introduction

In the past few years the pharmacotherapy of T2DM has changed dramatically with the addition of new classes of drugs to achieve tighter glycemic control to reduce the risk of developing microvascular and macrovascular complications and to improve the quality of patients' lives. Despite the introduction of new chemical classes of drugs and the effort spent on drug development, the appropriate glycemic control in most patients with T2DM is still under target and may require intensive multiple drug therapy, increasing the risk of developing adverse drug effects and drug-drug interactions (Stolar *et al.*, 2008).

The use of herbal medicine for the treatment of diabetes mellitus has been known for centuries (Yeh *et al.*, 2003). I have established in previous chapters (chapter 3-6) the efficiency and mechanism of action of one particular GS extract named OSA®. However, in this chapter, I screened for more phytochemicals to identify potential therapeutic agents to treat T2DM. Many plants have been reported efficacy in the treatment of T2DM (Grover *et al.*, 2002), and recently extracts of *Costus pictus* (CP) have been reported to show antidiabetic properties (Gireesh et al., 2009, Jayasri et al., 2008, Jayasri et al., 2009a, Jothivel et al., 2007, Shilpa et al., 2009). The plant, commonly known as spiral ginger, belongs to the Costaceae family and grows in gardens as an ornamental climbing plant (Benny, 2004, George *et al.*, 2007). The antidiabetic activity of CP extracts has been tested chronically in animals *in vivo*, where it was reported to reduce blood glucose levels in rats in which hyperglycemia had been induced by administering the β-cell toxins alloxan or streptozotocin (STZ) (Gireesh *et al.*, 2009, Jayasri *et al.*, 2008, Jothivel *et al.*, 2007). The precise mechanism of the glucose-lowering effect of CP is not completely clear

but it may be due to 1) an inhibition of α-amylase and α-glucosidase enzymes resulting in reduced carbohydrate absorption (Jayasri *et al.*, 2009a); 2) an increase in GLUT4 translocation and glucose uptake in insulin-responsive target tissues (Shilpa *et al.*, 2009); or 3) a direct stimulation of insulin secretion from pancreatic β-cells (Gireesh *et al.*, 2009).

The aim of this chapter was, therefore, to determine whether an aqueous extract of CP acutely and directly stimulates insulin secretion from the mouse MIN6 β-cell line and from primary mouse and human islets and to investigate the effect of chronic CP treament on insulin gene expression from mouse islets. Many insulin secretagogues initiate insulin secretion by increasing cytosolic Ca^{2+} ($[Ca^{2+}]_i$) through facilitating extracellular Ca^{2+} entry into β-cells via voltage-gated Ca^{2+} channels (VGCC) in the plasma membrane, so I have also examined the dependence of CP-induced insulin secretion on Ca^{2+} .

7.2 Materials and Methods

7.2.1 Plant material and preparation

CP leaves were extracted as described in section 2.1.2. The lyophilized powder was prepared as 100 mg/ml stock in water and diluted as appropriate in Gey & Gey buffer.

7.2.2 MIN6 cells maintenance

MIN6 cells (passage 32-39) were maintained as described in section 2.3.2. MIN6 cells grow as adherent monolayers on negatively-charged tissue culture plastic. The medium was changed every 3-4 days and when the cell confluency reached ≈ 70-

80% the MIN6 cells were detached for use in experiments by incubation with 0.1% trypsin/0.02% EDTA.

7.2.3 Formation of MIN6 pseudoislets (PIs)

MIN6 cells were cultured in bacterial Petri dishes to prevent the adhesion of the cells to the substrate, resulting in the formation of three dimensional islet-like cell clusters known as pseudoislets. PIs were maintained as described in section 2.3.3. The medium was changed every 3-4 days and PIs were used in the experiments after 7-10 days.

7.2.4 Mouse and human islets isolation

Mouse and human islets were isolated and cultured as described in section 2.4 and 2.5 for 24 hrs before use in experiments.

7.2.5 Insulin secretion

7.2.5.1 Insulin secretion from MIN6 monolayer cells

Static secretion experiments were carried as described in section 2.7.1. The cells were incubated with buffer containing 2mM glucose in the presence or absence of CP extract (0.06-1.0 mg/ml) for 30 min at 37°C. At the end of the incubation period, 100µl of incubation medium was removed and stored at -20°C until insulin was measured by RIA.

7.2.5.2 Insulin secretion from MIN6 PIs, mouse and human islets

To measure the time-course of the effects of CP extract on insulin secretion, perifusion experiments using MIN6 PIs, isolated mouse and human islets were performed (section 2.7.2). PIs or islets were transferred into chambers lined with 1

μm pore-size nylon filter and perifused with physiological buffer supplemented with 2mM glucose, 2mM $CaCl_2$ and 0.5 mg/ml BSA, in a temperature-controlled (37°C) environment. At the start of each experiment the PIs or islets were perifused for 60 min at a flow rate of 0.5 ml/min, during which time the perifusate was discarded. At t=60 min, the tissues were perifused with buffer supplemented with either 2mM or 20mM glucose in the presence or absence of 0.1 mg/ml of CP extract. Perifusate samples were collected every 2 min and stored at -20°C until insulin content was determined by RIA.

7.2.6 Total insulin content of mouse islets

The chronic effect of CP on total insulin content of mouse islets was measured as described in section 2.8. Mouse islets (5 islets/well) were incubated for 24hrs with DMEM supplemented with 2mM glucose in the presence or absence of 0.1 mg/ml CP. Following 24hrs, the islets were washed with PBS, sonicated in acidified alcohol and stored at -20°C until assayed for insulin content by RIA.

7.2.7 Cell viability

The effects of CP on membrane integrity were assessed using a Trypan Blue exclusion test (section 2.11). MIN6 monolayers or mouse islets that had been exposed to CP extract (1.0 mg/ml) for 30 min were incubated with 0.1% (w/v) Trypan Blue dye for 15 min at 37°C. The cells were then washed with PBS and visualized under a light microscope. Images were captured using a Nikon Coolpix 4500 digital camera (Surrey, UK).

7.2.8 Ca^{2+} microfluorimetry

The effects of CP extract on $[Ca^{2+}]_i$ were assessed using single cell calcium microfluorimetry as described in section 2.12. Briefly, MIN6 cells were seeded on ethanol-washed glass coverslips at a density of 50,000 cells/coverslip and allowed to adhere overnight in DMEM under standard tissue culture conditions. The cells were loaded with 5μM of the Ca^{2+}-fluorophore Fura-2/AM for 30 min at 37°C. The coverslips were placed in a steel chamber which was mounted into a heated platform (37°C) on the stage of an Axiovert 135 Research Inverted Microscope. The cells were perifused with 0.1 mg/ml CP in the presence or absence of the Ca^{2+} chelator, EGTA (0.1mM), or nifedipine (10μM), a voltage-gated Ca^{2+} channel (VGCC) blocker, at a flow rate of 1 ml/min. Cells were illuminated alternately at 340 and 380nm, and emitted light at 510nm was detected using a CCD camera.

7.2.9 Insulin gene expression

The effect of CP on PPI mRNA expression was assessed by quantitative RT-PCR. 150 mouse islets were pre-incubated with 2mM glucose and then incubated with 2mM glucose in the presence or absence of 0.1 mg/ml CP or 20mM glucose. Total RNA was extracted by Qiagen RNeasy mini kit (section 2.15.1) and reverse transcribed to cDNA by mmLV-RT (section 2.15.2). PPI and actin, as a house keeping gene, mRNA levels were determined using SYBR green as fluorescence indicator (section 2.16). Specific primers were used to amplify 125 and 285 bp amplicons of PPI and actin, respectively. PPI expression was normalized by actin and expressed as fold increase over basal (2mM glucose).

7.2.10 Data analysis

Data are represented as mean ± SEM. In perifusion experiment with more than one treatment, the mean represents the area under the curve. Differences between treatment groups were assessed using one way analysis of variance (ANOVA), Student's t-test, or Bonferroni's multiple comparison test as appropriate, and differences between treatments were considered significant at $P< 0.05$.

7.3 Results

7.3.1 Effect of CP extract on insulin secretion from MIN6 monolayers and MIN6 membrane integrity

The effect of CP on insulin secretion from MIN6 cell monolayers at a basal concentration of glucose (2mM) is shown in Figure 7.1. Thirty min exposure of MIN6 cells to the CP extract (0.06-1.0 mg/ml) caused a concentration-dependent increase in insulin secretion ($P<0.01$) which could not be attributed to the extract causing non-specific leakage of insulin from the cells by damaging their plasma membranes. Thus, the effect of CP extract on membrane integrity was assessed using the Trypan Blue exclusion test. Incubating MIN6 cells or mouse islets with 0.1% (w/v) Trypan Blue dye for 15 min in the presence of CP extract (1.0 mg/ml) was not accompanied by increased Trypan Blue uptake (Figure 7.2).

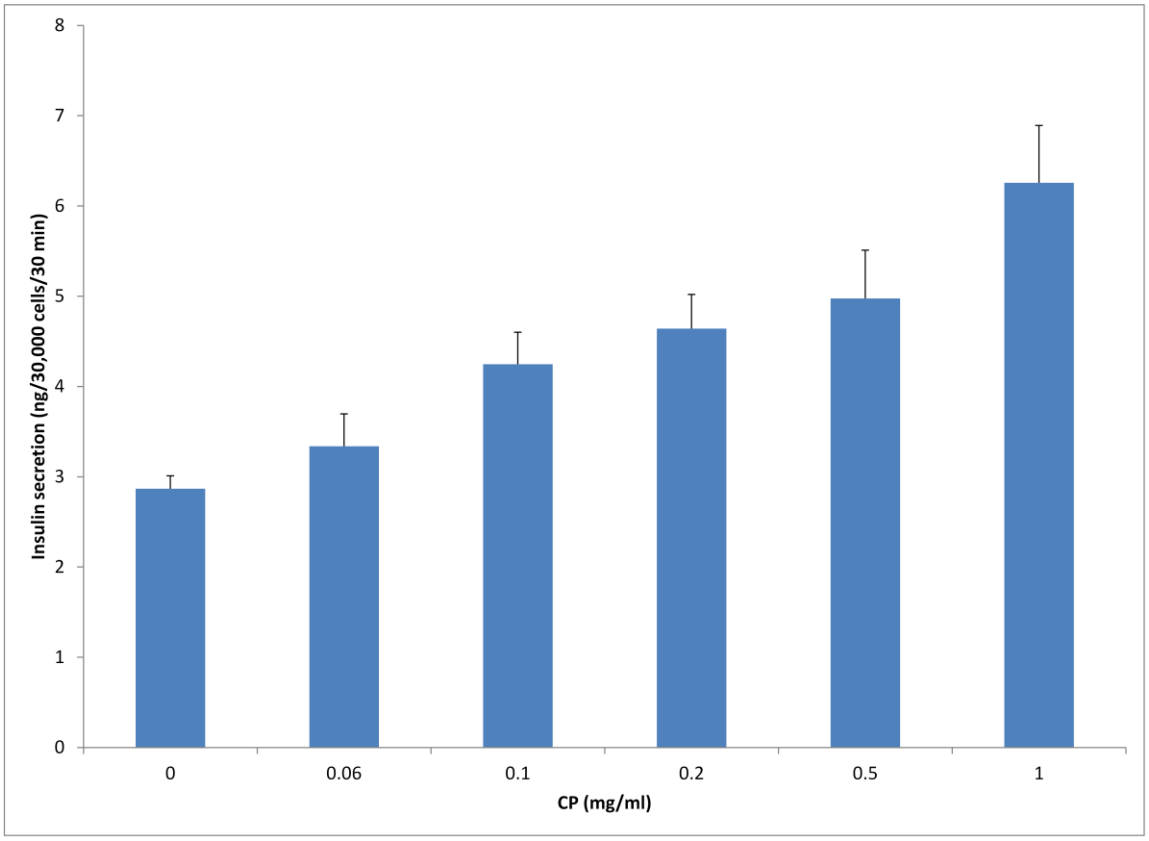

Figure 7.1: Effect of CP extract on insulin secretion from MIN6 cell monolayers. MIN6 cells were preincubated with buffer supplemented with 2mM glucose for 2 hrs then incubated for 30 min at 37 °C with CP extract (0.06-1.0 mg/ml). Insulin content of the supernatant was measured by RIA. CP extract induced a concentration-dependent increase ($p<0.01$) in insulin secretion. Data are mean + SEM, n=12 for each experimental treatment.

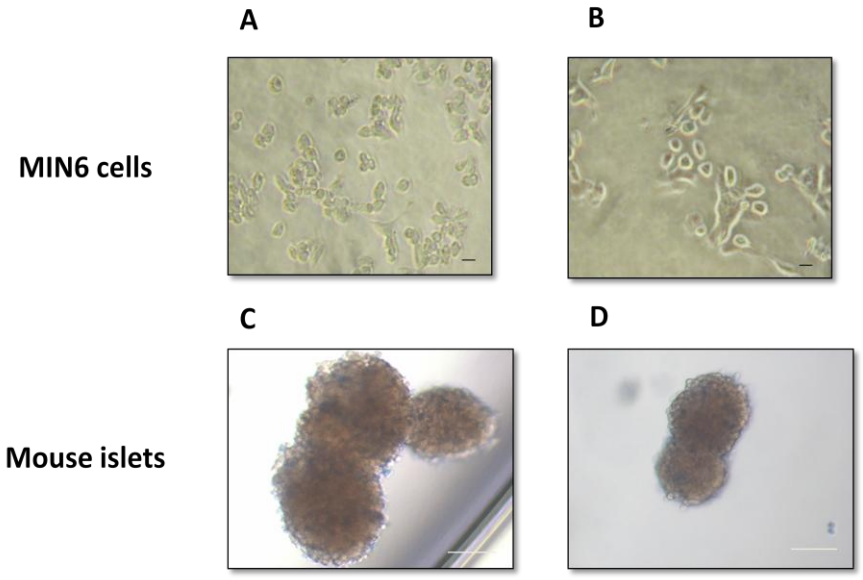

Figure 7.2: Effect of CP extract on MIN6 cell and mouse islets viability. Membrane integrity was measured by the Trypan Blue exclusion method. MIN6 cells or mouse islets were exposed to 1.0 mg/ml CP for 30 min after which they were incubated with 0.1% Trypan Blue dye in PBS at 37 °C for 15 min. The micrographs in panels A, B, C and D show MIN6 cells and mouse islets that had been incubated with 2mM glucose in the absence (A, C) or presence (B, D) of 1.0 mg/ml CP after staining with 0.1% (w/v) Trypan Blue dye. MIN6 cells: Bar shows 10µm, mouse islets: Bar shows 50µm.

7.3.2 Effect of CP extract on insulin secretion from MIN6 PIs, isolated mouse and human islets

A multichannel, temperature-controlled perifusion system was used to examine the effects of CP extract on the pattern and rate of insulin secretion. MIN6 PIs, mouse and human islets were perifused with buffers supplemented with 0.1 mg/ml CP extract at glucose concentrations selected to mimic conditions of fasting blood glucose (2mM) and uncontrolled hyperglycemia (20mM). In the presence of 2mM glucose, the CP extract induced a rapid but transient increase in insulin secretion from MIN6 PIs, reaching a peak of 323 ± 60% basal ($p<0.01$) after 4-6 min (Figure 7.3). The rate of insulin secretion subsequently subsided to almost basal levels despite the continued presence of the CP extract. Similarly, CP-induced insulin secretion from perifused mouse (Figure 7.4) and human (Figure 7.5) islets was also rapid in onset but transient during the 20 min exposure to CP.

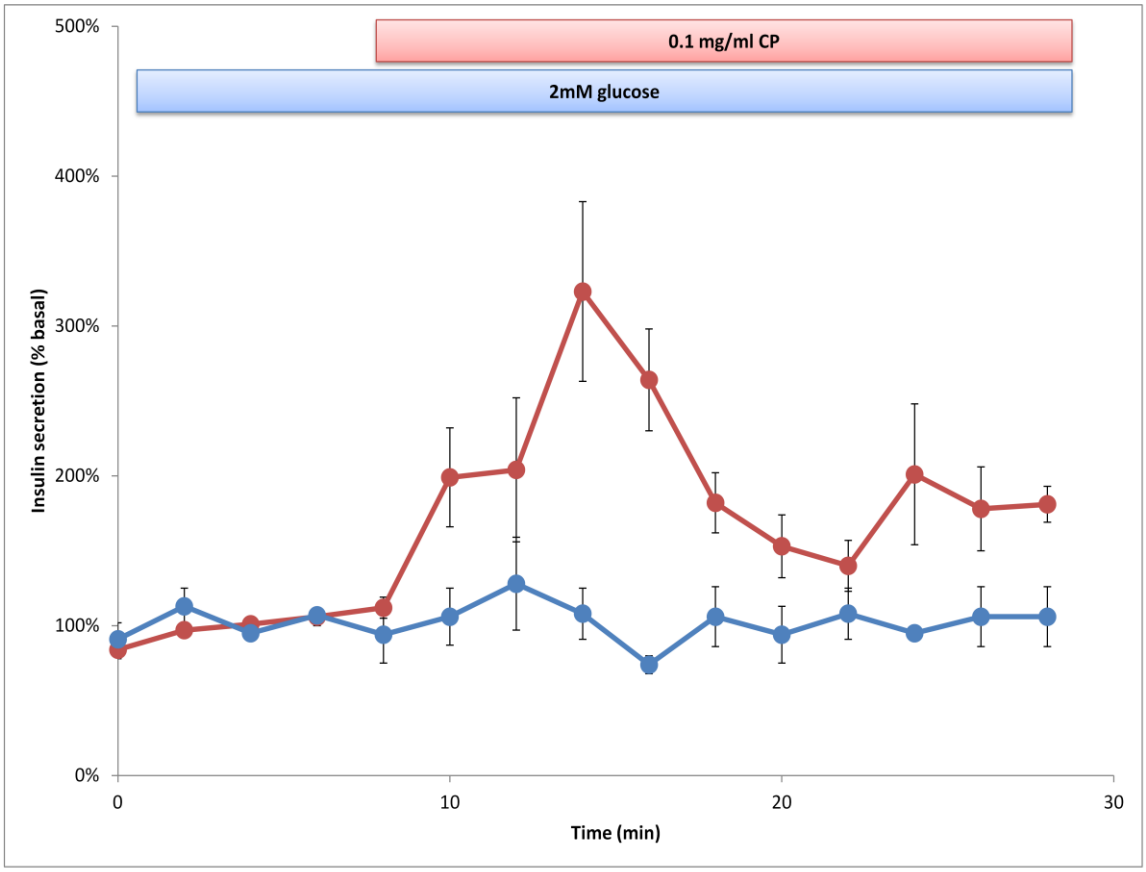

Figure 7.3: Effect of CP extract (0.1 mg/ml) on insulin secretion from MIN6 PIs at a substimulatory glucose concentration. MIN6 PIs were perifused with physiological salt solution supplemented with either 0.1 mg/ml CP (●) or vehicle (●) in the presence of 2mM glucose. Samples were collected every 2 min and insulin content was measured by RIA. Insulin secretion data are expressed as % of basal (2mM glucose). Insulin secretion was significantly stimulated in the presence of 0.1 mg/ml CP at 2mM glucose (P<0.05). Data show mean ± SEM, n=4 per each treatment.

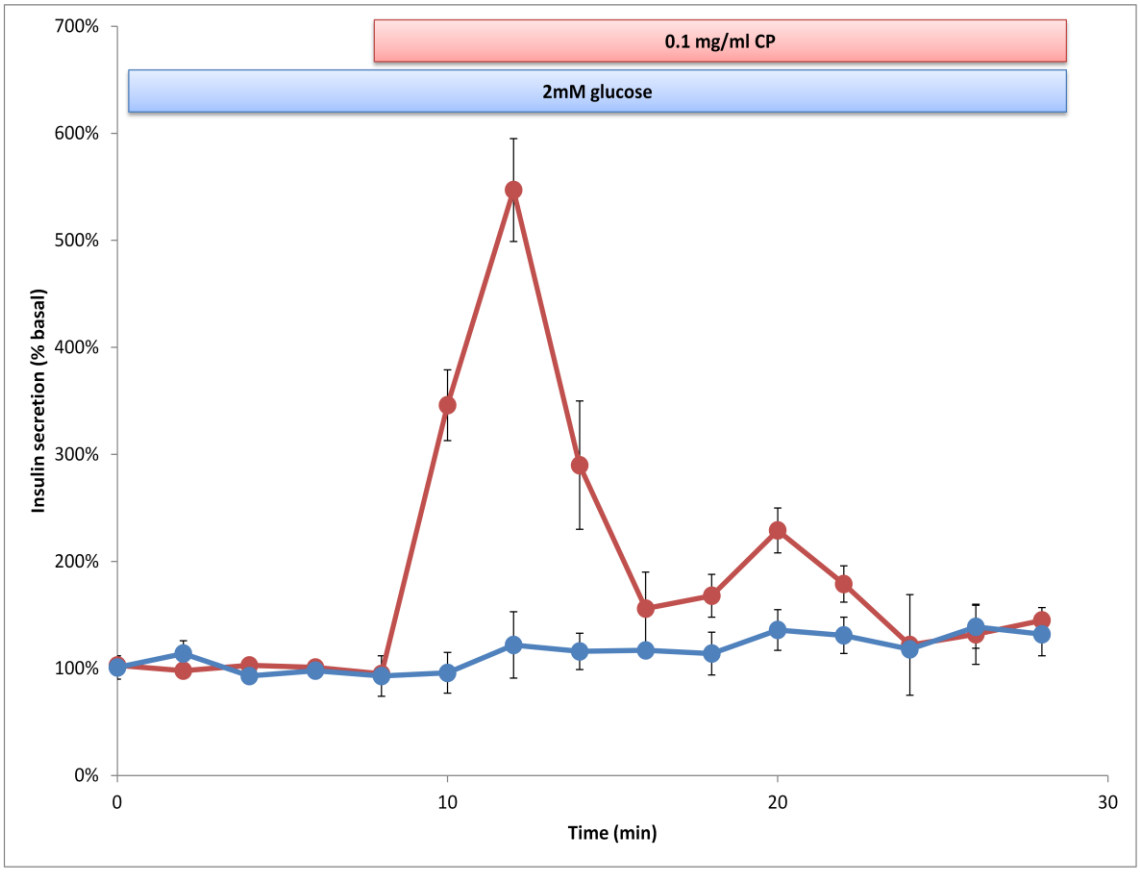

Figure 7.4: Effect of CP extract (0.1 mg/ml) on insulin secretion from primary mouse islets at a substimulatory glucose concentration. Mouse islets were perifused with physiological salt solution supplemented with either 0.1 mg/ml CP (●) or vehicle (●) in the presence of 2mM glucose. Samples were collected every 2 min and insulin content was measured by RIA. Insulin secretion data are expressed as % of basal (2mM glucose). Insulin secretion was significantly stimulated in the presence of 0.1 mg/ml CP at 2mM glucose ($p<0.05$). Data show mean ± SEM, n=4 per each treatment.

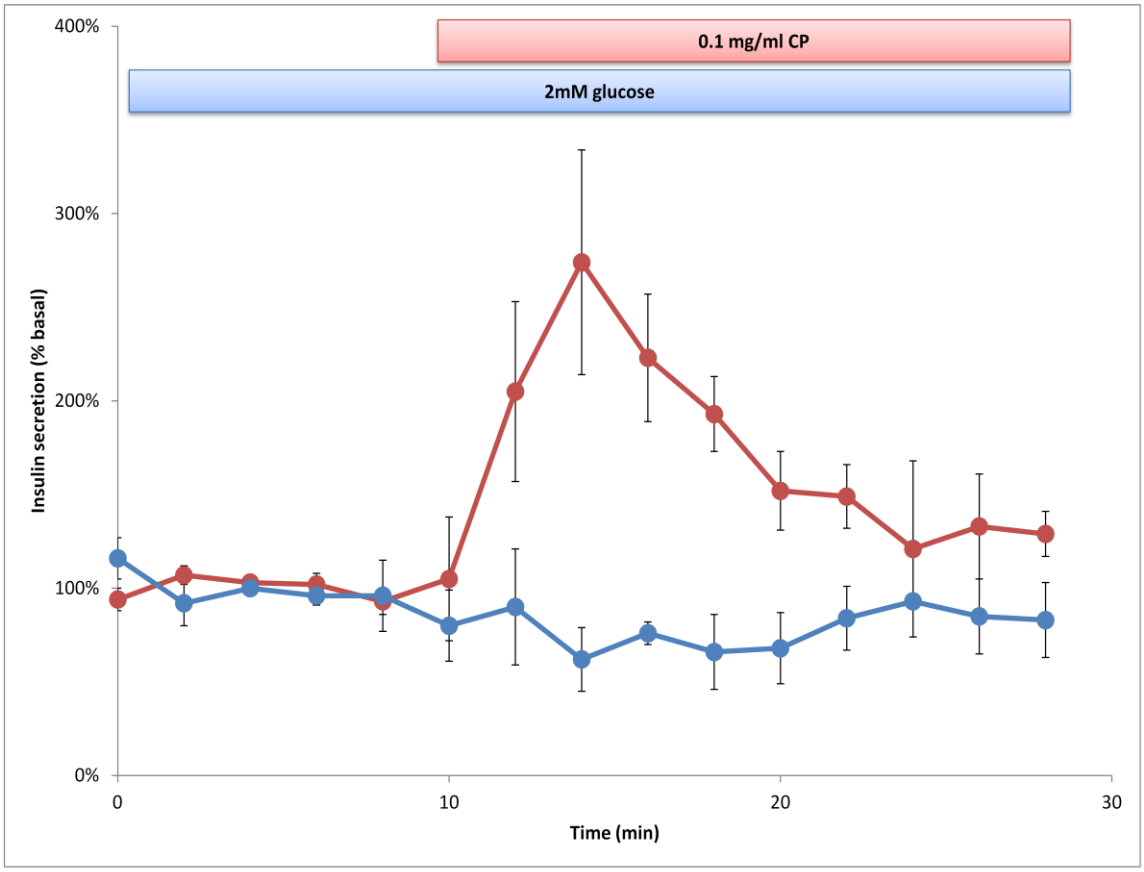

Figure 7.5: Effect of CP extract (0.1 mg/ml) on insulin secretion from primary human islets at a substimulatory glucose concentration. Human islets were perifused with physiological salt solution supplemented with either 0.1 mg/ml CP (●) or vehicle (●) in the presence of 2mM glucose. Samples were collected every 2 min and insulin content was measured by RIA. Insulin secretion data are expressed as % of basal (2mM glucose). Insulin secretion was significantly stimulated in the presence of 0.1 mg/ml CP at 2mM glucose ($p<0.05$). Data show mean ± SEM, n=4 per each treatment.

The CP extract (0.1 mg/ml) did not potentiate glucose-induced (20mM) insulin release from MIN6 PIs (Figure 7.6) nor from mouse (Figure 7.7) or human islets (Figure 7.8). In these experiments, exposing MIN6 PIs, mouse or human islets to 20mM glucose evoked a bi-phasic and maintained increase in insulin secretion as expected. Addition of CP extract slightly elevated insulin release from MIN6 PIs and mouse islets over the first phase of glucose-induced insulin secretion but this effect was not statistically significant, neither when assessing the rate of insulin secretion at individual time points, nor when comparing area under the curve estimates of the total mass of insulin secreted during the experiment.

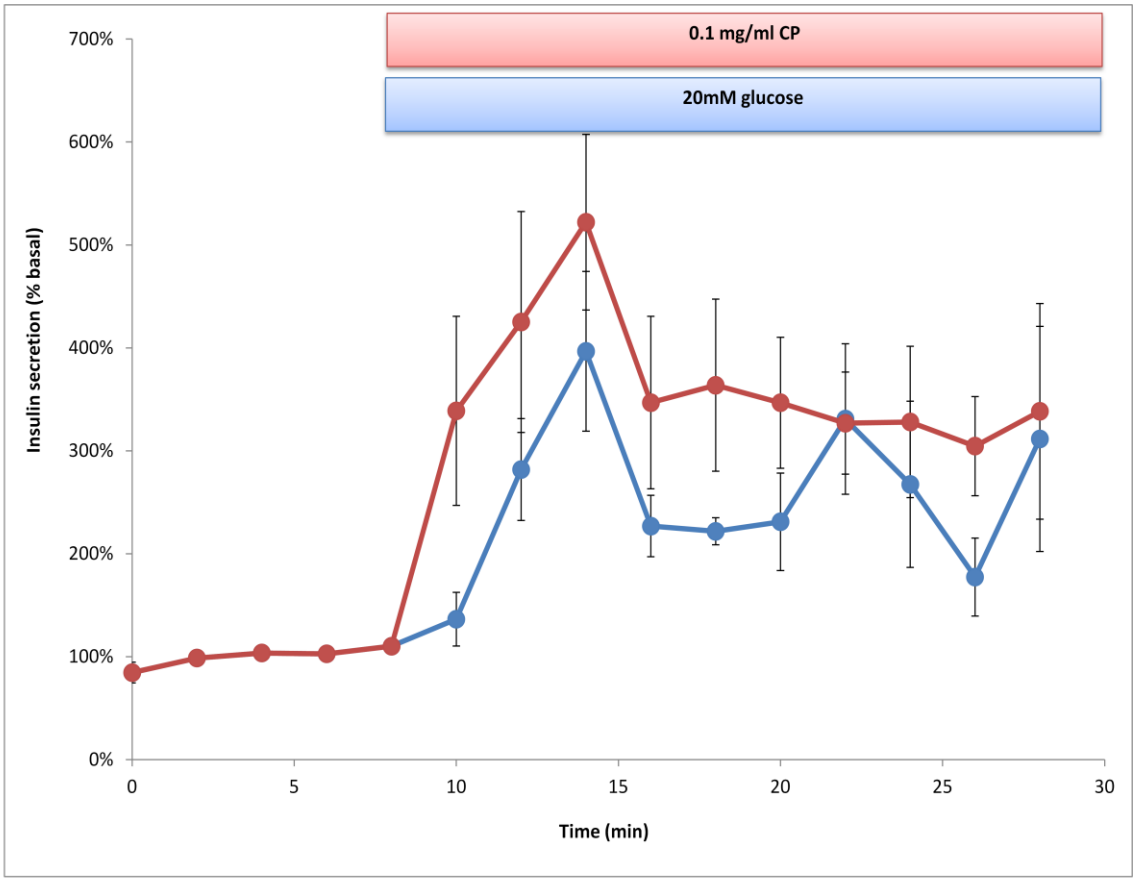

Figure 7.6: Effect of CP extract (0.1 mg/ml) on insulin secretion from MIN6 PIs at a stimulatory glucose concentration. MIN6 PIs were perifused with physiological salt solution supplemented with 20mM glucose in the presence (●) or absence (●) of 0.1 mg/ml CP, as shown by the bars. Samples were collected every 2 min and insulin content was measured by RIA. Data are expressed as % of basal (2mM glucose). Insulin secretion was not significantly potentiated in the presence of 0.1 mg/ml CP extract at 20mM glucose (p>0.2). Data show mean ± SEM, n=4 per each treatment.

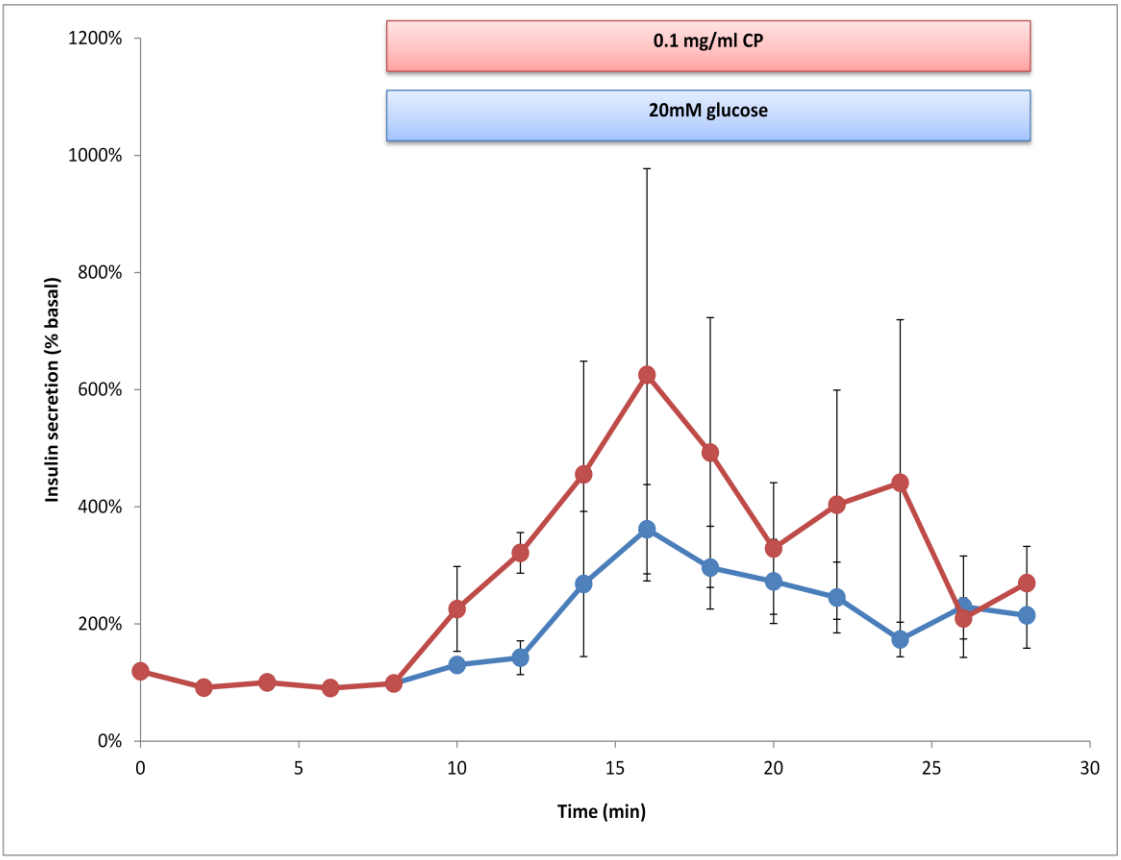

Figure 7.7: Effect of CP extract (0.1 mg/ml) on insulin secretion from primary mouse islets at a stimulatory glucose concentration. Mouse islets were perifused with physiological salt solution supplemented with 20mM glucose in the presence (●) or absence (●) of 0.1 mg/ml CP, as shown by the bars. Samples were collected every 2 min and insulin content was measured by RIA. Data are expressed as % of basal (2mM glucose). Insulin secretion was not significantly potentiated in the presence of 0.1 mg/ml CP extract at 20mM glucose (p>0.2). Data show mean ± SEM, n=4 per each treatment.

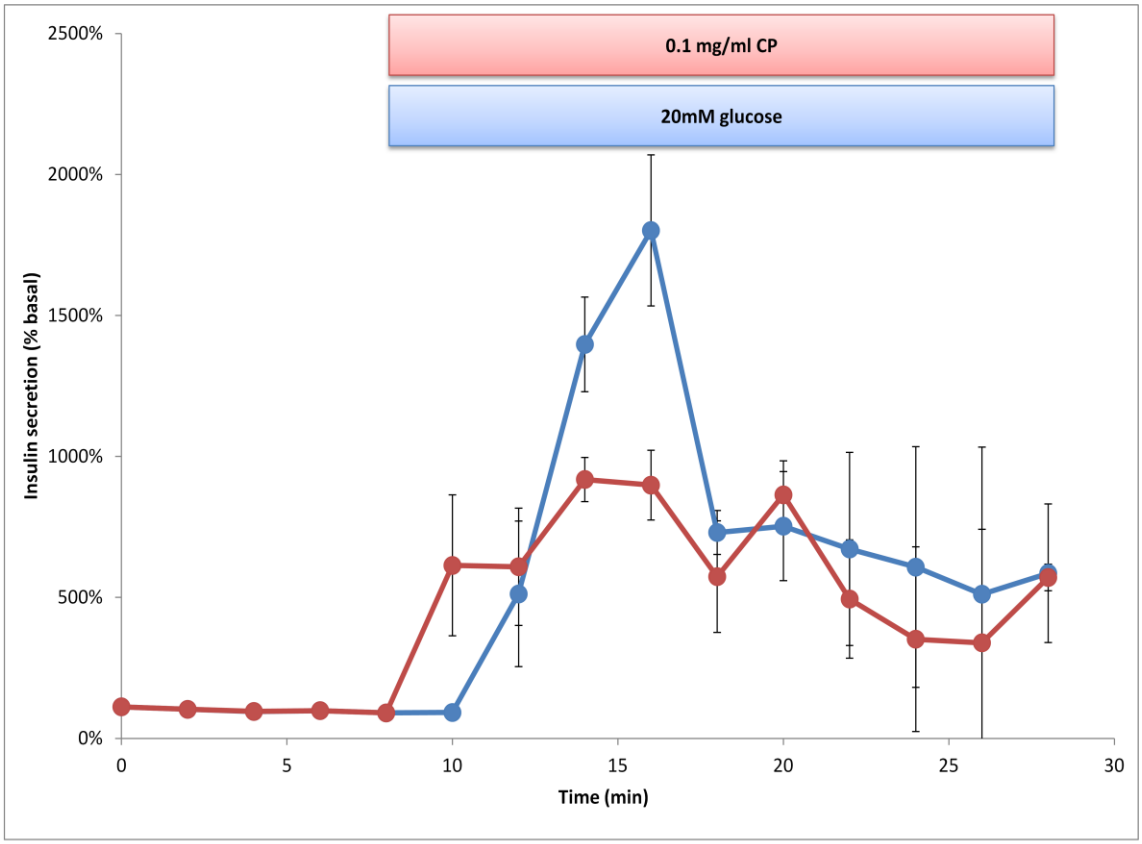

Figure 7.8: Effect of CP extract (0.1 mg/ml) on insulin secretion from primary human islets at a stimulatory glucose concentration. Human islets were perifused with physiological salt solution supplemented with 20mM glucose in the presence (●) or absence (●) of 0.1 mg/ml CP, as shown by the bars. Samples were collected every 2 min and insulin content was measured by RIA. Data are expressed as % of basal (2mM glucose). Insulin secretion was not significantly potentiated in the presence of 0.1 mg/ml CP extract at 20mM glucose (p>0.2). Data show mean ± SEM, n=4 per each treatment.

7.3.3 Effect of CP extract on MIN6 cell $[Ca^{2+}]_i$

Exposure to CP extract (0.1 mg/ml) at 2mM glucose was associated with an increase in $[Ca^{2+}]_i$ in Fura-2-loaded MIN6 cells (Figure 7.9). The elevations in $[Ca^{2+}]_i$ levels were delayed in onset, with a lag time of approximately 3 min, consistent with the time-course of the effects of the extract on insulin secretion (Figure 7.3) and similar to the time course seen in similar experiments using OSA® (chapter 5). The CP-induced increase in $[Ca^{2+}]_i$ was completely abolished in the absence of extracellular Ca^{2+} or in the presence of nifedipine. MIN6 cells that had been exposed to CP showed further elevation of $[Ca^{2+}]_i$ levels upon exposure to 100µM ATP (basal to peak amplitude: 0.3±0.01, $p<0.01$, 30/30 cells).

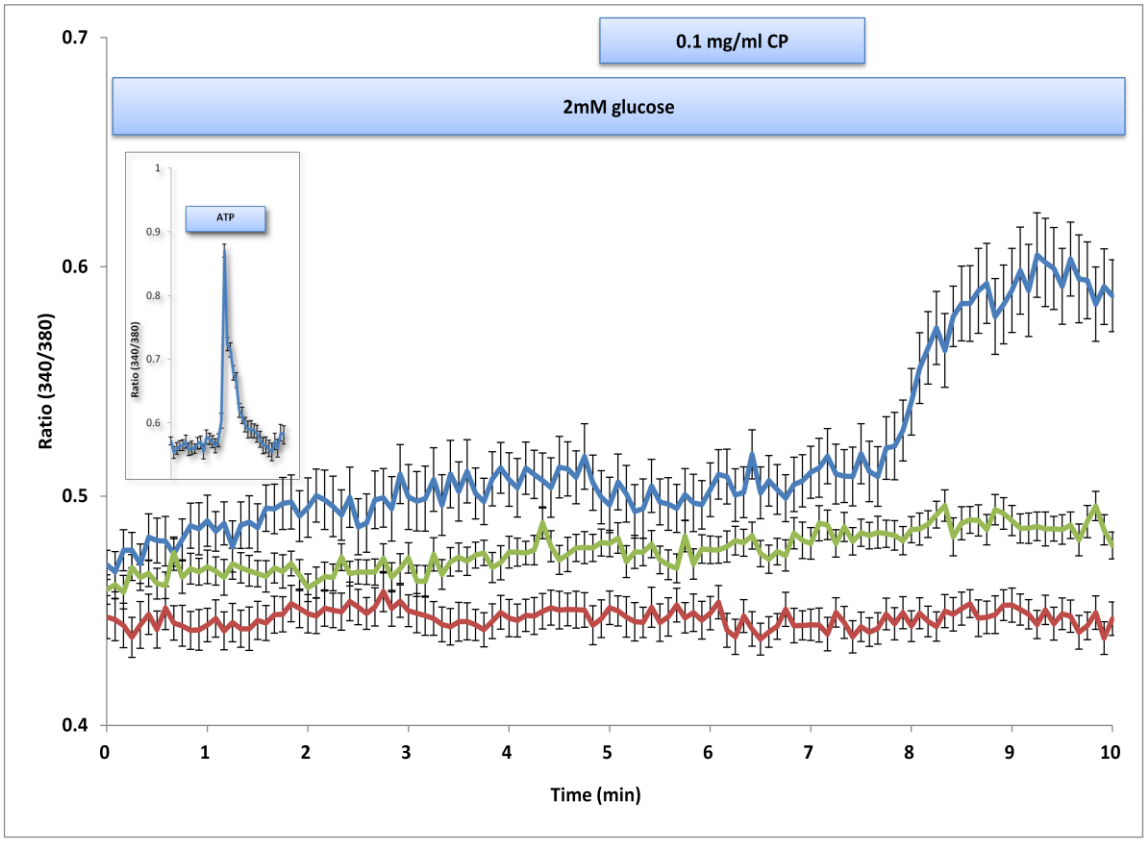

Figure 7.9: Effect of CP extract on intracellular Ca^{2+} levels in MIN6 β-cells. Fura-2-loaded MIN6 cells were perifused throughout with a buffer containing 2mM glucose and supplemented with 0.1 mg/ml CP extract for 3 min, as shown by the upper bar, in the presence (—) or absence (—) of extracellular Ca^{2+} and in the presence of nifedipine (—). Changes in $[Ca^{2+}]_i$ were determined by single cell microfluorimetry and expressed as 340/380nm ratiometric data. CP significantly (P<0.01) elevated $[Ca^{2+}]_i$ which was completely abolished in the absence of extracellular Ca^{2+} or in the presence of nifedipine (P<0.01). ATP (inset) also caused elevations in $[Ca^{2+}]_i$ in cells which had been previously exposed to CP. Data are mean ± SEM, n=30-34 cells for each experimental treatment. All observations are representative of at least two experiments.

7.3.4 Effect of CP extract on preproinsulin mRNA expression

Quantitative measurement of PPI mRNA levels from mouse islets exposed to 0.1 mg/ml CP for 24 hrs showed no increase in insulin gene transcription as compared to 2mM glucose (Figure 7.10). However, 20mM glucose, as expected, raised the levels of mRNA encoding PPI ($p<0.05$).

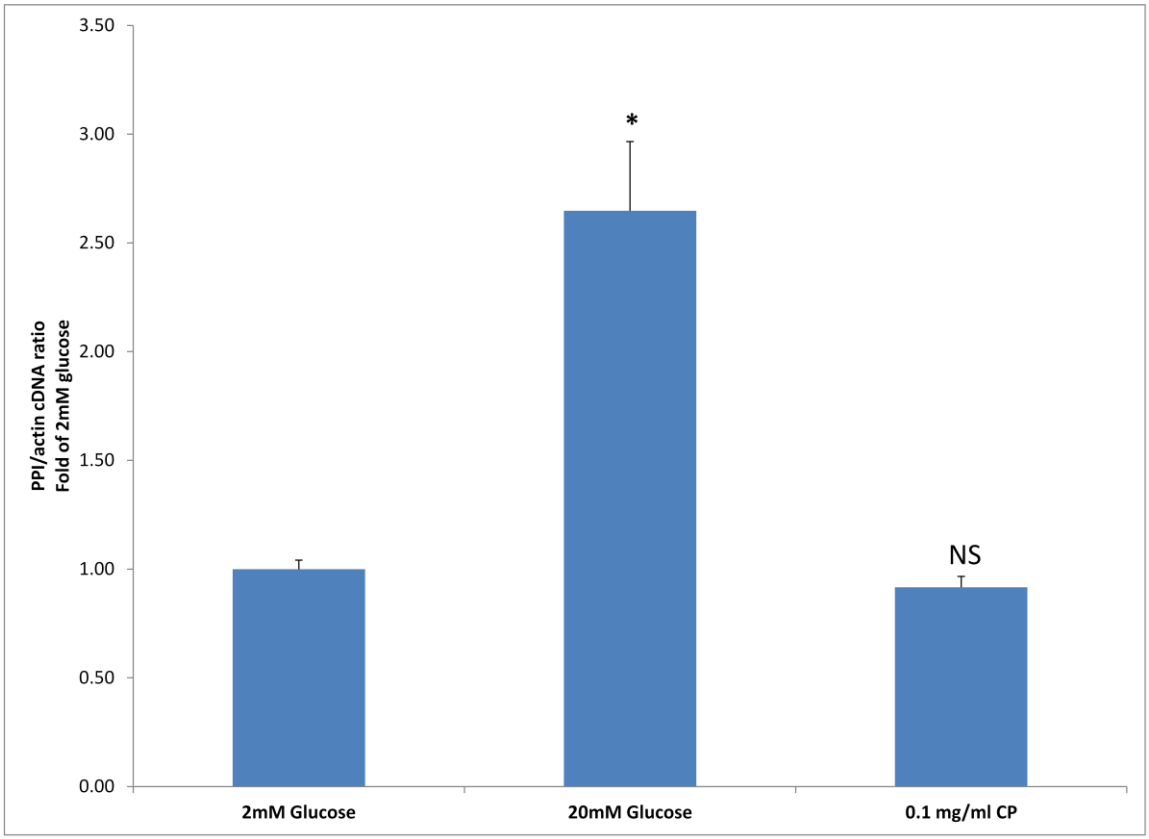

Figure 7.10: Effect of CP on preproinsulin mRNA expression in mouse islets. 150 mouse islets were preincubated with 2mM glucose and then incubated with 20mM glucose or 2mM glucose supplemented with either vehicle or 0.1 mg/ml CP for 24 hrs. Quantification of PPI was carried out as described in Materials and Methods. PPI mRNA levels were normalized to actin mRNA. Unlike 20mM glucose (*p<0.05), CP caused no significant increase in PPI expression at 24 hrs as compared to 2mM glucose (p>0.2). Data show mean + SEM, n=3. NS: not significant.

7.3.5 Effect of CP extract on mouse total insulin content

Prolonged exposure of mouse islets to CP was not associated with any changes in islet total insulin content. The total insulin content of islets incubated in the presence of 2mM glucose alone was 29.5 ± 5.5 ng/islet. Addition of CP did not cause any changes in islet total insulin content (28.7 ± 2.1 ng/islet, p>0.2)

7.4 Discussion

The previous chapters have discussed the role of OSA® as a potential antidiabetic agent. In this chapter I investigated the role of another promising plant extract, *Costus pictus* (CP), which has reported to have glucose-lowering activity in diabetic rats. The beneficial antidiabetic effect of CP seen in hyperglycemic rats was

reported following chronic and prolonged treatment with the plant extract. Thus, 28 days oral administration of the same aqueous CP extract as used in the current study to hyperglycemic rats at 2 gm/kg body weight induced a significant ($p<0.001$) reduction in fasting blood glucose levels, associated with increased serum insulin levels (Jayasri *et al.*, 2008). Other studies have also reported similar results (Gireesh *et al.*, 2009, Jothivel *et al.*, 2007). It is difficult to investigate cellular mechanisms of action using *in vivo* models, so in our current study I investigated the acute effect of a CP extract *in vitro* using MIN6 cells and primary mouse and human islets. MIN6 cells, which are a transformed insulin-secreting β-cell line derived from a mouse insulinoma, are a useful experimental model for studies of insulin secretion because, unlike other β-cell lines, they contain a relatively high insulin content (Ishihara *et al.*, 1993, Persaud, 1999).

Our preliminary data using MIN6 cells grown as adherent monolayers demonstrated that CP extract caused a concentration-dependent increase in insulin secretion, and that the extract was capable of initiating an insulin secretory response in the absence of a stimulatory concentration of glucose. In all our experiments, the basal glucose concentration was maintained at 2mM, a sub-stimulatory concentration of glucose, to eliminate any possible contribution of glucose to the secretory response.

Different chemical constituents including saponins, flavonoids, glycosides and other compounds have been isolated and characterized from a wide range of medicinal plant extracts. Triterpene saponins have been shown to exert a wide range of pharmacological activities including anti-diabetic, anti-viral, anti-inflammatory,

anti-allergic and anti-bacterial effects. The anti-diabetic effect seen with CP may be also mediated by these saponins but this is still to be determined.

Insulin is released from β-cells *in vitro* in either controlled or uncontrolled manners. Regulated or controlled insulin release involves membrane depolarization, Ca^{2+} influx and granule exocytosis, whereas unregulated or uncontrolled insulin release usually occurs due to a compromised plasma membrane and increased membrane permeability. Most plant extracts contain different chemical constituents that may damage the plasma membrane. It has been reported that high content of saponins may compromise plasma membranes leading to uncontrolled release of insulin. Therefore the effect of CP on plasma membrane integrity was determined by Trypan Blue exclusion test. CP extract did not compromise plasma membrane viability even at a concentration as high as 1.0 mg/ml, suggesting that its effects on insulin secretion in our experiments were due to an activation of a regulated exocytotic response.

Data from static incubation experiment using MIN6 cells as monolayers showed that CP caused a concentration-dependent increase in insulin secretion. In these experiments, I used late passage MIN6 cells (p.39) and it is well-documented these late passage cells in static secretion experiments lose their ability to respond to various stimuli such as glucose and α-ketoisocaproic acid. The secretory responses of MIN6 cells to those stimuli can be largely restored if they configured into three-dimensional islet-like clusters (pseudoislets), probably because of enhanced β-cell to β-cell communication within the pseudoislet structures (Hauge-Evans *et al.*, 1999). Therefore, for our subsequent perifusion measurements of the effects of CP extract on insulin secretion, the MIN6 cells were configured as pseudoislets to

ensure maximum insulin secretory responses. Perifusion experiments have the additional advantages of measuring the rate and duration of insulin output, which facilitate the detection of relatively transient responses of the extract. These experiments confirmed the observations obtained using monolayer cells that CP extract acutely initiated insulin secretion in the presence of a substimulatory concentration of glucose, and further revealed that the effect was transient. These observations are in accordance with the lack of effect of CP extract on plasma membrane permeability because such damage is associated with irreversible leakage of insulin from compromised cells. In addition, CP extract induced an insulin secretory response from primary mouse and human islets confirming that the extract had a direct stimulatory effect in primary β-cells. Furthermore, the direct stimulatory effect of CP extract on mouse islets was not associated with increases in insulin expression at either mRNA or protein levels, further supporting the results of our perifusion experiments which reported a transient effect of CP on insulin secretion.

The initiation of insulin secretion by CP could not be attributed to the presence of high K^+ levels in the plant extract since, in a previuosly published report, trace element analysis of CP leaves using proton-induced X-ray emission indicated that the K^+ concentration was only 0.4±0.12μg/ml (Jayasri *et al.*, 2008). Thus, CP leaf extracts contain, at most, micromolar concentrations of K^+ while millimolar concentrations are required to stimulate insulin secretion (Wollheim and Sharp, 1981).

Although CP slightly potentiated the first, but not the second, phase of glucose-induced insulin secretion from MIN6 PIs and mouse islets, the increment in insulin

secretion did not reach statistical significance. On the other hand, CP did not enhance insulin output over the bi-phasic glucose-induced insulin secretion from human islets. This may be a consequence of the human islets showing a robust glucose-induced secretory response (maximally 18 fold basal) and any small changes in insulin secretion that may have been caused by CP are likely to have been masked. A supra-physiological glucose concentration (20mM) was used in these experiments to preclude an action of the plant extracts through metabolism-induced generation of ATP. Our observations are in contrast to a recent report that aqueous CP extract stimulated insulin secretion above that induced by 20mM glucose (Gireesh *et al.*, 2009). The differences in reported effects of CP extracts most likely reflect differences in experimental protocols between studies. Our perifusion experiments were designed to look at rapid changes in the rate of insulin secretion over a minute-to-minute time scale, whereas the previous study (Gireesh *et al.*, 2009) used a static incubation protocol which found stimulatory effects on glucose-induced insulin secretion after prolonged (24h) exposure to the extract.

Many physiological insulin secretagogues act by facilitating the influx of extracellular Ca^{2+}, or the release of Ca^{2+} from intracellular stores leading to increased $[Ca^{2+}]_i$ and insulin exocytosis. Our measurements of $[Ca^{2+}]_i$ in Fura-2-loaded MIN6 cells demonstrated that the CP extract induced elevations in $[Ca^{2+}]_i$, consistent with its effects to initiate insulin secretion. The removal of extracellular Ca^{2+} or blockade of VGCC by nifedipine completely inhibited the CP-induced increases in $[Ca^{2+}]_i$, suggesting that CP raised cytosolic Ca^{2+} levels in β-cells by increasing Ca^{2+} influx through VGCC. The ability of the cells which had been exposed to CP to further increase $[Ca^{2+}]_i$ in response to ATP further demonstrated that the

extract did not impair the ability of the cells to maintain a membrane potential and Ca^{2+} gradient across the plasma membrane, consistent with the Trypan Blue measurements of membrane integrity.

In summary, our *in vitro* studies suggest that an important mechanism of action of *Costus pictus* extract is through a direct effect on islet β-cells to stimulate insulin secretion. Our measurements of $[Ca^{2+}]_i$ suggest that CP initiates an insulin secretory response by increasing Ca^{2+} influx through VGCC, consistent with a mode of action similar to that of other depolarizing agents such as sulphonylurea drugs. This ability to by-pass glucose metabolism and induce insulin secretion by depolarization-induced Ca^{2+} influx offers a mechanism for increasing insulin secretion from glucose-unresponsive β-cells in T2DM.

The data presented here and in previous chapters have shown that the effects of GS and CP extract on insulin secretion have distinct characteristics. First, although both extracts act directly on β-cells to initiate insulin secretion, the effect of GS was maintained throughout the stimulation period. Second, the GS, but not CP, extract potentiated glucose-induced insulin secretion. Third, both extracts increase $[Ca^{2+}]_i$ with similar time course suggestive of a common mechanism of action through Ca^{2+} influx. Finally, the GS extract, but not the CP extract, enhanced PPI mRNA expression, consistent with a therapeutic advantage in modulating β-cell insulin stores. Overall, when comparing the profiles of both extracts, GS extract may offer better therapeutic potential than CP extract. This type of "screening portfolio" allows identification of useful plant-based remedies, which will be discussed in detail in the General Discussion (chapter 8).

Chapter 8

General discussion

8.1 Introduction

Diabetes mellitus is a global health problem affecting both developed and developing countries. It is defined as a metabolic disorder characterized by an elevation of blood glucose concentration leading to chronic hyperglycemia and is associated with abnormal metabolism of carbohydrates, fat and protein. The prevalence of the disease is increasing and the estimated number of people with diabetes will be 440 million by the year 2030, more than double the current estimate (Internaional Diabetes Federation, 2009). Ninety-five percent of those individuals will have Type 2 diabetes mellitus (T2DM) which is characterized by β-cell dysfunction and worsening of insulin sensitivity in insulin-sensitive tissues. Recent studies have developed the concept that T2DM is associated with a progressive loss of the functional β-cell mass, with symptoms appearing when the β-cell mass is no longer sufficient to maintain glucose homeostasis. The risk of developing macrovascular and microvascular complications increases with untreated or poorly controlled T2DM as a result of long-standing hyperglycemia and insulin resistance. These complications can involve many different organs of the body leading to coronary heart disease, stroke, peripheral vascular disease, neuropathy, retinopathy and nephropathy (Defronzo *et al.*, 2004). Therefore, the major targets of T2DM treatment are reduction in hyperglycemia and improvement of insulin resistance. The current available therapies for the treatment of T2DM have been focused on correcting these abnormalities. However, some of these therapies are associated with serious adverse effects and complete glycemic control is yet far from achievement. Therefore, introducing and developing new drugs especially those from plant origin have been an active area of research.

There is no doubt that alternative medicine, especially herbal remedies, has attracted a lot of attention in the past few decades. This is due to the fact that almost 35-48% of people worldwide have used herbal medicine to treat various diseases including DM. Metformin, one of the current and effective antidiabetic drugs, was originally isolated from *Galega officinalis*, a plant which has been used in managing DM for centuries (Witters, 2001). Thus, identifying novel, effective extracts of plant origin to treat DM could offer inexpensive and widely available therapeutic options in the developing world.

More than 800 plants have been claimed to be effective in treating DM (Alarcon-Aguilara *et al.*, 1998). However, currently there are no defined criteria in the phytochemical society for bench-marking identification and screening of plant-based remedies as potential antidiabetic agents. Therefore, in this thesis I have identified certain characteristics which can be used as a screening tool to identify potential plant extracts as therapeutic agents for the treatment of DM.

8.2 Screening for potential plant extracts

We here suggest specific criteria that can be applied as a "screening portifolio" to identify potential therapeutic agents of plant origin. A useful plant extract should possess some or all of the following properties:

- Potentiate nutrient-induced insulin secretion to reduce post-prandial hyperglycemia.
- Stimulate insulin secretion while preserving β-cell insulin stores.
- Preserve β-cell mass by either stimulating neogenesis and proliferation or preventing apoptosis.

- Reduce the rate at which glucose enters the bloodstream by interfering with glucose absorption in the intestine.
- Improve diabetic symptoms either by direct stimulation of insulin secretion from β-cells or by reduction of insulin resistance in animal models of diabetes and in human subjects.

8.3 GS and CP as potential antidiabetic agents

Gymnema and Costus are genera in the family of Asclepiadaceae and Costaceae, respectively, containing 100 species among which the species GS and CP have a historical use as Ayurvedic medicine in treating various diseases, practically DM (Benny, 2004, Porchezhian and Dobriyal, 2003). The therapeutic benefits of GS and CP in treating DM reside in their leaves. Extracts of GS and CP leaves have been shown to contain many bioactive compounds that are responsible for their antidiabetic activities. Saponins and flavonoids have been extracted from CP leaves and may possibly contribute to the antihyperglycemic effects of CP extracts (Jayasri *et al.*, 2008, Jothivel *et al.*, 2007, Meléndez-Camargo *et al.*). Triterpene saponins including gymnemic acid (GA) have been isolated from GS leaves and are believed to mediate some of the effects of GS on DM (Sugihara *et al.*, 2000). GA-containing extracts (also known as low molecular weight extracts) have been documented to lower blood glucose levels and to increase insulin levels in animal models of DM and in human subjects (Balasubramaniam *et al.*, 1988, Baskaran *et al.*, 1990, Gupta, 1961, Gupta, 1963, Gupta and Variyar, 1961, Khare *et al.*, 1983, Shanmugasundaram *et al.*, 1981, Shanmugasundaram *et al.*, 1983, Shanmugasundaram *et al.*, 1988, Shanmugasundaram *et al.*, 1990b, Srivastava *et al.*, 1985, Srivastava *et al.*, 1986, Sugihara *et al.*, 2000). Most of these studies have used low molecular weight

extracts to establish the antidiabetic effect of GS. However, the activity of other extracts, especially high molecular weight extracts, has yet to be determined. Therefore, in this project I have studied the therapeutic potential of a high molecular weight extract named OSA® in a series of *in vivo* and *in vitro* experiments.

In this chapter I will compare the potential therapeutic efficacy of OSA® or CP using the criteria described above.

8.3.1 Direct stimulation of hormone release from β-cell line and primary islets

Both OSA® and CP caused concentration-dependent increases in insulin secretion from MIN6 monolayers at a substimulatory glucose concentration. The kinetic profiles of the insulin secretory responses induced by OSA® and CP were assessed in perifusion experiments with MIN6 PIs. At substimulatory glucose concentrations, OSA® induced a sustained increase in insulin secretion which was reversible upon withdrawal of OSA®. The sustained effect of OSA® should provide a therapeutic benefit of long-term control of blood glucose levels and thus reduces the frequency of dosage. Unlike OSA®, CP only transiently elevated insulin secretion which returned rapidly to basal levels in spite of the continuous presence of CP, suggesting that it may be of limited therapeutic efficacy in the face of prolonged hyperglycemia, as occurs in T2DM.

The insulinotropic effects of OSA® and CP were also observed in mouse and human islets, indicating a direct action on primary β-cells. In mouse and human islets, OSA® and CP initiated insulin secretion which was again sustained in the presence

of OSA® but only transient in the presence of CP. Although increasing insulin secretion at substimulatory glucose concentrations may increase the risk of developing hypoglycemia, SUs, which also stimulate insulin release at 2mM glucose, are still used successfully in the treatment of T2DM (Persaud and Jones, 2008), suggesting that OSA® and CP may be at least as effective as this commonly used class of T2DM drugs.

In addition to the initiation of insulin secretion, OSA® also potentiated glucose-induced insulin secretion from MIN6 PIs, mouse and human islets. OSA® increased insulin output over 20mM glucose, a supra-stimulatory glucose concentration, suggesting that OSA® did not act as a nutrient, nor by enhancing nutrient metabolism. The advantage of this effect is that OSA® can bypass glucose metabolism and stimulate insulin secretion in glucose unresponsive β-cells, similar to exendin-4, a GLP-1 agonist. However, OSA® has the benefit of not being degraded in the GI tract, unlike exendin-4, and thus be safe to be given orally. OSA®, not only increased insulin secretion at 2 and 20mM glucose, but also stimulated insulin secretion at more physiological glucose concentrations (5 and 10mM). This gives OSA® the advantage of exerting its insulinotropic action regardless of glucose levels. In contrast to OSA®, CP did not augment glucose-induced insulin secretion from the β-cell line nor from primary islets, suggesting that CP may have limited use as a therapeutic agent to treat hyperglycemia in T2DM.

OSA® also affected the secretion of other pancreatic hormones. Glucagon secretion was stimulated by OSA® in the presence of either 2mM glucose or 20mM arginine. Whether OSA® has a direct or indirect action on α-cells is yet to be determined.

However, the increase in glucagon secretion is not uncommon for insulinotropic agents. SUs, which are still used as a first-line therapy in T2DM treatment, are also reported to stimulate glucagon secretion (Bohannon *et al.*, 1982, MacDonald *et al.*, 2007).

8.3.2 Maintenance of cell viability

Any saponin-containing plant extracts may have deleterious effect on plasma membrane integrity because saponins have been shown to increase plasma membrane permeability through membrane pore formation (Ahnert-Hilger and Gratzl, 1988, Schulz, 1990). Neither OSA® nor CP caused any detectable damage to the plasma membrane at the therapeutic concentrations used in this thesis as demonstrated by the Trypan Blue exclusion test. Cells treated with effective concentrations OSA® or CP showed no increase in Trypan Blue uptake indicating an intact cell membrane. Maintaining the integrity of plasma membrane is important in triggering a regulated exocytosis of insulin.

8.3.3 Preservation of β-cell insulin stores

Maintaining insulin stores in β-cells following chronic stimulation of insulin secretion prevents β-cell exhaustion (Leibowitz, 2002) and thus prevents the gradual loss of secretory responses associated with the continuous use of insulin-secreting agents over prolonged periods of time. An effective pharmacological treatment for T2DM should therefore simultaneously stimulate both insulin secretion and insulin biosynthesis, to ensure that β-cell stores of insulin are maintained. The eventual failure of sulphonylureas as a front line therapy for

T2DM may be caused by their failure to stimulate insulin biosynthesis, leading to β-cell exhaustion and the requirement for insulin replacement therapy.

OSA® seems to fulfill the requirement of stimulating both insulin secretion and insulin biosynthesis. Our measurement of PPI mRNA levels indicated that OSA®, but not CP, significantly elevated the mRNA expression of PPI in chronically-treated mouse islets. In addition, the total insulin content of OSA® treated mouse islets remained unchanged as compared to vehicle-treated islets, despite the chronic stimulation of insulin secretion induced by OSA®.

The elevations in PPI mRNA levels without any change in total insulin content seen in OSA®-treated mouse islets will act to not only maintain β-cell insulin stores but also to prevent overloading β-cells with insulin, suggesting a therapeutic advantage of OSA® over some of the currently used insulin-secreting agents such as SUs.

8.3.4 Activation of crucial steps in stimulus-secretion coupling

Common intracellular mechanisms of increasing insulin secretion are by elevating $[Ca^{2+}]_i$ levels and/or activating other second messengers/protein kinases (Howell *et al.*, 1994). The insulin secretory responses to both OSA® and CP were associated with elevations in $[Ca^{2+}]_i$ concentrations in β-cells as assessed by Ca^{2+} microfluorimetry. Both OSA® and CP-induced increases in $[Ca^{2+}]_i$ levels were inhibited in the presence of EGTA or nifedipine indicating that both OSA® and CP increase cytosolic Ca^{2+} by facilitating Ca^{2+} entry through VGCC. These results were confirmed by perifusion experiments showing that OSA®-induced insulin secretion was partially inhibited by nifedipine.

The downstream elements of the signaling pathway of the insulin secretory response of OSA® were not well understood. The closure of K_{ATP}-channels and subsequent β-cell depolarization were ruled out as the cause for increasing β-cell $[Ca^{2+}]_i$ levels because opening K_{ATP}-channels by diazoxide did not affect OSA®-induced insulin secretion. However, protein kinase activation was partially involved in the secretory response to OSA® as evident by the inhibition of OSA®-induced insulin secretion by staurosporine, a non-selective serine/threonine protein kinase inhibitor. The exact nature of the protein kinase responsible for the OSA® effect on insulin secretion is unknown. PKCαβ and CamKII are known to be involved in the regulation of insulin secretion but were shown not to be involved in OSA®-induced insulin secretion. The ability of OSA® to increase insulin secretion independent of $[Ca^{2+}]_i$ might suggest an involvement of cAMP in the secretory action of OSA®, because cAMP has been reported to increase insulin secretion by sensitizing the secretion machinery to $[Ca^{2+}]_i$ without altering $[Ca^{2+}]_i$ concentration. Interestingly, the insulin secretion induced by OSA® was dissociated from cAMP formation because OSA® reduced $[cAMP]_i$ levels in β-cells in parallel to increasing insulin secretion.

Overall, our current data suggest two possible sites of action of OSA® in the β-cell, (as shown in Figure 8.1). The first is after K_{ATP}-channel closure and depolarization and leads to increased $[Ca^{2+}]_i$, so this may be a direct effect on a plasma membrane Ca^{2+} channel, or an associated receptor. The second site of action is at a late stage in the exocytotic pathway, after the activation of protein kinases, which is not inhibited by broad spectrum protein kinase activators. This may be a direct effect at the site of exocytosis, as has been postulated for some other insulin-releasing

agents such as arachidonic acid, or it may be through a receptor which affects exocytosis directly, as has been suggested for α-adrenoreceptors.

Although the precise mechanism(s) of action of OSA® have not yet been defined this does not prevent the use of OSA® as a therapeutic agent. For example, sulphonylureas were used clinically for many decades before the discovery of K_{ATP}-channels as their site of action. Similarly, metformin has been used in treating T2DM for decades despite the fact that its mechanism of action is not yet clear.

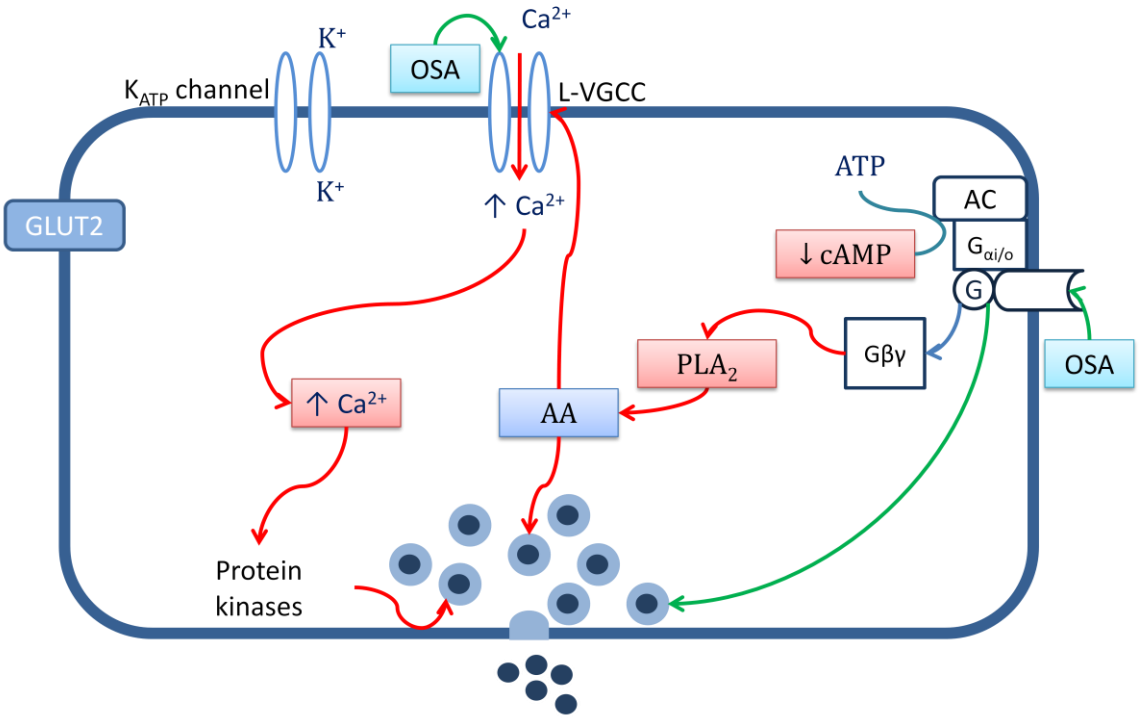

Figure 8.1: Model of OSA®-induced insulin secretion from β-cells. OSA® shares similar characteristic with arachidonic acid (AA). It acts beyond K_{ATP}-channel closure by facilitating Ca^{2+} entry through VGCC either directly or via a receptor. OSA® also partially activates protein kinases to induce insulin secretion. Other actions of OSA® may involve stimulation of insulin vesicles fusion and exocytosis.

8.3.5 Protection of β-cells against harmful insults

T2DM is associated with chronic elevation of cytokines, glucose and FFAs which can precipitate β-cell death through excessive induction of apoptosis via caspase-dependent and –independent pathways (Cnop *et al.*, 2005, Eizirik and Mandrup-

Poulsen, 2001, Johnson and Luciani, 2010, Lupi and Del Prato, 2008, Mandrup-Poulsen, 2001, Poitout and Robertson, 2008, Robertson *et al.*, 2004). Protecting against apoptosis may provide an important way to preserve β-cell mass and thus prevent the progression of T2DM. One successful example of this type of therapy is exendin-4, a GLP-1 agonist, which inhibited IL-1β induced apoptosis in β-cells *in vitro* suggesting a protective role of exendin-4 in β-cells (Ferdaoussi *et al.*, 2008). Exendin analogues or DPPIV inhibitors which inhibit the degradation of endogenous GLP-1 are now being adopted as an effective therapy for T2DM because they have the potential to reduce hyperglycemic by stimulating insulin secretion whilst maintaining the β-cell mass (Xu *et al.*, 1999). The data generated in our studies suggest that OSA® may act in a similar fashion. Thus, OSA® significantly reduced cytokine-induced caspase-3/7 levels in a β-cell line and primary mouse islets, consistent with a protective effect against cell loss via apoptosis. This effect was further emphasized by the data from the microarray analysis of OSA® and/or cytokine treated islets. Cytokines, as expected, elevated caspase-3 mRNA levels. Cytokines-treatment was associated with reduced expression of key genes involved cell survival and defenses, including AKT and MnSOD. OSA® partially reversed the effects of cytokines in mouse islets by reducing the levels of both caspase-3 mRNA and protein. In addition, OSA®-treatment of mouse islets in the presence of cytokines induced an elevation in some free radical scavengers, including MnSOD, suggesting that OSA® may have anti-oxidant activities in β-cells. Our enrichment analysis of the microarray data to identify pathways that were influenced by OSA® demonstrated that PI3K/AKT pathway may mediate some of the anti-apoptotic effects of OSA®. These studies have identified another potentially important mechanism through which OSA® may be an effective therapy for T2DM, and the

cytoprotective activities of OSA® in addition to its insulin secretagogue activity may allow OSA® to be used as an alternative therapy for T2DM.

8.3.6 Improvement of glycemia *in vivo*

Proving the efficacy of a potential antidiabetic drug in animal model of DM and in human subjects is a prequisite to use the drug therapeutically. In a small cohort study, administering OSA® (1 g/day) for 60 days to patients with T2DM significantly improved blood glucose levels pre- and post-prandially. Fasting and post-prandial blood glucose concentrations almost returned to normal levels after OSA® treatment, with no changes in either body weight or post-prandial glucose excursion but with elevations in plasma insulin and C-peptide levels indicating that improvement in glycemia by OSA® was not secondary to changes in either glucose absorption of food intake but rather secondary to a direct effect of OSA® on β-cells. These observations strongly support the use of OSA® as a β-cell-directed therapy for T2DM acting as an insulin-releasing agent.

In our animal study, a single dose of OSA® (500 mg/kg) to ob/ob mice, a T2DM model characterized by hyperglycemia, dramatically attenuated the glucose intolerance status of these animals during IP glucose tolerance tests. This effect of OSA® was not associated with any reduction in glucose absorption or with improvement in insulin resistance, again supporting a direct effect of OSA® on β-cells. The beneficial effects of OSA® seen in our animal and human studies were in agreement with the reported antihyperglycemic actions seen with other GS extracts.

Similar to the effects of OSA® in our *in vivo* studies , our colleagues have reported that aqueous CP extracts significantly reduced blood glucose levels and increased plasma insulin levels in STZ-treated hyperglycemic rats, an effect which was postulated to be due in part to a direct effect on β-cells.

8.4 Conclusion

The work described in this thesis highlights the potential importance of plant-based remedies in the treatment of T2MD. Certain screening criteria and characteristics were devised and applied to identify potential therapeutic agents of plant origin. To validate the screening process, two aqueous plant extracts, OSA® and CP, were studied using a series of functional endpoints to assess their potential usefulness as antidiabetic agents. When the profiles of both extracts were compared, they showed distinct characteristics from each other. The GS extract, OSA®, fulfilled almost all the criteria chosen for an effective antidiabetic agent, being an effective insulin secretagogue at non-toxic concentrations; inducing a simultaneous increase in insulin gene transcription to avoid β-cell exhaustion; having protective effects against apoptotic stimuli; being effective at lowering blood glucose *in vivo*; and being effective when delivered by the enteral route. In contrast, the CP extract was much less attractive as an antidiabetic agent. Although it was an insulin secretagogue, and non toxic, the CP extract would be therapeutically ineffective because it only caused a transient increase insulin secretion and was only effective under normoglycemic, but not hyperglycemic, conditions. These characteristics make it unsuitable for further functional studies as a therapeutic agent for T2DM.

In conclusion, these studies have highlighted the therapeutic potential of OSA®, and perhaps other GS extracts, as a low cost and readily available alternative therapy for the treatment of T2DM.

8.5 Future work

The work in this thesis is not yet complete unless the following is considered in future projects:

- OSA® is an alcoholic extract of a mixture of compounds and for OSA® to be used clinically it is required to fractionate and purify OSA® to isolate and identify the most active ingredient(s) using high performance liquid chromorography (HPLC) and mass chromotography (MS) techniques.
- Previous reports showed that crude or low molecular weight GS extracts reduced intestinal glucose absoption so the effect of OSA® on glucose absorption should also be investigated using in situ gut perifusion.

References

ACHENBACH, P., BONIFACIO, E., KOCZWARA, K. & ZIEGLER, A. G. 2005. Natural history of type 1 diabetes. *Diabetes,* 54 Suppl 2**,** S25-31.

AHMED, A. B., RAO, A. S. & RAO, M. V. 2010. In vitro callus and in vivo leaf extract of gymnema sylvestre stimulate beta-cells regeneration and anti-diabetic activity in wistar rats. *Phytomedicine,* 17**,** 1033-9.

AHNERT-HILGER, G. & GRATZL, M. 1988. Controlled manipulation of the cell interior by pore-forming proteins. *Trends in Pharmacological Sciences,* 9**,** 195-7.

AHREN, B. 1999. Potentiators and inhibitors of insulin secretion. *advances in molecular and cell biology,* 29**,** 175-98.

AHREN, B. 2000. Autonomic regulation of islet hormone secretion--implications for health and disease. *Diabetologia,* 43**,** 393-410.

AL-HASANI, H., TSCHOP, M. H. & CUSHMAN, S. W. 2003. Two birds with one stone: Novel glucokinase activator stimulates glucose-induced pancreatic insulin secretion and augments hepatic glucose metabolism. *Mol Interv,* 3**,** 367-70.

ALARCON-AGUILARA, F. J., ROMAN-RAMOS, R., PEREZ-GUTIERREZ, S., AGUILAR-CONTRERAS, A., CONTRERAS-WEBER, C. C. & FLORES-SAENZ, J. L. 1998. Study of the anti-hyperglycemic effect of plants used as antidiabetics. *Journal of Ethnopharmacology,* 61**,** 101-10.

AMMALA, C., ASHCROFT, F. M. & RORSMAN, P. 1993. Calcium-independent potentiation of insulin release by cyclic amp in single beta-cells. *Nature,* 363**,** 356-8.

ANDRALI, S. S., SAMPLEY, M. L., VANDERFORD, N. L. & OZCAN, S. 2008. Glucose regulation of insulin gene expression in pancreatic beta-cells. *Biochemical Journal,* 415**,** 1-10.

ARAI, K., ISHIMA, R., MORIKAWA, S., MIYASAKA, A., IMOTO, T., YOSHIMURA, S.*, et al.* 1995. Three-dimensional structure of gurmarin, a sweet taste-suppressing polypeptide. *Journal of Biomolecular NMR,* 5**,** 297-305.

ARAKI, E., OYADOMARI, S. & MORI, M. 2003. Impact of endoplasmic reticulum stress pathway on pancreatic beta-cells and diabetes mellitus. *Exp Biol Med (Maywood),* 228**,** 1213-7.

ASHCROFT, F. M. & ASHCROFT, J. H. 1992. Insulin secretion: Mechanism of insulin secretion. *In:* ASHCROFT, F. M. & ASHCROFT, S. J. (eds.) *Insulin molecular biology to pathology.* Oxford University press.

ASHCROFT, F. M. & RORSMAN, P. 1989. Electrophysiology of the pancreatic beta-cell. *Progress in Biophysics and Molecular Biology,* 54**,** 87-143.

BABU, D. A., DEERING, T. G. & MIRMIRA, R. G. 2007. A feat of metabolic proportions: Pdx1 orchestrates islet development and function in the maintenance of glucose homeostasis. *Molecular Genetics and Metabolism,* 92**,** 43-55.

BAILEY, C. J. & KRENTZ, A. 2010. Oral antidiabetic agents. *In:* HOLT, R., COCKRAM, C., FLYVBJERG, A. & GOLDSTEIN, B. J. (eds.) *Textbook of diabetes.* 4 ed. Chichester: Wiley-Blackwell.

BAILEY, E. M., GUEST, P. C. & HUTTON, J. C. 1992. Insulin biosynthesis: Insulin synthesis. *In:* ASHCROFT, F. M. & ASHCROFT, S. J. (eds.) *Insulin molecular biology to pathology.* Oxford University press.

BALASUBRAMANIAM, K., ARASARATNAM, V., SEEVARATNAM, S., THIRUMAGAL, K. & AGESWARAN, A. 1988. Hypoglycemic effect of gymnema sylvestre on diabetic patients. *Jaffna Medical Journal,* 23**,** 49-53.

BALLIAN, N. & BRUNICARDI, F. C. 2007. Islet vasculature as a regulator of endocrine pancreas function. *World Journal of Surgery,* 31**,** 705-14.

BAND, A. M., JONES, P. M. & HOWELL, S. L. 1992. Arachidonic acid-induced insulin secretion from rat islets of langerhans. *Journal of Molecular Endocrinology,* 8**,** 95-101.

BAND, A. M., JONES, P. M. & HOWELL, S. L. 1993. The mechanism of arachidonic acid-induced insulin secretion from rat islets of langerhans. *Biochimica et Biophysica Acta,* 1176**,** 64-8.

BASKARAN, K., KIZAR AHAMATH, B., RADHA SHANMUGASUNDARAM, K. & SHANMUGASUNDARAM, E. R. 1990. Antidiabetic effect of a leaf extract from gymnema sylvestre in non-insulin-dependent diabetes mellitus patients. *Journal of Ethnopharmacology,* 30**,** 295-300.

BASUDEV, H., JONES, P. M., PERSAUD, S. J. & HOWELL, S. L. 1993. Arachidonic acid-induced insulin secretion from rat islets of langerhans is not mediated by protein phosphorylation. *Molecular and Cellular Endocrinology,* 91**,** 193-9.

BENNY, M. 2004. Insulin plant in gardens. *natural product radiance,* 3**,** 349-50.

BERTRAND, L., HORMAN, S., BEAULOYE, C. & VANOVERSCHELDE, J. L. 2008. Insulin signalling in the heart. *Cardiovascular Research,* 79**,** 238-48.

BLONDE, L. 2009. Current antihyperglycemic treatment strategies for patients with type 2 diabetes mellitus. *Cleveland Clinic Journal of Medicine,* 76 Suppl 5**,** S4-11.

BOHANNON, N. V., LORENZI, M., GRODSKY, G. M. & KARAM, J. H. 1982. Stimulatory effects of tolbutamide infusion on plasma glucagon in insulin-dependent diabetic subjects. *Journal of Clinical Endocrinology and Metabolism,* 54**,** 459-62.

BOLDYS, A. & OKOPIEN, B. 2009. Inhibitors of type 2 sodium glucose co-transporters--a new strategy for diabetes treatment. *Pharmacological Reports,* 61**,** 778-84.

BRANDHORST, H., BRANDHORST, D., BRENDEL, M. D., HERING, B. J. & BRETZEL, R. G. 1998. Assessment of intracellular insulin content during all steps of human islet isolation procedure. *Cell Transplantation,* 7**,** 489-95.

BRATANOVA-TOCHKOVA, T. K., CHENG, H., DANIEL, S., GUNAWARDANA, S., LIU, Y. J., MULVANEY-MUSA, J.*, et al.* 2002. Triggering and augmentation mechanisms, granule pools, and biphasic insulin secretion. *Diabetes,* 51 Suppl 1**,** S83-90.

BRAUN, M., RAMRACHEYA, R., BENGTSSON, M., ZHANG, Q., KARANAUSKAITE, J., PARTRIDGE, C.*, et al.* 2008. Voltage-gated ion channels in human pancreatic beta-cells: Electrophysiological characterization and role in insulin secretion. *Diabetes,* 57**,** 1618-28.

BUSTIN, S. A. 2000. Absolute quantification of mrna using real-time reverse transcription polymerase chain reaction assays. *Journal of Molecular Endocrinology,* 25**,** 169-93.

CANTRELL, D. A. 2001. Phosphoinositide 3-kinase signalling pathways. *Journal of Cell Science,* 114**,** 1439-45.

CARDOZO, A. K., HEIMBERG, H., HEREMANS, Y., LEEMAN, R., KUTLU, B., KRUHOFFER, M.*, et al.* 2001a. A comprehensive analysis of cytokine-induced and nuclear factor-kappa b-dependent genes in primary rat pancreatic beta-cells. *Journal of Biological Chemistry,* 276**,** 48879-86.

CARDOZO, A. K., KRUHOFFER, M., LEEMAN, R., ORNTOFT, T. & EIZIRIK, D. L. 2001b. Identification of novel cytokine-induced genes in pancreatic beta-cells by high-density oligonucleotide arrays. *Diabetes,* 50**,** 909-20.

CERASI, E. 1992. Pathology of insulin deficiency: Aetiology of type ii diabetes. *In:* ASHCROFT, F. M. & ASHCROFT, S. J. (eds.) *Insulin molecular biology to pathology.* Oxford University press.

CHACHIN, M., YAMADA, M., FUJITA, A., MATSUOKA, T., MATSUSHITA, K. & KURACHI, Y. 2003. Nateglinide, a d-phenylalanine derivative lacking either a sulfonylurea or benzamido moiety, specifically inhibits pancreatic beta-cell-type k(atp) channels. *Journal of Pharmacology and Experimental Therapeutics,* 304**,** 1025-32.

CHAMPE, P. C., HARVEY, R. A. & FERRIER, D. R. 2005. *Metabolic effects of insulin and glucagon,* Philadelphia, Lappincott Williams & Wilkins.

CHATTERJI, A. K. 2005a. Therapeutic compositions: Us patent 6,946,151.

CHATTERJI, A. K. 2005b. Composition for diabetes treatment and prophylaxis: Us patent 6,949,262.

CHEN, D., LEE, S. L. & PETERFREUND, R. A. 2009. New therapeutic agents for diabetes mellitus: Implications for anesthetic management. *Anesthesia and Analgesia,* 108**,** 1803-10.

CHRISTIE, M. R. 1992. Pathology of insulin deficiency: Aetiology of type i diabetes immunological aspects. *In:* ASHCROFT, F. M. & ASHCROFT, S. J. (eds.) *Insulin molecular biology to pathology.* Oxford University press.

CHRISTIE, M. R. & ASHCROFT, S. J. 1984. Cyclic amp-dependent protein phosphorylation and insulin secretion in intact islets of langerhans. *Biochemical Journal,* 218**,** 87-99.

CLARK, A. R. & DOCHERTY, K. 1992. Insulin biosynthesis: The insulin gene. *In:* ASHCROFT, F. M. & ASHCROFT, S. J. (eds.) *Insulin molecular biology to pathology.* Oxford University press.

CLAUDIO, V. & LAGUA, T. 1995. *Nutrition and diet therapy reference dictionary,* New York, Springer.

CNOP, M., WELSH, N., JONAS, J. C., JORNS, A., LENZEN, S. & EIZIRIK, D. L. 2005. Mechanisms of pancreatic beta-cell death in type 1 and type 2 diabetes: Many differences, few similarities. *Diabetes,* 54 Suppl 2**,** S97-107.

COOK, D. L. & HALES, C. N. 1984. Intracellular atp directly blocks k+ channels in pancreatic b-cells. *Nature,* 311**,** 271-3.

COSTES, S., BROCA, C., BERTRAND, G., LAJOIX, A. D., BATAILLE, D., BOCKAERT, J.*, et al.* 2006. Erk1/2 control phosphorylation and protein level of camp-responsive element-binding protein: A key role in glucose-mediated pancreatic beta-cell survival. *Diabetes,* 55**,** 2220-30.

CREAGH, E. M., CONROY, H. & MARTIN, S. J. 2003. Caspase-activation pathways in apoptosis and immunity. *Immunological Reviews,* 193**,** 10-21.

DA SILVA XAVIER, G., VARADI, A., AINSCOW, E. K. & RUTTER, G. A. 2000. Regulation of gene expression by glucose in pancreatic beta -cells (min6) via insulin secretion and activation of phosphatidylinositol 3'-kinase. *Journal of Biological Chemistry,* 275**,** 36269-77.

DACHICOURT, N., SERRADAS, P., GIROIX, M. H., GANGNERAU, M. N. & PORTHA, B. 1996. Decreased glucose-induced camp and insulin release in islets of diabetic rats: Reversal by ibmx, glucagon, gip. *American Journal of Physiology,* 271**,** E725-32.

DAI, Y. S., AMBUDKAR, I. S., HORN, V. J., YEH, C. K., KOUSVELARI, E. E., WALL, S. J.*, et al.* 1991. Evidence that m3 muscarinic receptors in rat parotid gland couple to two second messenger systems. *American Journal of Physiology,* 261**,** C1063-73.

DECKELBAUM, R. J. & WILLIAMS, C. L. 2001. Childhood obesity: The health issue. *Obesity Research,* 9 Suppl 4**,** 239S-43S.

DEFRONZO, R., FERRANNINI, E., KEEN, H. & ZIMMET, D. 2004. *International textbook of diabetes mellitus,* Chichester, John Wiley & Sons.

DEL PRATO, S., MARCHETTI, P. & BONADONNA, R. C. 2002. Phasic insulin release and metabolic regulation in type 2 diabetes. *Diabetes,* 51 Suppl 1**,** S109-16.

DIWAN, P. V., MARGARET, I. & RAMAKRISHNA, S. 1995. Influence of gymnema sylvestre on inflammation *Inflammopharmacology,* 3**,** 271-7.

DODSON, G. & STEINER, D. 1998. The role of assembly in insulin's biosynthesis. *Current Opinion in Structural Biology,* 8**,** 189-94.

DONATH, M. Y., BONI-SCHNETZLER, M., ELLINGSGAARD, H., HALBAN, P. A. & EHSES, J. A. 2010. Cytokine production by islets in health and diabetes: Cellular origin, regulation and function. *Trends in Endocrinology and Metabolism,* 21**,** 261-7.

DONATH, M. Y. & HALBAN, P. A. 2004. Decreased beta-cell mass in diabetes: Significance, mechanisms and therapeutic implications. *Diabetologia,* 47**,** 581-9.

DONATH, M. Y., STORLING, J., MAEDLER, K. & MANDRUP-POULSEN, T. 2003. Inflammatory mediators and islet beta-cell failure: A link between type 1 and type 2 diabetes. *Journal of Molecular Medicine (Berl),* 81**,** 455-70.

DORMAN, J. S. & BUNKER, C. H. 2000. Hla-dq locus of the human leukocyte antigen complex and type 1 diabetes mellitus: A huge review. *Epidemiologic Reviews,* 22**,** 218-27.

EASOM, R. A. 1999. Cam kinase ii: A protein kinase with extraordinary talents germane to insulin exocytosis. *Diabetes,* 48**,** 675-84.

EIZIRIK, D. L. & MANDRUP-POULSEN, T. 2001. A choice of death--the signal-transduction of immune-mediated beta-cell apoptosis. *Diabetologia,* 44**,** 2115-33.

ELIASSON, L. 2003. Sur1 regulates pka-independent camp-induced granule priming in mouse pancreatic b-cells. *The Journal of General Physiology,* 121**,** 181-97.

ELIASSON, L., ABDULKADER, F., BRAUN, M., GALVANOVSKIS, J., HOPPA, M. B. & RORSMAN, P. 2008. Novel aspects of the molecular mechanisms controlling insulin secretion. *Journal of Physiology,* 586**,** 3313-24.

EVANS-MOLINA, C., GARMEY, J. C., KETCHUM, R., BRAYMAN, K. L., DENG, S. & MIRMIRA, R. G. 2007. Glucose regulation of insulin gene transcription and pre-mrna processing in human islets. *Diabetes,* 56**,** 827-35.

EVANS, J. L. 2002. Oxidative stress and stress-activated signaling pathways: A unifying hypothesis of type 2 diabetes. *Endocrine Reviews,* 23**,** 599-622.

FALQUI, L. 2005. B-cell function replacement by islet transplantation. *In:* CHIARELLI, F., DAHL-JORGENSEN, K. & W., K. (eds.) *Diabetes in childhood and adolescence.* Switzerland: Karger.

FERDAOUSSI, M., ABDELLI, S., YANG, J. Y., CORNU, M., NIEDERHAUSER, G., FAVRE, D.*, et al.* 2008. Exendin-4 protects beta-cells from interleukin-1 beta-induced apoptosis by interfering with the c-jun nh2-terminal kinase pathway. *Diabetes,* 57**,** 1205-15.

FRAYLING, T. M. 2007. Genome-wide association studies provide new insights into type 2 diabetes aetiology. *Nature Reviews Genetics,* 8**,** 657-62.

FURMAN, B., ONG, W. K. & PYNE, N. J. 2010. Cyclic amp signaling in pancreatic islets. *Advances in Experimental Medicine and Biology,* 654**,** 281-304.

FUSHIKI, T., KOJIMA, A., IMOTO, T., INOUE, K. & SUGIMOTO, E. 1992. An extract of gymnema sylvestre leaves and purified gymnemic acid inhibits glucose-stimulated gastric inhibitory peptide secretion in rats. *Journal of Nutrition,* 122**,** 2367-73.

GARROW, D. & EGEDE, L. E. 2006. Association between complementary and alternative medicine use, preventive care practices, and use of conventional medical services among adults with diabetes. *Diabetes Care,* 29**,** 15-9.

GEORGE, A., THANKAMMA, A., DEVI, V. K. R. & FERNANDEZ, A. 2007. Phytochemical investigation of insulin plant (costus pictus). *Asian Journal of Chemistry,* 19**,** 3427-30.

GEWIES, A. 2003. Intoroduction to apoptosis. *ApoReview***,** 1-26.

GEY, G. O. & GEY, M. J. 1936. Maintenance of human normal cells in continuous culture, preliminary report: Cultivation of mesoblastic tumors and normal cells and notes on methods of cultivation. *American Journal of Cancer,* 27**,** 45-76.

GIDDINGS, S. J., CHIRGWIN, J. M. & PERMUTT, M. A. 1985. Glucose regulated insulin biosynthesis in isolated rat pancreatic islets is accompanied by changes in proinsulin mrna. *Diabetes Research,* 2**,** 71-5.

GILLESPIE, K. M. 2006. Type 1 diabetes: Pathogenesis and prevention. *Canadian Medical Association Journal,* 175**,** 165-70.

GILON, P., RAVIER, M. A., JONAS, J. C. & HENQUIN, J. C. 2002. Control mechanisms of the oscillations of insulin secretion in vitro and in vivo. *Diabetes,* 51 Suppl 1**,** S144-51.

GIREESH, G., THOMAS, S. K., JOSEPH, B. & PAULOSE, C. S. 2009. Antihyperglycemic and insulin secretory activity of costus pictus leaf extract in streptozotocin induced diabetic rats and in in vitro pancreatic islet culture. *Journal of Ethnopharmacology,* 123**,** 470-4.

GOODMAN, H. 2003. *The pancreatic islets,* USA, Elsevier.

GRANNER, D. K. 2000. Hormones of pancreas and gastrointestinal tract. *In:* MURRAY, R. K., GRANNER, D. K., MAYES, P. A. & RODWELL, V. W. (eds.) *Harper's biochemistry.* 25 ed.: Appleton & Lang.

GROMADA, J., FRANKLIN, I. & WOLLHEIM, C. B. 2007. Alpha-cells of the endocrine pancreas: 35 years of research but the enigma remains. *Endocrine Reviews,* 28**,** 84-116.

GROVER, J. K., YADAV, S. & VATS, V. 2002. Medicinal plants of india with anti-diabetic potential. *Journal of Ethnopharmacology,* 81**,** 81-100.

GUPTA, S. S. 1961. Inhibitory effect of gymnema sylvestre (gurmar) on adrenaline-induced hyperglycemia in rats. *Indian Journal of Medical Sciences,* 15**,** 883-7.

GUPTA, S. S. 1963. Effect of gymnema sylvestre and pterocarpus marsupium on glucose tolerance in albino rats. *Indian Journal of Medical Sciences,* 17**,** 501-5.

GUPTA, S. S. & VARIYAR, M. C. 1961. Inhibitory effect of gymnema sylvestre (gurmar) on adreno-hypophysial activity in rats. *Indian Journal of Medical Sciences,* 15**,** 656-9.

GUPTA, S. S. & VARIYAR, M. C. 1964. Experimental studies on pituitary diabetes. Iv. Effect of gymnema sylvestre and coccinia indica against the hyperglycaemic response of somatotropin and corticotropin hormones. *Indian Journal of Medical Research,* 52**,** 200-7.

GYSEMANS, C., CALLEWAERT, H., OVERBERGH, L. & MATHIEU, C. 2008. Cytokine signalling in the beta-cell: A dual role for ifngamma. *Biochemical Society Transactions,* 36**,** 328-33.

HANSEN, A. M., CHRISTENSEN, I. T., HANSEN, J. B., CARR, R. D., ASHCROFT, F. M. & WAHL, P. 2002. Differential interactions of nateglinide and repaglinide on the human beta-cell sulphonylurea receptor 1. *Diabetes,* 51**,** 2789-95.

HARRIS, J. I., NAUGHTON, M. A. & SANGER, F. 1956. Species differences in insulin. *Archives of Biochemistry and Biophysics,* 65**,** 427-38.

HARRIS, T. E., PERSAUD, S. J. & JONES, P. M. 1997. Go 6976: An inhibitor of ca^{2+}/dag-dependent protein kinase c isoforms in islets of langerhans. *Biochemical Society Transactions,* 25**,** 118S.

HAUGE-EVANS, A. C., SQUIRES, P. E., PERSAUD, S. J. & JONES, P. M. 1999. Pancreatic beta-cell-to-beta-cell interactions are required for integrated responses to nutrient stimuli: Enhanced ca2+ and insulin secretory responses of min6 pseudoislets. *Diabetes,* 48**,** 1402-8.

HEINE, R. J. 1996. Role of sulfonylureas in non-insulin-dependent diabetes mellitus: Part ii--"the cons". *Hormone and Metabolic Research,* 28**,** 522-6.

HENQUIN, J. C., ISHIYAMA, N., NENQUIN, M., RAVIER, M. A. & JONAS, J. C. 2002. Signals and pools underlying biphasic insulin secretion. *Diabetes,* 51 Suppl 1**,** S60-7.

HILLS, C. E. & BRUNSKILL, N. J. 2008. Intracellular signalling by c-peptide. *Experimental Diabetes Resarch,* 2008**,** 635158.

HILLS, C. E. & BRUNSKILL, N. J. 2009. Cellular and physiological effects of c-peptide. *Clinical Science (Lond),* 116**,** 565-74.

HINKE, S. A. 2009. Epac2: A molecular target for sulfonylurea-induced insulin release. *Sci Signal,* 2**,** pe54.

HORIKOSHI, M., HARA, K., ITO, C., SHOJIMA, N., NAGAI, R., UEKI, K.*, et al.* 2007. Variations in the hhex gene are associated with increased risk of type 2 diabetes in the japanese population. *Diabetologia,* 50**,** 2461-6.

HOWELL, S. L. 1984. The mechanism of insulin secretion. *Diabetologia,* 26**,** 319-27.

HOWELL, S. L., JONES, P. M. & PERSAUD, S. J. 1994. Regulation of insulin secretion: The role of second messengers. *Diabetologia,* 37 Suppl 2**,** S30-5.

HU, S., WANG, S., FANELLI, B., BELL, P. A., DUNNING, B. E., GEISSE, S.*, et al.* 2000. Pancreatic beta-cell k(atp) channel activity and membrane-binding studies with nateglinide: A comparison with sulfonylureas and repaglinide. *Journal of Pharmacology and Experimental Therapeutics,* 293**,** 444-52.

HUANG, G. C., ZHAO, M., JONES, P., PERSAUD, S., RAMRACHEYA, R., LOBNER, K.*, et al.* 2004. The development of new density gradient media for purifying human islets and islet-quality assessments. *Transplantation,* 77**,** 143-5.

HUI, H., DOTTA, F., DI MARIO, U. & PERFETTI, R. 2004. Role of caspases in the regulation of apoptotic pancreatic islet beta-cells death. *Journal of Cellular Physiology,* 200**,** 177-200.

ILLUMINA. 2010. *Gene expression microarray data quality control* [Online]. USA: illumina. Available: http://www.illumina.com/Documents/products/technotes/technote_gene_expression_data_quality_control.pdf 2011].

IMOTO, T., MIYASAKA, A., ISHIMA, R. & AKASAKA, K. 1991. A novel peptide isolated from the leaves of gymnema sylvestre--i. Characterization and its suppressive effect on the neural responses to sweet taste stimuli in the rat. *Comparative Biochemistry and Physiology A Comparative Physiology,* 100**,** 309-14.

IN'T VELD, P. & MARICHAL, M. 2010. Microscopic anatomy of the human islet of langerhans. *Advances in Experimental Medicine and Biology,* 654**,** 1-19.

INGALLS, A. M., DICKIE, M. M. & SNELL, G. D. 1950. Obese, a new mutation in the house mouse. *Journal of Heredity,* 41**,** 317-8.

INTERNAIONAL DIABETES FEDERATION 2009. *Diabetes atlas,* Brussels, IDF.

ISHIHARA, H., ASANO, T., TSUKUDA, K., KATAGIRI, H., INUKAI, K., ANAI, M.*, et al.* 1993. Pancreatic beta cell line min6 exhibits characteristics of glucose metabolism and glucose-stimulated insulin secretion similar to those of normal islets. *Diabetologia,* 36**,** 1139-45.

ISLAM, M. S. 2010. Calcium signaling in the islets. *Advances in Experimental Medicine and Biology,* 654**,** 235-59.

JAYASRI, M., GUNASEKARAN, S., RADHA, A. & MATHEW, T. 2008. Anti-diabetic effect of *costus pictus* leaves in normal and streptozotocin-induced diabetic rats. *International Journal of Diabetes and Metabolism,* 16**,** 117-22.

JAYASRI, M., RADHA, A. & MATHEW, T. L. 2009a. ∝-amylase and ∝-glucosidase inhibitory activity of costus pictus d. Don in the management of diabetes. *Journal of Herbal Medicine and Toxicology,* 3**,** 91-4.

JAYASRI, M. A., LAZAR, M. & RADHA, A. 2009b. A report on the antioxidant activity of leaves and rhizomes of *costus pictus* d. Don. *International Journal of Integrative Biology,* 5**,** 20-6.

JELSEMA, C. L. & AXELROD, J. 1987. Stimulation of phospholipase a2 activity in bovine rod outer segments by the beta gamma subunits of transducin and its inhibition by the alpha subunit. *Proceedings of the National Academy of Sciences of the United States of America,* 84**,** 3623-7.

JOHNSON, J. D. & LUCIANI, D. S. 2010. Mechanisms of pancreatic beta-cell apoptosis in diabetes and its therapies. *Advances in Experimental Medicine and Biology,* 654**,** 447-62.

JOHNSON, J. E. 1995. Methods for studying cell death and viability in primary neuronal cultures. *Methods in Cell Biology,* 46**,** 243-76.

JONES, P. M., BURNS, C. J., BELIN, V. D., RODERIGO-MILNE, H. M. & PERSAUD, S. J. 2004. The role of cytosolic phospholipase a(2) in insulin secretion. *Diabetes,* 53 Suppl 1**,** S172-8.

JONES, P. M., COURTNEY, M. L., BURNS, C. J. & PERSAUD, S. J. 2008. Cell-based treatments for diabetes. *Drug Discov Today,* 13**,** 888-93.

JONES, P. M. & PERSAUD, S. 1998. Protein kinases, protein phosphorylation, and the regulation of insulin secretion from pancreatic beta-cells. *Endocrine Reviews,* 19**,** 429-61.

JONES, P. M. & PERSAUD, S. J. 1993. Arachidonic acid as a second messenger in glucose-induced insulin secretion from pancreatic beta-cells. *Journal of Endocrinology,* 137**,** 7-14.

JONES, P. M., PERSAUD, S. J. & HARRIS, T. E. 1999. Signal transduction: Protein phosphorylation and the regulation of insulin secretion. *advances in molecular and cell biology,* 29**,** 303-34.

JOTHIVEL, N., PONNUSAMY, S. P., APPACHI, M., SINGARAVEL, S., RASILINGAM, D., DEIVASIGAMANI, K.*, et al.* 2007. Anti-diabetic activity of methanol leaf extract of *costus pictus* d. Don in alloxan-induced diabetic rats. *Journal of Health Science,* 53**,** 655-63.

KANETKAR, P., SINGHAL, R. & KAMAT, M. 2007. Gymnema sylvestre: A memoir. *J Clin Biochem Nutr,* 41**,** 77-81.

KANG, G., CHEPURNY, O. G., MALESTER, B., RINDLER, M. J., REHMANN, H., BOS, J. L.*, et al.* 2006. Camp sensor epac as a determinant of atp-sensitive potassium channel activity in human pancreatic beta cells and rat ins-1 cells. *Journal of Physiology,* 573**,** 595-609.

KANG, G., LEECH, C. A., CHEPURNY, O. G., COETZEE, W. A. & HOLZ, G. G. 2008. Role of the camp sensor epac as a determinant of katp channel atp sensitivity in human pancreatic beta-cells and rat ins-1 cells. *Journal of Physiology,* 586**,** 1307-19.

KAO, J. P. 1994. Practical aspects of measuring [ca^{2+}] with fluorescent indicators. *Methods in Cell Biology,* 40**,** 155-81.

KASAI, H., HATAKEYAMA, H., OHNO, M. & TAKAHASHI, N. 2010. Exocytosis in islet beta-cells. *Advances in Experimental Medicine and Biology,* 654**,** 305-38.

KHARE, A. K., TONDON, R. N. & TEWARI, J. P. 1983. Hypoglycaemic activity of an indigenous drug (gymnema sylvestre, 'gurmar') in normal and diabetic persons. *Indian Journal of Physiology and Pharmacology,* 27**,** 257-8.

KIM, D. & CHUNG, J. 2002. Akt: Versatile mediator of cell survival and beyond. *J Biochem Mol Biol,* 35**,** 106-15.

KIM, K. A. & LEE, M. S. 2009. Recent progress in research on beta-cell apoptosis by cytokines. *Frontiers in Bioscience,* 14**,** 657-64.

KNIP, M. 2005. Etiological aspects of type 1 diabetes. *In:* CHIARELLI, F., DAHL-JORGENSEN, K. & W., K. (eds.) *Diabetes in childhood and adolescence.* Switzerland: Karger.

KNUTSON, K. L. & HOENIG, M. 1994. Identification and subcellular characterization of protein kinase-c isoforms in insulinoma beta-cells and whole islets. *Endocrinology,* 135**,** 881-6.

LAKEY, J. R., WARNOCK, G. L., BRIERTON, M., AO, Z., HERING, B. J., LONDON, N.*, et al.* 1997. Development of an automated computer-controlled islet isolation system. *Transplantation Proceedings,* 29**,** 1956.

LARSEN, C. M., WADT, K. A., JUHL, L. F., ANDERSEN, H. U., KARLSEN, A. E., SU, M. S.*, et al.* 1998. Interleukin-1beta-induced rat pancreatic islet nitric oxide synthesis requires both the p38 and extracellular signal-regulated kinase 1/2 mitogen-activated protein kinases. *Journal of Biological Chemistry,* 273**,** 15294-300.

LEACH, M. J. 2007. Gymnema sylvestre for diabetes mellitus: A systematic review. *Journal of Alternative and Complementary Medicine,* 13**,** 977-83.

LEBOVITZ, H. E. 2004. Oral antidiabetic agents: 2004. *Medical Clinics of North America,* 88**,** 847-63, ix-x.

LEBOVITZ, H. E. & BANERJI, M. A. 2001. Insulin resistance and its treatment by thiazolidinediones. *Recent Progress in Hormone Research,* 56**,** 265-94.

LEECH, C. A., CASTONGUAY, M. A. & HABENER, J. F. 1999. Expression of adenylyl cyclase subtypes in pancreatic beta-cells. *Biochemical and Biophysical Research Communications,* 254**,** 703-6.

LEECH, C. A., HOLZ, G. G., CHEPURNY, O. & HABENER, J. F. 2000. Expression of camp-regulated guanine nucleotide exchange factors in pancreatic beta-cells. *Biochemical and Biophysical Research Communications,* 278**,** 44-7.

LEIBIGER, B., WAHLANDER, K., BERGGREN, P. O. & LEIBIGER, I. B. 2000. Glucose-stimulated insulin biosynthesis depends on insulin-stimulated insulin gene transcription. *Journal of Biological Chemistry,* 275**,** 30153-6.

LEIBOWITZ, G. 2002. Glucose-regulated proinsulin gene expression is required for adequate insulin production during chronic glucose exposure. *Endocrinology,* 143**,** 3214-20.

LEROITH, D. & ACCILI, D. 2008. Mechanisms of disease: Using genetically altered mice to study concepts of type 2 diabetes. *Nature Clinical Practice Endocrinology and Metabolism,* 4**,** 164-72.

LI, G., HIDAKA, H. & WOLLHEIM, C. B. 1992. Inhibition of voltage-gated ca^{2+} channels and insulin secretion in hit cells by the ca^{2+}/calmodulin-dependent protein kinase ii inhibitor kn-62: Comparison with antagonists of calmodulin and l-type Ca^{2+} channels. *Molecular Pharmacology,* 42**,** 489-8.

LINDGREN, C. M. & MCCARTHY, M. I. 2008. Mechanisms of disease: Genetic insights into the etiology of type 2 diabetes and obesity. *Nature Clinical Practice Endocrinology and Metabolism,* 4**,** 156-63.

LINDSTROM, P. 2007. The physiology of obese-hyperglycemic mice [ob/ob mice]. *ScientificWorldJournal,* 7**,** 666-85.

LINDSTROM, P. 2010. Beta-cell function in obese-hyperglycemic mice [ob/ob mice]. *Advances in Experimental Medicine and Biology,* 654**,** 463-77.

LIU, X., YE, W., YU, B., ZHAO, S., WU, H. & CHE, C. 2004. Two new flavonol glycosides from gymnema sylvestre and euphorbia ebracteolata. *Carbohydrate Research,* 339**,** 891-5.

LONGUET, C., BROCA, C., COSTES, S., HANI, E. H., BATAILLE, D. & DALLE, S. 2005. Extracellularly regulated kinases 1/2 (p44/42 mitogen-activated protein kinases) phosphorylate synapsin i and regulate insulin secretion in the min6 beta-cell line and islets of langerhans. *Endocrinology,* 146**,** 643-54.

LUPI, R. & DEL PRATO, S. 2008. Beta-cell apoptosis in type 2 diabetes: Quantitative and functional consequences. *Diabetes and Metabolism,* 34 Suppl 2**,** S56-64.

MACDONALD, P. E., DE MARINIS, Y. Z., RAMRACHEYA, R., SALEHI, A., MA, X., JOHNSON, P. R.*, et al.* 2007. A k atp channel-dependent pathway within alpha cells regulates glucagon release from both rodent and human islets of langerhans. *PLoS Biol,* 5**,** e143.

MACDONALD, P. E., JOSEPH, J. W. & RORSMAN, P. 2005. Glucose-sensing mechanisms in pancreatic beta-cells. *Philosophical Transactions of the Royal Society of London. Series B: Biological Sciences,* 360**,** 2211-25.

MADISON, J. M. & YAMAGUCHI, H. 1996. Muscarinic inhibition of adenylyl cyclase regulates intracellular calcium in single airway smooth muscle cells. *American Journal of Physiology,* 270**,** L208-14.

MAEDLER, K. 2002. Glucose-induced beta cell production of il-1beta contributes to glucotoxicity in human pancreatic islets. *Journal of Clinical Investigation,* 110**,** 851-60.

MAIESE, K., MORHAN, S. D. & CHONG, Z. Z. 2007. Oxidative stress biology and cell injury during type 1 and type 2 diabetes mellitus. *Curr Neurovasc Res,* 4**,** 63-71.

MANDRUP-POULSEN, T. 2001. Beta-cell apoptosis: Stimuli and signaling. *Diabetes,* 50 Suppl 1**,** S58-63.

MANNI, P. E. & SINSHEIMER, J. E. 1965. Constituents from gymnema sylvestre leaves. *Journal of Pharmaceutical Sciences,* 54**,** 1541-4.

MATSCHINSKY, F., LIANG, Y., KESAVAN, P., WANG, L., FROGUEL, P., VELHO, G.*, et al.* 1993. Glucokinase as pancreatic beta cell glucose sensor and diabetes gene. *Journal of Clinical Investigation,* 92**,** 2092-8.

MEISELMAN, H. L. & HALPERIN, B. P. 1970. Human judgments of gymnema sylvestre and sucrose mixtures. *Physiology and Behavior,* 5**,** 945-8.

MEISELMAN, H. L. & HALPERN, B. P. 1970. Effects of gymnema sylvestre on complex tastes elicited by amino acids and sucrose. *Physiology and Behavior,* 5**,** 1379-84.

MELÉNDEZ-CAMARGO, M. E., CASTILLO-NÁJERA, R., SILVA-TORRES, R. & CAMPOS-ALDRETE, M. E. Evaluation of the diuretic effect of the aqueous extract of costus pictus d. Don in rat. *Proceedings of the Western Pharmacology Society,* 49**,** 72-4.

MELLOUL, D. 2008. Role of nf-kappab in beta-cell death. *Biochemical Society Transactions,* 36**,** 334-9.

MELLOUL, D., MARSHAK, S. & CERASI, E. 2002. Regulation of insulin gene transcription. *Diabetologia,* 45**,** 309-26.

MHASKAR, K. S. & CAIUS, J. F. 1930. A study of indian medicinal plants. Ii. Gymnema sylvestre. *Indian medical research memoirs,* 16**,** 1-35.

MIDDLETON, J. E. & GRIFFITHS, W. J. 1957. Rapid colorimetric micro-method for estimating glucose in blood and c. S. F. Using glucose oxidase. *British Medical Journal,* 2**,** 1525-7.

MIKI, T., NAGASHIMA, K. & SEINO, S. 1999. The structure and function of the atp-sensitive k+ channel in insulin-secreting pancreatic beta-cells. *Journal of Molecular Endocrinology,* 22**,** 113-23.

MURAKAMI, N., MURAKAMI, T., KADOYA, M., MATSUDA, H., YAMAHARA, J. & YOSHIKAWA, M. 1996. New hypoglycemic constituents in "gymnemic acid" from gymnema sylvestre. *Chemical and Pharmaceutical Bulletin,* 44**,** 469-71.

MURAYAMA, T., KAJIYAMA, Y. & NOMURA, Y. 1990. Histamine-stimulated and gtp-binding proteins-mediated phospholipase a2 activation in rabbit platelets. *Journal of Biological Chemistry,* 265**,** 4290-5.

MURCHISON, D. & GRIFFITH, W. H. 2007. Calcium buffering systems and calcium signaling in aged rat basal forebrain neurons. *Aging Cell,* 6**,** 297-305.

NAKAGAWA, Y., NAGASAWA, M., YAMADA, S., HARA, A., MOGAMI, H., NIKOLAEV, V. O*., et al.* 2009. Sweet taste receptor expressed in pancreatic beta-cells activates the calcium and cyclic amp signaling systems and stimulates insulin secretion. *PLoS One,* 4**,** e5106.

NAKAMURA, Y., TSUMURA, Y., TONOGAI, Y. & SHIBATA, T. 1999. Fecal steroid excretion is increased in rats by oral administration of gymnemic acids contained in gymnema sylvestre leaves. *Journal of Nutrition,* 129**,** 1214-22.

NARENDRAN, P., ESTELLA, E. & FOURLANOS, S. 2005. Immunology of type 1 diabetes. *Quarterly Journal of Medicine,* 98**,** 547-56.

NEWSHOLME, E. A., BEVAN, S. J., DIMITRIADIS, G. D. & KELLY, R. P. 1992. Insulin action: Physiological aspects of insulin actions. *In:* ASHCROFT, F. M. & ASHCROFT, S. J. (eds.) *Insulin molecular biology to pathology.* Oxford University press.

NICHOLS, C. G. & KOSTER, J. C. 2002. Diabetes and insulin secretion: Whither katp? *American Journal of Physiology Endocrinology and Metabolism,* 283**,** E403-12.

NICOL, D. S. & SMITH, L. F. 1960. Amino-acid sequence of human insulin. *Nature,* 187**,** 483-5.

NIELSEN, D. A., WELSH, M., CASADABAN, M. J. & STEINER, D. F. 1985. Control of insulin gene expression in pancreatic beta-cells and in an insulin-producing cell line, rin-5f cells. I. Effects of glucose and cyclic amp on the transcription of insulin mrna. *Journal of Biological Chemistry,* 260**,** 13585-9.

NINOMIYA, Y. & IMOTO, T. 1995. Gurmarin inhibition of sweet taste responses in mice. *American Journal of Physiology,* 268**,** R1019-25.

NOLAN, T., HANDS, R. E. & BUSTIN, S. A. 2006. Quantification of mrna using real-time rt-pcr. *Nat Protoc,* 1**,** 1559-82.

OHMORI, R., IWAMOTO, T., TAGO, M., TAKEO, T., UNNO, T., ITAKURA, H*., et al.* 2005. Antioxidant activity of various teas against free radicals and ldl oxidation. *Lipids,* 40**,** 849-53.

OKABAYASHI, Y., TANI, S., FUJISAWA, T., KOIDE, M., HASEGAWA, H., NAKAMURA, T., *et al.* 1990. Effect of gymnema sylvestre, r.Br. On glucose homeostasis in rats. *Diabetes Research and Clinical Practice,* 9**,** 143-8.

PALTI, Y., DAVID, G. B., LACHOV, E., MIDA, Y. H. & SCHATZBERGER, R. 1996. Islets of langerhans generate wavelike electric activity modulated by glucose concentration. *Diabetes,* 45**,** 595-601.

PAPADIMITRIOU, A., KING, A. J., JONES, P. M. & PERSAUD, S. J. 2007. Anti-apoptotic effects of arachidonic acid and prostaglandin e2 in pancreatic beta-cells. *Cellular Physiology and Biochemistry,* 20**,** 607-16.

PATRONA, C. & PESKAR, B. A. 1987. *Radioimmunoassay in basic and clinical pharmacology,* Germany, Springer-Verlag

PAVLOVIC, D., ANDERSEN, N. A., MANDRUP-POULSEN, T. & EIZIRIK, D. L. 2000. Activation of extracellular signal-regulated kinase (erk)1/2 contributes to cytokine-induced apoptosis in purified rat pancreatic beta-cells. *European Cytokine Network,* 11**,** 267-74.

PERSAUD, S. & JONES, P. 2008. Beta-cell-based therapies for type 2 diabetes. *European Endocrinology,* 4**,** 36-9.

PERSAUD, S. J. 1999. Pancreatic β-cell lines: Their roles in β-cell research and diabetes therapy. *advances in molecular and cell biology,* 29**,** 21-46.

PERSAUD, S. J., AL-MAJED, H., RAMAN, A. & JONES, P. M. 1999. Gymnema sylvestre stimulates insulin release in vitro by increased membrane permeability. *Journal of Endocrinology,* 163**,** 207-12.

PERSAUD, S. J., ASARE-ANANE, H. & JONES, P. M. 2002. Insulin receptor activation inhibits insulin secretion from human islets of langerhans. *FEBS Letters,* 510**,** 225-8.

PERSAUD, S. J., JONES, P. M. & HOWELL, S. L. 1993. Staurosporine inhibits protein kinases activated by Ca^{2+} and cyclic amp in addition to inhibiting protein kinase c in rat islets of langerhans. *Molecular and Cellular Endocrinology,* 94**,** 55-60.

PERSAUD, S. J., MULLER, D., BELIN, V. D., KITSOU-MYLONA, I., ASARE-ANANE, H., PAPADIMITRIOU, A., *et al.* 2007. The role of arachidonic acid and its metabolites in insulin secretion from human islets of langerhans. *Diabetes,* 56**,** 197-203.

PHILIPPE, J., PACHECO, I. & MEDA, P. 1994. Insulin gene transcription is decreased rapidly by lowering glucose concentrations in rat islet cells. *Diabetes,* 43**,** 523-8.

PIPELEERS, D., KIEKENS, R. & IN'T VELD, P. 1992. The pancreatic β-cell: Morphology of the pancreatic β-cell. *In:* ASHCROFT, F. M. & ASHCROFT, S. J. (eds.) *Insulin molecular biology to pathology.* Oxford University press.

PLUM, L., BELGARDT, B. F. & BRUNING, J. C. 2006. Central insulin action in energy and glucose homeostasis. *Journal of Clinical Investigation,* 116**,** 1761-6.

POITOUT, V., HAGMAN, D., STEIN, R., ARTNER, I., ROBERTSON, R. P. & HARMON, J. S. 2006. Regulation of the insulin gene by glucose and fatty acids. *Journal of Nutrition,* 136**,** 873-6.

POITOUT, V. & ROBERTSON, R. P. 2008. Glucolipotoxicity: Fuel excess and beta-cell dysfunction. *Endocrine Reviews,* 29**,** 351-66.

PORCHEZHIAN, E. & DOBRIYAL, R. M. 2003. An overview on the advances of gymnema sylvestre: Chemistry, pharmacology and patents. *Pharmazie,* 58**,** 5-12.

PORTE, D., JR., BASKIN, D. G. & SCHWARTZ, M. W. 2005. Insulin signaling in the central nervous system: A critical role in metabolic homeostasis and disease from c. Elegans to humans. *Diabetes,* 54**,** 1264-76.

PORTE, D., JR. & KAHN, S. E. 2001. Beta-cell dysfunction and failure in type 2 diabetes: Potential mechanisms. *Diabetes,* 50 Suppl 1**,** S160-3.

PORTE, D., JR., SMITH, P. H. & ENSINCK, J. W. 1976. Neurohumoral regulation of the pancreatic islet a and b cells. *Metabolism: Clinical and Experimental,* 25**,** 1453-6.

PRATT, J. 1989. On the history of the discovery of insulin. *In:* VON ENGELHARDT, D. (ed.) *Diabetes its medical and cultural history.* Berlin: Springer-Verlag.

PROMEGA. 2009. *Caspase-glo 3/7 assay* [Online]. Promega. Available: http://www.promega.com/resources/protocols/technical-bulletins/101/caspase-glo-37-assay-protocol/ [Accessed 25 october 2010].

QUESADA, I., TUDURI, E., RIPOLL, C. & NADAL, A. 2008. Physiology of the pancreatic alpha-cell and glucagon secretion: Role in glucose homeostasis and diabetes. *Journal of Endocrinology,* 199**,** 5-19.

RABINOVITCH, A., BLONDEL, B., MURRAY, T. & MINTZ, D. H. 1980. Cyclic adenosine-3',5'-monophosphate stimulates islet b cell replication in neonatal rat pancreatic monolayer cultures. *Journal of Clinical Investigation,* 66**,** 1065-71.

RANG, H., DALE, M., RITTER, J. & MOORE, P. 2003. *Pharmacology*, Churchill-Livingston.

RAO, G. S. & SINSHEIMER, J. E. 1971. Constituents from gymnema sylvestre leaves. 8. Isolation, chemistry, and derivatives of gymnemagenin and gymnestrogenin. *Journal of Pharmaceutical Sciences,* 60**,** 190-3.

REGAZZI, R. 1999. Mechanism of insulin exocytosis. *advances in molecular and cell biology,* 29**,** 151-72.

RENA, G., GUO, S., CICHY, S. C., UNTERMAN, T. G. & COHEN, P. 1999. Phosphorylation of the transcription factor forkhead family member fkhr by protein kinase b. *Journal of Biological Chemistry,* 274**,** 17179-83.

RENDELL, M. & KIRCHAIN, W. 2000. Pharmacotherapy of type 2 diabetes mellitus. *Annual Pharmacology,* 34**,** 878-95.

ROBERTSON, R. P., HARMON, J., TRAN, P. O. & POITOUT, V. 2004. Beta-cell glucose toxicity, lipotoxicity, and chronic oxidative stress in type 2 diabetes. *Diabetes,* 53 Suppl 1**,** S119-24.

ROGLIC, G., UNWIN, N., BENNETT, P. H., MATHERS, C., TUOMILEHTO, J., NAG, S*., et al.* 2005. The burden of mortality attributable to diabetes: Realistic estimates for the year 2000. *Diabetes Care,* 28**,** 2130-5.

SAHU, N. P., MAHATO, S. B., SARKAR, S. K. & PODDAR, G. 1996. Triterpenoid saponins from gymnema sylvestre. *Phytochemistry,* 41**,** 1181-5.

SARKAR, S. A., KUTLU, B., VELMURUGAN, K., KIZAKA-KONDOH, S., LEE, C. E., WONG, R*., et al.* 2009. Cytokine-mediated induction of anti-apoptotic genes that are linked to nuclear factor kappa-b (nf-kappab) signalling in human islets and in a mouse beta cell line. *Diabetologia,* 52**,** 1092-101.

SCHADEWALDT, H. 1989. The history of diabetes mellitus. *In:* VON ENGELHARDT, D. (ed.) *Diabetes its medical and cultural history.* Berlin: Springer-Verlag.

SCHULZ, I. 1990. Permeabilizing cells: Some methods and applications for the study of intracellular processes. *Methods in Enzymology,* 192**,** 280-300.

SHAFIEE-NICK, R., PYNE, N. J. & FURMAN, B. L. 1995. Effects of type-selective phosphodiesterase inhibitors on glucose-induced insulin secretion and islet phosphodiesterase activity. *British Journal of Pharmacology,* 115**,** 1486-92.

SHANMUGASUNDARAM, E. R., GOPINATH, K. L., RADHA SHANMUGASUNDARAM, K. & RAJENDRAN, V. M. 1990a. Possible regeneration of the islets of langerhans in streptozotocin-diabetic rats given gymnema sylvestre leaf extracts. *Journal of Ethnopharmacology,* 30**,** 265-79.

SHANMUGASUNDARAM, E. R., RAJESWARI, G., BASKARAN, K., RAJESH KUMAR, B. R., RADHA SHANMUGASUNDARAM, K. & KIZAR AHMATH, B. 1990b. Use of gymnema sylvestre leaf extract in the control of blood glucose in insulin-dependent diabetes mellitus. *Journal of Ethnopharmacology,* 30**,** 281-94.

SHANMUGASUNDARAM, E. R., VENKATASUBRAHMANYAM, M., VIJENDRAN, N. & SHANMUGASUNDARAM, K. R. 1988. Effect of an isolate from gymnema sylvestre r.Br. In the control of diabetes mellitus and associated pathological changes. . *Ancient Science of Life,* 7**,** 183-94.

SHANMUGASUNDARAM, K. R., PANNEERSELVAM, C., SAMUDRAM, P. & SHANMUGASUNDARAM, E. R. 1981. The insulinotropic activity of gymnema sylvestre, r. Br. An indian medical herb used in controlling diabetes mellitus. *Pharmacological Research Communications,* 13**,** 475-86.

SHANMUGASUNDARAM, K. R., PANNEERSELVAM, C., SAMUDRAM, P. & SHANMUGASUNDARAM, E. R. 1983. Enzyme changes and glucose utilisation in diabetic rabbits: The effect of gymnema sylvestre, r.Br. *Journal of Ethnopharmacology,* 7**,** 205-34.

SHIBASAKI, T., SUNAGA, Y. & SEINO, S. 2004. Integration of atp, camp, and Ca^{2+} signals in insulin granule exocytosis. *Diabetes,* 53 Suppl 3**,** S59-62.

SHIGEMATSU, N., ASANO, R., SHIMOSAKA, M. & OKAZAKI, M. 2001. Effect of long term-administration with gymnema sylvestre r. Br on plasma and liver lipid in rats. *Biological and Pharmaceutical Bulletin,* 24**,** 643-9.

SHILPA, K., SANGEETHA, K. N., MUTHUSAMY, V. S., SUJATHA, S. & LAKSHMI, B. S. 2009. Probing key targets in insulin signaling and adipogenesis using a methanolic extract of costus pictus and its bioactive molecule, methyl tetracosanoate. *Biotechnol Lett,* 31**,** 1837-41.

SHIMIZU, K., IINO, A., NAKAJIMA, J., TANAKA, K., NAKAJYO, S., URAKAWA, N.*, et al.* 1997a. Suppression of glucose absorption by some fractions extracted from gymnema sylvestre leaves. *Journal of Veterinary Medical Science,* 59**,** 245-51.

SHIMIZU, K., OZEKI, M., IINO, A., NAKAJYO, S., URAKAWA, N. & ATSUCHI, M. 2001. Structure-activity relationships of triterpenoid derivatives extracted from gymnema inodorum leaves on glucose absorption. *Japanese Journal of Pharmacology,* 86**,** 223-9.

SHIMIZU, K., OZEKI, M., TANAKA, K., ITOH, K., NAKAJYO, S., URAKAWA, N.*, et al.* 1997b. Suppression of glucose absorption by extracts from the leaves of gymnema inodorum. *Journal of Veterinary Medical Science,* 59**,** 753-7.

SIMONDS, W. F. 1999. G protein regulation of adenylate cyclase. *Trends in Pharmacological Sciences,* 20**,** 66-73.

SINSHEIMER, J. E. & MCILHENNY, H. M. 1967. Constituents from gymnema sylvestre leaves. Ii. Nitrogenous compounds. *Journal of Pharmaceutical Sciences,* 56**,** 732-6.

SINSHEIMER, J. E. & RAO, G. S. 1970. Constituents from gymnema sylvestre leaves. Vi. Acylated genins of the gymnemic acids--isolated and preliminary characterization. *Journal of Pharmaceutical Sciences,* 59**,** 629-32.

SINSHEIMER, J. E., RAO, G. S. & MCILHENNY, H. M. 1970. Constuents from gymnema sylvestre leaves. V. Isolation and preliminary characterization of the gymnemic acids. *Journal of Pharmaceutical Sciences,* 59**,** 622-8.

SLADEK, R., ROCHELEAU, G., RUNG, J., DINA, C., SHEN, L., SERRE, D.*, et al.* 2007. A genome-wide association study identifies novel risk loci for type 2 diabetes. *Nature,* 445**,** 881-5.

SMEEKENS, S. P., MONTAG, A. G., THOMAS, G., ALBIGES-RIZO, C., CARROLL, R., BENIG, M.*, et al.* 1992. Proinsulin processing by the subtilisin-related proprotein convertases furin, pc2, and pc3. *Proceedings of the National Academy of Sciences of the United States of America,* 89**,** 8822-6.

SMITS, P., BIJLSTRA, P. J., RUSSEL, F. G., LUTTERMAN, J. A. & THIEN, T. 1996. Cardiovascular effects of sulphonylurea derivatives. *Diabetes Research and Clinical Practice,* 31 Suppl**,** S55-9.

SRIVASTAVA, Y., BHATT, H. V., JHALA, C., NIGAM, S. K., KUMAR, A. & VERMA, Y. 1986. Oral gymnema sylvestre r.Br. Leaf extracts inducing protacted longevity and hypoglycemia in alloxan diabetic rats: Review and experimental study. *International Journal of Crude Drug Research,* 24**,** 171-6.

SRIVASTAVA, Y., NIGAM, S. K., BHATT, H. V., VERMA, Y. & PREM, A. S. 1985. Hypoglycemic and life-prolonging properties of gymnema sylvestre leaf extract in diabetic rats. *Israel Journal of Medical Sciences,* 21**,** 540-2.

STAIGER, H., MACHICAO, F., STEFAN, N., TSCHRITTER, O., THAMER, C., KANTARTZIS, K.*, et al.* 2007. Polymorphisms within novel risk loci for type 2 diabetes determine beta-cell function. *PLoS One,* 2**,** e832.

STEIL, D. 1999. Diabetes mellitus. *In:* DIPIRO, J., TALBERT, R., YEE, G., MARTZKE, G., WELLS, B. & POSEY, M. (eds.) *Pharmacotherapy a pathophysiologic approach.* New York: McGrem-Hill.

STOLAR, M. W., HOOGWERF, B. J., GORSHOW, S. M., BOYLE, P. J. & WALES, D. O. 2008. Managing type 2 diabetes: Going beyond glycemic control. *Journal of Managed Care Pharmacy,* 14**,** s2-19.

SUGIHARA, Y., NOJIMA, H., MATSUDA, H., MURAKAMI, T., YOSHIKAWA, M. & KIMURA, I. 2000. Antihyperglycemic effects of gymnemic acid iv, a compound derived from gymnema sylvestre leaves in streptozotocin-diabetic mice. *J Asian Nat Prod Res,* 2**,** 321-7.

SUN, G. Y., XU, J., JENSEN, M. D. & SIMONYI, A. 2004. Phospholipase a2 in the central nervous system: Implications for neurodegenerative diseases. *Journal of Lipid Research,* 45**,** 205-13.

SUTTISRI, R., LEE, I. S. & KINGHORN, A. D. 1995. Plant-derived triterpenoid sweetness inhibitors. *Journal of Ethnopharmacology,* 47**,** 9-26.

SWANSTON-FLATT, S. K., FLATT, P. R., DAY, C. & BAILEY, C. J. 1991. Traditional dietary adjuncts for the treatment of diabetes mellitus. *Proceedings of the Nutrition Society,* 50**,** 641-51.

SZEGEZDI, E., LOGUE, S. E., GORMAN, A. M. & SAMALI, A. 2006. Mediators of endoplasmic reticulum stress-induced apoptosis. *EMBO Rep,* 7**,** 880-5.

TABUCHI, H. 2000. Regulation of insulin secretion by overexpression of Ca^{2+}/calmodulin-dependent protein kinase ii in insulinoma min6 cells. *Endocrinology,* 141**,** 2350-60.

TERASAWA, H., MIYOSHI, M. & IMOTO, T. 1994. Effect of long-term adminstration of gymnema sylveste watery-extract on variations of body weight, plasma glucose, serum triglyceride, total cholesterol and insulin in wistar fatty rats. *Yonago Acta Medica,* 37**,** 117-27.

THAMS, P., ANWAR, M. R. & CAPITO, K. 2005. Glucose triggers protein kinase a-dependent insulin secretion in mouse pancreatic islets through activation of the k+atp channel-dependent pathway. *European Journal of Endocrinology / European Federation of Endocrine Societies,* 152**,** 671-7.

TIAN, Y. & LAYCHOCK, S. G. 2001. Protein kinase c and calcium regulation of adenylyl cyclase in isolated rat pancreatic islets. *Diabetes,* 50**,** 2505-13.

TOMINAGA, M., KIMURA, M., SUGIYAMA, K., ABE, T., IGARASHI, K., IGARASHI, M.*, et al.* 1995. Effects of seishin-renshi-in and gymnema sylvestre on insulin resistance in streptozotocin-induced diabetic rats. *Diabetes Research and Clinical Practice,* 29**,** 11-7.

TRIPLITT, C. L. 2007. New technologies and therapies in the management of diabetes. *American Journal of Managed Care,* 13 Suppl 2**,** S47-54.

TRITOS, N. A. & KOKKOTOU, E. G. 2006. The physiology and potential clinical applications of ghrelin, a novel peptide hormone. *Mayo Clinic Proceedings,* 81**,** 653-60.

TURNER, R. & NEIL, A. 1992. Pathology of insulin deficiency: Introduction to diabetes. *In:* ASHCROFT, F. M. & ASHCROFT, S. J. (eds.) *Insulin molecular biology to pathology.* Oxford University press.

VAN SCHAFTINGEN, M. & SCHUIT, F. 1999. Signal recognition: Glucose and primary stimuli. *advances in molecular and cell biology,* 29**,** 199-226.

VANDEKOPPEL, S., CHOE, H. M. & SWEET, B. V. 2008. Managed care perspective on three new agents for type 2 diabetes. *Journal of Managed Care Pharmacy,* 14**,** 363-80.

WANG, L. F., LUO, H., MIYOSHI, M., IMOTO, T., HIJI, Y. & SASAKI, T. 1998. Inhibitory effect of gymnemic acid on intestinal absorption of oleic acid in rats. *Canadian Journal of Physiology and Pharmacology,* 76**,** 1017-23.

WANG, Z. & THURMOND, D. C. 2009. Mechanisms of biphasic insulin-granule exocytosis - roles of the cytoskeleton, small gtpases and snare proteins. *Journal of Cell Science,* 122**,** 893-903.

WARREN, R. P., WARREN, R. M. & WENINGER, M. G. 1969. Inhibition of the sweet taste by gymnema sylvestre. *Nature,* 223**,** 94-5.

WASSMUTH, R., KOCKUM, I., KARLSEN, A., HAGOPIAN, W., BARMEIER, H., DUBE, S., *et al.* 1992. Pathology of insulin deficiency: Aetiology of type i diabetes genetic aspects. *In:* ASHCROFT, F. M. & ASHCROFT, S. J. (eds.) *Insulin molecular biology to pathology.* Oxford University press.

WATSON, E. L., JACOBSON, K. L., DIJULIO, D. H. & DOWD, F. J. 1993. Biphasic effects of carbachol on stimulated camp accumulation in mouse parotid acini. *American Journal of Physiology,* 265**,** C1061-8.

WELSH, M., NIELSEN, D. A., MACKRELL, A. J. & STEINER, D. F. 1985. Control of insulin gene expression in pancreatic beta-cells and in an insulin-producing cell line, rin-5f cells. Ii. Regulation of insulin mrna stability. *Journal of Biological Chemistry,* 260**,** 13590-4.

WELSH, N., CNOP, M., KHARROUBI, I., BUGLIANI, M., LUPI, R., MARCHETTI, P., *et al.* 2005. Is there a role for locally produced interleukin-1 in the deleterious effects of high glucose or the type 2 diabetes milieu to human pancreatic islets? *Diabetes,* 54**,** 3238-44.

WEYER, C., BOGARDUS, C., MOTT, D. M. & PRATLEY, R. E. 1999. The natural history of insulin secretory dysfunction and insulin resistance in the pathogenesis of type 2 diabetes mellitus. *Journal of Clinical Investigation,* 104**,** 787-94.

WILLIAMS, G. & PICKUP, J. (eds.) 2004. *Handbook of diabetes*: Blackwell.

WINZELL, M. S. & AHREN, B. 2007. G-protein-coupled receptors and islet function-implications for treatment of type 2 diabetes. *Pharmacology and Therapeutics,* 116**,** 437-48.

WITTERS, L. A. 2001. The blooming of the french lilac. *Journal of Clinical Investigation,* 108**,** 1105-7.

WOLF, G. 2001. Insulin resistance associated with leptin deficiency in mice: A possible model for noninsulin-dependent diabetes mellitus. *Nutrition Reviews,* 59**,** 177-9.

WOLLHEIM, C. B. & SHARP, G. W. 1981. Regulation of insulin release by calcium. *Physiological Reviews,* 61**,** 914-73.

WORLD HEALTH ORGANIZATION. 2006. *Definition and diagnosis of diabetes mellitus and intermediate hyperglycemia* [Online]. WHO Press.

XU, G., STOFFERS, D. A., HABENER, J. F. & BONNER-WEIR, S. 1999. Exendin-4 stimulates both beta-cell replication and neogenesis, resulting in increased beta-cell mass and improved glucose tolerance in diabetic rats. *Diabetes,* 48**,** 2270-6.

YACKZAN, K. S. 1969. Biological effects of gymnema sylvestre fractions. Ii. Electrophysiology--effect of gymnemic acid on taste receptor response. *Alabama Journal of Medical Sciences,* 6**,** 455-63.

YALOW, R. S. & BERSON, S. A. 1960. Immunoassay of endogenous plasma insulin in man. *Journal of Clinical Investigation,* 39**,** 1157-75.

YAMAGATA, K. 2003. Regulation of pancreatic beta-cell function by the hnf transcription network: Lessons from maturity-onset diabetes of the young (mody). *Endocrine Journal,* 50**,** 491-9.

YE, W., LIU, X., ZHANG, Q., CHE, C. T. & ZHAO, S. 2001. Antisweet saponins from gymnema sylvestre. *Journal of Natural Products,* 64**,** 232-5.

YE, W. C., ZHANG, Q. W., LIU, X., CHE, C. T. & ZHAO, S. X. 2000. Oleanane saponins from gymnema sylvestre. *Phytochemistry,* 53**,** 893-9.

YEH, G. Y., EISENBERG, D. M., KAPTCHUK, T. J. & PHILLIPS, R. S. 2003. Systematic review of herbs and dietary supplements for glycemic control in diabetes. *Diabetes Care,* 26**,** 1277-94.

YOSHIKAWA, M., MURAKAMI, T., KADOYA, M., LI, Y., MURAKAMI, N., YAMAHARA, J.*, et al.* 1997a. Medicinal foodstuffs. Ix. The inhibitors of glucose absorption from the leaves of gymnema sylvestre r. Br. (asclepiadaceae): Structures of gymnemosides a and b. *Chemical and Pharmaceutical Bulletin,* 45**,** 1671-6.

YOSHIKAWA, M., MURAKAMI, T. & MATSUDA, H. 1997b. Medicinal foodstuffs. X. Structures of new triterpene glycosides, gymnemosides-c, -d, -e, and -f, from the leaves of gymnema sylvestre r. Br.: Influence of gymnema glycosides on glucose uptake in rat small intestinal fragments. *Chemical and Pharmaceutical Bulletin,* 45**,** 2034-8.

ZAWALICH, W. S. & ZAWALICH, K. C. 1996. Regulation of insulin secretion by phospholipase c. *American Journal of Physiology,* 271**,** E409-16.

ZEGGINI, E., SCOTT, L. J., SAXENA, R., VOIGHT, B. F., MARCHINI, J. L., HU, T.*, et al.* 2008. Meta-analysis of genome-wide association data and large-scale replication identifies additional susceptibility loci for type 2 diabetes. *Nature Genetics,* 40**,** 638-45.

ZEGGINI, E., WEEDON, M. N., LINDGREN, C. M., FRAYLING, T. M., ELLIOTT, K. S., LANGO, H.*, et al.* 2007. Replication of genome-wide association signals in uk samples reveals risk loci for type 2 diabetes. *Science,* 316**,** 1336-41.

ZHANG, H., NAGASAWA, M., YAMADA, S., MOGAMI, H., SUZUKI, Y. & KOJIMA, I. 2004. Bimodal role of conventional protein kinase c in insulin secretion from rat pancreatic beta cells. *Journal of Physiology,* 561**,** 133-47.

ZHU, X. M., XIE, P., DI, Y. T., PENG, S. L., DING, L. S. & WANG, M. K. 2008. Two new triterpenoid saponins from gymnema sylvestre. *J Integr Plant Biol,* 50**,** 589-92.

Appendix 1

In vivo human study

Human study

Patient cohort

Eleven patients (7 female, 4 male) were recruited and consented for an *in vivo* study of the effects of OSA® administration on blood glucose and insulin levels. The mean age of the cohort was 50.1±3 years (female: 50.7±4; male: 49±5, p>0.2) with a range from 36 to 70 years. The mean body weight at the outset of the trial was 58.7±7.6 kg (female: 57.7±3.0; male: 60.5±2.8, p>0.2) with a range from 45 to 70 kg. Patients were recruited, following local ethical approval, from Burdwan Medical College clinic, West Bengal, and were either newly diagnosed with T2DM, or had previously been treated with standard pharmacological regimens. Exclusion criteria were pregnancy, pre-existing heart disease, hypertension or respiratory disorders, and failure of compliance with the protocol. This study was performed by C.R. Maity, S.K. Chatterjee, N. Koley, T. Biswas and A.K. Chatterji.

Treatment and analysis

OSA® was administered orally in a capsule form at a dose of 500mg (2x250mg capsules) two times each day before food intake for 60 days, giving a total daily dose of 1g OSA®. Blood samples were taken at the start of the trial (day 0) and at the completion of the trial (day 60), and body weight was recorded at the start and completion of the trial. Blood glucose was estimated by a colorimetric glucose-oxidase method (Middleton and Griffiths, 1957) and insulin and C-peptide were measured in serum samples by radioimmunoassay (RIA) (Claudio and Lagua, 1995).

Statistical analysis

Data are represented as mean ± SEM unless otherwise stated. Differences between treatment groups were assessed using analysis of variance (ANOVA) and Bonferroni's T test for multiple comparisons or Student's paired T test (two tailed), as appropriate. Differences between treatment groups were considered significant when $p< 0.05$.

Effect of chronic OSA® administration in humans with T2DM

Daily oral administration of OSA® for 60 days produced significant improvements in glycemic control, as shown in Figure 1. Thus, in 10/11 patients OSA® treatment was associated with a reduction in fasting blood glucose levels (Figure 1), with a mean reduction from 162±23 to 119±17 mg/dl ($p<0.005$). Post-prandial blood glucose levels (Figure 2) also showed significant reductions in 10/11 patients, with a reduction from 291±10 to 236±30 mg/dl ($p<0.02$). OSA® treatment had no significant effect on the extent of the post-prandial excursion in plasma glucose (day 0, 132±10 mg/dl; day 60, 117±26 mg/dl, $p>0.2$), nor on body weight over the 60 day period of the trial (day 0, 58.7±7.6 kg; day 60, 53.9±7.3 kg, $p>0.2$). One patient showed no reduction in either fasting or post-prandial blood glucose levels and no change in body weight during the treatment period.

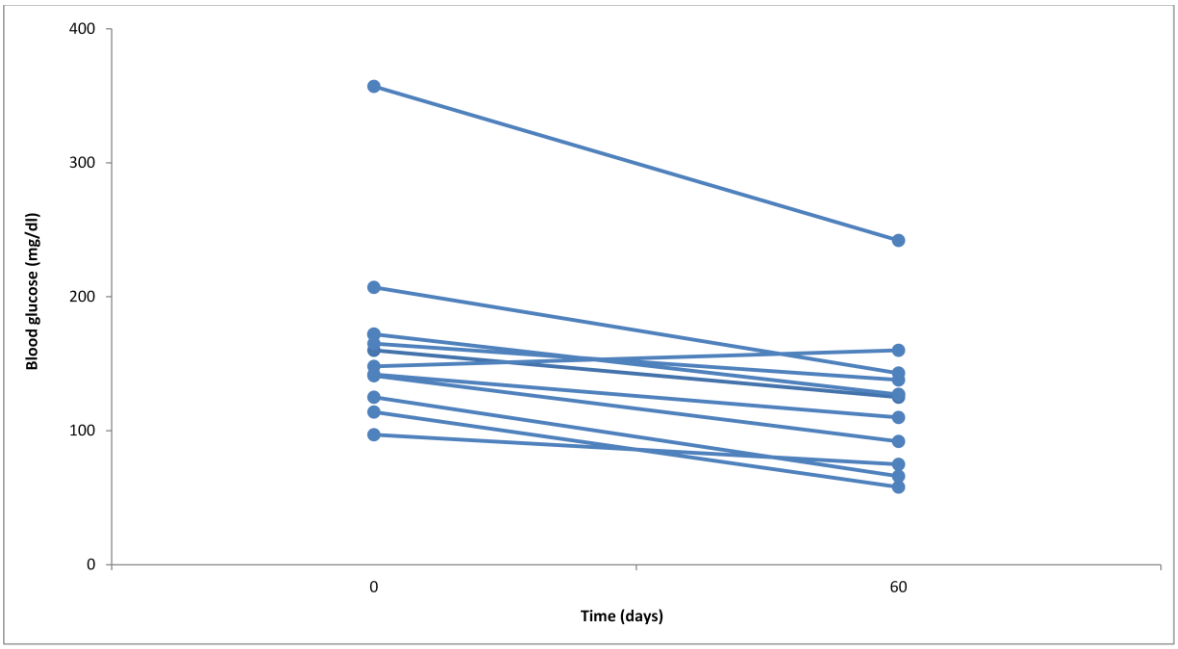

Figure 1: Effect of OSA® on fasting blood glucose levels of patients with Type 2 diabetes mellitus. OSA® (1000mg/day) was administered orally and fasting blood glucose levels were determined at the start (t=0 day) and completion (t=60 days) of the study as described in the Materials and Methods. Data show blood glucose levels of individual patients in mg/dl at two time points (0, 60 days). Fasting glucose levels were significantly reduced (P<0.005) after 60 days of treatment with OSA®, n=11.

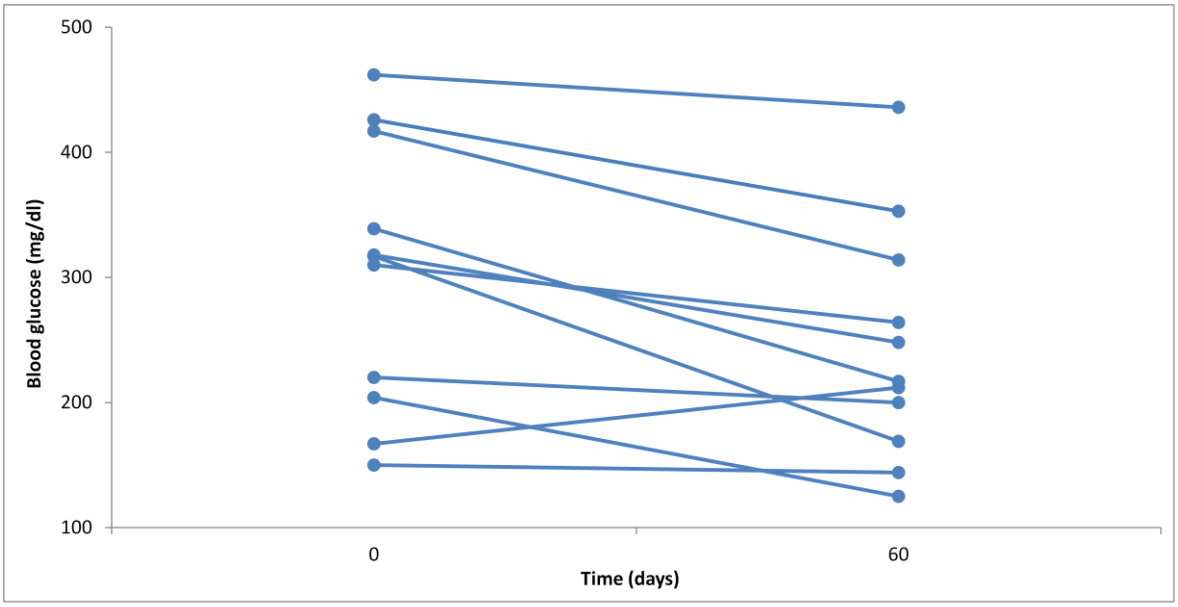

Figure 2: Effect of OSA® on post-prandial blood glucose levels of patients with Type 2 diabetes mellitus. OSA® (1000mg/day) was administered orally and post-prandial blood glucose levels were determined at the start (t=0 day) and completion (t=60 days) of the study as described in the Materials and Methods. Data show blood glucose levels of individual patients in mg/dl at two time points (0, 60 days). Post-prandial glucose levels were significantly reduced (P<0.02) after 60 days of treatment with OSA®, n=11.

The improvements in glycemic control in response to OSA® treatment were associated with increased circulating levels of insulin and/or C-peptide in all patients, as shown in Figure 3 and 4. Thus 60 days treatment with OSA® induced a mean increase in serum insulin (Figure 3) from 24±9 to 32±6 μU/ml ($p<0.001$), with a corresponding increase in serum C-peptide (Figure 4) from 298±42 to 447±48 pmol/l ($p<0.05$).

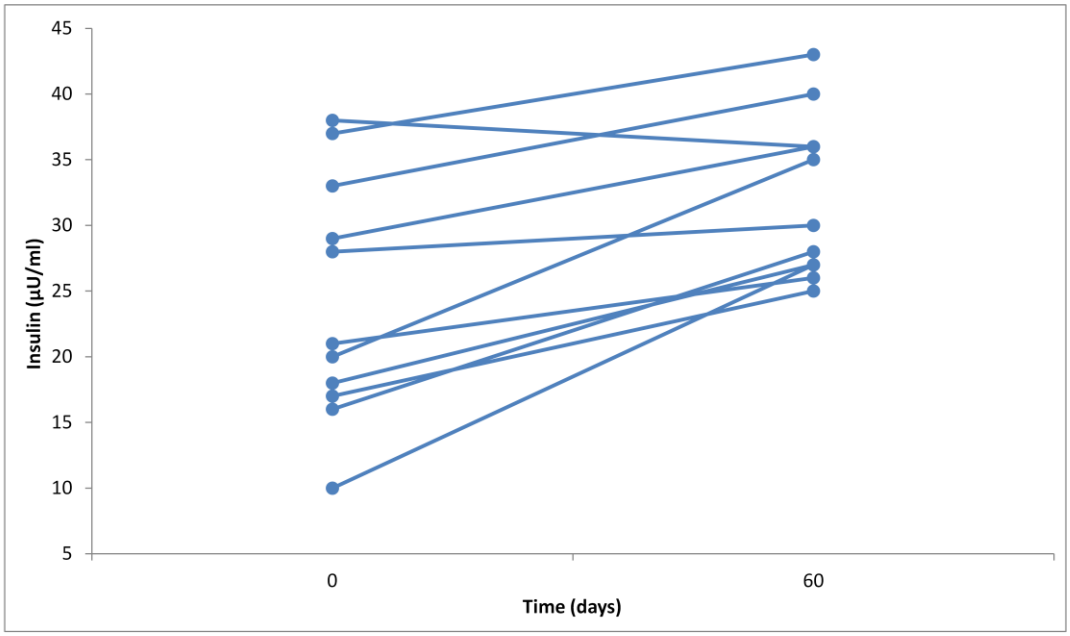

Figure 3: Effect of daily oral administration of OSA® on plasma insulin levels of patients with Type 2 diabetes mellitus. Administration of OSA® (1000mg/day) for 60 days significantly ($p<0.001$) increased circulating levels of insulin. Data show the plasma levels of insulin (µU/ml) for each patient before and after treatment, n=11.

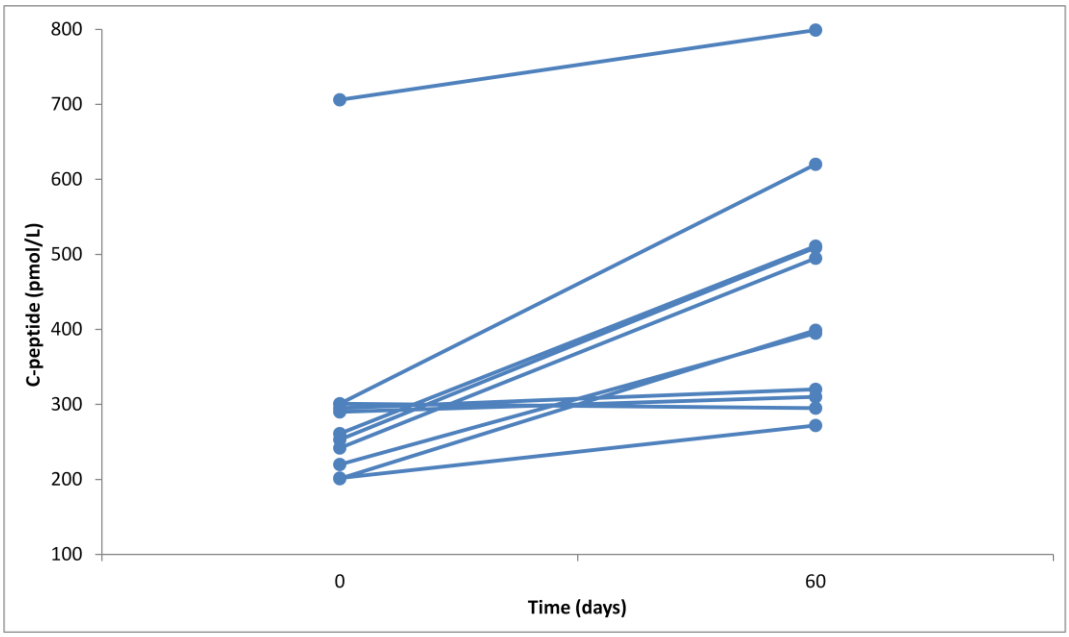

Figure 4: Effect of daily oral administration of OSA® on C-peptide levels of patients with Type 2 diabetes mellitus. Administration of OSA® (1000mg/day) for 60 days significantly ($p<0.05$) increased circulating levels of C-peptide. Data show the plasma levels of C-peptide (pmol/l) for each patient before and after treatment, n=11.

Appendix 2

PCR

Mouse preproinsulin (insulin I & II)

Insulin I (Ins I) Gene ID: 16333 mRNA accession #: NM_008386

Insulin II (Ins II) Gene ID: 16334 mRNA accession #: NM_008387

Product size: 125bp

Forward primer: 5'-CCACCCAGGCTTTTGTCA-3'

Reverse primer: 5'- TTGTGGGTCCTCCACTTCA-3'

Assay conditions: Activation: 95C° for 10mins

Cycling: (melting 95C° for 10 sec; annealing 58C° for 10 sec; extension 72C° for 10 sec; fluorescence measurement x 40)

Melt: 65-95C° in 1C° increments

Gel electrophoresis of PCR product

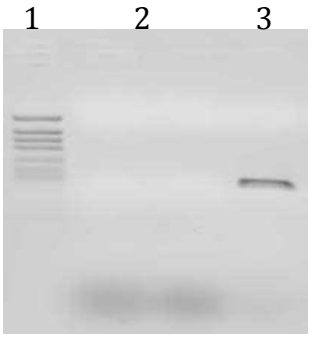

Marker NC -RT Islets

Marker: PBSII + SK/Hpall (40 ng/µl)

Melting temperature: ~88C°

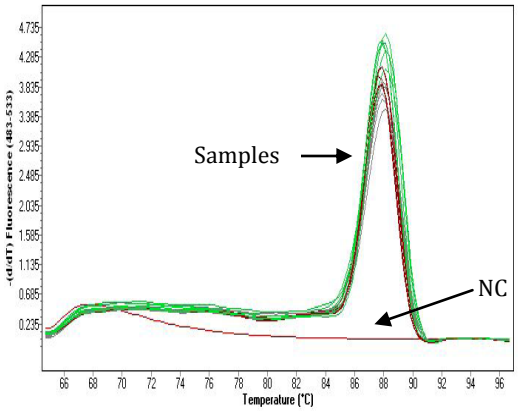

Standard series: from purified PCR product

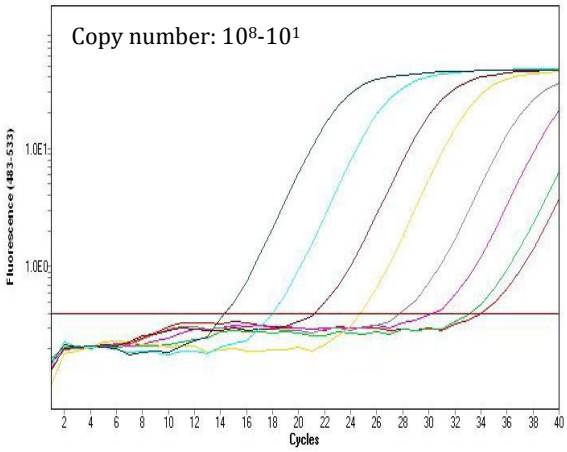

Linear regression of standard series & assay efficiency

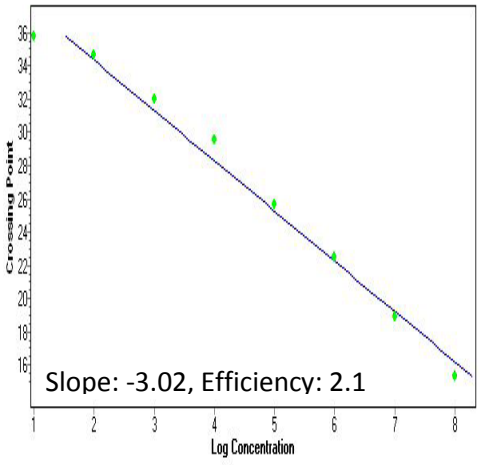

Mouse actin (Actb)

Gene ID: 11461 mRNA accession #: NM_007393 Product size: 285bp

Forward primer: 5'- ATGAAGTGTGACGTTGACATCCGT-3'
Reverse primer: 5'- CCTAGAAGCATTTGCGGTGCACGATG-3'

Assay conditions: Activation: 95C° for 10mins

Cycling: (melting 95C° for 10 sec; annealing 58C° for 10 sec; extension 72C° for 10 sec; fluorescence measurement x 36)

Melt: 65-95C° in 1C° increments

Gel electrophoresis of PCR product

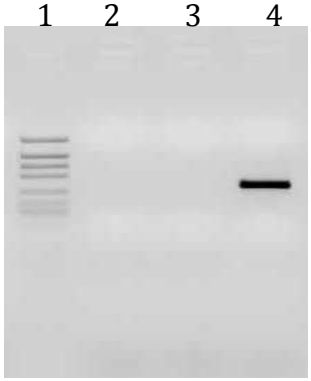

Marker NC -RT Islets

Melting temperature: ~88C°

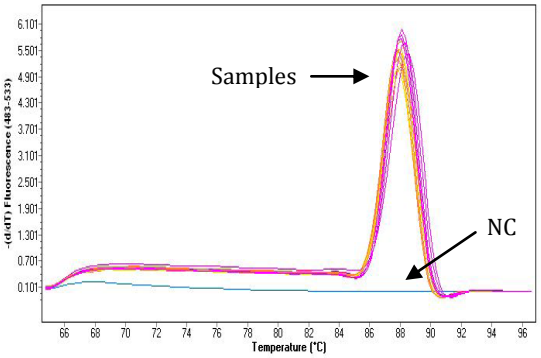

Marker: PBSII + SK/HpaII (40 ng/µl)

Standard series: from purified PCR product

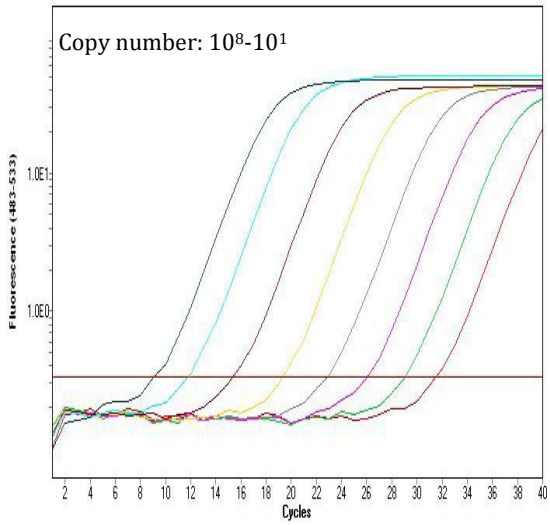

Linear regression of standard Series & assay efficiency

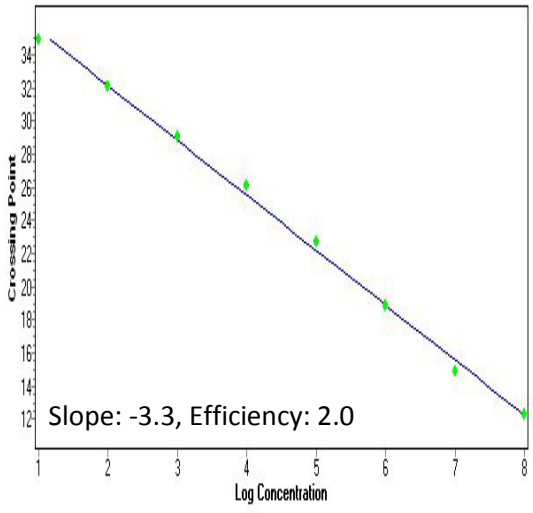

Appendix 3

Microarray experiment

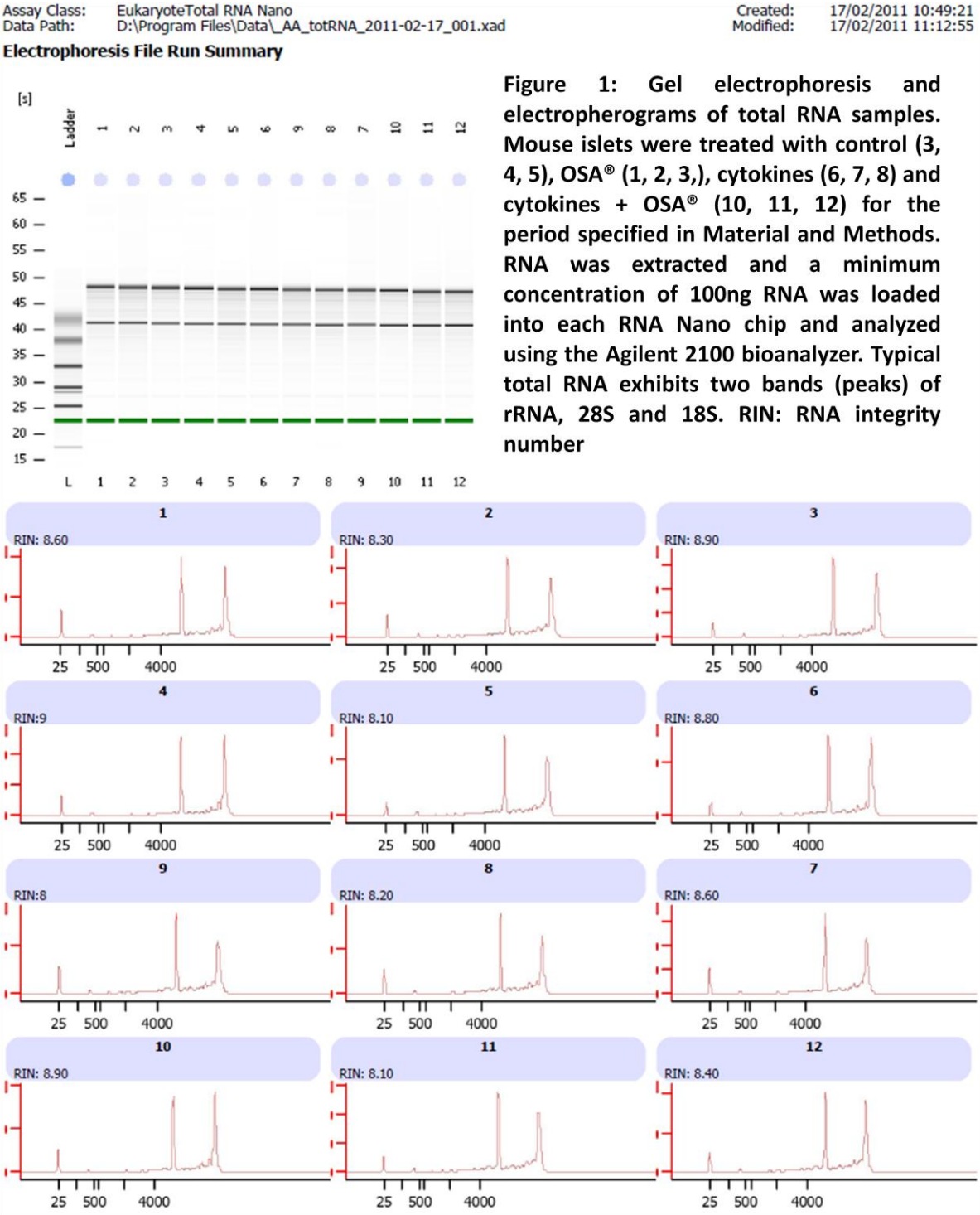

Figure 1: Gel electrophoresis and electropherograms of total RNA samples. Mouse islets were treated with control (3, 4, 5), OSA® (1, 2, 3,), cytokines (6, 7, 8) and cytokines + OSA® (10, 11, 12) for the period specified in Material and Methods. RNA was extracted and a minimum concentration of 100ng RNA was loaded into each RNA Nano chip and analyzed using the Agilent 2100 bioanalyzer. Typical total RNA exhibits two bands (peaks) of rRNA, 28S and 18S. RIN: RNA integrity number

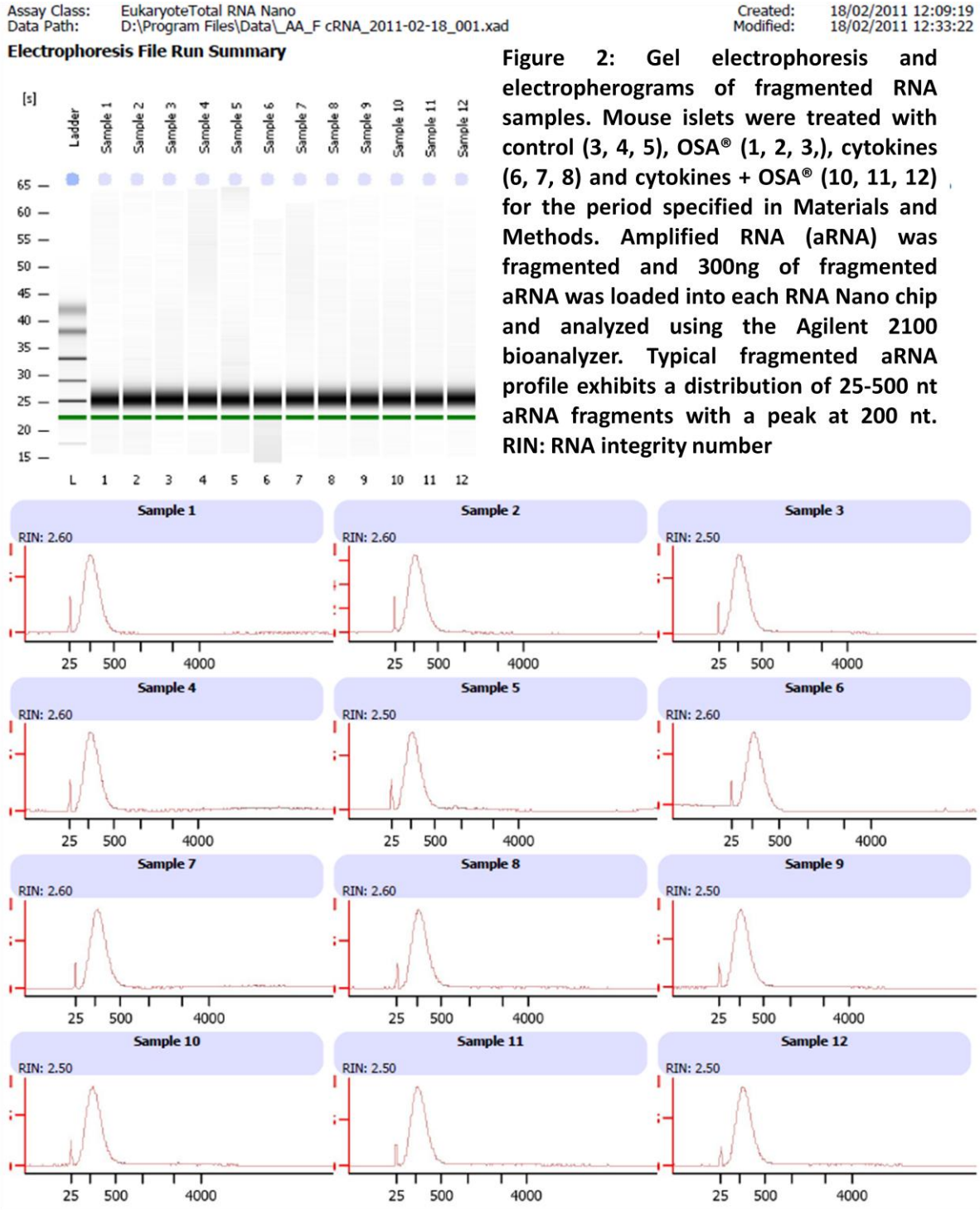

Figure 2: Gel electrophoresis and electropherograms of fragmented RNA samples. Mouse islets were treated with control (3, 4, 5), OSA® (1, 2, 3,), cytokines (6, 7, 8) and cytokines + OSA® (10, 11, 12) for the period specified in Materials and Methods. Amplified RNA (aRNA) was fragmented and 300ng of fragmented aRNA was loaded into each RNA Nano chip and analyzed using the Agilent 2100 bioanalyzer. Typical fragmented aRNA profile exhibits a distribution of 25-500 nt aRNA fragments with a peak at 200 nt. RIN: RNA integrity number

Expression Console™ 1.1.2800.19935

AFFYMETRIX

Figure 3: Signal distribution (in normal and log scale) and Pearson's correlation of hybridized samples. Quality control checks were performed for each Affymetrix array chip loaded with hybridization cocktail containing fragmented aRNA of control (4, 5, 6), OSA® (1, 2, 3), cytokines (7, 8, 9) and cytokines + OSA® (10, 11, 12). The wash/stain of each chip was carried out using Fluidics station 450 and the chips were scanned using GeneChip® Scanner 3000 7G. Image acquisition was done using Affymetrix GeneChip® Command Console (AGCC) and signals were analyzed with MAS 5.0.

Signal Histogram - MAS5

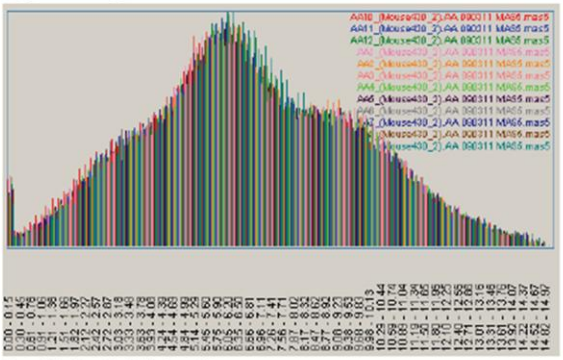

Log Probe Cell Intensity

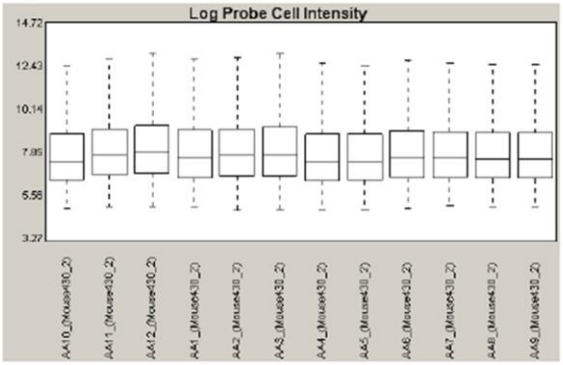

Pearson's Correlation (signal)

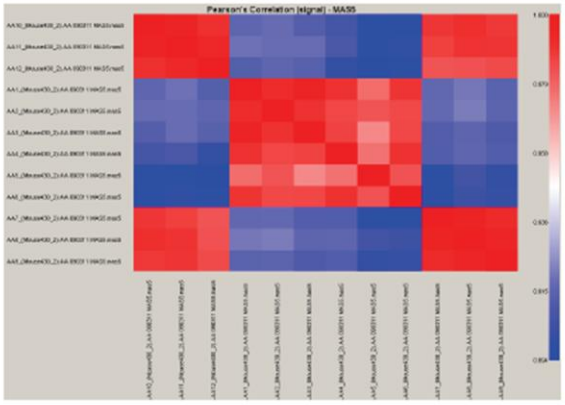

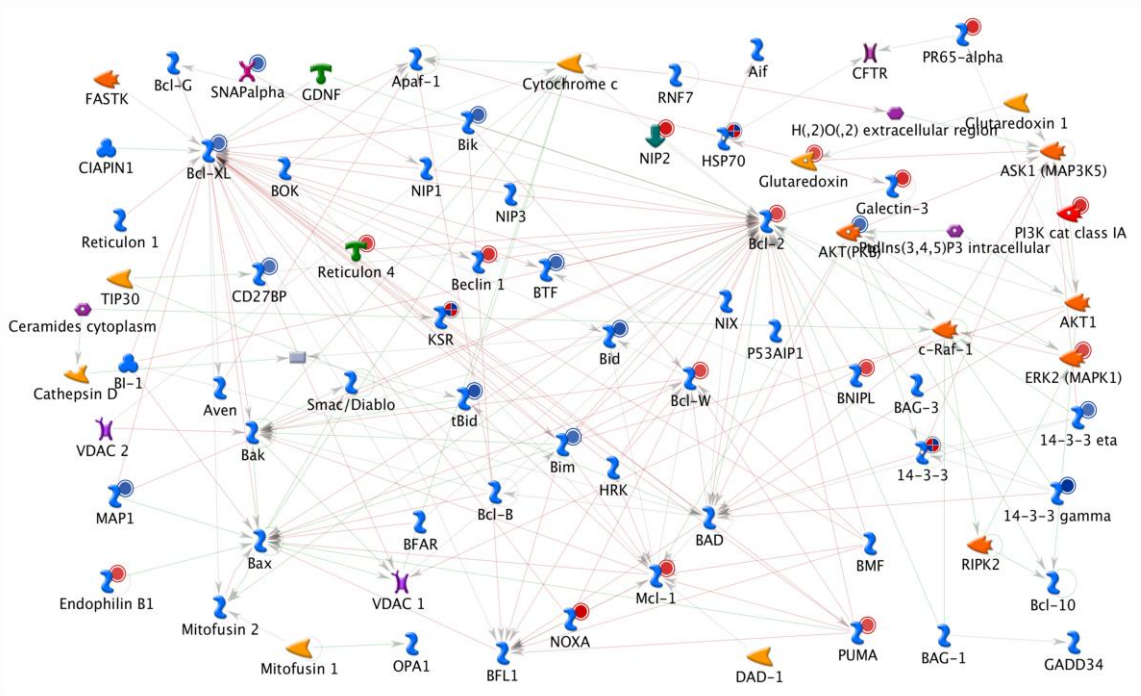

Figure 4: GeneGO process network of apoptotic mitochondria. Genes that were upregulated were highlighted by red circle and genes that were downregulated were highlighted by blue circle.

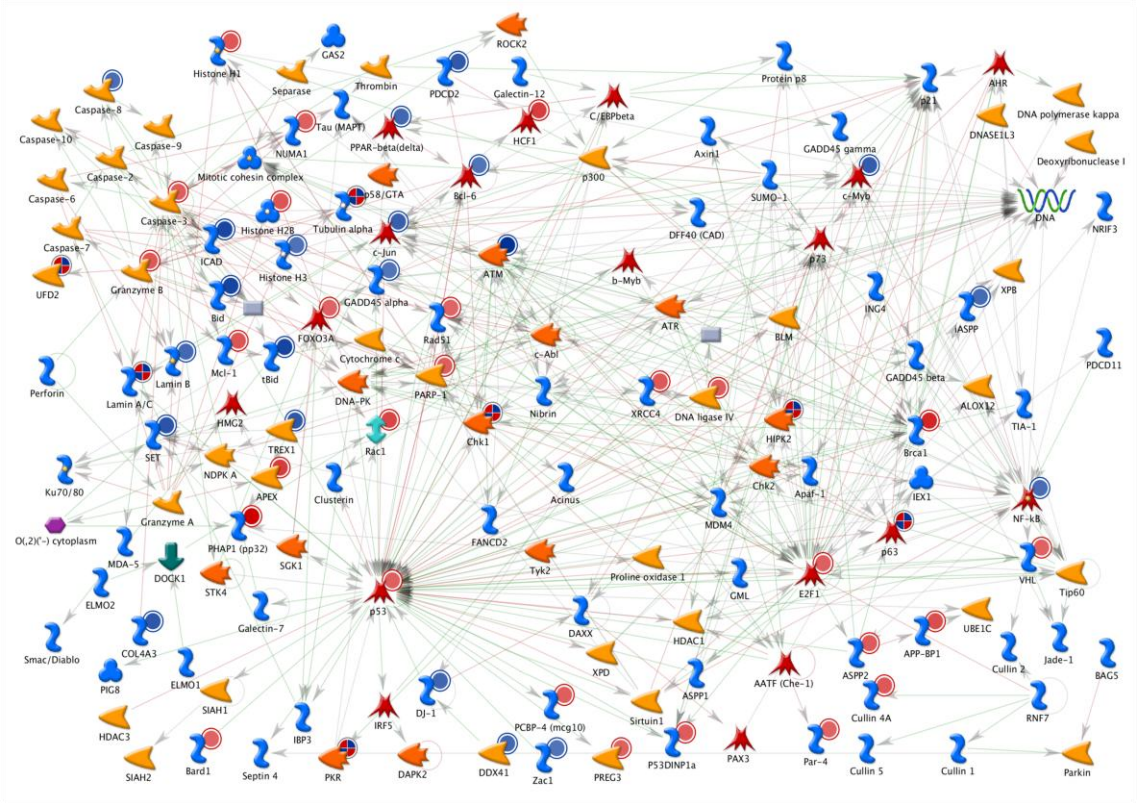

Figure 5: GeneGO process network of apoptotic nucleus. Genes that were upregulated were highlighted by red circle and genes that were downregulated were highlighted by blue circle.

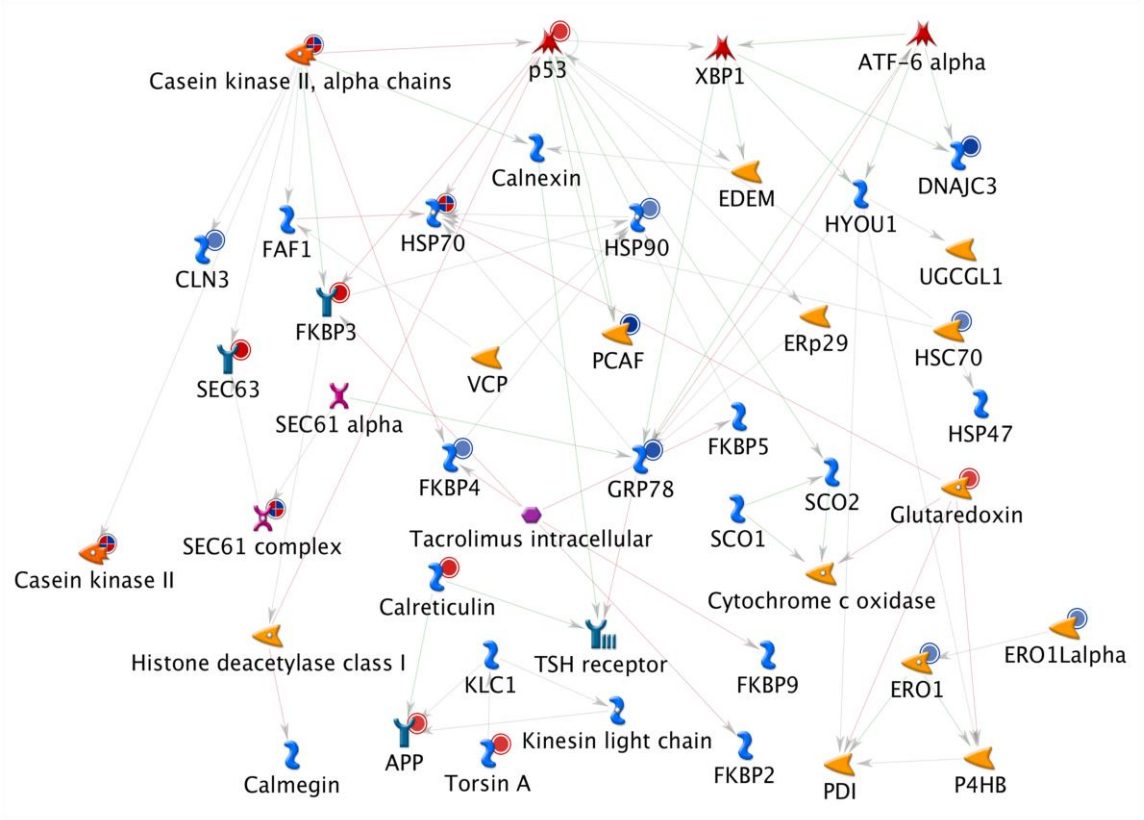

Figure 6: GeneGO process network of ER stress. Genes that were upregulated were highlighted by red circle and genes that were downregulated were highlighted by blue circle.

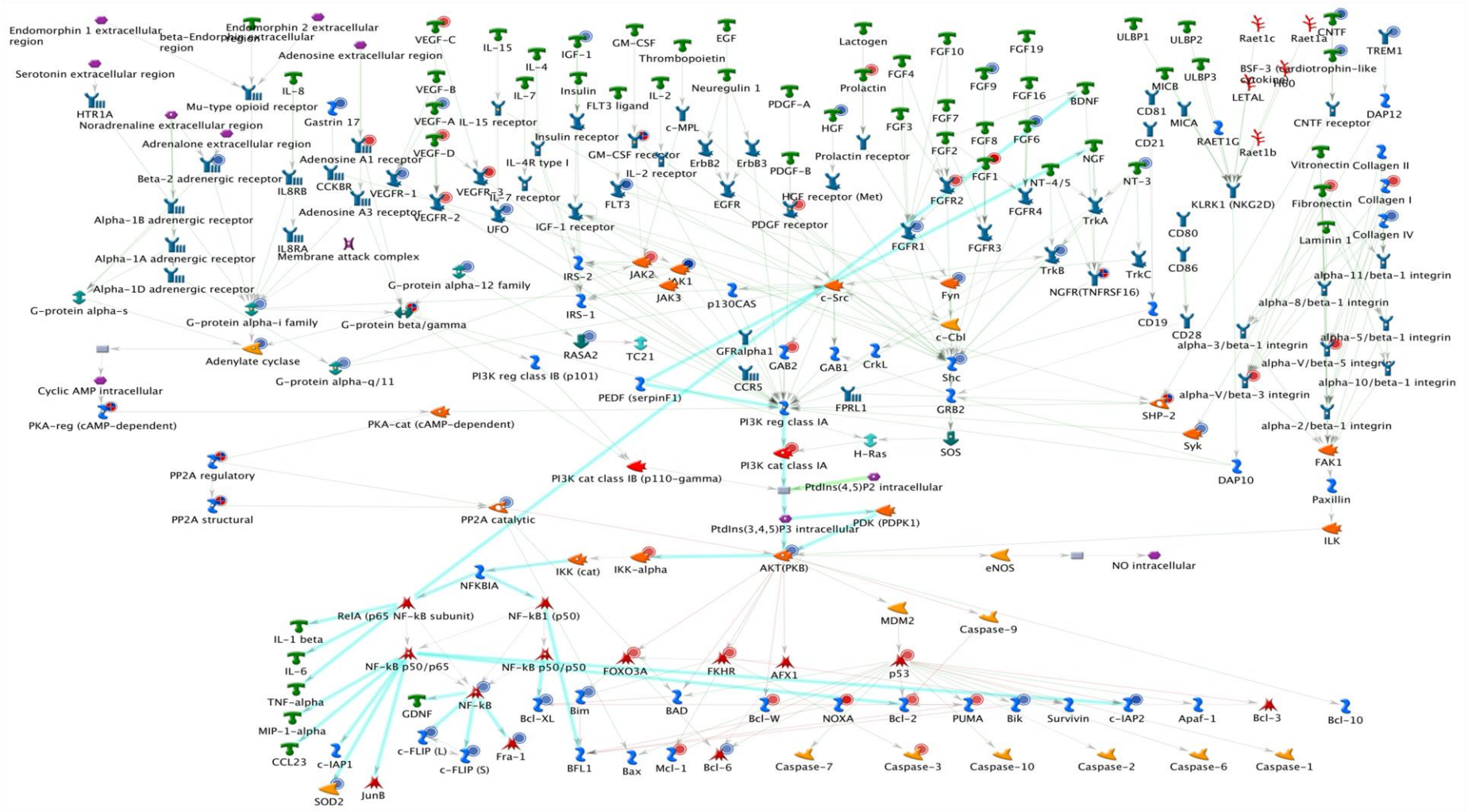

Figure 7: GeneGO process network of apoptosis and PI3K/AKT. Genes that were upregulated were highlighted by red circle and genes that were downregulated were highlighted by blue circle.

List of publications

1. Liu B, Asare-Anane H, Al-Romaiyan A, Huang GC, Amiel S, Jones P, Persaud SJ. Characterisation of the insulinotropic activity of an aqueous extract of *Gymnema sylvestre* in mouse B-cells and human islets of Langerhans. Cell physiol biochem 2009; 23: 125-132.
2. Al-Romaiyan A, Liu B, H. Asare-Anane H, Maity CR, Chatterjee SK, Koley N, Biswas T, Chatterji AK, Huang G-C, Amiel SA, Persaud SJ and Jones PM. A novel *Gymnema sylvestre* extract stimulates insulin secretion from human islets *in vivo* and *in vitro*. Phytother res 2010; 24(9):1370-1376
3. Al-Romaiyan A, Jayasri MA, Mathew TL, Huang GC, Amiel S, Jones PM, Persaud SJ. *Costus pictus* extracts stimulate insulin secretion from mouse and human islets of Langerhans *in vitro*. Cell Physiol Biochem. 2010;26(6):1051-8. Epub 2011 Jan 4.
4. Al-Romaiyan A, Liu B, Huang GC, Amiel S, Jones PM, Persaud SJ. A *Gymnema sylvestre* extract stimulates insulin secretion from isolated mouse and human islets of Langerhans *in vitro*: role of extracellular Ca^{2+} and protein kinases. Diabetes, Obesity & Metabolism, 2011, submitted.
5. Al-Romaiyan A, Persaud SJ and Jones PM. Screening of novel plant extracts for potential use as anti-diabetic drugs: *Gymnema sylvestre* and *Costus pictus* as examples. Journal of Ethnopharmacology, 2011, submitted.